

# Anatomy of the eye and orbit

- Anatomical terms of reference
- Osteology of the skull and orbits
- Structure of the eye
- Orbital contents
- Cranial nerves associated with the eye and orbit
- Ocular appendages (adnexa)
- Anatomy of the visual pathway

## Anatomical terms of reference

The internationally accepted terminology for description of the relations and position of structures in the body requires reference to a series of imaginary planes (Fig. 1-1). Thus, relative positions of anatomical structures are referred to in terms of: *medial* (nearer the median or mid-sagittal plane) and *lateral* (away from this plane); *anterior* and *posterior* refer to the front and back surfaces of the body; *superior* (cranial or rostral) or *inferior* (caudal) refer to position in the vertical; *superficial* and *deep* specify distance from the surface of the body. A combination of terms can be used to describe the relative position of structures that do not fit exactly any of the other terms, e.g. ventrolateral, postero-medial, etc.

## Osteology of the skull and orbits

### GENERAL ARRANGEMENT AND FEATURES OF THE SKULL

The skull is divided into two parts: an upper part shaped like a bowl, which contains the brain, known as the *cranium* or *neurocranium*; and a lower part, the *facial skeleton* or *viscerocranium*. The cranium can be further subdivided into the cranial vault and cranial base.

The skull is composed of a large number of separate bones that are united by *sutures* (fibrous immovable joints). The cranium consists of eight bones (only two are paired), the facial skeleton consists of 14 bones, of which only two are single (Fig. 1-2A,B). The skull contains a number of cavities that reflect its multiple functions:

- *cranial cavity* – houses, supports and protects the brain
- *nasal cavity* – concerned with respiration and olfaction
- *orbits* – contain the eyes and adnexa
- *oral cavity* – start of gastrointestinal tract, responsible for mastication and initial food processing; houses taste receptors.

Many of the cranial bones contain air-filled spaces, the paranasal sinuses (Fig. 1-3). Most of the anatomical features of the whole skull relevant to the study of the eye and orbits are indicated in Figure 1-2A and B (*norma frontalis* and *norma lateralis*). (See video 1-1).



## OSTEOLOGY OF THE ORBIT

The orbital cavities, situated between the cranium and facial skeleton, are separated from each other by the nasal cavity and the ethmoidal and sphenoidal air sinuses (Fig. 1-3A–C). Each bony orbit accommodates and protects the eye and adnexa, and serves to transmit the nerves and vessels that supply the face around the orbit. Parts of the following bones contribute to the walls of the orbit: maxilla, frontal, sphenoid, zygomatic, palatine, ethmoid and lacrimal (Figs 1-4 and 1-5A,B). Each orbit is roughly the shape of a quadrilateral pyramid whose base is the *orbital margin* and whose apex narrows at the *optic canal*. Each orbit has a floor, roof, medial wall and lateral wall (Fig. 1-4). (See video 1-2).



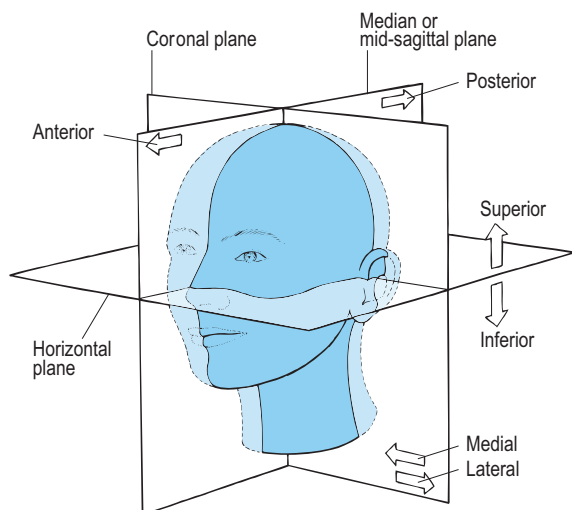


**FIGURE 1-1** Diagram illustrating anatomical planes of reference.

The floor tapers off before reaching the apex; therefore the apex of the pyramid is triangular in shape. The orbit is widest approximately 1.5 cm behind the orbital margin. The medial walls are approximately parallel to the mid-sagittal plane, while the lateral walls are oriented at an angle of approximately 45° to this plane. The *orbital aperture* is directed forwards, laterally and slightly downwards, a characteristic of primates and indeed predators which require binocular vision. Nerves and muscles passing from the apex into the orbit pass forward and laterally (Fig. 1-3A,B). The orbit is approximately 40 mm in height, 40 mm in width and 40 mm in depth. The volume is approximately 30 mL, of which one-fifth is occupied by the eye.

### The walls of the orbit

The bones that make up the roof, floor and medial and lateral walls are summarized in Figure 1-4.

### Features of the orbital roof

- *Fossa for the lacrimal gland*: lies in the anterolateral aspect of the roof behind the zygomatic process of the frontal bone.
- *Trochlear fossa (fovea)*: lies in the anteromedial aspect of the roof, 4 mm from the margin, and is the site at which the trochlea (small pulley) is attached. The tendon of the superior oblique passes through the trochlea.

- *Anterior and posterior ethmoidal canals*: Positioned at the junction of roof and medial wall above the frontoethmoidal suture (Fig. 1-5A). They transmit the anterior and posterior ethmoidal nerves and vessels.

**Relations.** The roof, which is thin and translucent except at the lesser wing of the sphenoid, separates the orbit from the anterior cranial fossa and frontal lobes of the brain. Anteriorly, the frontal sinus lies above the orbit.

### Features of the medial orbital wall

- This wall is oblong in shape and thin (0.2–0.4 mm). The four bones that comprise this wall are separated by vertical sutures (Figs 1-4 and 1-5A).
- *Lacrimal fossa* for the lacrimal sac: it is bound by anterior and posterior lacrimal crests and is continuous below with the *nasolacrimal canal* (Fig. 1-5B).

**Relations.** This is the thinnest of the walls and is largely transparent or semitransparent – the ethmoidal air sinuses can easily be seen through this wall in a dried skull (Fig. 1-5A,B). Medial to this wall in an anterior to posterior sequence lie the anterior, middle, posterior ethmoidal air cells and the sphenoidal sinus.

### Features of the orbital floor

- The floor slopes slightly downwards from the medial to the lateral wall.
- It is crossed by the *infraorbital groove*, which runs forward from the *inferior orbital fissure*. Before it reaches the orbital margin this fissure becomes the *infraorbital canal*, which opens as the *infraorbital foramen* 4 mm below the orbital margin on the anterior surface of the maxilla (Figs 1-3C, 1-4 and 1-5A).

**Relations.** The floor separates the orbit from the maxillary sinus, the bone being only 0.5–1 mm in thickness (Fig. 1-3C).

### Features of the lateral orbital wall (Fig. 1-4)

- *Spina recti lateralis*: a small bony spine on the greater wing of the sphenoid near the apex of the orbit which gives origin to part of the lateral rectus.
- *Zygomatic foramen*: transmits zygomatic nerve and vessels to temporal fossa and cheek (zygomaticotemporal nerve and zygomaticofacial nerve) (Fig. 1-5B).

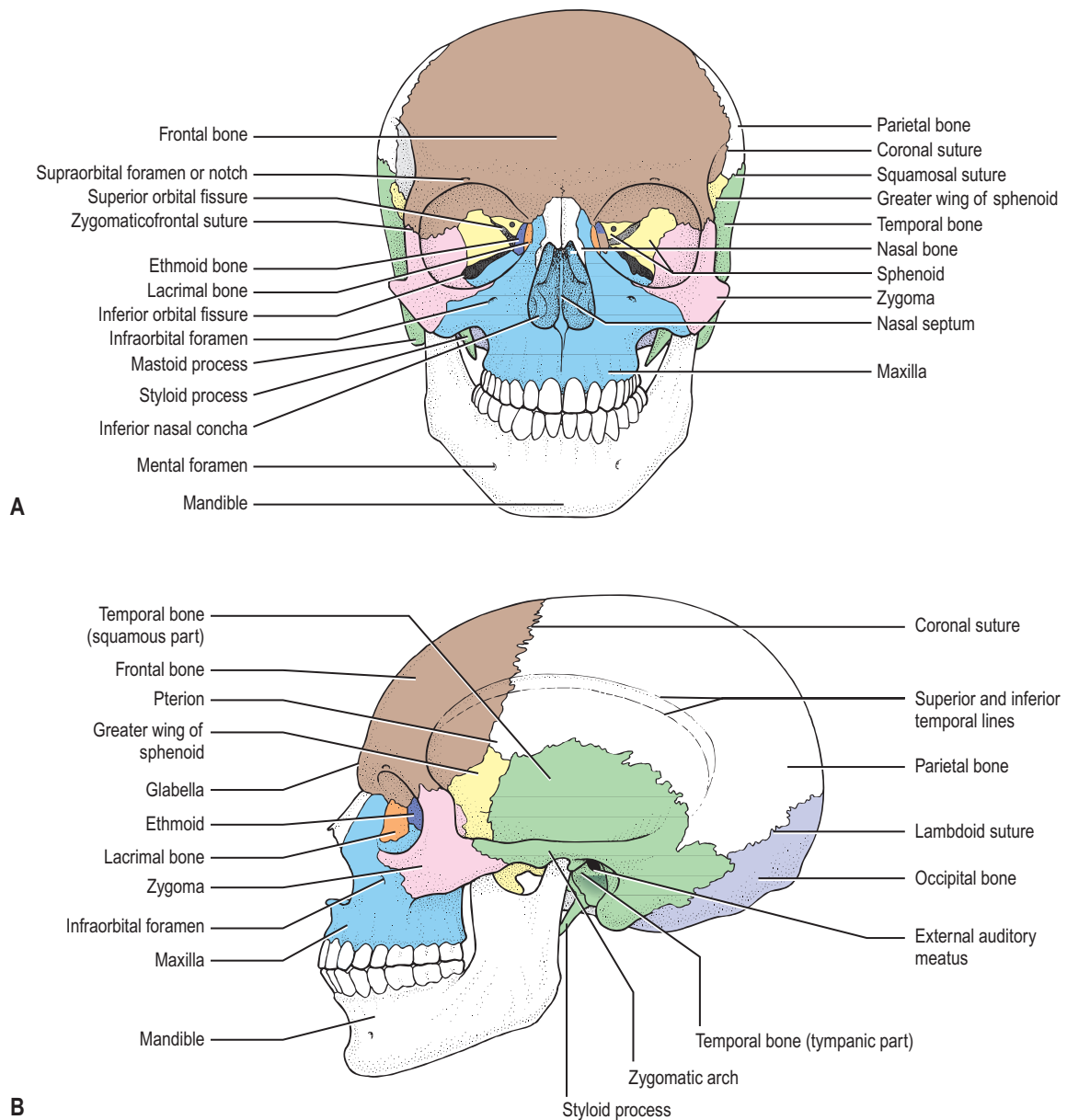


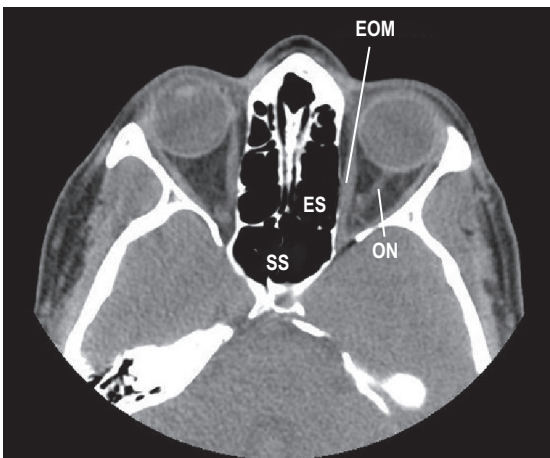
**FIGURE 1-2** Osteology of the skull. Two views of the skull: (A) norma frontalis; and (B) norma lateralis to illustrate the individual bones and important anatomical landmarks.

- **Lateral orbital tubercle:** forms the attachment of the check ligament of the lateral rectus, suspensory ligament (Lockwood's) of the eye, superior transverse ligament (Whitnall's) and aponeurosis of levator palpebrae superioris.
- Foramina for small veins that communicate with middle cranial fossa.

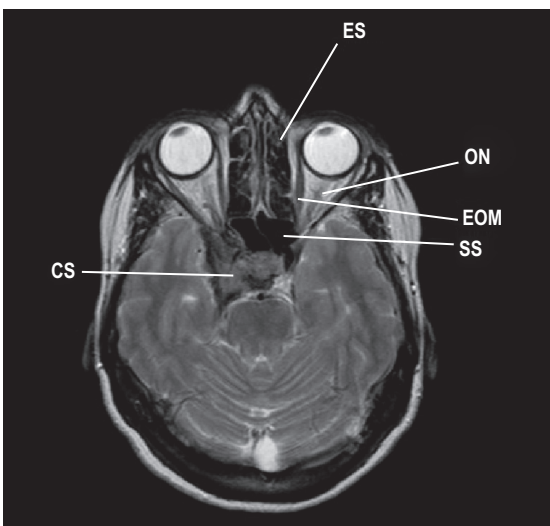
**Relations.** Laterally – skin, temporal fossa and middle cranial fossa in an anterior–posterior sequence (Fig. 1-3A).

#### Orbital margin, fissures and optic canal

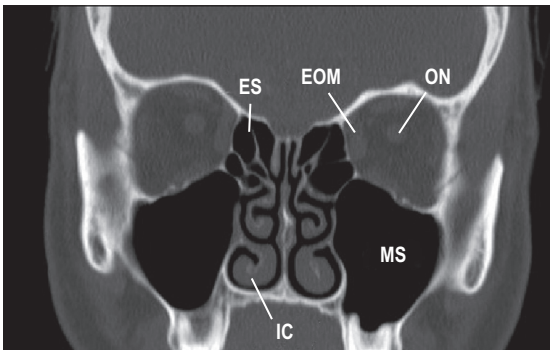
**Orbital margin.** This is a thickened rim of bone that helps protect the orbital contents. It is made up of three bones: the frontal, zygomatic and maxilla



A



B

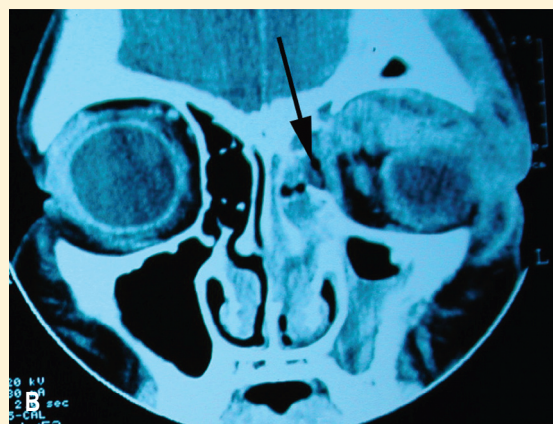


C

## BOX 1-1 CLINICAL CORRELATES

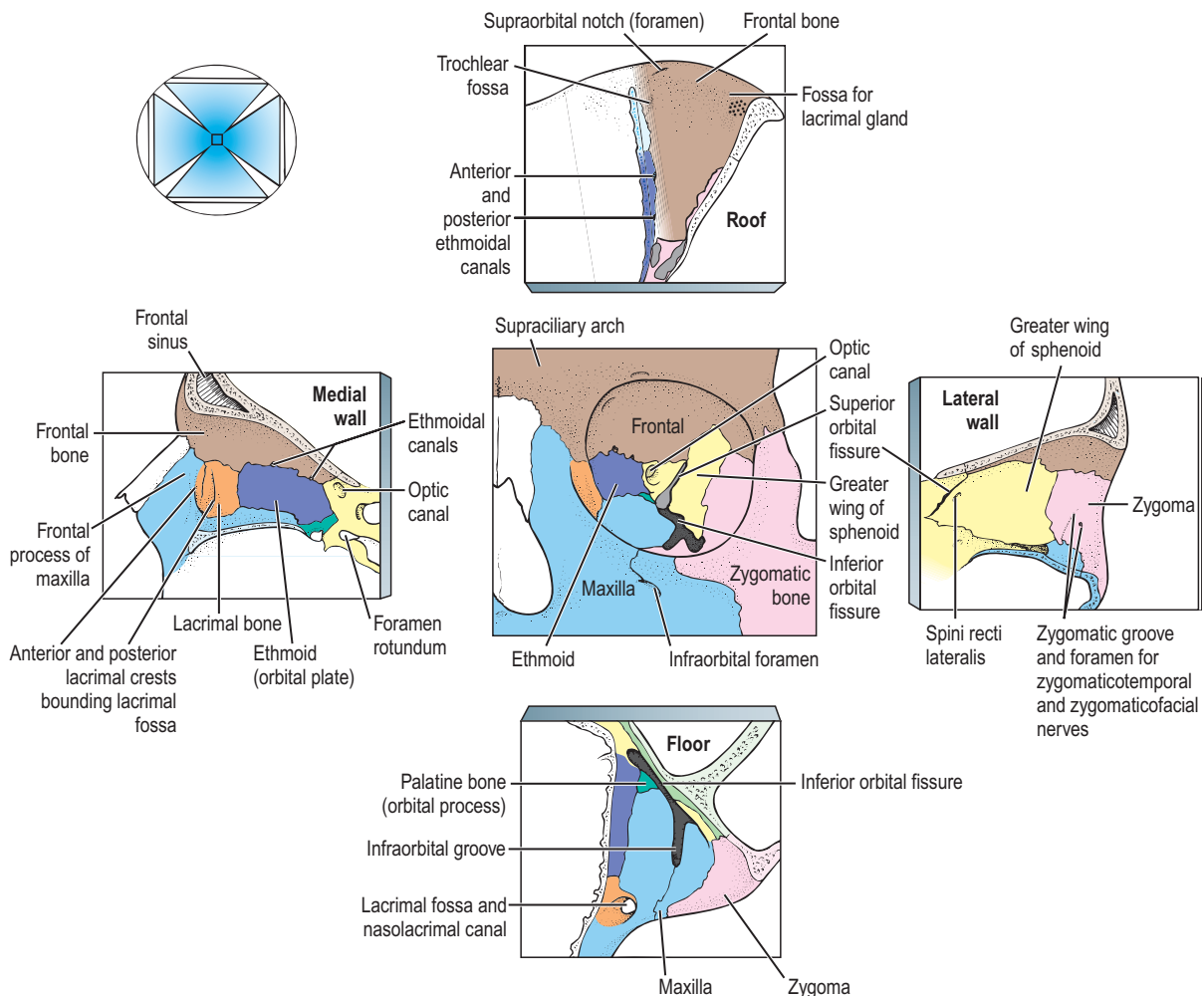
### Orbital cellulitis

This condition may be a consequence of infection spreading from the air sinuses to the orbit via the paper-thin medial wall (*lamina papyracea*) that separates the two. An example is shown of a patient with orbital cellulitis following creation of a drainage fistula (A). A coronal CT (B) illustrates the communication with the ethmoidal sinuses and nasal cavity (arrow).



(Images courtesy of Dr Alan McNab.)

**FIGURE 1-3** Transverse (A,B) and coronal (C) computed tomography (CT: A and C) and magnetic resonance imaging (MRI: B) scans of the head displaying the major relations of the orbits. Features identifiable in the scans include ethmoid air cells/sinuses (ES), maxillary sinus (MS), sphenoid sinus (SS), nasal cavity (NC), inferior nasal concha (IC), extraocular muscle (EOM), optic nerve (ON) and cavernous sinus (CS).

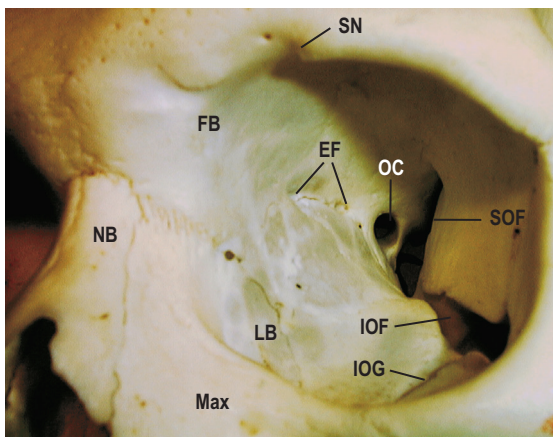
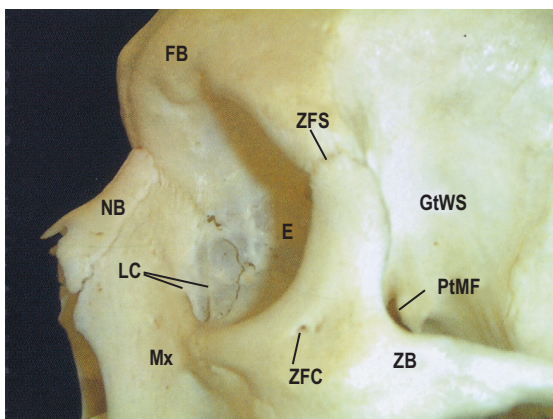


**FIGURE 1-4** Osteology of the orbit. The central diagram illustrates the anterior view of the intact left orbit, the four surrounding diagrams ('exploded orbit' – see inset, top left) show the individual bones which form the roof, floor, medial and lateral walls and other noteworthy features. **Roof:** orbital plate of the frontal bone and small area of lesser wing of the sphenoid. **Medial wall:** frontal process of the maxilla, lacrimal bone, orbital plate of the ethmoid and the body of the sphenoid. **Floor:** orbital plate of the maxilla, orbital surface of the zygoma and the orbital process of the palatine bone. **Lateral wall:** orbital surfaces of greater wing of sphenoid posteriorly and zygomatic bone anteriorly.

(Figs 1-4 and 1-5A,B). The lateral margin does not reach as far anteriorly as the medial margin (see Figs 1-2B and 1-5B). The medial margin is sharp and distinct in its lower half because of the anterior lacrimal crest, but is indistinct superiorly (Figs 1-4 and 1-5B).

**Superior orbital fissure.** This communication between the orbital and cranial cavities lies between the roof and lateral wall of the orbit and is bounded by the lesser and greater wings of sphenoid (Figs 1-4,

1-5A and 1-6). It is wider at its medial end and narrowest at its lateral end. It is around 22 mm long and is separated from the optic foramen above by the posterior root of the lesser wing of the sphenoid. The part of the common tendinous ring that gives origin to the lateral rectus spans between the narrow and wide parts of the fissure. Structures passing above or outside the tendinous ring or annulus include the lacrimal nerve, frontal nerve, trochlear nerve, superior ophthalmic vein and recurrent branch of the lacrimal

**A****B**

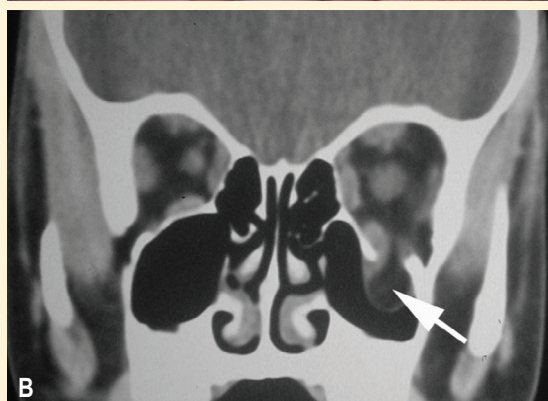
**FIGURE 1-5** (A) Anterior view of the bony orbit showing important osteological features of the apex including the relation of the superior orbital fissure (SOF), optic canal (OC) and inferior orbital fissure (IOF). IOG, inferior orbital groove; LB, lacrimal bone; EF, anterior and posterior ethmoidal foramina; SN, supraorbital notch; FB, frontal bone; NB, nasal bone; Max, maxilla. (B) Lateral view of the orbit. ZB, zygomatic bone; PtMF, pterygomaxillary fissure; GtWS, greater wing of the sphenoid; ZFS, zygomaticofrontal suture; ZFC, zygomaticofacial canal; LC, lacrimal crest; E, ethmoid bone; Mx, maxilla.

artery. The latter anastomoses with the orbital branch of the middle meningeal artery and may more commonly travel in a small crano-orbital foramen lateral to the superior orbital fissure. Structures passing within the ring, and thus within the apex of the muscle cone, include the oculomotor nerve (superior and inferior divisions), abducent nerve, nasociliary nerve, sympathetic root of the ciliary ganglion, and variably the inferior ophthalmic vein (Fig. 1-6).

## BOX 1-2 CLINICAL CORRELATES

### Orbital blow-out fractures

The floor, although thicker than the medial wall, is more often involved in orbital blow-out fractures, probably because it lacks the buttress-like supports of the ethmoidal air cells and the protection of the nose. Tumour spread to or from the maxillary sinus may occur via the floor of the orbit.

**A****B**

An example of ocular motility being compromised in left eye following blow-out fracture (A) and a coronal CT (B) showing the herniation of orbital contents into the roof of the maxillary sinus (arrow).

(Images courtesy of Dr Alan McNab.)

**Inferior orbital fissure.** This fissure lies between the lateral wall and floor of the orbit below the superior orbital fissure. It forms a communication between the orbit and the infratemporal fossa and pterygopalatine fossa. It runs forward and laterally for approximately 20 mm and ends 20 mm from the orbital margin (Figs 1-4 and 1-5A). The fissure is narrowest in the middle section and in life is covered by periorbita and a sheet

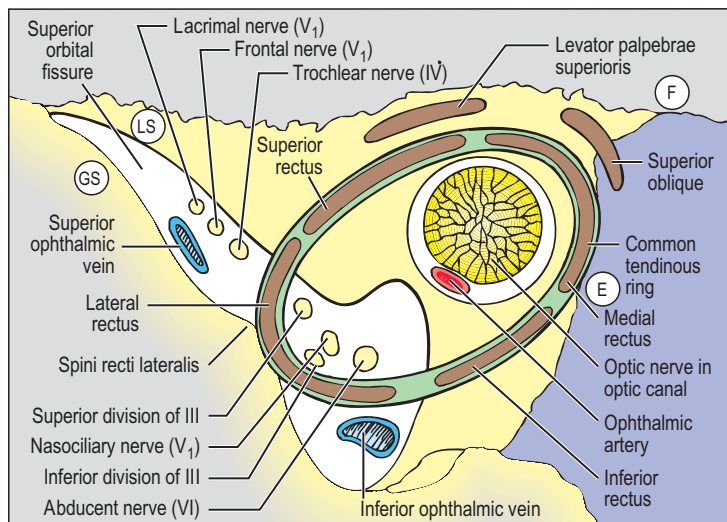


**FIGURE 1-6** Schematic diagram of the superior orbital fissure and optic canal in the right orbit. Note the origins of the extraocular muscles from the common tendinous ring and the relative position of the cranial nerves and vessels as they enter or exit the orbit. GS, greater wing of sphenoid; LS, lesser wing of sphenoid; F, frontal bone; E, ethmoid. The positions of the veins are variable. The first letters of each of the structures passing through the superior orbital fissure (LFTSNIA) form a well-known mnemonic.

of smooth muscle of unknown function, the orbitalis or ‘muscle of Müller’. It transmits the infraorbital nerve, zygomatic nerve, branches from the pterygopalatine ganglion and the inferior ophthalmic vein may communicate with the pterygoid venous plexus below.

**Optic canal.** This is a bony channel in the sphenoid that passes anteriorly, inferiorly and laterally ( $36^\circ$ ) from the middle cranial fossa to the apex of the orbit. The canal is formed by the two roots of the lesser wing of the sphenoid. The optic canals are 25 mm apart posteriorly and 30 mm anteriorly. Each is funnel-shaped and narrowest anteriorly where its opening into the orbit is oval with sharp upper and lower borders and a prolonged roof (10–12 mm in length). The opening at the cranial aspect is oval with a prolonged floor. The sphenoidal and posterior ethmoidal air sinuses are important medial relations, and the olfactory tracts are superior relations of the canal. The canal transmits the *optic nerve* with its meningeal coverings and the *ophthalmic artery*, which lies below and then lateral to the nerve within the dural sheath for part of its course (Fig. 1-6). Sympathetic nerve fibres accompany the artery.

## PARANASAL SINUSES

The paranasal sinuses (Figs 1-3, 1-7 and Video 1.3) comprise the frontal, ethmoidal, sphenoidal and

maxillary sinuses. They are air-filled cavities in the skull that are in communication with the nasal cavity via a series of apertures. Infection commonly spreads from the nasal cavity into the sinuses. The sinuses function to warm and moisten the air, add resonance to the voice and lighten the skull. They vary in size and shape between individuals.

Additional content available at <https://expertconsult.inkling.com/>.

## CRANIAL CAVITY (FIG. 1-8A,B AND EFIG. 1-1)

The cranial cavity houses the brain, cerebral vessels, the meninges, meningeal vessels and the intracranial portions of the cranial nerves. The base of the cranial cavity can be subdivided for descriptive purposes into three fossae: anterior, middle and posterior. Accounts of the detailed anatomy of these fossae can be found in any standard anatomy text; therefore only features of relevance to the eye and orbit in the anterior and middle cranial fossae will be described.

For discussion of posterior cranial fossa see <https://expertconsult.inkling.com/>.

### Cranial fossae

**Anterior cranial fossa.** The anterior cranial fossa is limited in front and laterally by the frontal bone and posteriorly by the lesser wing of the sphenoid. Its floor is formed by the orbital plate of the frontal bone, the cribriform plate of the ethmoid (with a median

### FRONTAL SINUSES (FIGS 1-4 AND 1-7)

The frontal sinuses are paired and lie behind the superciliary arches within the frontal bone (eFig. 1-1). They are separated from each other or further subdivided by thin bony septa that are not necessarily in the midline. The sinuses may extend as far laterally as the zygomatic process of the frontal bone. Each is approximately triangular and extends highest above the medial end of the eyebrow (Fig. 1-7). Each sinus opens into the middle meatus of the nasal cavity, either through the ethmoidal infundibulum or directly via the frontonasal duct. The mucosal lining is supplied by the supraorbital nerves and vessels; hence, referred pain from frontal sinusitis is experienced along the course of the supraorbital nerve.

Recent geometric morphometric studies (elliptic Fourier analysis) of the outlines of frontal sinuses from large numbers of radiographic images have confirmed a long-held belief that each individual's frontal sinus is distinct and unique. This may have important applications for personal identification in the context of forensics.

### ETHMOIDAL SINUSES (AIR CELLS)

#### (FIGS 1-3A–C AND 1-7)

These thin-walled sinuses are for the most part situated in the lateral mass of the ethmoid, although frontal, maxillary, lacrimal, sphenoidal and palatine bones contribute to the walls. They are variable in number and are grouped into anterior, middle and posterior. The general pattern of drainage of the sinuses is as follows: the anterior opens into the hiatus semilunaris, the middle on to the bulla ethmoidalis (both middle meatus) and the posterior into the superior meatus. They are related to the frontal sinus anteriorly, the sphenoidal sinus posteriorly, the nasal cavity medially and below, and laterally the orbit (Fig. 1-7A).

### SPHENOVIDAL SINUS (FIGS 1-3A,B AND 1-7)

This sinus lies within the body of the sphenoid bone and possesses an indented roof because of the pituitary fossa that lies above and houses the pituitary gland (Fig. 1-8). It may be divided by a variable midline septum. A transverse ridge in the lateral wall marks the position of the internal carotid artery (within the cavernous sinus). Other important relations of the sinus include the optic chiasma and nerves above, the nasal cavity below, the ethmoidal

sinuses anteriorly, and the paired cavernous sinuses laterally (Fig. 1-9C). The sphenoidal sinus drains into the superior meatus or sphenoethmoidal recess. Surgical access to the pituitary gland may be gained via the nasal cavity and sphenoidal sinus; hence, surgeons must be aware of the above-mentioned relations.

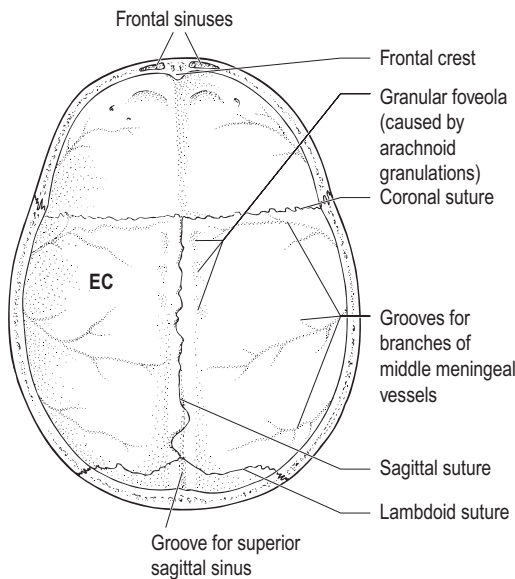
### MAXILLARY SINUS (FIGS 1-3C AND 1-7)

These are the largest of the paranasal air sinuses. They are pyramidal in shape and lie within the body of the maxilla. The *base* forms part of the lateral wall of the nasal cavity and the *apex* is within the zygomatic process. Each sinus is in communication with the middle meatus of the nasal cavity via an aperture, the maxillary hiatus, on its base, which empties into the lower part of the hiatus semilunaris. The opening is positioned high on this wall and therefore does not facilitate gravitational drainage in the upright position. The *nasolacrimal duct* lies in a thin bony canal in the anterior part of the base. The orbital plate forms the *roof* of the sinus and floor of the orbit.

### ORBITAL FLOOR FRACTURES

Rapid traumatic compression of the orbital contents, such as occurs during squash ball injuries, can lead to blow-out fractures; orbital contents may herniate into the maxillary sinus. It was once thought that orbital contents, including extraocular muscles, became trapped in the fractured floor, thus restricting range of movement and explaining the diplopia suffered by these patients. However, recent studies have indicated that in many cases only orbital fibroadipose tissue is trapped in the damaged floor of the orbit (see p. 6).

The *floor* of the maxillary sinus is formed by the alveolar process housing a variable number of the roots of the first and second molars that protrude into the sinus, and may be separated from the sinus by only a thin covering of bone or mucous membrane. Thus sinusitis may present as referred pain such as toothache and vice versa. In addition, abscesses in the maxillary sinus may result from infection of these roots. The *anterior/lateral wall* is directed on to the face, and access for drainage of maxillary obstructions or other surgical procedures in the sinus may be gained by this route. The *posterior wall* faces the infratemporal fossa.



**eFIGURE 1-1** Features of the vault interior.

### POSTERIOR CRANIAL FOSSES

This is the deepest of the three cranial fossae, its floor lying below the level of the middle fossa. Its roof is formed by the tentorium cerebelli. It lodges the hind-brain: the cerebellum, pons and medulla oblongata. The fossa is bound anteriorly by the superior border of the petrous temporal bone and the dorsum sella, and surrounds the foramen magnum, the cerebellum being housed in the cerebellar fossae on the squamous part of the occipital bone. Features and openings on the floor of the posterior cranial fossa are not as relevant to the eye and orbit as those in the anterior or middle fossae; however, readers should be able to identify the following: foramen magnum, jugular foramen, hypoglossal canal, internal acoustic meatus, grooves for the sigmoid and transverse sinuses, internal occipital protuberance and clivus (Fig. 1-8A,B).

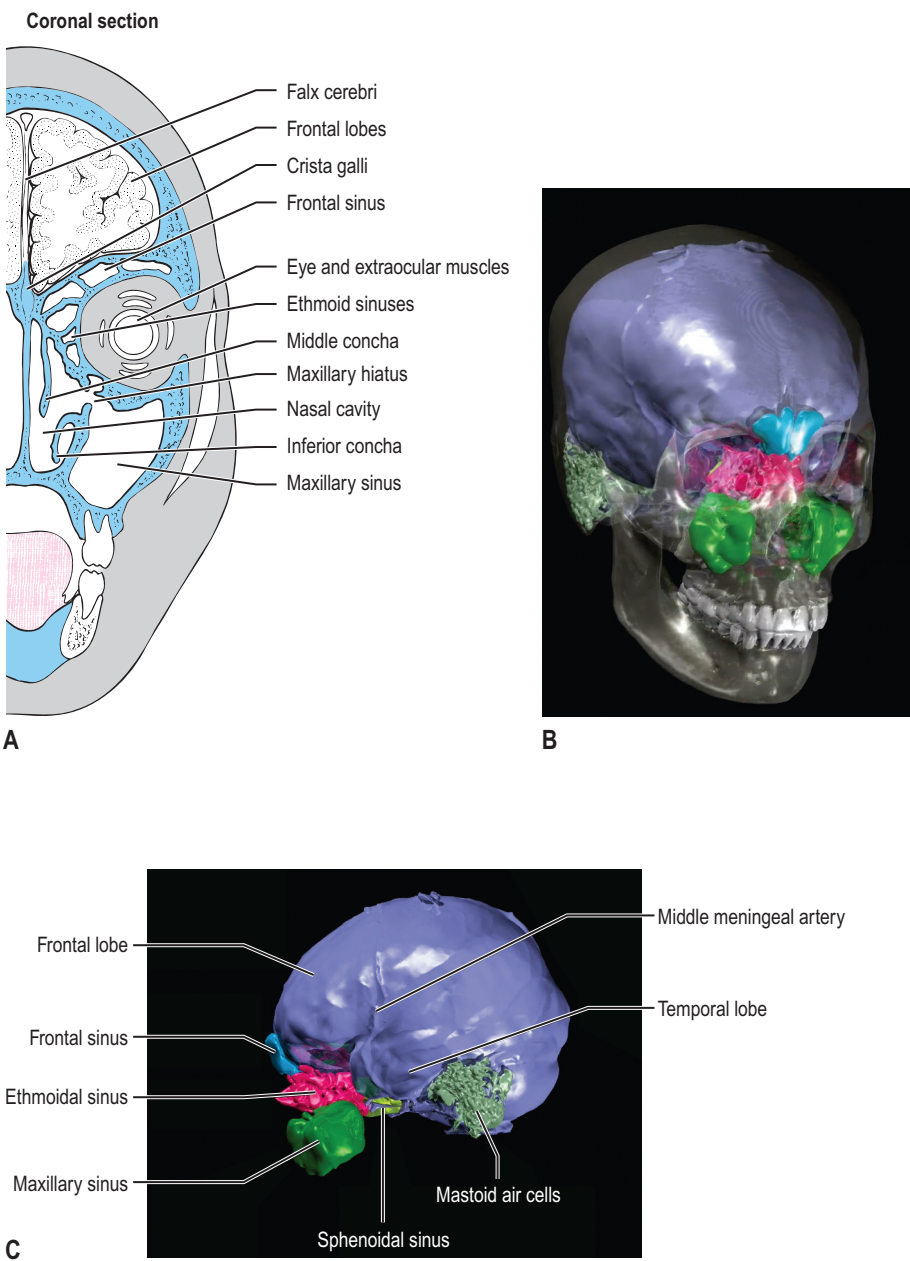


**FIGURE 1-7** (A) Diagram of a coronal section of the head revealing most of the paranasal sinuses except the sphenoid sinus. (B) 3D visualization of paranasal sinuses as seen from anterior aspect and (C) lateral aspect. See [http://www.oucom.ohio.edu/dbms-witmer/3D\\_human.htm](http://www.oucom.ohio.edu/dbms-witmer/3D_human.htm) or <https://expertconsult.inkling.com/> for 3D pdf movies of skull and more details of paranasal sinus anatomy.

crest-like ridge, the crista galli, which forms the anterior attachment of the falx cerebri), and the lesser wings and anterior part of the body (jugum) of the sphenoid. The perforations of the cribriform plate transmit the olfactory nerves. The orbital plate of the frontal bone separates the orbit below from the frontal

lobes of the cerebral hemispheres, whose sulci and gyri cause surface impressions on the bone. Projecting posteriorly from the lesser wings of the sphenoid are the anterior clinoid processes that overhang the middle cranial fossa and give attachment to the free edge of the tentorium cerebelli.

**Middle cranial fossa.** The middle cranial fossa lies at a lower plane than the anterior cranial fossa but is higher than the posterior cranial fossa. Its floor is shaped like a butterfly, with a narrow central or median part and expanded lateral parts. It is bound anteriorly by the posterior free edge of the lesser wing of the sphenoid, the anterior clinoid processes, and the anterior margin of the sulcus chiasmaticus (Fig. 1-8A,B). Posteriorly it extends to the superior borders of the petrous temporal bones and dorsum sellae of the sphenoid, and laterally it is bound by the squamous part of the temporal bone, part of the parietal bones, and the greater wings of the sphenoid. Features and foramina of the floor of the middle cranial fossa and the structures that they transmit are summarized in Table 1-1.

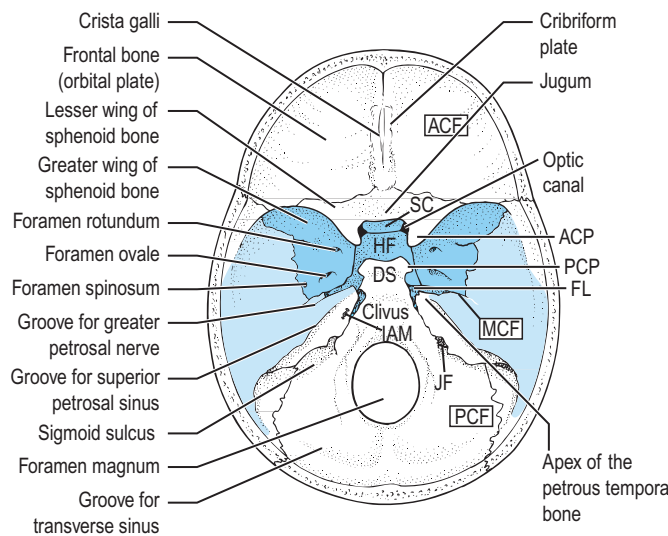
**Pituitary fossa.** The pituitary fossa (hypophyseal fossa) is an indentation in the roof of the body of the sphenoid bone in the middle cranial fossa. It is bound anteriorly by the tuberculum sellae, in front of which lies the sulcus chiasmatica, and posteriorly by the

dorsum sellae, a ridge of bone at either end of which lies the posterior clinoid processes. The pituitary fossa houses the pituitary gland or *hypophysis cerebri*. This is connected by a thin stalk – the pituitary stalk (or tuber cinereum) – to the brain. The fossa is roofed by a sheet of dura mater, the *diaphragma sella* (Fig. 1-9C,D) which is attached in front to the tuberculum and behind to the dorsum sellae. The pituitary stalk passes through a small opening in the roof. The right and left cavernous sinuses are important lateral relations (Fig. 1-9C).

### The meninges (Fig. 1-9A,B and eFig. 1-2A)

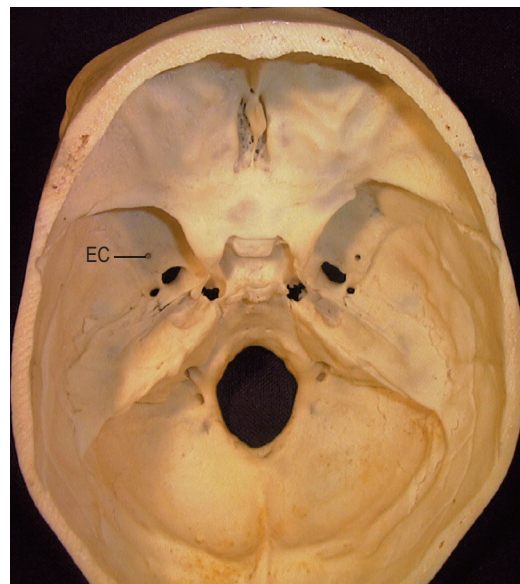
The brain and spinal cord are surrounded by three layers of meninges: a tough *pachymeninx*, the dura mater, and the *leptomeninges* consisting of the arachnoid mater and pia mater. Between the arachnoid and pia is the subarachnoid space filled with cerebrospinal fluid.

**Dura mater.** The *dura mater* is theoretically ‘divided’ into an endosteal layer (really the periosteum on the

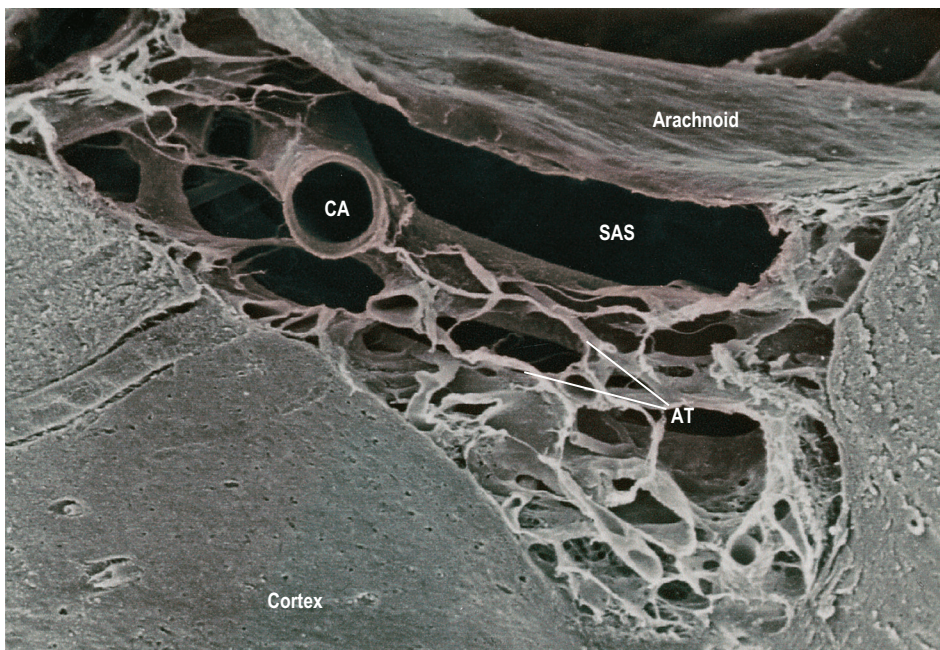
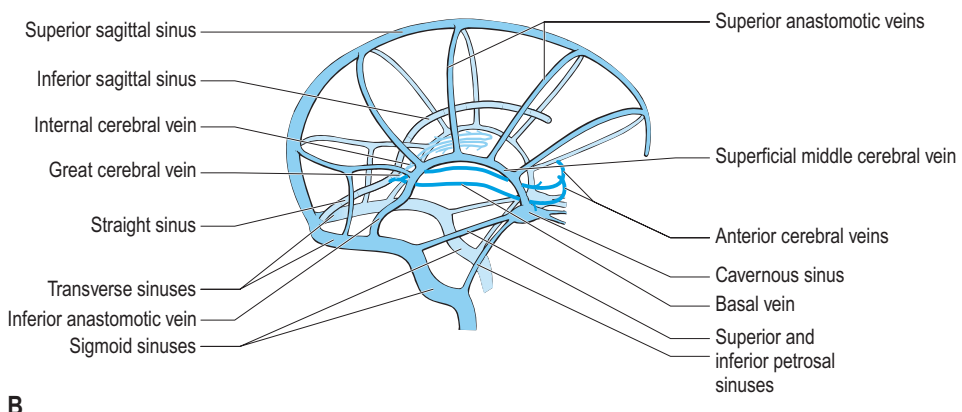


A

**FIGURE 1-8** Osteology of the cranial cavity. (A) The boundaries of the anterior (ACF), middle (MCF) and posterior (PCF) cranial fossae together with major foraminae and important landmarks on the base of the skull. HF, hypophyseal fossa; DS, dorsum sella; SC, sulcus chiasmaticus; IAM, internal auditory meatus; JF, jugular foramen and fossa; ACP, anterior clinoid process; PCP, posterior clinoid process; FL, foramen lacerum. (B) Photograph of cranial cavity to illustrate features shown in (A): EC, emissary canal.



B

**A****B**

**eFIGURE 1-2** (A) Scanning electron micrograph of the meninges and cortex of the brain showing the arrangement of the arachnoid trabeculae (AT) supporting the cerebral arteries (CA) as they course through the subarachnoid space (SAS) ( $\times 100$ ). (B) Schematic diagram of the dural venous sinuses and their connections with cerebral veins.

**TABLE 1-1 Summary of features on the floor of the middle cranial fossa**

Feature/foramen	Position	Relevance
Sulcus chiasmaticus	Between the two optic canals anterior to tuberculum sella	Only rarely does optic chiasma lie in contact with this region
Sella turcica ('Turkish saddle')	Central part of sphenoid body between the two cavernous sinuses	The central hollow, the hypophyseal fossa, houses the pituitary gland. Anterior and posterior clinoid processes give attachment to the free and attached margins of the tentorium cerebelli
Optic canal	Between the two roots of the lesser wing of the sphenoid	Transmits optic nerve, ophthalmic artery, sympathetic nerves and meningeal coverings
Superior orbital fissure	Between the lesser and greater wings of the sphenoid. Lies at apex of cavernous sinus	Transmits trochlear, abducent and oculomotor nerves and terminal branches of ophthalmic nerve
Foramen rotundum	Pierces greater wing of sphenoid	Transmits maxillary nerve and small veins from cavernous sinus
Foramen ovale	Pierces greater wing of sphenoid	Transmits mandibular nerve, accessory meningeal artery and occasionally the lesser petrosal nerve
Foramen spinosum	Posterolateral to foramen ovale	Transmits middle meningeal artery and vein and meningeal branch of the mandibular nerve
Foramen lacerum	At apex of petrous temporal bone	The upper end transmits the internal carotid artery before it enters the cavernous sinus. Also transmits sympathetic nerves and a small plexus of veins. The lower end is covered by connective tissue and pierced only by small branches of the ascending pharyngeal artery
Trigeminal impression	Anterior surface of petrous temporal bone behind foramen lacerum	Occupied by trigeminal ganglion in trigeminal cave. Joined on lateral aspect by grooves for the greater and lesser petrosal nerves
Tegmen tympani and arcuate eminence	Tegmen is a thin plate of temporal bone over middle ear cavity. Arcuate eminence is produced by superior semicircular canal in petrous temporal bone	Infections in middle ear may spread through thin plate of bone to middle cranial fossa and temporal lobe of the brain

inner surface of the skull) and a meningeal layer; however, on the whole they are fused except where they separate to form *dural venous sinuses* and *dural folds* (Fig. 1-9A,B). The latter are connective tissue septae that extend into the cranial cavity and serve to subdivide it into compartments. In association with the cerebrospinal fluid they aid in providing physical support and protection for the brain. The position and form of the dural folds are summarized diagrammatically in Figure 1-9A.

The *dural venous sinuses* are valveless, highly specialized, firm-walled veins within the cranial cavity which drain venous blood from the brain and cranial bones (Fig. 1-9B). In common with other veins the sinuses are lined by vascular endothelial cells; however, their walls contain no smooth muscle cells. The

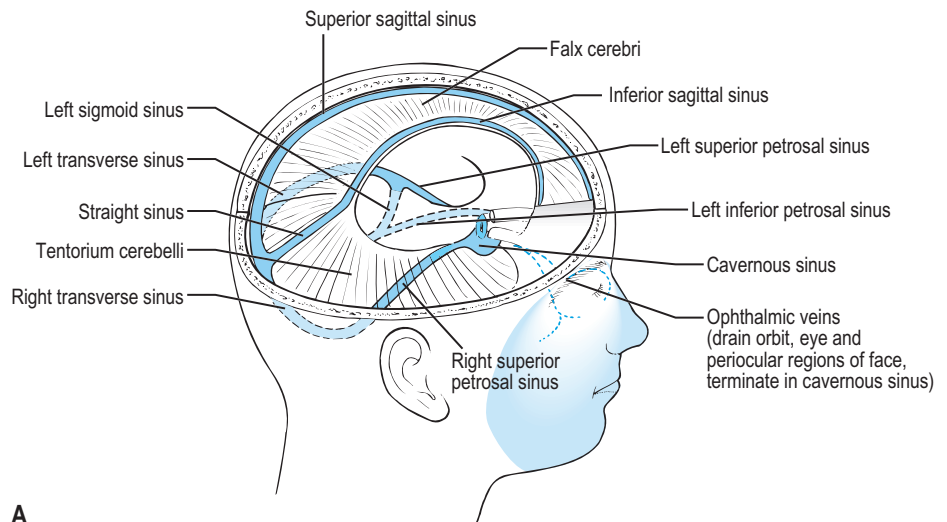
arrangement of the sinuses is summarized in Fig. 1-9A and eFig. 1-2B.

Of particular note to those studying the eye and orbit is the pair of cavernous sinuses lying either side of the body of the sphenoid (Fig. 1-9C,D).

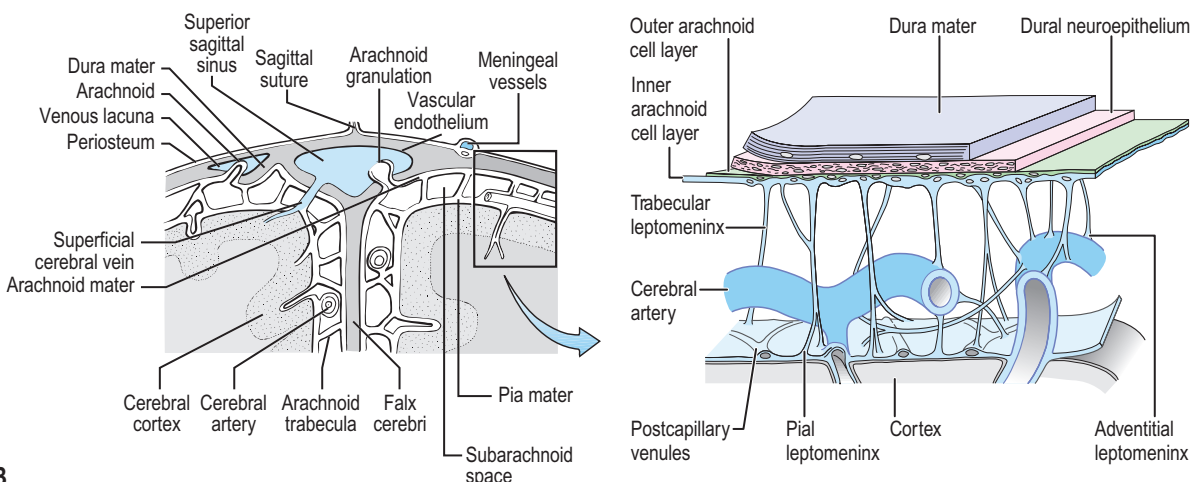
The importance of the *cavernous sinuses* (Fig. 1-9C,D) lies in their *position, relations* and extensive *communications*. Each cavernous sinus is around 2–3 cm long in the sagittal plane and consists of a series of incompletely fused venous channels or a single venous channel partially subdivided by *trabeculae*. It has walls of dura mater, like other venous sinuses.

**Position.** There is one cavernous sinus on either side of the body of the sphenoid. The sinus extends from the superior orbital fissure in front to the apex of the petrous temporal bone behind.

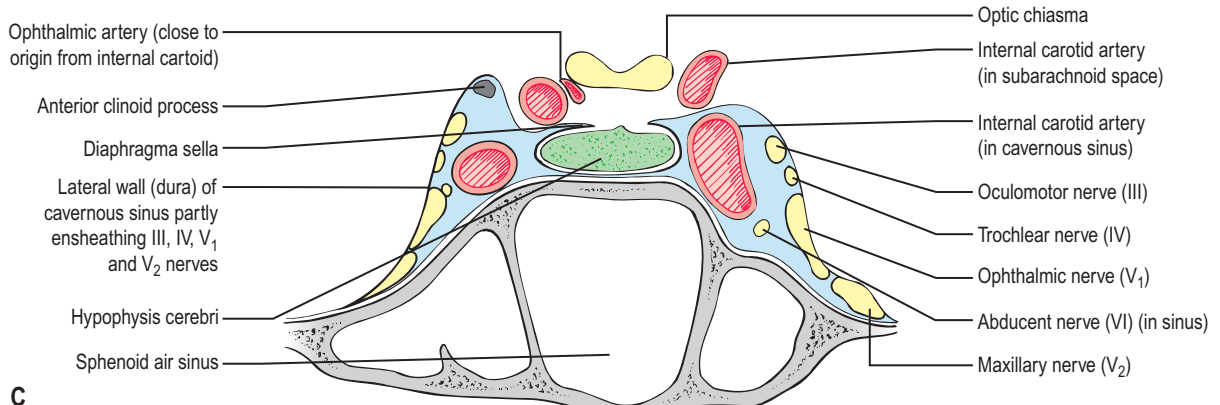




A



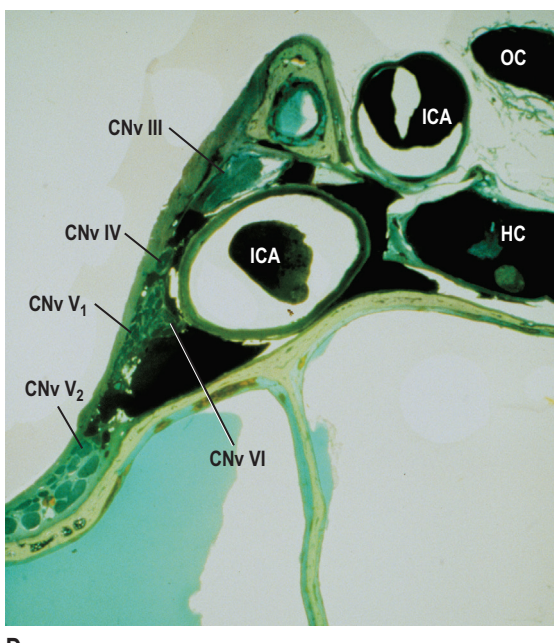
B



C

**FIGURE 1-9** (A) The interior of the cranium with the brain removed to illustrate the arrangement of the dural folds and some of the related dural venous sinuses. (B) The meninges as seen in coronal section in the region of the superior sagittal sinus. Inset higher-power diagrammatic representation of the meningeal layers. (C) Coronal section approximately midway along the body of the sphenoid bone to reveal the paired cavernous sinuses, one on either side. Note the position of the cranial nerves (II, III, IV, V<sub>1</sub>, V<sub>2</sub> and VI), internal carotid artery (cut in two places, within and above the sinus) and hypophysis cerebri (pituitary gland).

*Continued*



D

**FIGURE 1-9, cont'd (D)** High-power view of the left cavernous sinus (coronal plane, 100  $\mu\text{m}$  thick section of low-viscosity nitrocellulose resin-embedded specimen) upon which eFig. 1-2B was based. OC, optic chiasma; HC, hypophysis cerebri; ICA, internal carotid artery.

**Relations.** These are summarized in Figure 1-9C and D (coronal section).

**Communications.** The sinuses communicate with each other via the anterior and posterior intercavernous sinuses. Tributaries draining into the sinuses anteriorly include the superior and inferior ophthalmic veins (which drain the eye and orbit as well as areas of skin around the periorbital region of the face and nose), and the sphenoparietal sinuses. The superficial cerebral vein from the brain drains into the sinus from above (eFig. 1-2B).

Blood from each sinus may, depending on relative pressures, drain via the superior and inferior petrosal sinuses either directly to the internal jugular veins (inferior petrosal) or to the transverse sinuses and thus to the internal jugular veins. Other exits include venous plexi around the internal carotid artery or veins traversing the foramen ovale or sphenoidal emissary foramen to communicate with the pterygoid plexus and other veins in the region of the skull base.

Communications with the vertebral venous plexus in the epidural space also exist via the basilar venous plexus on the clivus.

The major dural folds (Fig. 1-9A) are falk cerebri, tentorium cerebelli, cavum trigeminale and dia-phragma sella.

Additional content available at <https://expertconsult.inkling.com/>

The meningeal arteries lie within the inner (or periosteal) layer of dura with their accompanying veins (Fig. 1-9B) and are responsible for the many fine grooves that ramify over the inner surface of the cranium (see Fig. 1-8B and eFig. 1-1).

The largest and most important of these is the middle meningeal artery, which enters the skull through the foramen spinosum. These arteries supply the meninges and diploë (bone marrow of cranial bones), but they do not supply the brain.

**Arachnoid mater** (eFig. 1-2A). The arachnoid (Gk. spider) is a delicate fibrocellular layer beneath the dura (separated by potential subdural space) that is connected to the pia mater covering the brain by numerous fibrocellular bands that cross the cerebrospinal fluid-filled subarachnoid space. This arrangement has led some to consider the leptomeninges as a conjoined pia–arachnoid membrane. The arachnoid bridges over the sulci, gyri and other irregularities on the brain surface, thus creating the subarachnoid cisterns or enlargements in the subarachnoid space (Fig. 1-9B, inset, and eFig. 1-2A).

Specialized regions of arachnoid, the *arachnoid villi* and *granulations* (fibrous aggregations of villi), project into several of the dural venous sinuses (Fig. 1-9B) and act as one-way pressure-sensitive valves allowing cerebrospinal fluid to drain from the subarachnoid space into the dural venous sinuses. Structures passing to and from the brain to the skull or its foramina, such as cranial nerves, must traverse the subarachnoid space. In addition, all cerebral arteries and veins lie in this space (eFig. 1-2A).

Since the arachnoid fuses with the perineurium of cranial nerves, the cerebrospinal fluid-containing subarachnoid space extends for a short distance around all cranial nerves. In particular it surrounds the optic nerve in a cuff-like manner as far as the posterior surface of the eye.

### Falx Cerebri

A sickle-shaped fold with its attached border in the mid-sagittal plane from the crista galli to the tentorium cerebelli behind. It lies in the vertical fissure between the two cerebral hemispheres, its lower border lying above the corpus callosum. The superior sagittal sinus is situated in the attached border and the inferior sagittal sinus is in the lower free border of the falx cerebri.

**Tentorium Cerebelli.** This fold lies approximately in a horizontal plane at 90° to the falx, although it is elevated centrally (hence 'tent-like'). It separates the occipital lobe of each cerebral hemisphere above from the cerebellum in the posterior cranial fossa below. The free edge forms the boundary of the tentorial notch, which separates the forebrain from the hindbrain and 'houses' the midbrain. Sinuses related to the tentorium include the straight sinus, right and left transverse sinuses, superior petrosal sinuses and cavernous sinuses.

**Cavum Trigeminale.** A blind-ended dural recess whose entrance is in the posterior cranial fossa. It is formed by an invagination of the dura beneath the free edge of the tentorium and is roofed by dura on the floor of the middle cranial fossa. It houses the trigeminal ganglion, which sits

in a shallow hollow on the apex of the petrous temporal bone, and some accompanying vessels. The ganglion is surrounded by cerebrospinal fluid continuous with the subarachnoid space of the posterior cranial fossa.

**Diaphragma Sellae.** A small circular fold of dura over the sella turcica that is pierced centrally by the infundibulum (Fig. 1-9C). It blends laterally with the roof of the cavernous sinus (Fig. 1-9D).

The area above the tentorium is known as the supratentorial compartment; that below is the infratentorial compartment. The cranial dura of the supratentorial compartment is innervated by sensory branches of the trigeminal nerve, and stimulation of these nerves (stretching, inflammation, compression) gives rise to frontal or parietal headache. The infratentorial compartment is supplied by branches of the upper cervical nerves, and stimulation of these sensory nerves may therefore manifest as occipital and neck pain.

The neck rigidity accompanying acute meningitis of the infratentorial region is most likely the result of reflex contractions, or spasm, of posterior neck musculature in response to stretching of the inflamed cranial and spinal cord meninges.

### BOX 1-3 CLINICAL CORRELATES

#### ARTERIOVENOUS FISTULAS IN THE CAVERNOUS SINUS

These cause a variety of symptoms including pulsating protrusion of the globe and congestion of the vessels of the lids and conjunctiva owing to raised venous pressure. Patients complain of hearing noises resembling rushing water, probably because of increased flow rates in the labyrinthine plexus, which is in communication with the cavernous sinus via the superior petrosal sinus.

#### CAVERNOUS SINUS THROMBOSIS

Cavernous sinus thrombosis as a sequel to infection spreading to the sinus, from such diverse initial sites as the nose, lids, behind the ear, bony labyrinth, pharynx and temporomandibular joint, can give rise to a variety of symptoms explainable on the basis of structures affected in and around the sinus. Facial pain may be the result of the involvement of the ophthalmic nerve ( $V_1$ ). Lateral rectus paralysis may follow involvement of the abducent nerve. Involvement of the other oculomotor nerves is less common because they are more protected in the lateral wall of the sinus. Thrombosis is usually bilateral because of the communications via the intercavernous sinuses. Papilloedema may result from obstruction of central retinal venous return.

### BOX 1-4 CLINICAL CORRELATES

#### Extradural and subdural haematomas

Damage to middle meningeal vessels, especially the frontal branch of the middle meningeal artery and vein (the latter lying closest to the bone), may result from blows to the head, especially in the temporal region (the pterion; see Figs 1-2B, 1-5B, 1-8B) where the bones are thinnest and most likely to fracture. Slow venous, or more rapid arterial, bleeding will lead to an extradural (epidural) haematoma with a resultant rise in intracranial pressure. Coma and death will occur if such a haematoma is not drained as soon as possible after symptoms of raised intracranial pressure, including papilloedema, manifest. A subdural haematoma may occur if the trauma results in brain laceration or tearing of intradural veins.

process, although they may be part of the system necessary for focusing and transmitting the light on to the retina, for example cornea, lens, iris and ciliary body, or they may be necessary for nourishing and supporting the tissues of the eye, for example the choroid, aqueous outflow system and lacrimal apparatus.

#### GENERAL SHAPE, SIZE AND POSITION OF THE EYE

The eye is approximately a sphere 2.5 cm in diameter with a volume of 6.5 mL. However, in reality it is the parts of two spheres, a smaller one anteriorly, the cornea, that has a greater curvature than the sclera, which constitutes the large sphere. The cornea forms one-sixth of the circumference of the globe and has a radius of 7.8 mm; the remaining five-sixths is formed by the sclera, which has a radius of 11.5 mm. There is variation in size between individuals but the average axial length of the globe is 24 mm (range 21–26 mm). The diameter is 23 mm and the horizontal length approximately 23.5 mm. Small eyes (<20 mm) are hyperopic or hypermetropic, while large eyes (26–29 mm) are myopic. The eye is situated in the anterior portion of the orbit, closer to the lateral than the medial wall and nearer the roof than the floor. The eye is made up of three basic layers or coats, often known as tunics (Fig. 1-10). These are the fibrous (corneoscleral) coat, the uvea or uveal tract (composed of choroid, ciliary body and iris), and the neural layer (retina). The coats surround the contents, namely the lens and the transparent media (aqueous humour and vitreous body).



**Pia mater** (Fig. 1-9B and eFig. 1-2A). The pia mater, a vascular fibrocellular membrane that is thicker than the arachnoid, closely follows the contours of the brain. Vessels entering or leaving the brain parenchyma carry a pial sheath with them. Pial tissue is rich in astrocytes, which extend along the vessel walls and form an important component of the blood–brain barrier. The perivascular spaces surrounding these vessels, the so-called Virchow–Robin spaces, are potentially in communication with the cerebrospinal fluid of the subarachnoid space and may be dilated in pathological states.

### Structure of the eye

The eye (Fig. 1-10) is a highly specialized organ of photoreception, the process by which light energy from the environment produces changes in specialized nerve cells in the retina, the rods and cones. These changes result in nerve action potentials, which are subsequently relayed to the optic nerve and then to the brain, where the information is processed and consciously appreciated as vision. All the other structures in the eye are secondary to this basic physiological

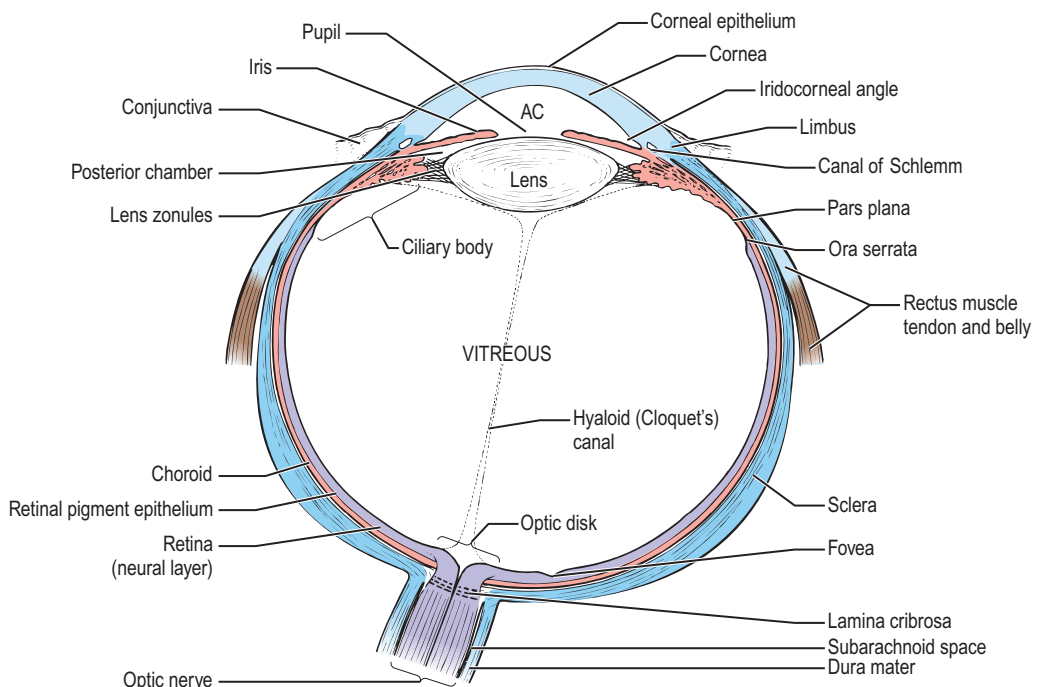


**FIGURE 1-10** Schematic diagram of the human eye in horizontal section revealing the major components and the arrangement of the three layers. AC, anterior chamber. The corneoscleral envelope (blue), the uveal tract (orange/red) and the inner neural layer (purple).

The cornea and sclera together form a tough fibrous envelope that protects the ocular tissues. The fibrous coat also provides important structural support for intraocular contents and for attachment of extraocular muscles. The cornea meets the sclera at a region known as the limbus or corneoscleral junction.

## THE CORNEA

The surface of the cornea (air–tissue interface) and associated tear film is responsible for most of the refraction of the eye. The transparency of the cornea is its most important property, although because of its highly exposed position it must also present a tough physical barrier to trauma and infection. Corneal transparency is the result of a number of related factors: its avascularity; the regularity and smoothness of the covering epithelium; and the regular arrangement of the extracellular and cellular components in the stroma, which is dependent on the state of hydration, metabolism and nutrition of the stromal elements.

### Shape

The cornea is smaller in the vertical (10.6 mm) than in the horizontal (11.7 mm) diameter; however, viewed

from behind, the circumference appears circular. The central radius is 7.8 mm with the peripheral corneal curvature being less marked. The cornea is also thicker at the periphery (0.67 mm) than in the centre (0.52 mm).

### Structure

The cornea is composed of five layers (Fig. 1-12A).

**Corneal epithelium (Fig. 1-12B).** The corneal epithelium is a stratified (possessing five or six layers) squamous non-keratinized epithelium (the superficial cells are flattened, nucleated and non-keratinized). It is 50–60 µm in thickness and adjacent cells are held together by numerous desmosomes and to the underlying basal lamina by hemidesmosomes and anchoring filaments (Fig. 1-12B). The anterior surface of the corneal epithelium is characterized by numerous microvilli and microplicae (ridges) whose glycocalyx coat interacts with, and helps stabilize, the precorneal tear film. New cells are derived from mitotic activity in the limbal basal cell layer (see p. 211) and these displace existing cells both superficially and centripetally. The corneal epithelium responds rapidly to

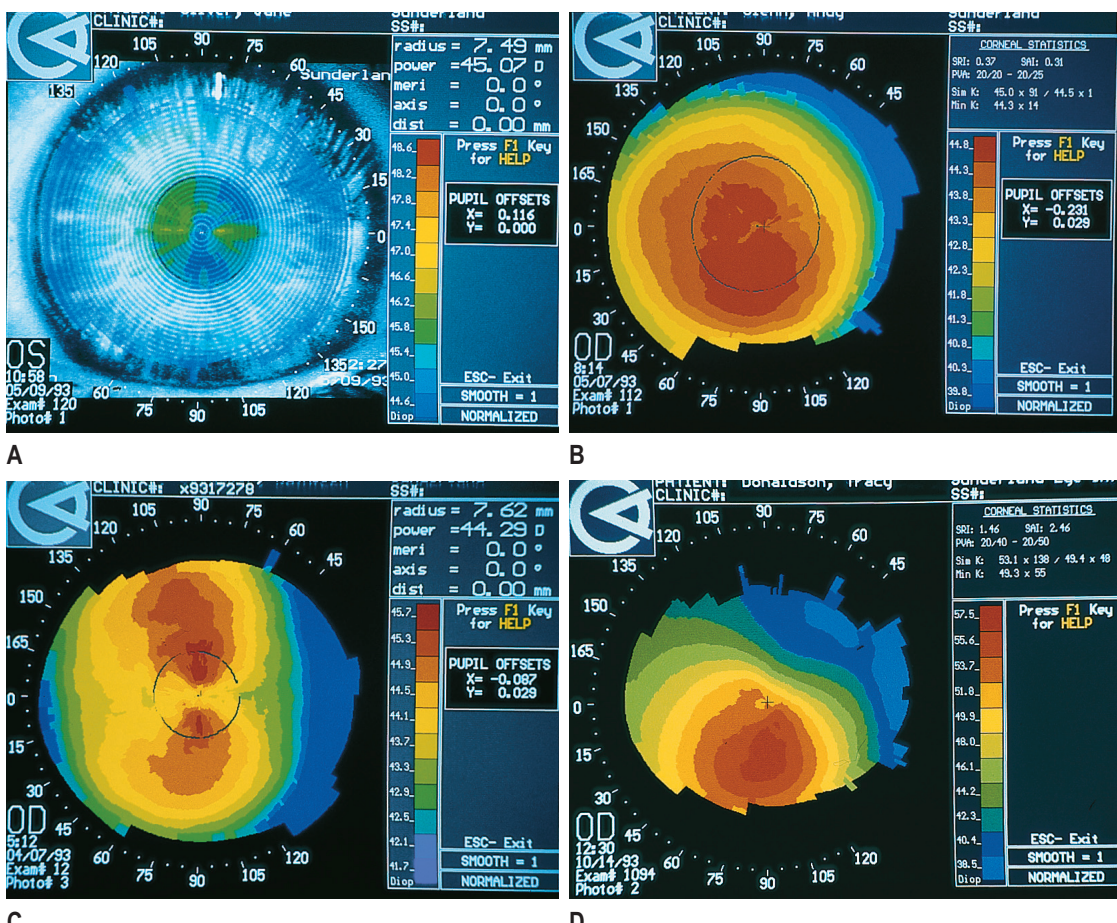
## BOX 1-5 CLINICAL CORRELATES

### ASTIGMATISM

Astigmatism is usually the result of differences in the radius of curvature in the vertical and horizontal meridians. Abnormalities in corneal curvature can be readily demonstrated by computerized video keratography, which applies the principle of projecting placido rings onto the corneal surface from which topographic maps can be constructed (Fig. 1-11).

repair disruptions in its integrity by amoeboid sliding movements of cells on the wound margin followed by cell replication.

The basal epithelial cells rest on a thin, but prominent, *basal lamina* (lamina lucida, 25 nm; lamina densa, 50 nm). Corneal epithelial adhesion is maintained by a basement membrane complex, which anchors the epithelium to Bowman's layer via a complex mesh of anchoring fibrils (type VII collagen) and anchoring plaques (type VI collagen), which interact



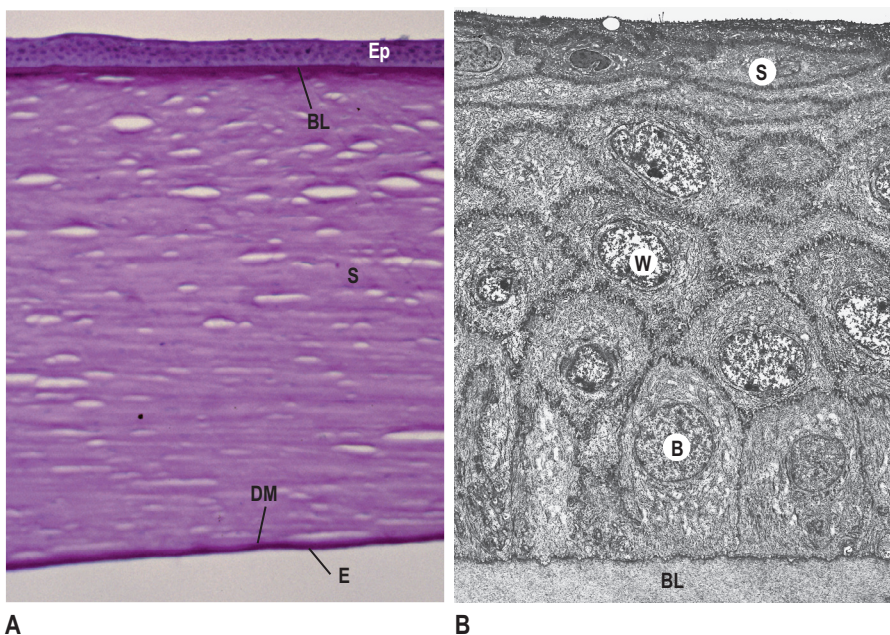


**FIGURE 1-12** Histology and ultrastructure of the cornea and its constituent layers. **(A)** Low-power light micrograph showing the five layers of the human cornea. Ep, epithelium; BL, Bowman's layer; S, substantia propria or stroma; DM, Descemet's membrane; E, endothelium. **(B)** Electron micrograph of the corneal epithelium. B, basal cell layer; W, wing cells; S, superficial cells; BL, Bowman's layer. Original magnifications: **A**,  $\times 80$ ; **B**,  $\times 3000$ . (Part B courtesy of W.R. Lee and D. Aitken.)

with the lamina densa and the collagen fibrils of Bowman's layer. The corneal epithelium is devoid of melanocytes. Myeloid-derived major histocompatibility complex (MHC) class II antigen-positive dendritic cells (Langerhans cells) are present in the limbus and peripheral cornea (Fig. 1-12), but decline sharply in density in a centripetal gradient, and are rare in the central cornea. However, MHC class II-negative dendritic cells have been identified in the mouse central cornea and recent *in vivo* confocal microscopy (IVCM) (Fig. 1-13) suggests that the normal human central corneal epithelium contains dendritic cells although their immunophenotype cannot be ascertained from IVCM. The comparative paucity of potential antigen-presenting cells, such as dendritic cells, and the avascular nature of the cornea are considered factors crucial to the success of corneal grafting (see Ch. 7).

**Anterior limiting lamina (Bowman's layer).** Bowman's layer (a modified acellular region of the stroma; 8–12  $\mu\text{m}$  thick) consists of fine, randomly arranged, collagen fibrils (20–30 nm diameter, types I, III, V and VI). The anterior surface is well delineated and is

separated from the epithelium by the thin basal lamina, while the posterior boundary merges with the stroma (Fig. 1-12A). Bowman's layer terminates abruptly at the limbus.

**Substantia propria or corneal stroma (Fig. 1-14 A–C).** The corneal stroma is a dense connective tissue of remarkable regularity. It makes up the vast majority of the cornea and consists predominantly of 2  $\mu\text{m}$  thick, flattened, collagenous lamellae (200–250 layers) oriented parallel to the corneal surface and continuous with the sclera at the limbus. Between the lamellae lie extremely flattened, modified fibroblasts known as keratocytes. These cells are stellate in shape with thin cytoplasmic extensions containing conspicuously few distinctive organelles (Fig. 1-14A–C) when viewed in conventional cross-sections. However, frontal sections reveal an abundance of organelles and a novel network of fenestrations on their surface which may facilitate the diffusion of metabolites or the mechanical 'anchoring' or attachment of collagen bundles (Fig. 1-14A). The density of keratocytes in the anterior stroma is 20 000–24 000 cells/ $\text{mm}^2$  and that density decreases

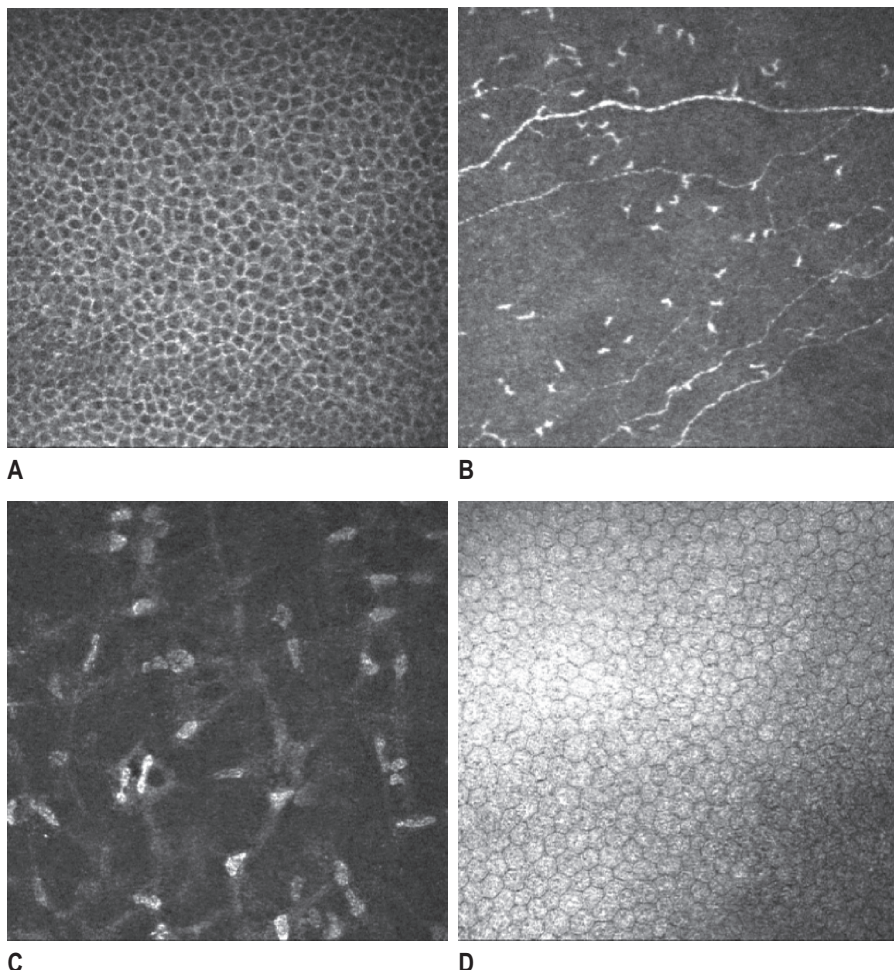


**FIGURE 1-13** *In vivo* confocal microscopy (IVCM) of the human cornea is a powerful non-invasive instrument used in the clinical evaluation of corneal abnormalities and normal structure of the tear film, cornea and conjunctiva. IVCM images are obtained by performing 'optical sections' of the cornea using non-coherent white light. Cells and matrix components with differing reflective properties within the transparent cornea can be imaged. The advantage of a 'confocal' approach is that only information in a narrow focal plane, approximately 4–25 µm in thickness, is analysed or collected by the microscope and scattering of light from structures outside the focal plane is thus minimized. The optics allow the light beam to be scanned (in the x and y axes) in a narrow area at one focal plane before shifting in depth to another plane of 'focus' (z axis) where the scan is repeated. Thus a series of optical 'slices' of high lateral resolution (1–2 µm) can be obtained from the entire cornea and, because of small differences in brightness/contrast, cellular detail can be visualized. This provides information that is normally the realm of conventional light microscopic and *ex vivo* laser scanning fluorescence confocal microscopic studies of processed tissues and whole mounts. The images are 'slices' at differing depths in the cornea from superficial to deep: (A) epithelium; (B) sub-basal nerve plexus and dendriform cells, which may represent Langerhans cells; (C) keratocytes in the posterior stroma; (D) corneal endothelial cells. (Images courtesy of Prof. C. McGhee.)

posteriorly before increasing again near Descemet's membrane (Fig. 1-13C). Keratocytes are connected by gap junctions to their neighbouring cells and arranged in a corkscrew pattern spiralling from the epithelium to the endothelium. The collagenous lamellae form a highly organized orthogonal ply, adjacent lamellae

being oriented at right angles, with the exception of the anterior third in which the lamellae display a more oblique orientation. The collagen fibres (Fig. 1-14C, inset) are predominantly of type I (30 nm diameter, 64–70 nm banding) with some type III, V and VI also present. The transparency of the cornea is highly

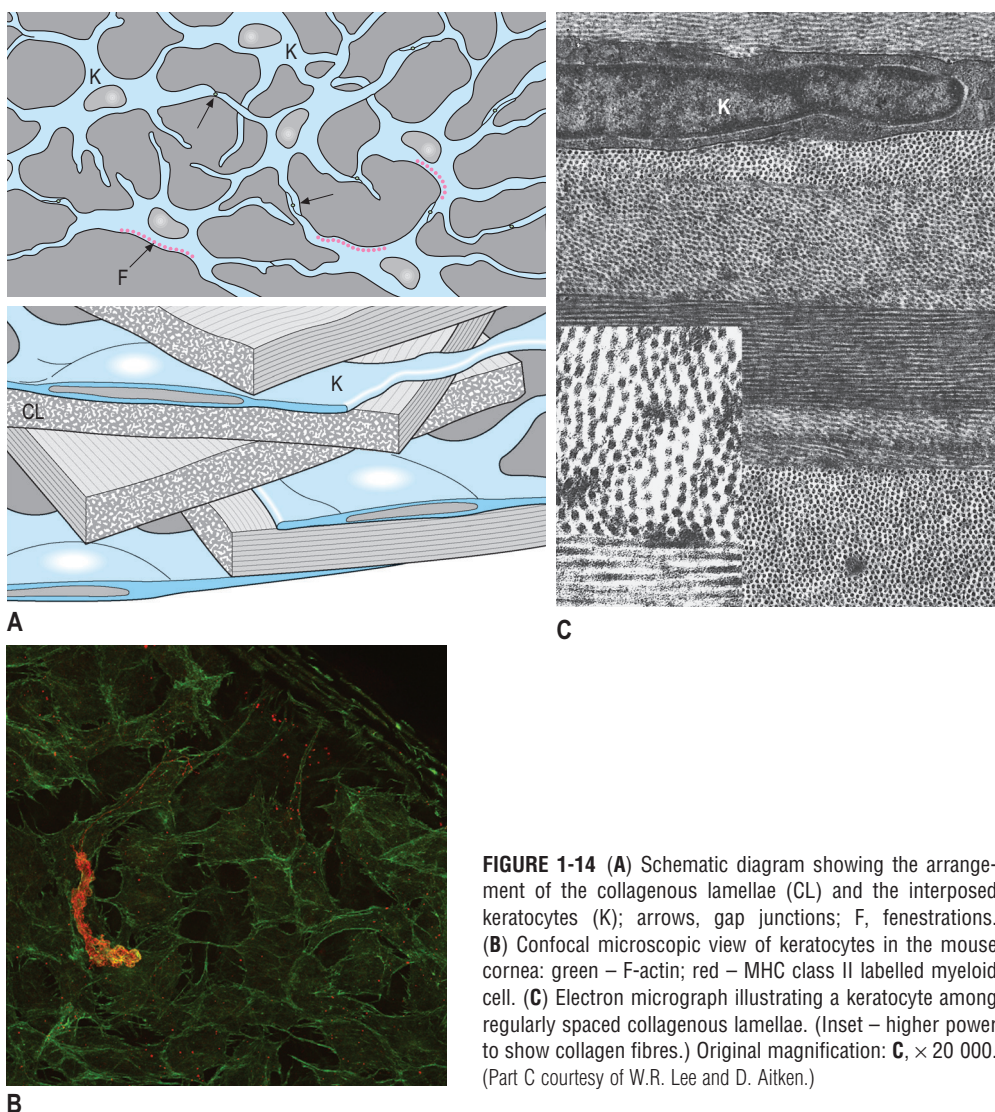


**FIGURE 1-14** (A) Schematic diagram showing the arrangement of the collagenous lamellae (CL) and the interposed keratocytes (K); arrows, gap junctions; F, fenestrations. (B) Confocal microscopic view of keratocytes in the mouse cornea: green – F-actin; red – MHC class II labelled myeloid cell. (C) Electron micrograph illustrating a keratocyte among regularly spaced collagenous lamellae. (Inset – higher power to show collagen fibres.) Original magnification: C,  $\times 20\,000$ . (Part C courtesy of W.R. Lee and D. Aitken.)

dependent on the regular diameter (influenced by the presence of type V collagen in particular) and spacing of the collagen fibres (interfibrillary distance), which in turn is regulated by glycosaminoglycans (GAG) and proteoglycans forming bridges between the collagen fibrils. The GAGs in the human cornea are predominantly keratan sulphate and chondroitin (dermatan) sulphates (see Ch. 4). The corneal stroma normally contains no blood or lymphatic vessels, but sensory nerve fibres are present in the anterior layers en route to the epithelium (see below and Fig. 1.13). Studies

using transgenic mice in which eGFP (enhanced green fluorescent protein) is expressed on all CX<sub>3</sub>CR1 positive monocyte derived cells has revealed extensive populations of resident tissue macrophages throughout the corneal stroma, some of which have recently described membrane nanotube cell–cell communications (Fig. 1-15).

**Posterior limiting lamina (Deszemet's membrane)** (**Figs 1-12A and 1-16A**). This is a thin, homogeneous, discrete, periodic acid–Schiff-positive layer

between the posterior stroma and the endothelium, from which it can become detached. It is 8–12 µm in thickness and represents the modified basement membrane of the corneal endothelium. It consists of two parts, an anterior third that is banded and a homogeneous or non-banded posterior two-thirds. It is rich in basement membrane glycoproteins, laminin and type IV collagen. The anterior banded region is reported to contain type VIII collagen. Types V and VI collagen may be involved in maintaining adherence at the interface of Deszemet's membrane with the most posterior lamellae of the stroma. Deszemet's membrane is continuous peripherally with the cortical zone of the trabeculae in the trabecular meshwork. Microscopic wart-like protuberances (Hassall–Henle bodies) containing 'long banded' (100 nm) deposits of unknown nature appear in the periphery of Deszemet's membrane with age. It is frequently thickened at its peripheral termination (Schwalbe's line, the anterior limit of the trabecular meshwork). If disrupted, Deszemet's membrane tends to curl inwards towards the anterior chamber.

**Corneal endothelium.** The corneal endothelium, a simple squamous epithelium on the posterior surface of the cornea, has a critical role in maintaining corneal hydration and thus transparency.

Fluid is constantly being lost via evaporation at the ocular surface, a fact illustrated by increased corneal thickness after a night of lid closure and when an impermeable lens is placed over the epithelium. The endothelial cells rest on Deszemet's membrane (Fig. 1-16A) and form an uninterrupted polygonal or hexagonal array, or mosaic (Fig. 1-16B), which can be clearly seen *in vivo* with the aid of specular microscopy and *in vivo* confocal microscopy (Fig. 1-13). The cells are 5–6 µm in height and 18–20 µm in diameter. Their lateral surfaces are highly interdigitated and possess apical junctional complexes that, together with abundant cytoplasmic organelles including mitochondria (Fig. 1-16A), are indicative of their crucial role in active fluid transport.

In the normal human cornea endothelial cells are generally considered to have low regenerative capacity and lost cells are quickly replaced by spreading of adjacent cells. However, there is some evidence that putative endothelial stem cells are located in

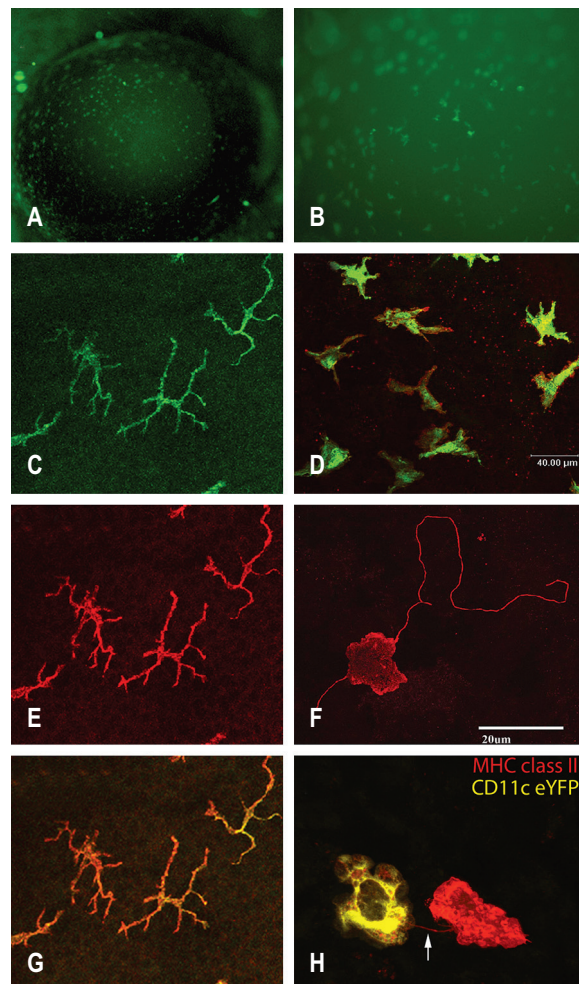


**FIGURE 1-15** (A, B) Low- and high-power *in vivo* fluorescent microscopy of the cornea of a normal CX3CR1-GFP transgenic mouse in which all myeloid cells (macrophages and dendritic cells) are labelled with green fluorescent protein (GFP). Note the regular array of corneal stromal macrophages. (C–H), Confocal microscopy of immune cells in the normal cornea. C, E, G is the same field of corneal epithelium from a corneal flatmount from a CX3CR1-GFP mouse: C – GFP (green); E – MHC class II (red); and G – combined image. D, CD11b<sup>+</sup> (red) stromal macrophages in the same mouse cornea. F – MHC class II<sup>+</sup> putative dendritic cell [DC] (see Ch. 7 for details of DC function) with a membrane nanotube extending from the cytoplasm. H, Putative DC joined to a MHC class II<sup>+</sup> macrophage.

centripetally arranged 'niches' or columns in the extreme peripheral cornea. Damage to corneal endothelial cells and density below 800 cells/mm<sup>2</sup> leads rapidly to oedema and swelling of the stroma, with resultant loss of transparency (see Ch. 4, p. 213).

### BOX 1-6 AGEING CHANGES

There are approximately 350 000 endothelial cells per cornea (3000–4000 cells/mm<sup>2</sup> at birth, falling to 2500 cells/mm<sup>2</sup> in middle age and 2000 cells/mm<sup>2</sup> in old age). Consequently, with age, the dense, regular hexagonal arrangement typical of the young cornea is replaced by fewer cells of more heterogeneous size and shape.

A density lower than 1500 cells/mm<sup>2</sup> in a potential donor cornea is considered unsuitable for transplantation.

### Nerve supply of the cornea

The cornea is richly supplied by sensory fibres derived from the ophthalmic division of the trigeminal nerve, mainly via the long ciliary nerves. Occasionally the inferior cornea receives some branches from the maxillary division of the trigeminal. Nerve bundles enter the peripheral cornea in a radial manner and as they travel centrally below the anterior one-third of the stroma and approximately 1 mm from the limbus they lose their perineurium and myelin sheaths. This alteration in myelination is thought to be related to the importance for transparency. They divide into smaller branches and begin to change direction towards the epithelium where they must pierce Bowman's layer, whereupon they further divide into smaller bundles to form the subepithelial or subbasal plexus in the interface between Bowman's layer and the basal aspect of the corneal epithelium. There are apparently no specialized end organs associated with these terminal axons, which are predominantly within the size range 0.1–0.5 µm consistent with A-delta and C fibres that function to transmit the sensory modalities of pain and temperature. Individual beaded fibres penetrate the epithelial layers and terminate in the superficial layers in the form of an intraepithelial plexus. There are approximately 7000 nociceptors per mm<sup>2</sup> in the human corneal epithelium.

### THE SCLERA

The sclera (Fig. 1-17A-D) forms the principal part of the outer fibrous coat of the eye and functions both to protect the intraocular contents and to maintain the shape of the globe when distended by intrinsic intraocular pressure. The globe shape is maintained

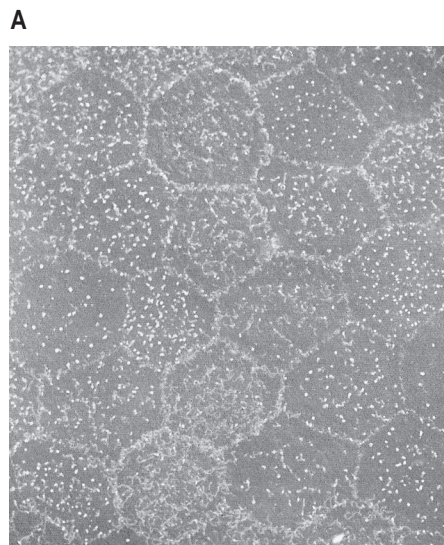
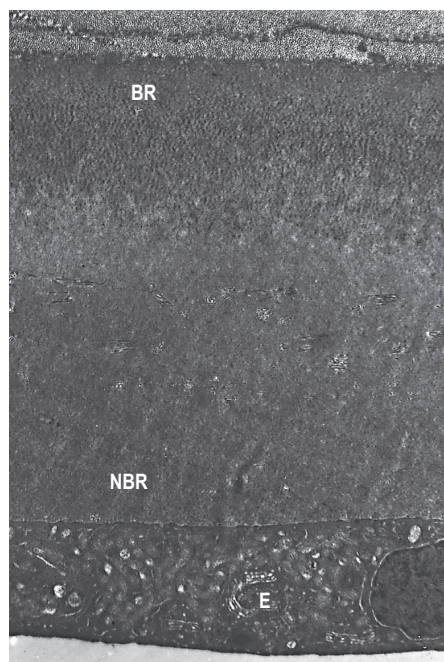


**FIGURE 1-16** (A) Electron micrograph of Deszemet's membrane and corneal endothelium (E) to illustrate the banded region (BR) and non-banded region (NBR). (B) An *en face* view of the inner surface of the corneal endothelium as seen by scanning electron microscopy. Note the homogeneous hexagonal array of endothelial cells. A similar but less detailed view of the endothelium can be achieved in the living patient with the aid of specular microscopy. Original magnifications: A,  $\times 7000$ ; B,  $\times 1200$ . (Courtesy of W.R. Lee and D. Aitken; Part A courtesy of Springer-Verlag.)

## BOX 1-7 CLINICAL CORRELATES

Larger myelinated nerve fibres can often be seen during slit-lamp examination as fine whitish fibres radiating into the cornea from the limbus. *In vivo confocal microscopy* has greatly added to our understanding of the distribution of corneal nerves in healthy and diseased corneas (see Fig. 1-13). Due to their position in the anterior stroma and their radial arrangement, many are damaged during refractive procedures such as LASIK (Excimer laser *in situ* keratomileusis). Damage to the corneal epithelium and intraepithelial nerve terminals can cause a great deal of pain.

Reactivation of latent herpes simplex virus in the trigeminal ganglion occurs following damage to nerve terminals (cold, exposure to ultraviolet light, trauma, corticosteroids), and activated virus is transmitted to the cornea along sensory nerve branches, leading to recurrent herpes simplex keratitis and superficial corneal ulceration.

even during contraction of the extraocular muscles, whose tendons insert on its surface. The sclera is relatively avascular and in adults appears white externally. The viscoelastic nature of the sclera (great tensile strength, extensibility and flexibility) allows only limited distension and contraction to accommodate minor variations in intraocular pressure.

The sclera is thickest posteriorly (1 mm) and thinnest (0.3–0.4 mm) behind the insertions of the aponeurotic tendons of the extraocular muscles. It is covered by the *fascia bulbi* posteriorly and the conjunctiva anteriorly. The sclera consists of dense irregular connective tissue comprising extracellular matrix and matrix-secreting fibroblasts. The matrix consists principally of collagen type I, although types III, IV, V, VI, VIII, XII and XIII have been identified (Rada et al., 2006). Unlike the cornea, the scleral collagenous lamellae are irregularly arranged (Fig. 1-17D) and are interspersed with elastic fibres, each consisting of an elastin core surrounded by longitudinally arranged microfibrils composed of a number of glycoproteins including fibrillin. The opaque nature of the sclera, in contrast to the transparency of the cornea, can be partly ascribed to this irregular arrangement of the collagen fibres (Fig. 1-17D), but also to the variable fibre diameter (25–250 nm), variable and irregular fibrillar spacing, higher water content, and the reduced coating of GAGs on collagen fibres. Indeed, the sclera contains one-quarter of the proteoglycan and GAG content of the cornea. Dermatan sulphate and

## BOX 1-8 CLINICAL CORRELATES

### Buphtalmos

The corneoscleral envelope of children with congenital glaucoma responds to raised intraocular pressure by irreversibly stretching, owing to the immaturity of the collagen fibres, thus producing the characteristically enlarged buphtalmos ('ox-eye') of this condition.

## BOX 1-9 CLINICAL CORRELATES

The yellowing of the eyeball in jaundice is the result of bilirubin deposition in the conjunctiva and not the sclera. Abnormal thinning of the sclera, such as occurs in some connective tissue disorders, e.g. Ehlers–Danlos syndrome, may also lead to a blue tinge. Localized thinning of the stromal collagenous layers may lead to staphyloma (bulging).

chondroitin sulphate proteoglycans are the most abundant in the sclera.

Collagen fibrils take up tensile force and are aligned with the direction of greatest tensile strength. The arrangements of scleral collagen can be studied using the 'split-line' technique, which has revealed that the collagen fibrils in the outer sclera are arranged in bundles that course in whorls, loops and arches, particularly around the muscle insertions and optic nerve (Fig. 1-17C). The collagen fibrils on the internal aspect of the sclera are arranged in a rhombic pattern (Fig. 1-17D).

The sclera extends anteriorly from the limbus to the lamina cribrosa posteriorly (Fig. 1-17A and Fig. 1-42). The scleral collagen fibrils are arranged in circles or figure-of-eight patterns at the lamina cribrosa. Structures that transverse the sclera are shown in Figure 1-17A. Histologically the sclera has three layers: the lamina fusca, stroma and episclera (Fig. 1-17B).

## LIMBUS AND AQUEOUS OUTFLOW PATHWAYS (Fig. 1-18)

It is becoming increasingly appreciated that the limbus (Fig. 1-18A–C) is more than the border zone between the cornea and sclera; it has multiple functions including nourishment of the peripheral cornea, corneal wound healing, immunosurveillance of the ocular surface and hypersensitivity responses; it contains the pathways of aqueous humour outflow and is thus involved in the control of intraocular pressure.

Surgical incisions to access the anterior chamber for cataract and glaucoma surgery are made at the limbus. The limbus is 1.5–2.0 mm in width and the change in the radius of curvature between the sclera and cornea produces a shallow *external scleral sulcus* and an *internal scleral sulcus*; the latter is deepened by the *scleral spur* and houses the canal of Schlemm and trabecular meshwork. The longitudinal ciliary muscle fibres attach to the posterior aspect of the *scleral spur*, and its anterior surface gives rise to the corneoscleral trabeculae.

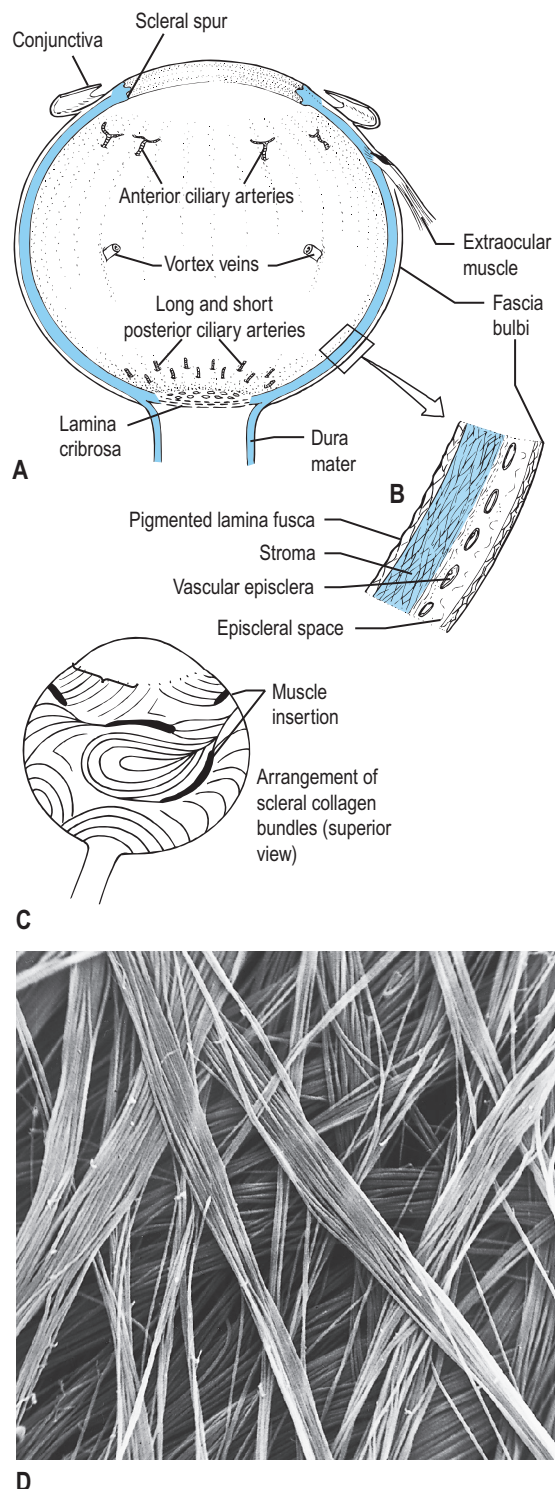
Several important transitions take place at the limbus (Fig. 1-18A–C).

- The regularly arranged corneal lamellae give way to the more random array of lamellae in the sclera. The corneal termination is V-shaped (Fig. 1-18B,C).
- The stratified squamous non-keratinized corneal epithelium with its parallel internal and external surfaces gives way to conjunctival epithelium, characterized by a folded basal surface and interdigitating subepithelial connective tissue (sometimes forming distinct papillae) (Fig. 1-18B).
- The conjunctival epithelium contains goblet cells and a rich network of MHC class II<sup>+</sup> CD11c<sup>+</sup> dendritic (Langerhans) cells (see section on conjunctiva, p. 83).
- Loops or arcades of conjunctival capillaries (derived from the anterior ciliary arteries) and lymphatic capillaries terminate at the limbus. The smaller vessels are not under neuronal control and are particularly susceptible to the

#### BOX 1-10 AGEING CHANGES

The ‘blue’ sclera of infants is the result of the underlying choroidal pigment showing through the thin collagenous stroma. In elderly individuals, fat deposition in the sclera may produce a yellowish hue.

**FIGURE 1-17** (A) Schematic diagram of the isolated sclera and structures that blend with it (muscle tendons and optic nerve dura) or traverse its substance. (B) The scleral layers. (C) The pattern of orientation of the collagen bundles in the scleral stroma in relation to the extraocular muscle tendinous insertions. (D) Collagen bundles in sclera. Original magnification: D,  $\times 7000$  (Part D courtesy of Dr A. Thale and Tillmann, 1993.)



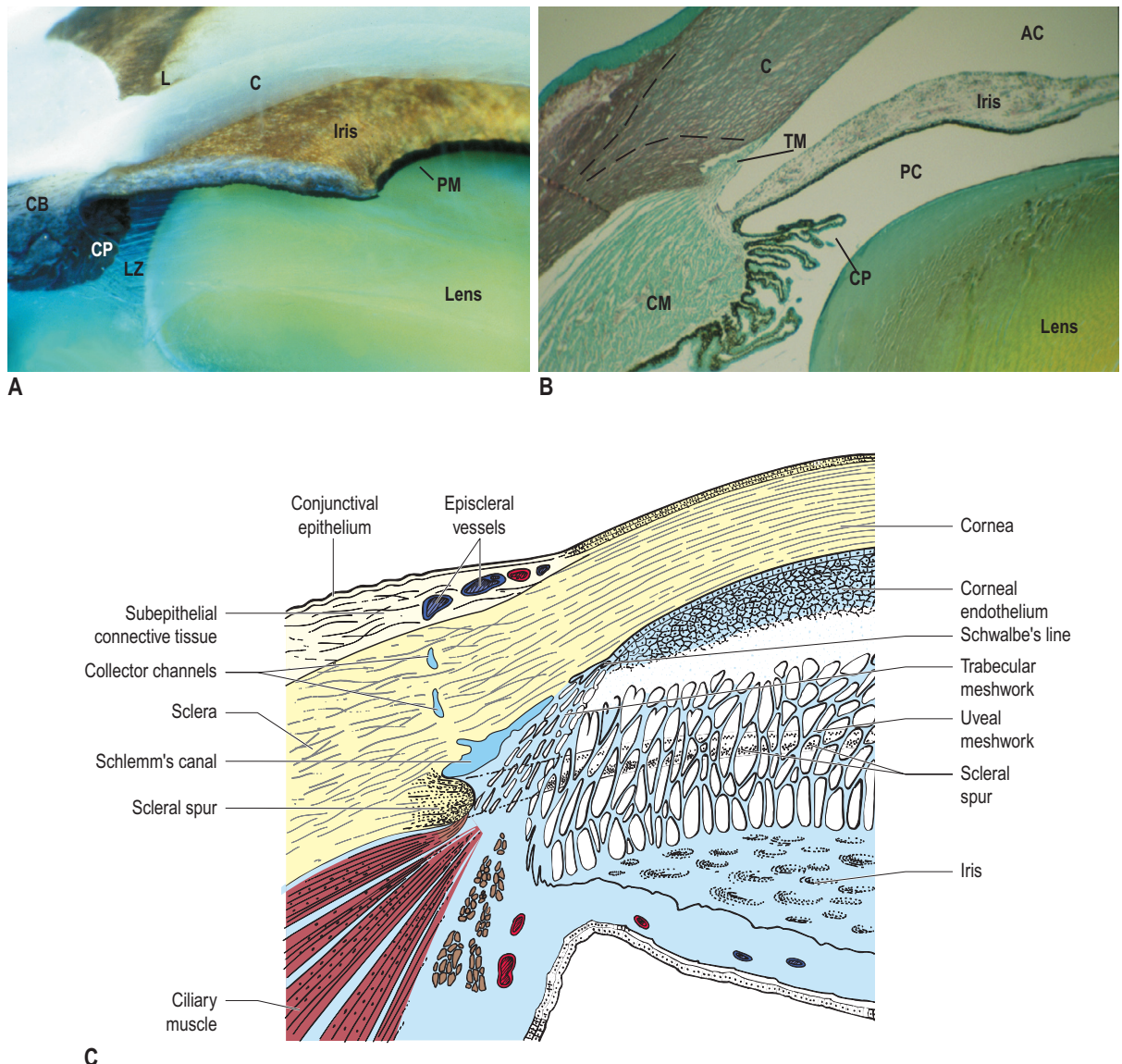


**FIGURE 1-18** (A) Macroscopic photograph of the anterior segment of a primate eye, which is almost identical to the human eye. Note the heavily pigmented limbus (L) characteristic of primates: C, cornea; CB, ciliary body; CP, ciliary processes; LZ, lens zonules; PM, pupillary margin. (B) Histology section of the primate anterior segment (Van Gieson stain). Dotted line indicates the corneoscleral junction: AC, anterior chamber; CM, ciliary muscle; PC, posterior chamber; C, cornea; CP, ciliary processes. (C) Three-dimensional schematic diagram of important features in and around the iridocorneal angle and corneoscleral limbus. Original magnifications: A and B,  $\times 50$ .

effects of vasoactive amines (e.g. histamine, leukotrienes, prostaglandins) released by local immune cells (see below).

- Descemet's membrane and Bowman's layer terminate in this region.

- The loose conjunctival subepithelial vascularized connective tissue (substantia propria), containing immunocompetent cell types such as mast cells, plasma cells and lymphocytes, tapers off at the limbus and is absent in the cornea (Fig. 1-18B).

## BOX 1-11 DEFINITIONS

### Anatomical and surgical limbus

Definitions of the limits and markings of the limbus vary among anatomists, pathologists and surgeons. The anatomical (histological) limbus is defined by a line that follows the V-shaped transition of corneal lamellae to scleral lamellae (Fig. 1-18B). Pathologists define the limbus as a block of tissue bordered anteriorly by a line passing through the termination of Schwalbe's line and the junction of the conjunctival and corneal epithelium (corneolimbal junction), and posteriorly by a line from the scleral spur perpendicular to the tangent of the external surface. Surgeons usually cut close to the blue-grey transition zone seen on external examination, and incisions made here will pass anterior to the trabecular meshwork and Schlemm's canal (Fig. 1-18B,C).

### Aqueous outflow pathways

In the chamber or iridocorneal angle, partially nestled in the internal scleral sulcus, lies a complex wedge-shaped circumferential band of specialized, sponge-like, connective tissue, the *trabecular meshwork*, with the *canal of Schlemm* (*sinus venosus sclerae*) on its outer aspect (Figs 1-18B,C and 1-19A). The base of the trabecular meshwork is formed posteriorly by the scleral spur, the anterior face of the ciliary muscle and the iris root. The apex of the meshwork terminates anteriorly at Schwalbe's line and the adjacent innermost corneal lamellae (Figs 1-18 and 1-19A). The trabecular meshwork can be further subdivided into three anatomical zones: the innermost *uveal meshwork* with cord-like trabeculae; the *corneoscleral meshwork* with flattened sheet-like trabeculae (Fig. 1-19D); and the outermost *cirriform meshwork* beneath the inner wall of Schlemm's canal (Fig. 1-19E). The cirriform meshwork, unlike the rest of the trabecular meshwork, is not arranged in lamellae but consists of trabecular cells enmeshed in a loose extracellular matrix of collagen (types I, III and IV), elastic-like fibres and proteoglycans. This layer is thought to be the main site of resistance to aqueous outflow. The elastic cores of the trabeculae are continuous with the elastic fibres in the cirriform meshwork, which are in turn connected to the inner wall of Schlemm's canal via 'connecting fibres'. The anterior ciliary muscle fibres terminate in the elastic cores of the trabeculae. As the ciliary muscle contracts and moves inwards, the

three-dimensional trabecular meshwork can be expanded, which results in an increase in the amount of 'free' spaces in the cribriform meshwork. This in turn allows greater aqueous outflow, thus increasing aqueous outflow facility.

Aqueous humour passes from the anterior chamber through the *intertrabecular* and *intratrabecular spaces*, which are lined by trabecular cells. These cells envelop the trabeculae (Fig. 1-19D) and maintain the state of hydration of the connective tissue core in a similar manner to corneal endothelium. In addition, trabecular cells are also phagocytic, trapping and removing debris from the aqueous humour as it percolates through the tortuous intertrabecular and intratrabecular spaces which narrow as Schlemm's canal is approached (Figs 1-18C and 1-19A).

Schlemm's canal (*sinus venosus sclerae*) is an endothelium-lined 36 mm long circumferential channel filled with aqueous humour. It measures 200–400 µm in the anteroposterior axis, is seldom more than 50–60 µm deep and is often septate. The canal is drained by 25–35 *collector channels* (20–90 µm in diameter) and between two and eight *aqueous veins* (of Ascher) (up to 100 µm in diameter). These either join deep, intrascleral and episcleral venous plexuses which drain into conjunctival veins or, in the case of aqueous veins, may drain directly into superficial conjunctival veins. The majority of aqueous humour (70–90%) leaves the anterior chamber through the trabecular meshwork and Schlemm's canal ('conventional' outflow pathways). The inner wall of the canal is characterized, in well-preserved and properly fixed eyes, by transcellular channels or giant vacuoles (Fig. 1-19B,C). There is good evidence to suggest that these intracellular vacuoles, with openings on both the trabecular and luminal aspects, function to drain the great bulk of aqueous humour. The number and size of vacuoles and their openings or pores vary in a pressure-sensitive manner. Small quantities of aqueous may also pass between endothelial cells in the canal wall.

A proportion (10–30%) of aqueous humour drains via the 'non-conventional' aqueous outflow pathways. This route is not pressure sensitive and consists of the intercellular spaces between ciliary muscle fibres and the loose connective tissue of the suprachoroidal space. From here, aqueous traverses the sclera via the

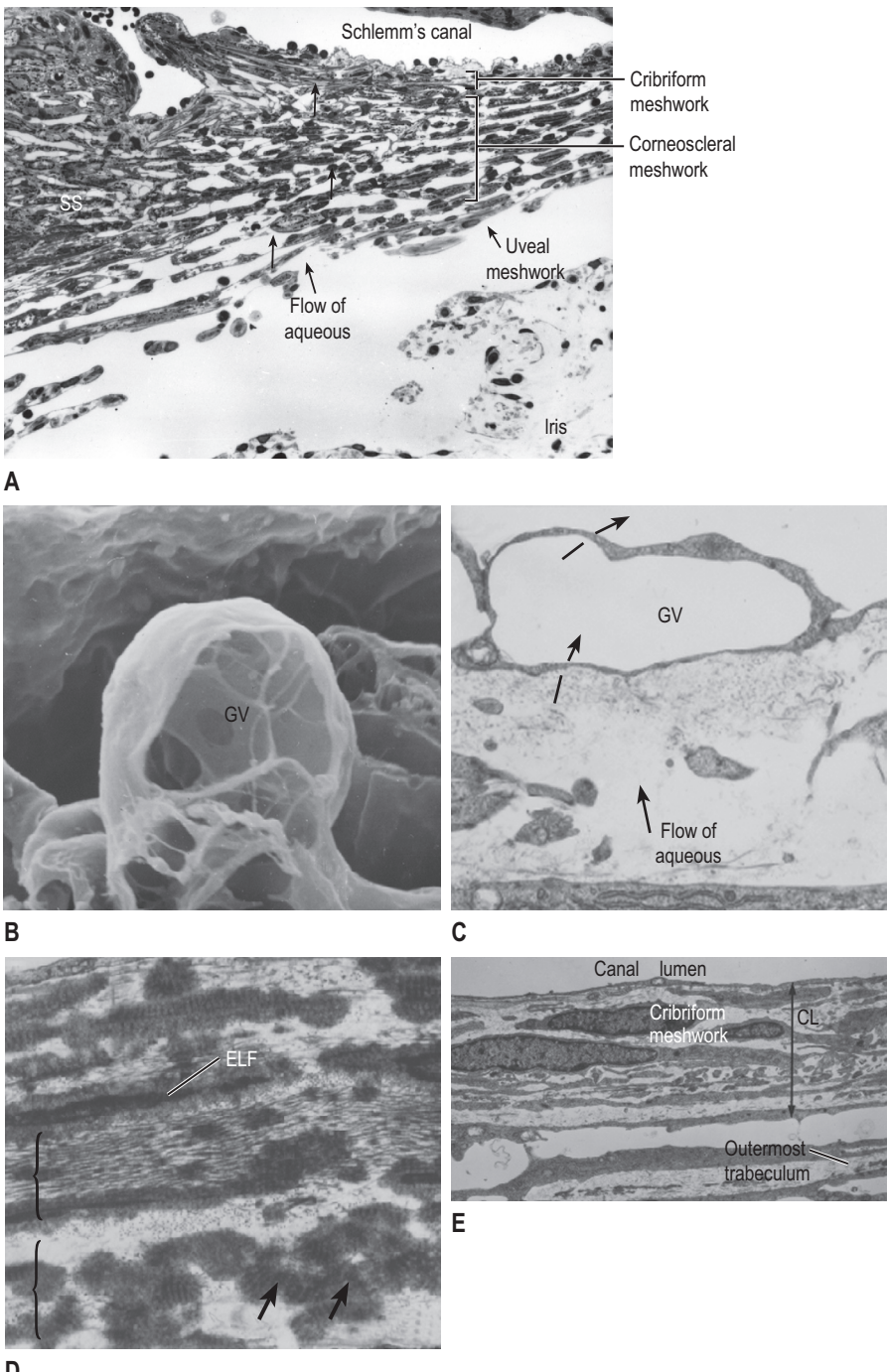


**FIGURE 1-19** Histology and ultrastructure of the trabecular meshwork and Schlemm's canal. **(A)** Light micrograph showing the scleral spur (SS), Schlemm's canal and the three zones of the meshwork: the uveal, corneoscleral and cribriform meshworks. The path of aqueous through the inter- and intratrabecular spaces is indicated by arrows. **(B)** 'Giant vacuole' (GV) in the inner wall of Schlemm's canal as seen by scanning electron microscopy. **(C)** Transmission electron micrograph of a 'giant vacuole'. The flow of aqueous is indicated by the arrows. This particular section does not include the basal or luminal pores seen in some 'giant vacuoles'. **(D)** Electron micrograph of a trabecula cut in cross-section showing the layered arrangement of the extracellular components: CZ, cortical zone; ELF, elastic-like fibres; arrows, 'long spacing collagen'. **(E)** High-power micrograph of the cribriform meshwork or layer showing the lack of trabecular organization. Fibrocyte-like cells are loosely arranged in various types of extracellular matrix. Original magnifications: **A**,  $\times 340$ , **B** and **C**,  $\times 7000$ , **D**,  $\times 13\,000$ , **E**,  $\times 5000$ . (From McMenamin, Lee and Aitken, 1986, *Ophthalmology*, with permission.)

connective tissue sheaths of nerves and vessels that pierce its substance (see Fig. 1-17A).

### Uveal tract or uvea

The uveal tract (L. *uva* = grape), the middle vascular pigmented layer of the eye, consists of the *iris*, *ciliary body* and *choroid* (see Fig. 1-10). These three components are continuous with one another and have an opening anteriorly, the *pupil*, and posteriorly the choroid is deficient at the *optic nerve canal*. The uveal tract is analogous to the vascular pia-arachnoid of the brain and optic nerve, with which it anastomoses at the optic nerve head. The choroid is described on p. 55; the iris and ciliary body are described below.

## THE IRIS

The iris (Fig. 1-20A,B) is a thin, heavily pigmented, contractile circular disk analogous to the diaphragm of a camera. It is suspended in the frontal or coronal plane anterior to the lens and ciliary body, and is surrounded by aqueous humour. The iris separates the

### BOX 1-12 CLINICAL CORRELATES

#### GLAUCOMA

Glaucoma is defined as a progressive optic nerve neuropathy. For most forms of glaucoma, elevated intraocular pressure and ageing remain important risk factors, although low tension or normal tension forms of glaucoma are common. However, in many forms of this condition pathological changes in the trabecular meshwork and Schlemm's canal may be responsible for increased resistance to aqueous outflow and raised, or diurnal fluctuations in, intraocular pressure (IOP). In *congenital glaucoma* there is malformation of the complex three-dimensional arrangement of the trabeculae and excess extracellular matrix in the outer meshwork. Physical blockage of the inner surface of the chamber angle by the iris occurs in *closed-angle glaucoma*; this may be a primary or a secondary process (see p. 512). Various forms of obstruction in the trabecular meshwork may give rise to *open-angle glaucoma* (see p. 512); the cause of the primary form of this condition is unknown, although there is evidence to indicate that excessive deposition of extracellular elements may occur in the cribiform meshwork. Secondary forms of open-angle glaucoma may be the result of debris such as lens proteins, melanin, macrophages and haemorrhagic products physically obstructing the intertrabecular and intratrabecular spaces, thus causing raised IOP (see p. 512).

anterior and posterior chambers, which are in continuity through an opening, the *pupil*, which lies slightly inferonasal to the centre of the iris. The iris is attached by its *root* at the angle (iridocorneal) of the anterior chamber where it merges with the ciliary body and trabecular meshwork. The free edge is known as the *pupillary margin*.

The iris is 12 mm in diameter with a circumference of 37 mm. It is cone-shaped with the pupil margin positioned more anteriorly than the root. The pupil margin rests on the lens, without whose support, for example in aphakic patients, it becomes tremulous (iridonesis). The size of the pupil regulates the amount of light entering the eye and is dependent on the state of contraction of the intrinsic pupillary muscles, the *dilator* and *sphincter pupillae*. The pupil may vary from 1 to 8 mm in diameter and there may be a slight degree of asymmetry between right and left eyes in normal individuals.

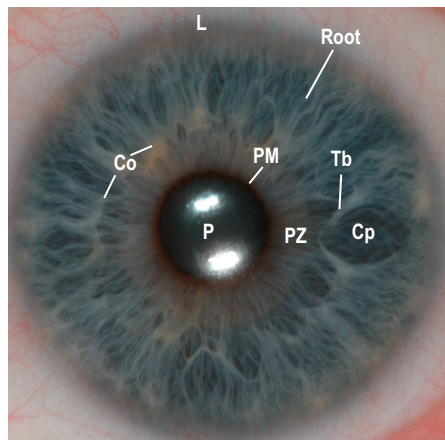
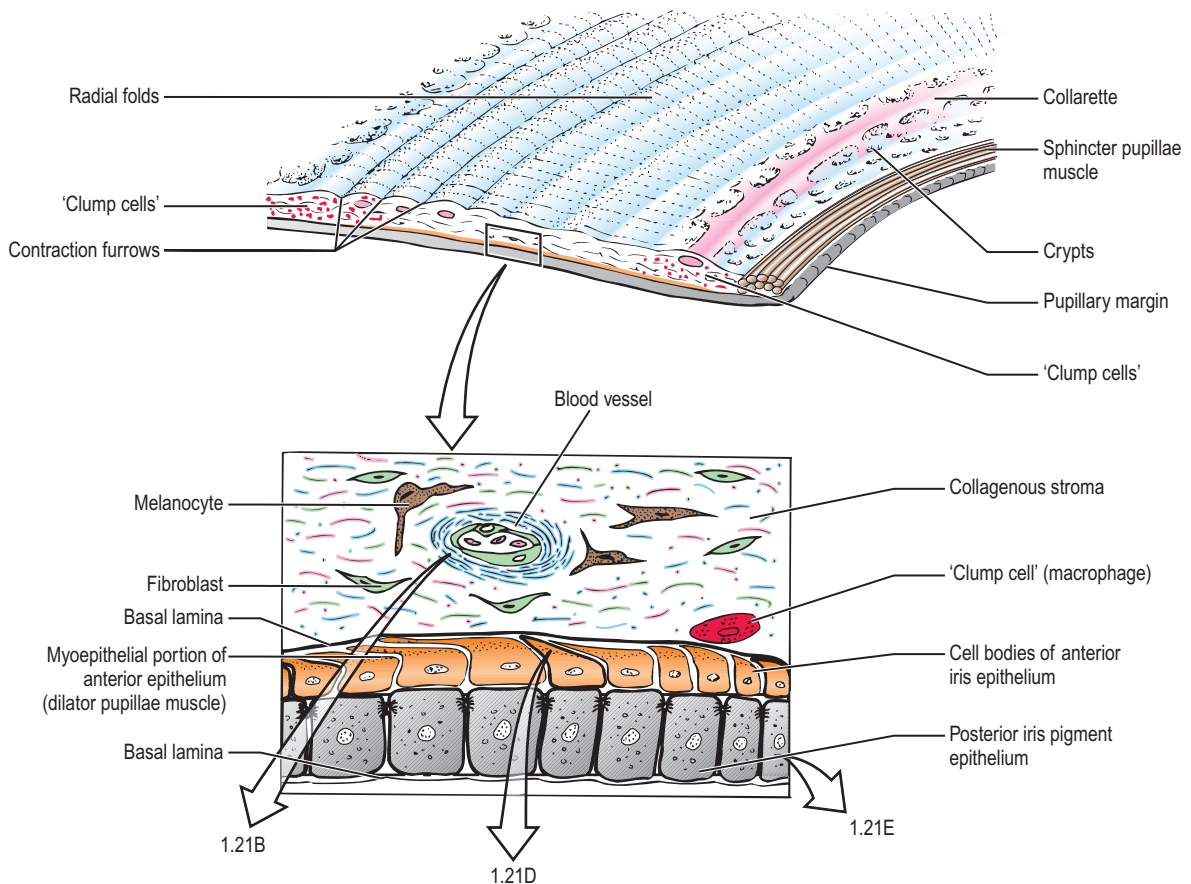
#### Structure (Fig. 1-20A,B)

The pupil margin and iris root are thin, and hence more susceptible to tearing in contusion injuries (iridodialysis). The anterior surface is divided into two zones, the *ciliary zone* and *pupil zone*, by the thickened region known as the *collarette*. The anterior surface is characterized by *radial streaks* (straight when the pupil is contracted and wavy when dilated) and *contraction furrows* (more noticeable in dilated irides). The surface of the iris appears smooth in dark irides, in which the intrastromal melanocytes are heavily pigmented, and more irregular in blue irides, which have a less heavily pigmented stroma. The blue appearance of some irides is because of absorption of long wavelengths and reflectance of shorter wavelengths, especially by the collagenous stroma.

#### Microscopic anatomy

The iris consists of four layers: anterior border layer, stroma, dilator pupillae muscle and posterior pigment epithelium.

**Anterior border layer (Figs 1-20B and 1-21A).** This layer is not covered by a layer of epithelial cells, as early anatomists believed, but is in fact made up of modified stroma consisting of a dense collection of fibroblasts, melanocytes and a few interspersed

**A****B**

**FIGURE 1-20** The structure of the iris. (A) Clinical macroscopic image of a blue iris. Note the pupil (P), pigmented pupil margin (PM) and pupillary zone (PZ) separated from the ciliary portion by the collarette (Co). The root is attached at the iridocorneal angle deep to the limbus (L). Note the fine collagenous trabecula (Tb), some of which form the boundaries of ovoid crypts (Cp). (B) Top diagram: surface features of a portion of the iris. Bottom diagram: high-power exploded view summarizing the arrangement of the pigmented (posterior) and non-pigmented (anterior) layers.

collagen fibres. This layer is deficient in areas; consequently the iris stroma is in free communication with the aqueous humour in the anterior chamber. Larger deficiencies in the anterior border layer are evident macroscopically as *crypts*. Aggregates of heavily pigmented melanocytes in this layer appear as *naevi*.

**Stroma (Fig. 1-21C–E).** This consists of loose connective tissue containing fibroblasts, melanocytes and collagen fibres (types I and III). The loose nature of this tissue, and its free communication via openings in the anterior border layer, allows fluid to move in and out of the stroma quickly during dilation and contraction. The iris stroma in humans contains numerous mast cells and macrophages, many of which are perivascular (see Fig. 1-21C and Ch. 7). Many of the macrophages are heavily pigmented, and a subgroup may form large ovoid ‘clump cells’ (of Koganei), which tend to accumulate near the iris root and sphincter pupillae muscle (Fig. 1-20B). Lying free within the stroma close to the pupil margin is the *sphincter pupillae* muscle, a circumferential ring of smooth muscle fibres about 1 mm in width. The sphincter muscle consists of muscle bundles, each comprising six to eight smooth muscle cells, which are continuous via gap junctions and surrounded by a basal lamina. This muscle is innervated by parasympathetic nerve fibres derived from the oculomotor nerve (postganglionic fibres from the ciliary ganglion travel via the short ciliary nerves) although sympathetics also terminate in this muscle. The unusual embryological origin of this muscle from the neuroectoderm is described in Chapter 2.

**Dilator pupillae muscle.** This is a layer of myoepithelial cells derived from the *anterior iris epithelium*. The basal processes of this epithelium are 4 µm in thickness and extend up to 50–60 µm in a radial direction, while the apices of the myoepithelial cells are lightly pigmented and closely apposed to the apical aspect of the *posterior pigment epithelium* (Figs 1-20B and 1-21A,E). The *dilator pupillae muscle* is innervated by non-myelinated sympathetic fibres whose cell bodies are situated in the superior cervical sympathetic ganglion. Its parasympathetic innervation seems less significant. The dilator pupillae extends only as far centrally as the outer margin of the sphincter pupillae.

**Posterior pigment epithelium (Fig. 1-21E).** This heavily pigmented layer consists of large cuboidal epithelial cells that appear black macroscopically on examination of the posterior surface of the iris. The posterior layer is derived from the inner neuroectodermal layer of the optic cup (see Ch. 2). The cells extend for a short distance on to the anterior iris surface at the pupillary margin; this forms the black ruff seen on the pupil margin during slit-lamp examination of the eye (Fig. 1-20A). The posterior pigmented epithelial layer forms a series of radially arranged furrows (most evident near the pupil margin) and circumferential contraction folds (most evident in the periphery).

### Pupil movements

Mydriasis (dilation) occurs in conditions of low light intensity and in states of excitement or fear. It is a result of the action of the dilator pupillae muscle.

Miosis (contraction) occurs in more illuminated conditions, during convergence, and while sleeping. It is the result of the action of the sphincter pupillae muscle.

### Blood supply of the iris

The iris has a rich blood supply and extensive anastomoses. At the root there is an incomplete major ‘circle’ of the iris that is derived from anterior rami of the anterior ciliary arteries. Branches from here pass centripetally and form an incomplete minor arterial ‘circle’ at the level of the collarette.

The arteries have an unusual coiled form to accommodate the variable states of contraction of the iris. Veins lie close to the arteries, with larger veins primarily in the anterior stroma and smaller veins in the deeper layers. Veins drain posteriorly/centrifugally into the ciliary body and eventually the vortex veins (see Fig. 1-39A,E).

Iris capillaries are characterized by non-fenestrated endothelial cells that have a high density of endocytotic vesicles and tight junctions. This makes them less permeable to a variety of solutes than normal somatic vessels (hence they do not normally leak in fluorescein angiography). These vessels thus constitute an important component of the *blood–ocular barrier*. The basal lamina of the endothelial cells is thickened (0.5–3 µm) and further strengthened by perivascular collagenous/hyalinized layers (Fig. 1-21A,B). Periarteriolar smooth muscle cells are rare and elastic fibres are absent.

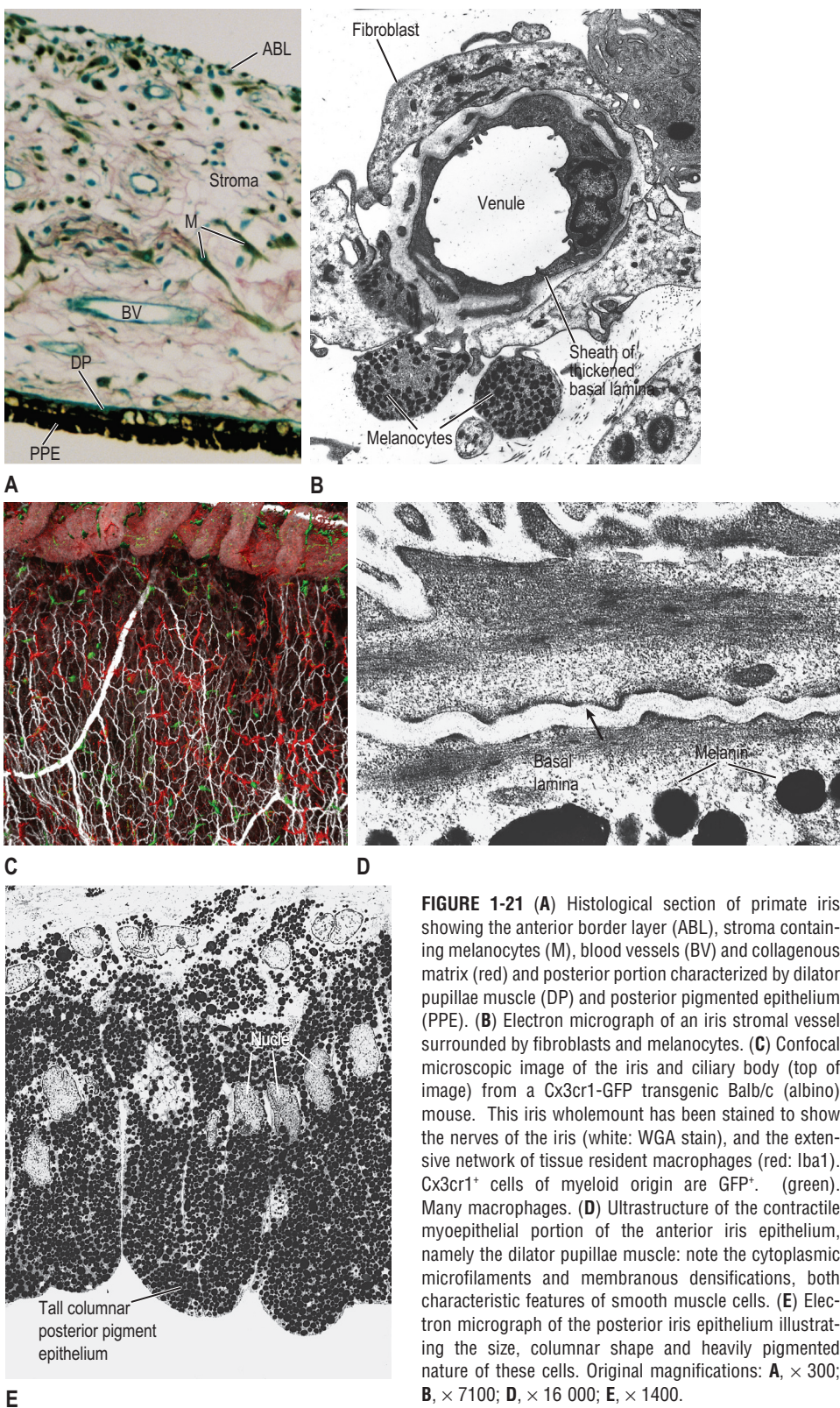


**FIGURE 1-21** (A) Histological section of primate iris showing the anterior border layer (ABL), stroma containing melanocytes (M), blood vessels (BV) and collagenous matrix (red) and posterior portion characterized by dilator pupillae muscle (DP) and posterior pigmented epithelium (PPE). (B) Electron micrograph of an iris stromal vessel surrounded by fibroblasts and melanocytes. (C) Confocal microscopic image of the iris and ciliary body (top of image) from a Cx3cr1-GFP transgenic Balb/c (albino) mouse. This iris wholmount has been stained to show the nerves of the iris (white: WGA stain), and the extensive network of tissue resident macrophages (red: Iba1). Cx3cr1<sup>+</sup> cells of myeloid origin are GFP<sup>+</sup> (green). Many macrophages. (D) Ultrastructure of the contractile myoepithelial portion of the anterior iris epithelium, namely the dilator pupillae muscle: note the cytoplasmic microfilaments and membranous densifications, both characteristic features of smooth muscle cells. (E) Electron micrograph of the posterior iris epithelium illustrating the size, columnar shape and heavily pigmented nature of these cells. Original magnifications: A,  $\times 300$ ; B,  $\times 7100$ ; D,  $\times 16\,000$ ; E,  $\times 1400$ .

### Nerve supply

The iris possesses a rich three-dimensional nerve plexus of myelinated and non-myelinated nerves. The sensory nerves are branches of the long and short ciliary nerves, themselves branches of the nasociliary nerve (ophthalmic division of the trigeminal). The autonomic innervation of the iris muscles is discussed above.

## THE CILIARY BODY

The ciliary body (Fig. 1-22A–D) is an approximately 5–6 mm wide ring of tissue that extends from the scleral spur anteriorly to the ora serrata posteriorly. Temporally it measures 5.6–6.3 mm, and nasally 4.6–5.2 mm. It is divided into two zones, an anterior *pars plicata* (corona ciliaris) and a posterior *pars plana* (Fig. 1-22A). The ciliary body is approximately triangular in cross-section; its base faces the anterior chamber and the apex blends posteriorly with the vascular choroid. The pars plicata is 2 mm wide and consists of 70 radially arranged folds known as *ciliary processes* (Fig. 1-22B), each of which is 0.5–0.8 mm high and 0.5 mm wide. The tips are paler as a result of decreased pigmentation. Minor ciliary processes may be present in the valleys between the major processes. The pars plana is an approximately 4 mm wide zone stretching from the posterior limits of the ciliary processes to the *ora serrata*, the sharp serrated or dentate junction where non-pigmented ciliary epithelium undergoes a sharp transition to become the neural retina.

The ciliary body can be divided histologically into the ciliary epithelium, ciliary body stroma and ciliary muscle (Fig. 1-22A). Each is described below in the context of the three principal functions of the ciliary body: (1) accommodation; (2) aqueous humour production; and (3) production of lens zonules, vitreal glycosaminoglycans and vitreal collagen.

### Accommodation

The anterior two-thirds of the ciliary body is occupied by the *ciliary muscle* which, in conjunction with the *lens zonules* (suspensory ligament) and the natural elastic nature of the lens fibres and capsule, functions to alter the refractive power of the lens. Histologically, the ciliary muscle in meridional sections consists of three groups of smooth muscle fibre bundles embedded in a vascular connective tissue stroma (Figs 1-18

and 1-22A). The stroma contains melanocytes, fibroblasts, and occasional immune cells such as mast cells, macrophages and lymphocytes.

The *outer longitudinal muscle fibres* are attached to the scleral spur and therefore indirectly to the corneoscleral trabeculae anteriorly; posteriorly they are anchored to the inner aspect of the sclera. The *middle oblique* or *radial muscle fibres* are continuous with inner corneoscleral trabeculae. The *inner circular muscle fibres* (one of the three so-called ‘Müller’s muscles’ associated with the eye and adnexa) appear as cross-sectional profiles in conventional meridional sections of the ciliary body (Figs 1-18C and 1-22A). A three-dimensional scheme has been proposed to explain the interrelationship between all three groups of muscle bundles; it appears that the fibres are all components of one interwoven fibre network (see Fig. 1-23 for summary).

The mode of action of the ciliary muscle is still controversial; however, it is generally agreed that during accommodation there is some degree of forward and inward shift of the ciliary body, which serves to slacken the tension on the zonules, thus increasing the refractive power of the lens (see pp. 35 and 217).

### Action of the ciliary muscle on aqueous outflow.

There is some evidence that contraction of the longitudinal ciliary muscle fibres causes an inwards and posterior movement of the scleral spur as well as an effect via extensions of these tendons to the inner wall of Schlemm’s canal, hence distending the inter- and intratrabecular spaces of the trabecular meshwork and preventing collapse of Schlemm’s canal during periods of high pressure. These have been proposed as modes of action of miotic drugs such as pilocarpine, which are used to increase aqueous outflow facility in patients with glaucoma.

### Production of aqueous humour

Aqueous humour is a clear colourless fluid actively secreted by the ciliary processes (for details of aqueous constituents see Ch. 5). The ciliary processes consist essentially of delicate finger-like protrusions of loose vascular connective tissue covered by a bilaminar cuboidal/columnar neuroepithelium, the outer pigmented and inner non-pigmented ciliary epithelium, both derived embryologically from the double neuroectoderm of the optic cup (see Ch. 2). The morphological basis of the blood–aqueous barrier is depicted

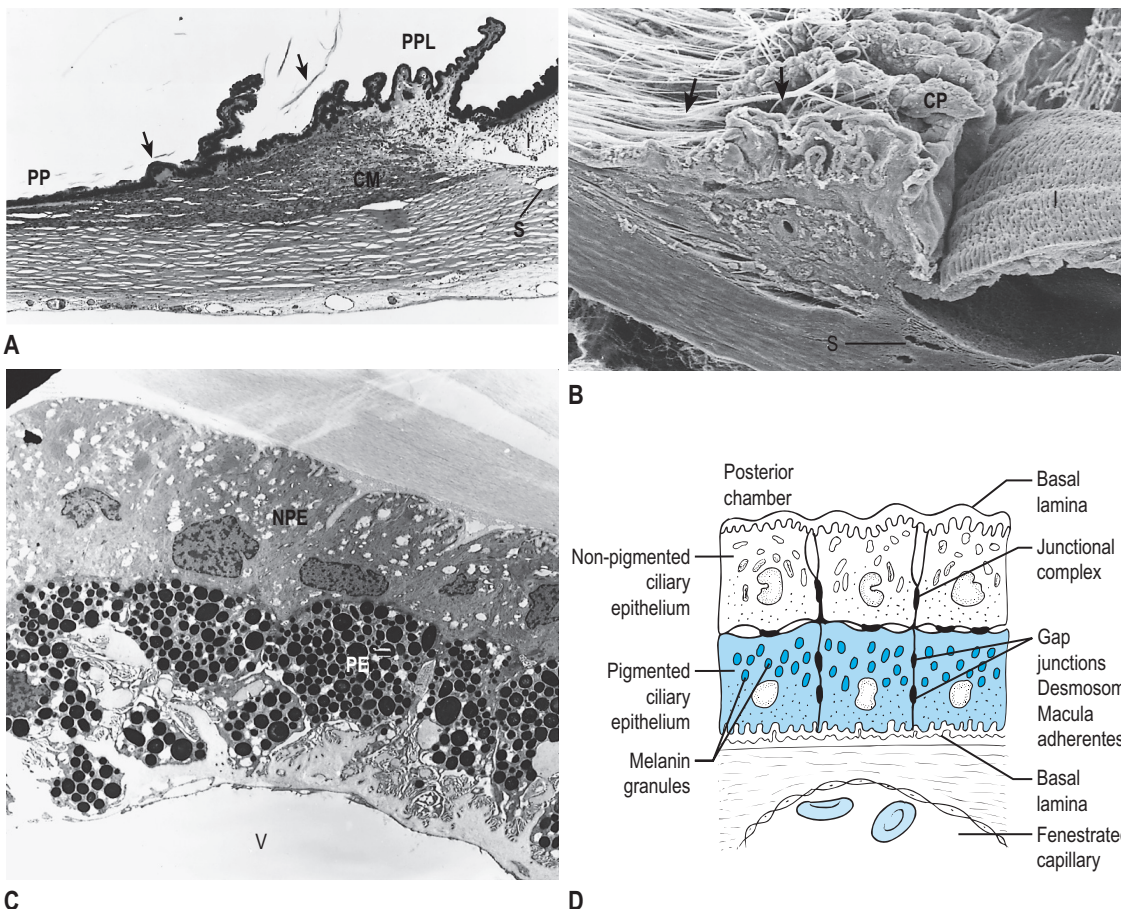


**FIGURE 1-22** (A) Histological section of the ciliary body showing the two major regions; the pars plana (PP) and the pars plicata (PPL) which includes the ciliary processes: CM, ciliary muscle; I, iris; S, Schlemm's canal. (B) Scanning electron micrograph of the inner surface of the ciliary processes (CP) and iris (I). Arrows in (A) and (B), zonular fibres. (C) Low-power electron micrograph of the pigmented (PE) and non-pigmented ciliary epithelia (NPE) of a ciliary process. Note the large fenestrated blood vessel (V) and the lens zonules blending with the basal lamina of the non-pigmented epithelium. (D) Diagrammatic representation of this double layer of epithelium, which constitutes the major site of the blood-aqueous barrier. Original magnifications: A,  $\times 40$ ; B,  $\times 45$ ; C,  $\times 1600$ . (Part A courtesy of W.R. Lee and Springer-Verlag.)

in Figure 1-22B. Aqueous humour is actively secreted by the inner non-pigmented ciliary epithelium whose apices are connected by junctional complexes including tight junctions. Macromolecules, having filtered through the highly permeable fenestrated stromal capillaries, pass between pigment epithelium cells held together only by punctate adherentes (macula adherentes)-like junctions or permeable band-like junctions (zonula adherentes), and are prevented from passing into the posterior chamber. The non-pigmented ciliary epithelium has morphological features characteristic of secretory epithelium, namely numerous mitochondria, and histochemically can be

shown to contain enzymes, such as carbonic anhydrase and ATPase, necessary for active fluid transport (see Ch. 4, p. 217).

#### Production of zonules, vitreal collagen and vitreal hyaluronic acid

The non-pigmented ciliary epithelial cells of the pars plana are cuboidal, columnar or irregular, depending on age and location. It is likely that these cells play a role in secretion of zonular fibres, the extracellular vitreal components, i.e. collagen and hyaluronic acid, and the inner limiting membrane, especially during embryonic development.

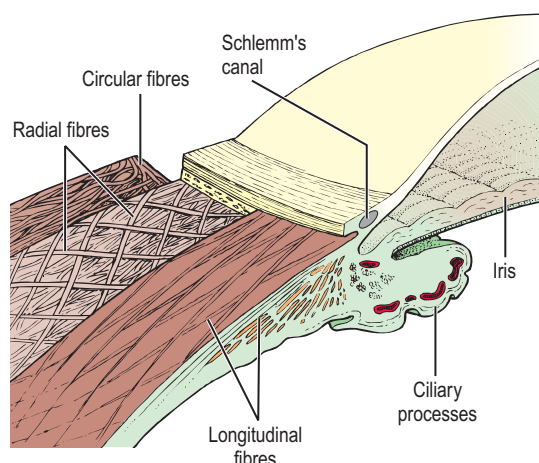


**FIGURE 1-23** Arrangement of the ciliary muscle fibres as seen on external view with the sclera removed. (After Rohen and Ciliarkörper, 1964.)

Some inner non-pigmented cells ‘tilt’ anteriorly, suggesting traction by the zonular fibres. The lens zonules (of Zinn) or suspensory ligament of the lens merge with the fibrous basal lamina material of the non-pigmented ciliary epithelium (Fig. 1-22C). The precise mode of zonule synthesis is still unclear. Tall non-pigmented ciliary epithelial cells in the pars plana have ultrastructural and histochemical features that indicate active hyaluronic acid secretion.

### Blood supply of the ciliary body

The blood supply of this region is derived from long posterior ciliary arteries and anterior ciliary arteries. The two long posterior ciliary arteries arise from the ophthalmic artery and after piercing the sclera near the optic nerve head they travel forward in the choroid in the medial and lateral horizontal plane and divide in the ciliary body before anastomosing with anterior ciliary branches, thus forming the major ‘circle’ of the iris (see p. 217, and Fig. 1-36). From this circle arises muscular and recurrent choroidal branches and the numerous branches that form the vascular plexus in the ciliary processes. Venous return occurs predominantly posteriorly through the system of vortex veins and less so through the anterior ciliary veins.

### Nerve supply of the ciliary body

The ciliary body has rich parasympathetic, sympathetic and sensory innervations.

**Parasympathetic innervation.** Preganglionic neurone cell bodies are located in the Edinger–Westphal nucleus which lies posterior to the main oculomotor nucleus in the rostral midbrain at the level of the superior colliculus. Their axons travel in the oculomotor (III) nerve and synapse with postganglionic cell bodies located in the ciliary ganglion. The postganglionic fibres travel to the eye in the short ciliary nerves and terminate as an extensive plexus in the ciliary muscle. The action is mediated by acetylcholine on muscarinic receptors (see Ch. 6, p. 355).

**Sympathetic innervation.** Preganglionic neurone cell bodies are situated in the lateral grey horn of the first thoracic segment of the spinal cord. Preganglionic fibres relay in the superior cervical ganglion (adjacent to vertebrae C2 and C3, behind the internal carotid artery). Postganglionic fibres leave the ganglia as the internal carotid nerve and plexus. These fibres may reach the orbit as either direct branches of the internal carotid plexus or by joining the ophthalmic division of the trigeminal and its main branch in the orbit, the nasociliary nerve. Sympathetic fibres may either pass directly to the retrobulbar plexus behind the eye or through the ciliary ganglion uninterrupted. From the ciliary ganglia, fibres are distributed via the short ciliary nerves to the blood vessels of the eye, including the ciliary body. Some terminal filaments of the internal carotid plexus may also be distributed via the ophthalmic artery and its branches. The sympathetic action is mediated by the action of norepinephrine on two subclasses of receptors,  $\alpha_1$  and  $\beta_2$  adrenoceptors, both of which are inhibitory (see Ch. 6, p. 358).

**Sensory innervation.** Sensory innervation is derived from the nasociliary nerve; however, the function of these fibres is unknown.

### THE LENS AND ZONULAR APPARATUS

The lens (Fig. 1-24) is a highly organized system of specialized cells (so-called lens ‘fibres’), which constitutes an important component of the optical system of the eye and fulfils the important function of altering the refractive index of light entering the eye to focus on the retina. While it has less refractive power (15 dioptres) than the cornea, the lens has the ability to change shape, under the influence of the ciliary

muscle, and thus alter its refractive power. The range of dioptric power diminishes with age (8 at 40 years, 1–2 by 60 years). The transparency of the lens is due to the shape, arrangement, internal structure and biochemistry of the lens cells or lens fibres.

### Position, size and shape

The lens, enclosed in its capsule, lies behind the iris and in front of the vitreous body. It is encircled by the ciliary processes and held in position by the zonular fibres laterally, the anterior vitreous face posteriorly (patellar fossa), and the iris anteriorly (see Fig. 1-10). It is normally transparent and avascular following regression of the pupillary membrane and tunica vasculosa lentis late in fetal development (see Ch. 2). It receives its nourishment from the aqueous and vitreous humours. It is a biconvex, ellipsoid structure with differing radius of curvature on the anterior and posterior surfaces. The anterior curvature is approximately 10 mm (range 8–14 mm) and the posterior curvature is approximately 6 mm (range 4.5–7.5 mm). The centre points of these surfaces, described as the *anterior* and *posterior poles*, are connected by an imaginary axis. The anterior pole lies 3 mm from the posterior corneal surface. The anterior and posterior surfaces are separated by the *equator*, which has a ridged (indented) appearance caused by the zonular fibres. In the adult eye the lens measures approximately 10 mm in diameter and has an axial length of 4 mm. The lens continues to grow (0.023 mm per year) and alters shape throughout life. It becomes rounder with age, especially after the age of 20 years.

### Structure

The lens comprises three parts: (1) the capsule; (2) anterior or lens epithelium; and (3) the lens fibres (Fig. 1-24A,D).

**Lens capsule.** The *lens capsule* is a thickened, smooth, basement membrane produced by the lens epithelium and lens fibres. It completely envelops the lens and has regions of variable thickness, being thickest pre- and post-equatorially (17–28 µm) and thinner at the posterior (2–3 µm) than at the anterior pole (9–14 µm). Ultrastructural examination reveals a fibrillar or lamellar appearance. The interfibrillar matrix consists of basement membrane glycoproteins (type IV collagen)

and sulphated GAGs which are responsible for its prominent periodic acid–Schiff-positive staining properties in histological sections. It possesses elastic properties and, when not under tension of the zonules, the capsule together with the cortex causes the lens to assume a more rounded shape.

**Lens epithelium.** This is a simple cuboidal epithelium (Fig. 1-24A,D) restricted to the anterior surface of the lens. The cells become more columnar at the equator. As they elongate, the apical portion comes to lie deeper to other, more anteriorly positioned, lens cells. These elongated lens cells are known as lens ‘fibres’ (Fig. 1-24D). The manner in which equatorial lens epithelial cells are transformed into lens fibres is depicted in Figure 1-24A. The cell nucleus and cell body sink deeper into the lens as further cells are laid down externally. Mitotic activity is maximal in the pre-equatorial and equatorial lens epithelium, known as the germinative zone (Fig. 1-24A).

**Lens fibres.** While each lens fibre is only a  $4 \times 7 \mu\text{m}$  hexagonal prismatic band in cross-section (Fig. 1-24C), it may be up to 12 mm (12 000 µm) in length. The apical portion of the elongated lens cell (or lens ‘fibre’) passes anteriorly, the basal portion posteriorly. The cell nucleus migrates anteriorly as the cell is pushed deeper in the lens, hence creating the anteriorly oriented *lens bow* (Fig. 1-24D). The meridionally oriented lens fibres extend the full length of the lens, meeting at the anterior and posterior sutures (Fig. 1-24A). Deeper (hence older) lens fibres are anucleate. Continual growth of the lens, by addition of superficial strips of new cells, produces a series of concentrically arranged laminae, similar to the layers of an onion (best seen by dissecting a fixed or frozen lens). In life, the outer *cortex* of the lens has a softer consistency than the hard central *nucleus*.

Lens fibres are tightly packed with little intercellular space. Neighbouring cells are linked by ball-and-socket cytoplasmic interdigitations (Fig. 1-24B,C) and numerous gap junctions. The junctions may aid maintenance of centrally positioned cells (via intercellular and molecular coupling or metabolic cooperation) some distance from the source of nutrition (aqueous humour). Superficially located lens fibres are rich in ribosomes, polysomes and rough endoplasmic

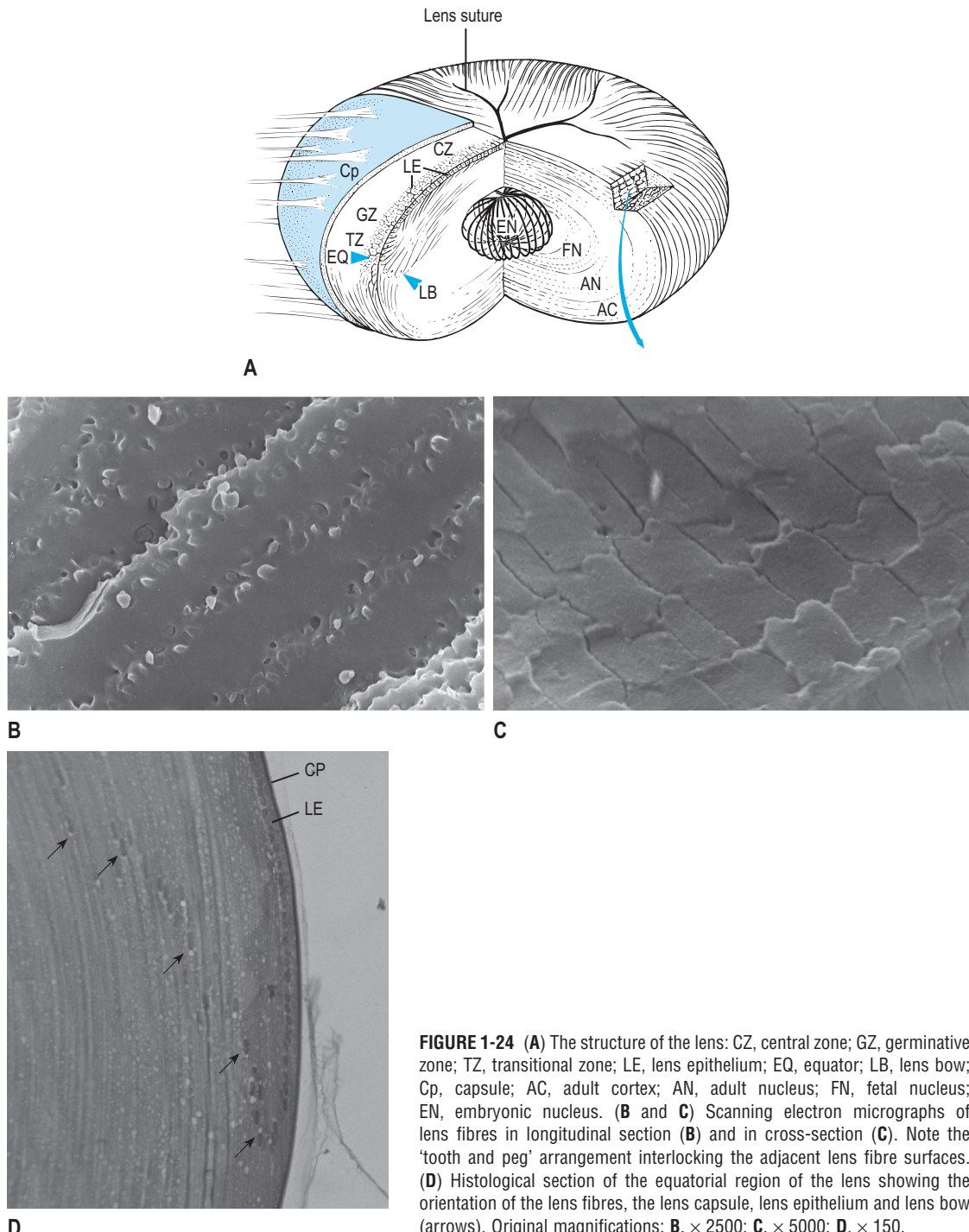


**FIGURE 1-24** (A) The structure of the lens: CZ, central zone; GZ, germinative zone; TZ, transitional zone; LE, lens epithelium; EQ, equator; LB, lens bow; Cp, capsule; AC, adult cortex; AN, adult nucleus; FN, fetal nucleus; EN, embryonic nucleus. (B and C) Scanning electron micrographs of lens fibres in longitudinal section (B) and in cross-section (C). Note the 'tooth and peg' arrangement interlocking the adjacent lens fibre surfaces. (D) Histological section of the equatorial region of the lens showing the orientation of the lens fibres, the lens capsule, lens epithelium and lens bow (arrows). Original magnifications: B,  $\times 2500$ ; C,  $\times 5000$ ; D,  $\times 150$ .

reticulum, and actively synthesize unique lens proteins, lens crystallins (see Ch. 4); however, the cytoplasm of mature lens fibres appears homogeneous. Lens fibres are rich in cytoskeletal elements oriented parallel to the long axis of the cell.

### Lens zonules (zonular apparatus)

The lens is held in position by a complex three-dimensional system of radially arranged zonules (zonules of Zinn or the suspensory ligament of the lens) (Fig. 1-25). These delicate fibres are attached to the lens capsule 2 mm anterior and 1 mm posterior to the equator, and arise from the pars plana region of the ciliary epithelium and pass forward closely related to the lateral surfaces of the ciliary processes (Fig. 1-25A,B). In humans, the zonules transmit the forces that flatten the lens, allowing the eye to focus on distant objects. However, the zonules are also present in non-accommodating species, where they presumably play a role in lens centration.

The zonules consist of dense, glassy bundles 5–30 µm in diameter. Each bundle consists of a series of fine fibres (0.35–1 µm in diameter), themselves composed of 10–12 nm diameter microfibrils. Biochemically, the zonules are unique, most closely resembling the periodontal ligament of the teeth. Proteomic analysis has revealed that the zonules are composed principally of fibrillin, a 350 kDa cysteine-rich glycoprotein. The zonular fibres are synthesized by cells of the non-pigmented ciliary epithelium. At their proximal end they emerge from the basal lamina of the ciliary epithelial cells. The distal portions of the zonular fibres connect to the lens capsule near the lens equator. In humans, the fibres appear to insert directly into the capsule and their tips can be seen to terminate below the capsular surface. The lens zonules are synthesized and maintained by cells in the non-pigmented

ciliary epithelium. The zonule is synthesized during embryonic and early postnatal development and it is likely that zonular proteins turn over slowly, if at all.

**Accommodation.** In the non-accommodated state, the ciliary body maintains tension on the zonules. During accommodation, movement of the ciliary body causes slackening of the zonules, whereupon the lens assumes an increased anterior curvature, with resultant increase in refractive power, owing to elasticity of the lens capsule and the outer cortical layers. Some authorities believe that there are two sorts of zonules: main zonules and ‘tension’ zonules, the latter being placed under tension during accommodation.

Posterior zonules are closely associated with the collagenous material of the anterior hyaloid membrane. Zonules running perpendicular to the main zonule stream form circumferential bands near the base of the ciliary processes or in the pars plana (posterior zonular girdle) and over the apices of the ciliary processes (anterior ciliary girdle).

### ANTERIOR AND POSTERIOR CHAMBERS

The cavity anterior to the lens and lens zonules is divided into two chambers by the iris. These two chambers, the larger anterior and smaller posterior, communicate through the pupil. The boundaries of these two chambers are shown in Figure 1-26.

### Posterior chamber

This is a very small irregularly shaped space whose size varies during accommodation. It is approximately triangular with its apex at the pupil margin; the base is formed by the ciliary processes; the posterior border is the lens and zonular apparatus; and the anterior border is the posterior surface of the iris. Aqueous humour secreted by the ciliary processes continually

### BOX 1-13 CLINICAL CORRELATES

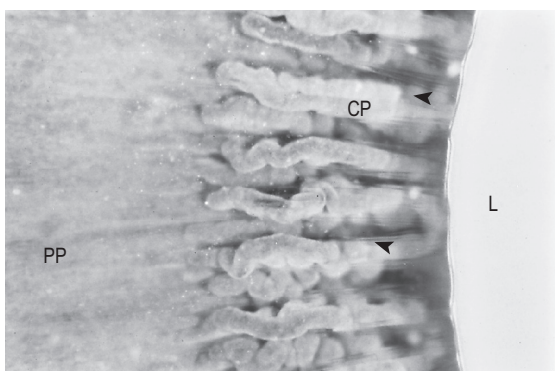
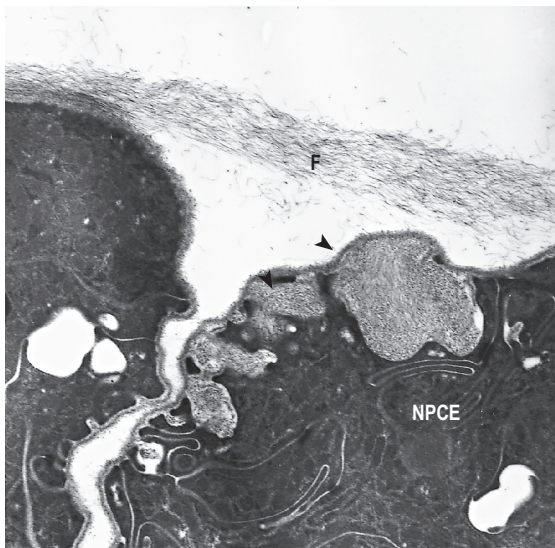
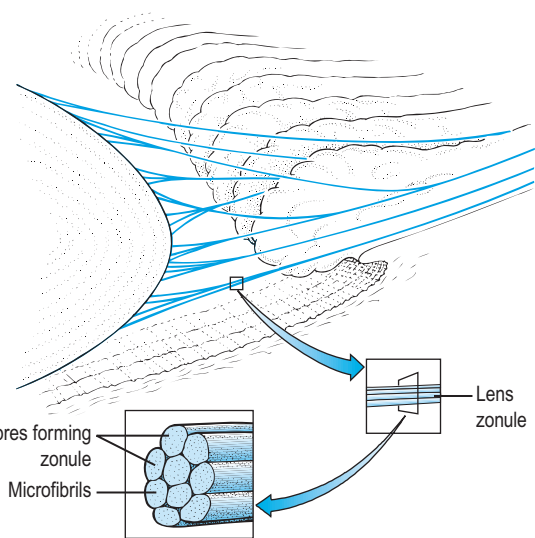
#### CATARACT

Cataract is the loss of normal lens transparency, besides the normal age-related yellowing, and may be caused by cumulative damage by ultraviolet light or perturbations in lens fibre biochemistry. Opacification may be the result of damage or disruption of the capsule, the lens fibre configuration or the lens epithelium (see Ch. 9).

### BOX 1-14 CLINICAL CORRELATES

#### Ectopic lentis in Marfan syndrome

In humans, mutations in the fibrillin-1 gene cause Marfan syndrome, a condition characterized by disturbances in connective tissue and skeletal elements. In these patients the zonules are disrupted and the lens dislocated or malpositioned within the eye – a condition known as ectopic lentis.

**A****C****B**

**FIGURE 1-25** Arrangement of the zonular fibres. **(A)** Macroscopic view of ciliary processes (CP) and intervening lens zonules (arrowheads) inserting into the lens capsule in a monkey eye: PP, pars plana; L, lens. **(B)** Arrangement of the different groups of lens zonules. **(C)** Electron micrograph showing the close association of zonular fibres (F) to the non-pigmented epithelial cells (NPCE) of the ciliary processes. Note the material similar to zonular fibres beneath the basal lamina of the epithelium (arrowheads). Original magnifications: **A**,  $\times 24$ ; **C**,  $\times 10\,500$ .

enters this chamber before passing through the pupil into the anterior chamber.

### Anterior chamber

The anterior chamber is bound in front by the cornea and posteriorly by the anterior iris surface and the pupillary portion of the lens. The lateral recess of the anterior chamber is formed by the iridocorneal angle occupied by the trabecular meshwork. The anterior chamber is deepest centrally (3 mm) and contains approximately 250  $\mu\text{L}$  of aqueous humour. Aqueous humour is produced at around 2–4  $\mu\text{L}/\text{minute}$ . A little passes back into the vitreous; however, the bulk flow of aqueous is from the posterior chamber through the

### BOX 1-15 CLINICAL CORRELATES

#### Ageing changes in the eye: presbyopia

This condition may develop around the age of 40–50 years when the elasticity of the lens markedly decreases and there is associated atrophy of the ciliary muscle fibres; consequently, the lens fails to change shape sufficiently during accommodation. This becomes evident as decreasing ability to read, i.e. use near vision.

pupil into the anterior chamber. The aqueous humour is drained from the anterior chamber via the conventional and non-conventional routes (see p. 21).

Aqueous humour has two principal functions. It is the medium by which the necessary metabolites are

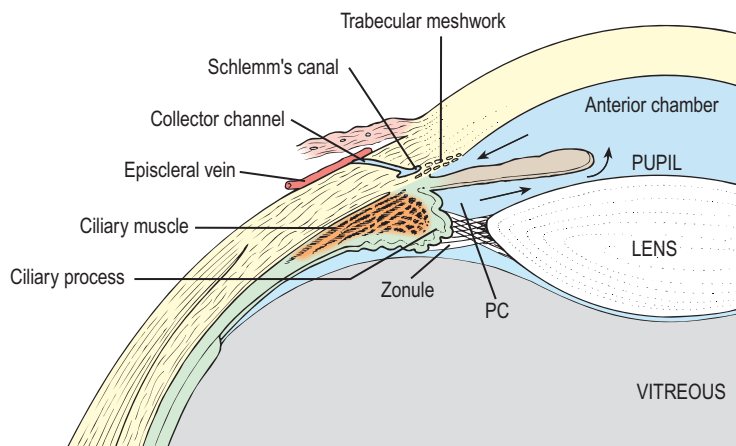


**FIGURE 1-26** Diagram of the anterior segment of the eye. The major pathway followed by aqueous humour from the posterior chamber (PC) to the anterior chamber and outflow pathways is shown by arrows.

transported to the avascular lens and cornea. It also removes toxic metabolic waste products of the cornea and iris. Second, it has a hydromechanical function in maintenance of intraocular pressure. This pressure depends on the balance between the *rate* of production of aqueous humour and its *resistance* to drainage. These two properties of aqueous humour, together with the fact that it is transparent, are necessary for the normal functioning of the eye (see p. 222).

## THE VITREOUS

The vitreous cavity (Fig. 1-27) is the largest cavity of the eye (two-thirds the volume of the eye, weight 3.9 g) and contains the vitreous humour or vitreous. It is bound anteriorly by the lens, posterior lens zonules and ciliary body, and posteriorly by the retinal cup. The vitreous is a transparent viscoelastic gel that is more than 98% water, with a refractive index of 1.33. Its viscosity is two to four times that of water. The main constituents of the vitreous, besides water, include hyaluronan (hyaluronic acid), collagens type II and IX, fibronectin, fibrillin and opicin. The gel structure of the vitreous body is dependent on the collagenous constituents and not the hyaluronan. The fine-diameter type II collagen fibres (8–12 nm in diameter) entrap large coiled hyaluronan molecules (see p. 240).

The vitreous is shaped like a sphere with an anterior depression, the *hyaloid fossa* (also known as the *patellar* or *lenticular fossa*) (Fig. 1-27A). The vitreous is traditionally regarded as consisting of two portions: a *cortical zone*, characterized by more

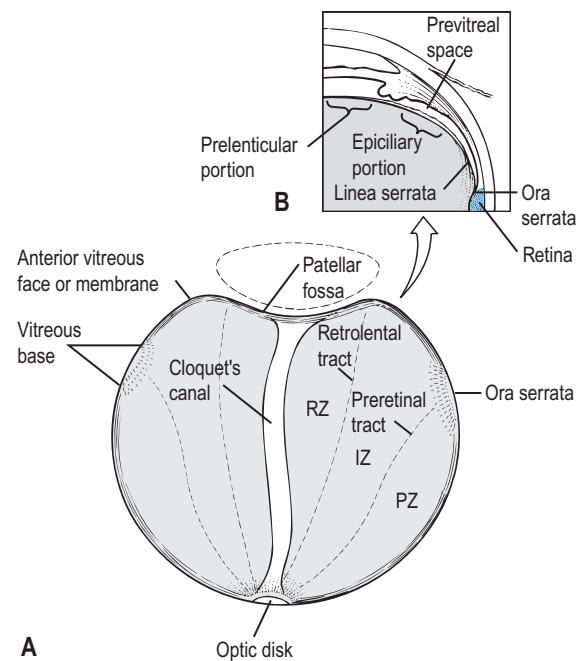


**FIGURE 1-27** (A) Diagram summarizing the anatomical zones of the vitreous (PZ, preretinal zone; IZ, intermediate zone; RZ, retrolental zone) and the major vitreal condensations (the retrolental tract, preretinal tract, vitreous base, anterior hyaloid face, vitreous cortex). (B) Higher power of the anterior vitreous face and its relation to the ciliary body and iris.

densely arranged collagen fibrils, and a more liquid *central vitreous*. The vitreous can be further subdivided for descriptive purposes into three major topographical zones, as shown in Figure 1-27A.

The cortical vitreous is attached by condensation of fine collagen fibrils at several points around its margin to (Fig. 1-27A,B):

- the peripheral retina and pars plana via the *vitreous base*, a 3–4 mm wide band
- the posterior lens capsule (*ligamentum hyaloide capsulare*)
- the retina along the margins of the optic disk (base of the hyaloid canal), although this is disputed (Sebag, 2004)
- the inner limiting membrane of the retina, especially near retinal vessels (most variable and weakest of attachments).

The *central vitreous* possesses less collagen than cortical vitreous. It is traversed by a central fluid-filled canal (hyaloid or Cloquet's canal), which represents the remnants of the course taken by the hyaloid artery that supplied the vitreous and lens in the fetal eye (see Ch. 2). The retrolental and intermediate zones in the human eye are semi-liquid. The existence of an ordered, organized, vitreal structure is still controversial owing to the problems of studying a gel that is 98.5–99.7% water.

The human vitreous begins to degenerate at adolescence, leading to the appearance of liquid-filled cavities and fibrillar strands, such as the retrolental, preretinal and other named tracts of significance only to vitreal specialists. Most of the central tracts (except preretinal) are mobile and change during eye movements. The posterior vitreous cortex may possess zones of reduced density or 'cortical holes' or pockets that, if present, occur close to the fovea, retinal vessels and any developmental anomalies. While these are normal features, secondary pathological holes may develop following various disease processes.

### Vitreous cells (Fig. 1-28A,B)

The vitreous is essentially acellular; however, occasional isolated cells may occur in the cortex, particularly near the vitreous base, optic disk and retinal vessels. Cells known as hyalocytes, which have the morphological, ultrastructural, immunophenotypic and functional characteristics of bone marrow-derived macrophages, are the main cell type in the vitreous. A marked vitreal cellular infiltrate is indicative of pathological or inflammatory processes in adjacent tissues, e.g. uveoretinitis.

### BOX 1-16 CLINICAL CORRELATES

#### Posterior vitreous detachment

The thin potential (subhyaloid or sublamellar) space between the surface of the cortical vitreous and the retina may fill with fluid in cases of vitreous detachment. The vitreous may detach relatively easily in the posterior segment where it is less weakly bound to the retina. The fluid may accumulate rapidly in the case of rhegmatogenous vitreous detachment and more slowly where the cortex is not ruptured (arrhegmatogenous vitreous detachment). The former is an age-related change in the vitreous. Vitreous detachment may predispose to retinal detachment (see Ch. 9).

### RETINA AND RETINAL PIGMENT EPITHELIUM (Fig. 1-29)

The retina is the innermost of the three coats of the eye. This layer is in the focal plane of the eye's optical system and is responsible for converting relevant information from the image of the external environment into neural impulses that are transmitted to the brain for decoding and analysis. It consists of two primary layers: an *inner neurosensory retina* and an outer simple epithelium, the *retinal pigment epithelium* (RPE). These two layers can be traced embryologically to the inner and outer layers of the invaginated optic cup (see Ch. 2). In the adult they are continuous anteriorly with the epithelial layers over the ciliary processes and posterior iris surface (see p. 28). Between the neural retina and RPE is a potential space, the *subretinal space*, across which the two layers must adhere. The neural retina is firmly attached only at its anterior termination, the ora serrata, and at the margins of the optic nerve head.

The retina is bound externally by Bruch's membrane and on its internal aspect by the vitreous (Fig. 1-26). It is continuous with the optic nerve posteriorly, the site of exit of ganglion cell axons from the eye.

#### Regions of the retina

Before considering the histological structure of the individual retinal layers (Fig. 1-29) and their constituent cell types, it is important that the reader appreciates the regional or topographical variations of the human retina (Fig. 1-30A,B).

There is often confusion regarding the terminology of the regions of the retina owing to the use of differing

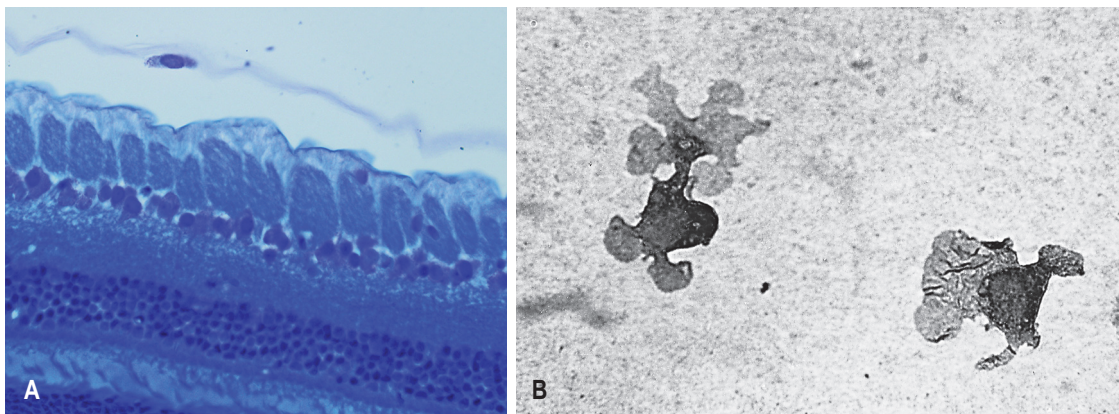


**FIGURE 1-28** (A) Section of the inner retina in primate eye showing a hyalocyte. (B) CD169<sup>+</sup> hyalocytes in the rat subhyaloid space (plan view, retinal whole mount).

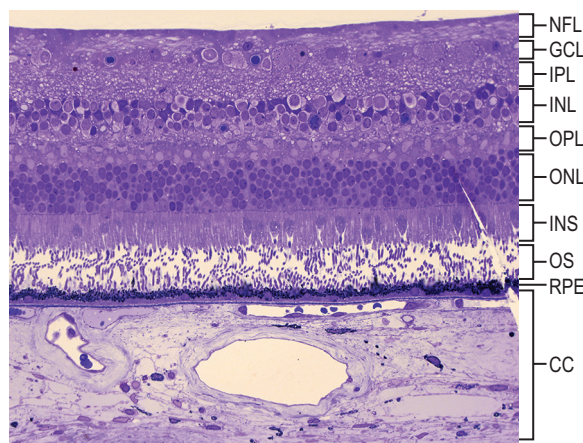


**FIGURE 1-29** Low-power micrograph of the human retina (resin histology): arrows, retinal vessels. Original magnification:  $\times 150$ . Abbreviations: see Fig. 1-32A.

terms by clinicians and anatomists. Figure 1-30A gives a summary of both terminologies.

1. The *posterior pole* or *central retina* (anatomically, *area centralis*) is a 5–6 mm diameter circular zone of retina situated between the superior and inferior temporal arteries. This region is cone-dominated and is characterized histologically by the presence of more than a single layer of ganglion cell bodies.
2. The *macula lutea* (anatomically, *fovea*) is a 1.5 mm diameter area in the posterior pole, 3 mm lateral to the optic disk. It is partly yellow as a result of yellow screening xanthophyll carotenoid

pigments (zeaxanthin and lutein) in the cone axons. This may serve to act as a short wavelength filter protecting against UV irradiation.

3. The *fovea centralis* (anatomically, *foveola*) is a central 0.35 mm wide zone in the macula, consisting of a depression surrounded by slightly thickened margins. Cone photoreceptors are concentrated here at maximum density to the exclusion of rods. The inner retinal layers in the margins of the pit (clivus) are displaced laterally (Fig. 1-30C). The foveal retina is avascular and relies on the choriocapillaris for nutritional support.
4. The *optic disk* lies 3 mm medial to the centre of the macula (fovea). There are no normal retinal layers in this zone (blind spot) as ganglion cell axons from the retina pierce the sclera to enter the optic nerve. This pale pink/whitish area is 1.8 mm in diameter with a slightly raised rim. The central retinal vessels emerge at the centre of the optic disk, pass over the rim, and radiate out to supply the retina (Figs 1-30A and, below, 1-34A). The vein usually lies lateral to the artery.
5. The *peripheral retina* is the remainder of the retina outside the posterior pole. The distance from the optic disk to the *ora serrata* is 23–24 mm on the temporal aspect and approximately 18.5 mm on the nasal aspect. The peripheral retina is 110–140  $\mu\text{m}$  in thickness, rich in rods, and possesses only one layer of ganglion cell bodies.

### BOX 1-17 CLINICAL CORRELATES

#### Retinal detachment

In this condition the neural retina separates from the retinal pigment epithelium (RPE), thus reopening the embryonic intraretinal space or optic ventricle (analogous to the ventricles of the brain), known in the adult as the *subretinal space*. Proteinaceous exudate tends to accumulate in the newly formed space (see Ch. 9). Adhesion of the neural layer and RPE is normally maintained by negative pressure, viscous proteoglycans in the subretinal space and electrostatic forces.

6. The *ora serrata* is the scalloped or dentate anterior margin of the sensory retina. At this transition zone, the neuroretina is continuous with the columnar non-pigmented epithelial cells of the pars plana. The ora serrata is around 1 mm closer to the limbus on the nasal than on the temporal side.

For descriptive purposes, the retina is divided into nasal and temporal halves by a vertical line through the fovea. The optic nerve head is often used as a central point to describe the retina as having supero- and inferonasal and supero- and inferotemporal quadrants. The area of the retina is approximately  $1250 \text{ mm}^2$  and varies in thickness from  $100 \mu\text{m}$  (periphery) to  $230 \mu\text{m}$  (near the optic nerve head) (Fig. 1-30B).

#### Retinal pigment epithelium (Fig. 1-31)

The retinal pigment epithelium (RPE) is a continuous monolayer of cuboidal/columnar epithelial cells, which extends from the margins of the optic nerve head to the ora serrata, where it is continuous with the pigment epithelium of the pars plana. This cell layer has many physical, optical, metabolic/biochemical and transport functions, which play a critical role in the normal visual process (Fig. 1-31A). These include: maintaining adhesion of the neurosensory retina; providing a selectively permeable barrier between the choroid and neurosensory retina; phagocytosis of rod, and to a lesser extent cone, outer segments; synthesis of interphotoreceptor matrix; absorption of light and reduction of light scatter within the eye, hence improving image resolution; and transport plus storage of metabolites and vitamins (especially vitamin A). The complex morphology of this neuroectoderm-derived epithelium reflects these multiple functions.

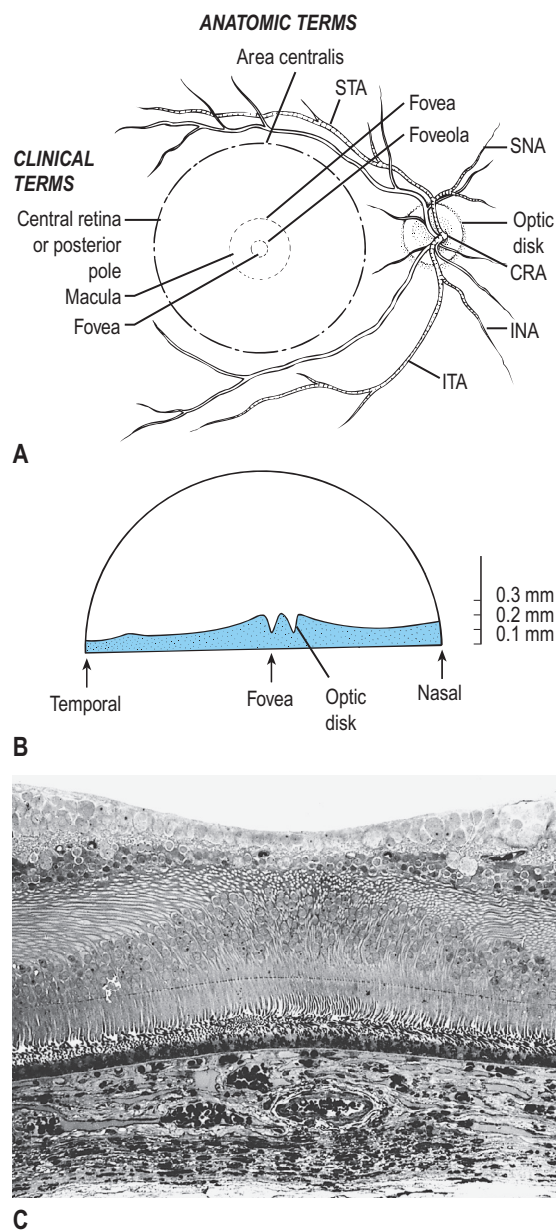


**FIGURE 1-30** (A) Anatomical and clinical terminology used to describe the regions of the retina: STA, superior temporal artery; ITA, inferior temporal artery; SNA, superior nasal artery; INA, inferior nasal artery; CRA, central retinal artery. (B) Regional variations in retinal thickness. (C) Section of the retina at the fovea. Original magnification:  $\times 150$ . (Courtesy of D. Aitken and W.R. Lee.)

**Cell size, shape and structure (Fig. 1-31).** The RPE cells vary in size and shape depending on age and location, being more columnar in the central retina (14 µm tall, 10 µm wide) and more flattened (10–14 µm tall, 60 µm wide) in the peripheral retina. The basal aspect of the cells lies on *Bruch's membrane* and their apical surface is intimately associated with the photoreceptor outer segments (Fig. 1-31A,B). When examined *en face* they form a highly organized hexagonal pattern of homogeneously sized cells (Fig. 1-31C). The number of RPE cells per eye varies from 4.2 million to 6.1 million. The correlation between structure and function of this monolayer is summarized diagrammatically in Figure 1-31A.

### Neurosensory retina (Figs 1-29 and 1-32)

The neurosensory retina is a thin transparent layer of neural tissue that in life has a red/purple tinge due to the presence of visual pigments; however, after death and in fixed specimens, it is white or opaque and often detached from the underlying RPE. Light stimuli are converted into neural impulses in the retina. These impulses are then partially integrated locally before transmission to the brain via the ganglion cell axons in the optic nerve. An appreciation of the anatomy of the neurosensory retina is crucial to an understanding of the physiology of vision (see Ch. 5).

The retina consists of several cell types among which neural cells predominate; other cell types include glial cells, vascular endothelium, pericytes and microglia. The three principal neurone cell types that relay impulses generated by light are photoreceptors, bipolar cells and ganglion cells, and their activity is modulated by other cell types such as horizontal cells, amacrine cells, and possibly by non-neuronal elements. It is the culmination of this neural processing concerning the visual image that is eventually transmitted to the brain along the optic nerve. Retinal cells are arranged in a highly organized manner, and in histological sections appear as eight distinct layers that include three layers of nerve cell bodies and two layers of synapses. The arrangement as seen in conventional histological section is shown in Figure 1-29 and the ultrastructural appearance is shown in Figure 1-32A. A simplified schematic diagram of retinal circuitry is shown in Figure 1-32B. Each of the principal cell types is described briefly below.

### BOX 1-18 AGEING CHANGES IN THE RETINAL PIGMENT EPITHELIUM

The retinal pigment epithelium (RPE) has low regenerative capacity in the normal human eye; therefore, cell loss is accommodated by hyperplasia of adjacent cells. Thus, in older eyes, the regular hexagonal array is lost and a heterogeneous mixture of sizes and shapes is more evident. Also evident with age is an increase in lipofuscin within the RPE which displays autofluorescent properties.

### Photoreceptors (Fig. 1-33)

There are two types of photoreceptor in the human eye: rods and cones. They are situated on the outer or 'scleral' aspect of the retina. There are approximately 115 million rods and 6.5 million cones in the human eye. Rods are responsible for sensing contrast, brightness and motion, while cones subserve fine resolution, spatial resolution and colour vision (see Ch. 5). The density of rods and cones varies in different regions of the retina, the periphery being rod-dominated (30 000/mm<sup>2</sup>) while cone density increases nearer the macula (150 000/mm<sup>2</sup> at the fovea), the fovea being exclusively cones.

Each photoreceptor consists of a long narrow cell with an inner and outer segment joined by a connecting stalk consisting of a modified cilium (Fig. 1-33). These inner and outer segments are 'separated' from the cell body by the outer limiting membrane. The nucleus is situated in the outer nuclear layer of the retina and axons pass into the outer plexiform layer where they form synaptic terminals (cone pedicle or rod spherule) with bipolar cells and interneurones (horizontal cells) (Fig. 1-32B). The outer segments of rods and cones are shaped precisely as their name implies. They contain the visual pigments that are responsible for absorption of light and initiation of the neuroelectrical impulse.

**Rod cells.** Rods are long (100–120 µm) slender cells whose outer segment contains the visual pigment rhodopsin sensitive to blue-green light (maximal spectral sensitivity 496 nm). Rods are highly sensitive photoreceptors and are used for vision in dark-dim conditions. The rhodopsin is contained within the membrane-bound lamellae or disks (up to 1000 per cell, 10–15 nm thick) that are enclosed by a single cell

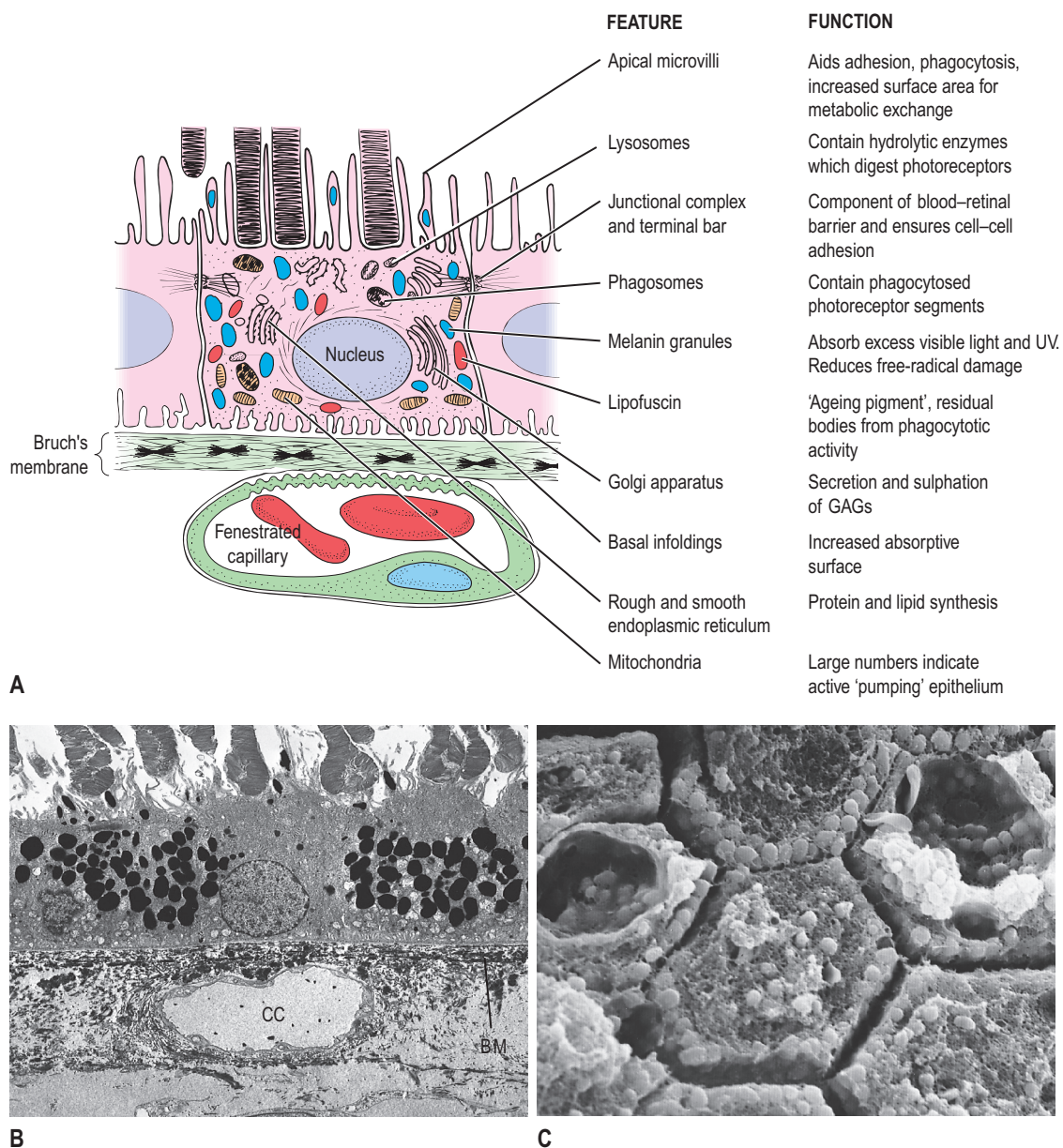


**FIGURE 1-31** (A) Diagram summarizing the main ultrastructural features of the retinal pigment epithelium (RPE). (B) Transmission electron micrograph of human RPE layer: CC, choriocapillaris; BM, Bruch's membrane. (C) Scanning electron micrograph of the apical surface of the retinal pigment epithelium. Note the hexagonal shape and the ovoid melanin granules, only visible because of post-mortem-induced disruption of the apical cell membrane. Original magnifications: **B**,  $\times 2600$ ; **C**,  $\times 3600$ . (Parts B and C courtesy of D. Aitken and W.R. Lee.)

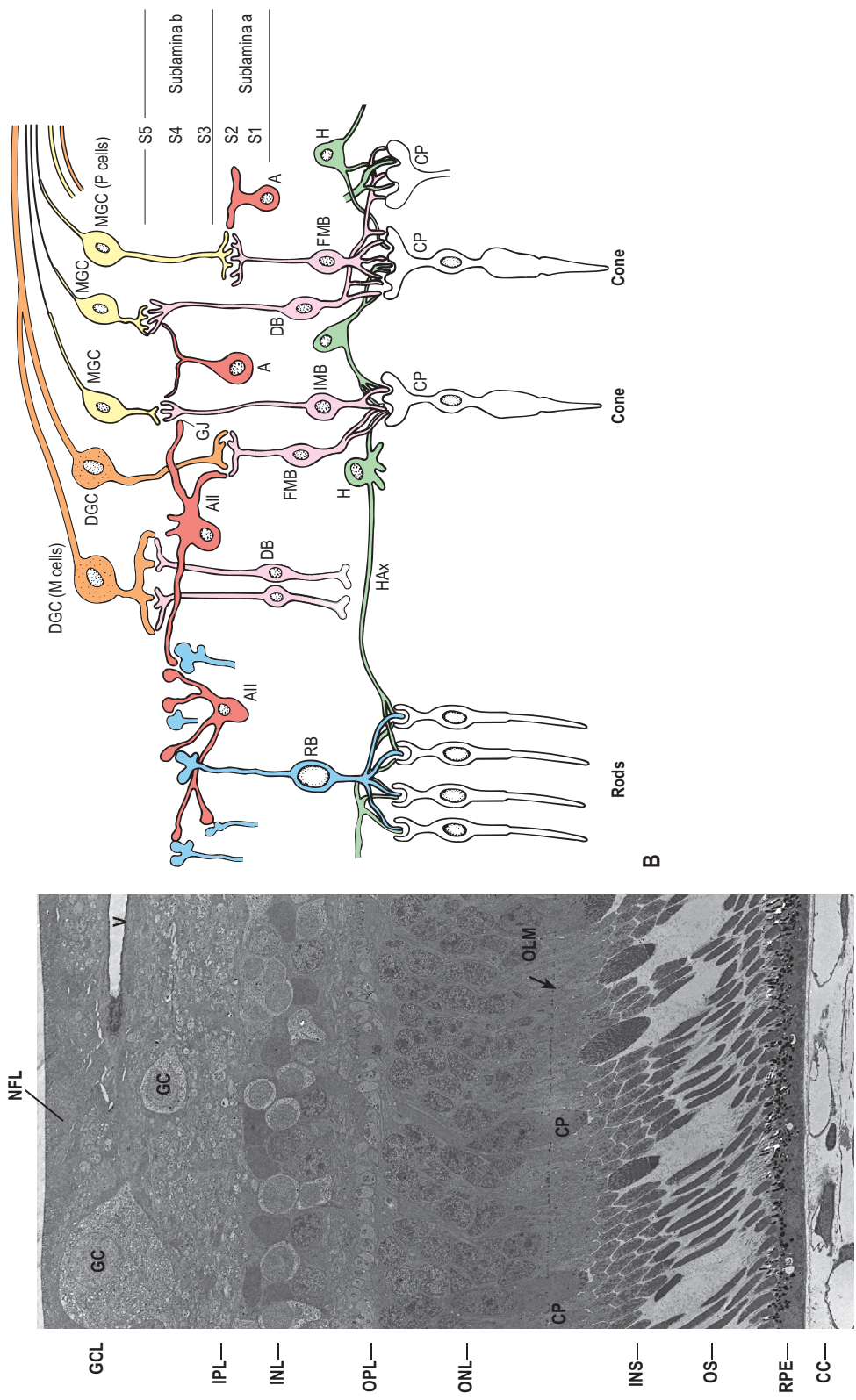


**FIGURE 1-32** (A) Low-power transmission electron micrograph of the primate retina demonstrating the layered arrangement: CC, choriocapillaris; RPE, retinal pigment epithelium; OS, outer segment; INS, inner segments; ONL, outer nuclear layer; OPL, outer plexiform layer; INL, inner nuclear layer; IPL, inner plexiform layer; GCL, ganglion cell layer; GC, ganglion cell; NFL, nerve fibre layer; V, retinal vessel; OLm, outer limiting membrane; CP, cone pedicle. Original magnification:  $\times 930$ . (B) Schematic diagram showing the arrangement and relations of the major cell types in the retina: RB, rod bipolar cell; CP, cone pedicle; H, horizontal cell; HAX, horizontal cell axon; A, cone amacrine cell; All, All (rod) amacrine cell; IMB, invaginating midget bipolar cell; FMB, flat midget bipolar cell; DB, diffuse bipolar cell; MGC, midget ganglion cell; DGC, diffuse ganglion cell; GJ, gap junction.

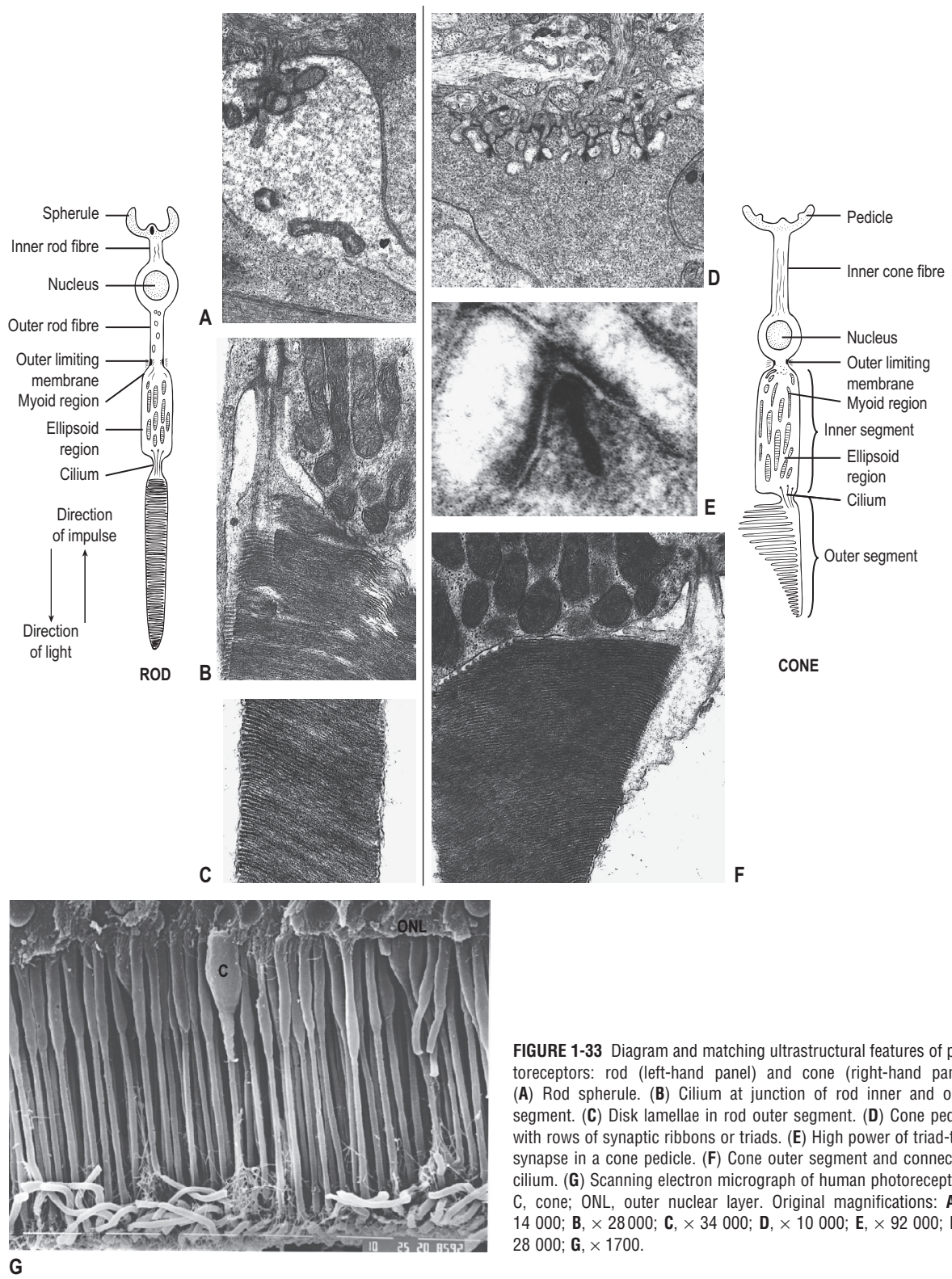


**FIGURE 1-33** Diagram and matching ultrastructural features of photoreceptors: rod (left-hand panel) and cone (right-hand panel). **(A)** Rod spherule. **(B)** Cilium at junction of rod inner and outer segment. **(C)** Disk lamellae in rod outer segment. **(D)** Cone pedicle with rows of synaptic ribbons or triads. **(E)** High power of triad-type synapse in a cone pedicle. **(F)** Cone outer segment and connecting cilium. **(G)** Scanning electron micrograph of human photoreceptors: C, cone; ONL, outer nuclear layer. Original magnifications: **A**,  $\times 14\,000$ ; **B**,  $\times 28\,000$ ; **C**,  $\times 34\,000$ ; **D**,  $\times 10\,000$ ; **E**,  $\times 92\,000$ ; **F**,  $\times 28\,000$ ; **G**,  $\times 1700$ .

membrane (a conceptually useful analogy is to liken them to coins stacked inside a stocking). Each outer segment is only 1–1.5 µm in width (Fig. 1-33A–C,G) and 25 µm in length. The disks are produced at the base of the outer segment (the ciliary connection) and over the course of 10 days travel to the tips, which are enclosed by the apical microvilli of the RPE. Here they are phagocytosed by the RPE cells in a circadian manner (predominantly shed in the early morning). The rods are separated by a modified extracellular ground substance known as interphotoreceptor matrix, which contains a 135 kDa glycolipoprotein, interphotoreceptor binding protein (IRBP). The inner half of the inner segment is known as the *myoid*, the outer half the *ellipsoid* (3 µm in length). The ellipsoid is connected to the outer segment by a modified cilium (nine doublet microtubules without a central pair) (Fig. 1-33B) whose basal body is situated in the ellipsoid. The cilium represents the embryological vestige of the ciliated neuroepithelial cells that line the primitive retinal or optic ventricle (see Ch. 2). The cilium acts as a conduit for metabolites and lipids between the inner and outer segments. The remainder of the ellipsoid contains numerous mitochondria, indicative of the high metabolic activity of these cells. The myoid region contains numerous organelles including Golgi apparatus, smooth endoplasmic reticulum, microtubules and glycogen, evidence of a metabolically and synthetically active cell.

**Cones (Fig. 1-33D–F).** In most diurnal animals two spectrally distinct cone types exist (one maximally sensitive to short wavelengths and one to long wavelengths; known as dichromatic retina); however, in diurnal Old World primates, apes and humans, a third type exists (trichromatic retina). The three types are generally referred to as blue, green and red (or the short, medium and long wavelength) sensitive cones. Cone outer segments are generally shorter than rods and are so called because they are generally conical (6 µm at the base, 1.5 µm at the tip); however, in the fovea they are long, slender and tightly packed (see Fig. 1-30C). The lamellae or disks in cones are not surrounded by a plasma membrane in the same manner as rods but are in free communication with the interphotoreceptor space. Cone disks have a greater lifespan than rods and are not produced in the same manner; in addition, they do not undergo

circadian phagocytosis by the RPE cells. They are surrounded by the long villous melanin-containing apical processes of the RPE.

Cones are about 60–75 µm in length. The outer segment is connected to the mitochondria-rich ellipsoid region (containing around 600 mitochondria per cell) of the inner segment by a cilium similar to that described in rods (Fig. 1-33F). The cell body of the cone can be easily identified histologically in the scleral aspect of the outer nuclear layer because of its large pale-staining nucleus and perinuclear cytoplasm (Figs 1-29 and 1-32A).

The cell bodies of rods and cones are connected by an *inner fibre* to specialized expanded synaptic terminals, known as *spherules* and *pedicles*, respectively. These synapse with bipolar and horizontal cells and contain many highly specialized presynaptic vesicles.

*Rod spherules* lie more scleral than the cone pedicles and are deeply indented by bipolar and horizontal cell processes (telodendria). A specialized region known as a *synaptic ribbon* is present between two adjacent nerve fibres. The horizontal cell telodendria penetrate deeply into the spherule; the bipolar cell dendrites (from one to four cells) have a shallower penetration. Up to five processes may be embedded in one spherule (Fig. 1-33A). There is no apparent contact between rod spherules; however, cone pedicles may be connected by gap junctions.

*Cone pedicles* are broader than rod spherules (7–8 µm) and have a pyramidal shape. In the cone pedicle there are up to 12 indentations, each of which contains three neuronal terminals (*triad*) (Fig. 1-33D,E). The central process in each triad is a midget bipolar cell dendrite (each may have multiple contacts with the same pedicle; Fig. 1-32B). The laterally disposed processes in the triad are horizontal cell processes that may also be involved in several triads on the one pedicle. Thus there may be up to 25 synaptic ribbons in each pedicle (Figs 1-32B and 1-33D,E). Each cone is usually contacted by all the horizontal cells (four to six) in the immediate area or field. Each pedicle also has numerous shallow indentations or synapses with flat diffuse bipolar cells (Fig. 1-32B).

### Bipolar cells (Figs 1-32B and 1-34A)

The retina contains approximately 35.7 million bipolar cells, which comprise several functional and morphological subtypes. They are primarily responsible for

transmitting signals from photoreceptors to ganglion cells, between which they are interposed. Their cell bodies lie in the *inner nuclear layer* and are oriented in a radial fashion parallel to the photoreceptors. Their single or multiple dendrites pass outwards to synapse principally with photoreceptors (but also with horizontal cells), while their single axon passes inwards and synapses with ganglion and amacrine cells. In the foveal region of the central retina the ratio of cones : bipolar cells : ganglion cells can be 1 : 1 : 1, whereas in the peripheral retina one bipolar cell receives stimuli from up to 50–100 rods. In intervening regions the ratio corresponds to the decreasing visual acuity present in the peripheral retina. This summation of stimuli is a crucial factor in the sensitivity of the rod system to low levels of illumination. Bipolar cells have been subdivided in humans into nine morphological subtypes (Figs 1-32B and 1-34A): one rod bipolar type and eight types of cone bipolars. The latter group can be subdivided into five types of diffuse cone bipolars and three types of midget bipolars.

**Rod bipolar cells.** Rod bipolar cells have a receptive field or dendritic tree, which is small in the central retina (15 µm wide, 10–20 rods) and larger in the peripheral retina (30 µm and 30–50 rods). These represent 20% of all bipolar cells and are most dense around the fovea. In the periphery they contact up to 50 rods and synapse with All amacrine cells; only rarely do they synapse directly with diffuse ganglion cells.

**Diffuse cone bipolar cells.** Diffuse cone bipolar cells are concerned with converging information from many cones. Their dendrites fan out (up to 70–100 µm) to end in clusters of between five and seven cone pedicles (can be as high as 15–20). The overlap of adjacent cells of this type is extensive in the perifoveal region.

**Midget bipolar cells.** Invaginating midget bipolar cells are the smallest of the bipolar cells whose dendrites penetrate the base of a single cone pedicle (occasionally two) to form a central element in triads. The near 1 : 1 ratio of midget bipolar cells to cones decreases peripherally. Their dendrites may synapse with amacrine cells and midget ganglion cells.

Flat midget bipolar cells connect single cones with single midget ganglion cells or more rarely may connect several cones. They are similar to invaginating midget bipolar cells except their dendrites do not invaginate deeply into the cone pedicle. Potentially, therefore, most cones can be in contact with these two types of midget bipolar cells (flat and invaginating midget) as well as the diffuse type.

Blue cone-specific bipolar cells (blue S-cone) are present in primates and humans and appear to make invaginating contact with only a limited number of cones in their territory, the suggestion being that these are specifically blue cones.

### Ganglion cells

The cell bodies of most ganglion cells are located in the innermost nucleated layer of the retina (ganglion cell layer) situated between the nerve fibre layer and the inner plexiform layer (Figs 1-29 and 1-32); however, ‘displaced’ ganglion cells have been identified in the inner nuclear layer. Ganglion cells are the last neuronal link in the retinal component of the visual pathway (Fig. 1-32B). Their axons form the nerve fibre layer on the innermost surface of the retina and synapse with cells in the lateral geniculate nucleus of the thalamus. The axons form bundles separated and ensheathed by glial cells (Fig. 1-34E). The bundles leave the eye to form the optic nerve. Upon exiting through the *lamina cribrosa*, the axons become myelinated with oligodendrocytes. There are up to seven layers of ganglion cell bodies in the central retina or fovea (ganglion cell layer is 60–80 µm thick) and as few as one cell layer in the peripheral retina (10–20 µm thick). There are approximately 1.2 million ganglion cells per retina; thus, theoretically, there are approximately 100 rods and four to six cones per ganglion cell. While they are functionally diverse, ganglion cells are characterized morphologically by a large cell body, abundant Nissl substance (arrays of rough endoplasmic reticulum) and a large Golgi apparatus (Fig. 1-34E). They are classified into different types on the basis of cell body size, dendritic tree spread, branching pattern and branching level in the five strata of the inner plexiform layer (Fig. 1-32B,C). Some ganglion cells in the macular area may contain yellow (xanthophyll carotenoid) pigment in the cytoplasm, although the cone axons and Müller cells are thought to also

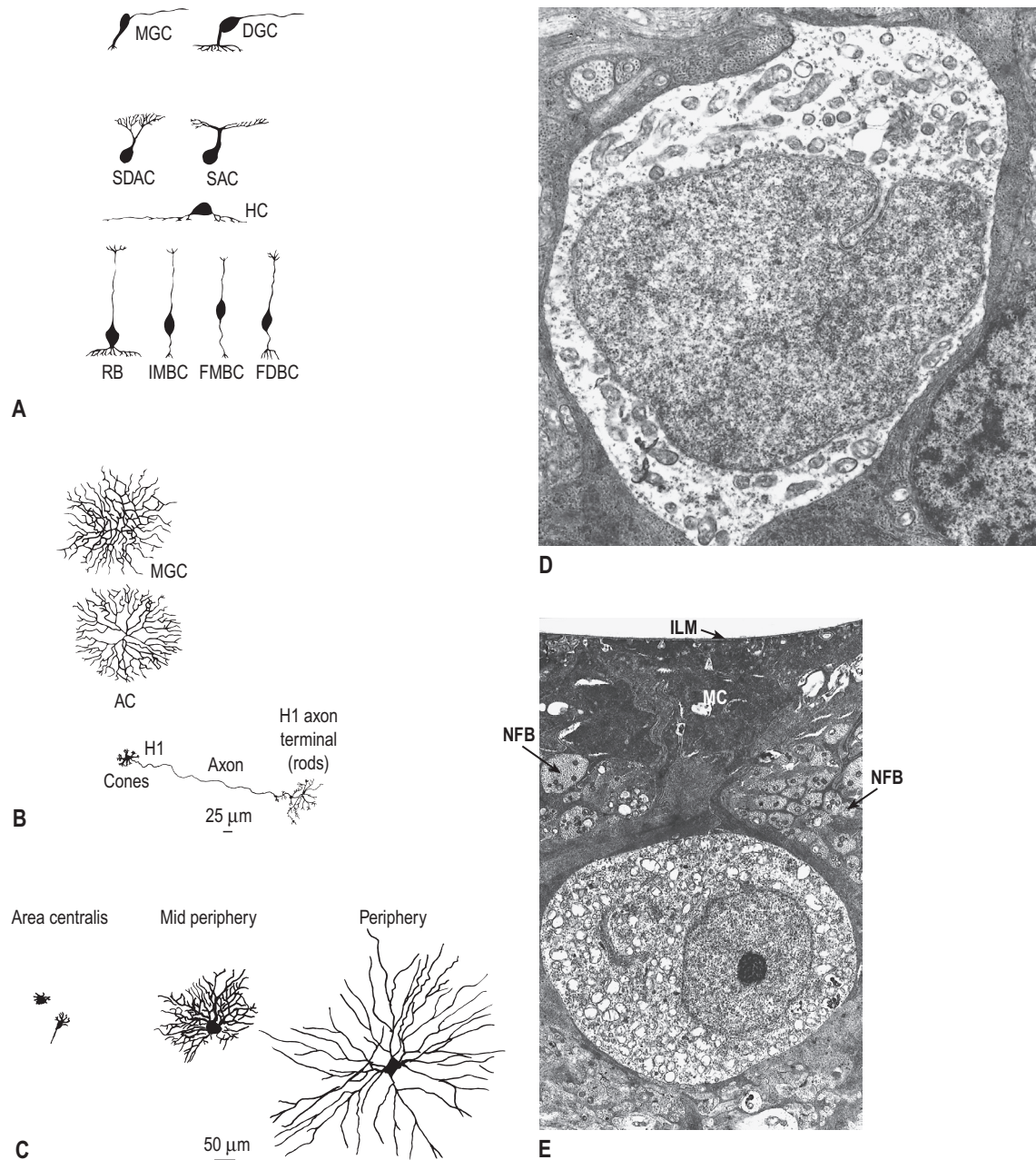


**FIGURE 1-34** (A) Diagram showing the arrangement and location of major neuronal cell types as seen in Golgi-stained preparations in relation to their position in the layers of the retina: DGC, diffuse ganglion cell; FDBC, flat diffuse bipolar cell; FMBC, flat midget bipolar cell; HC, horizontal cell; IMBC, invaginating midget bipolar cell; MGC, midget ganglion cell; RB, rod bipolar; SAC, stratified amacrine cell; SDAC, small diffuse amacrine cell. (B) Shape of dendritic fields of midget ganglion cell (MGC), amacrine cell (AC) and H1 horizontal cell (HC) as seen in Golgi preparations or single cell injections in retinal whole mounts. (C) Cat ganglion cells increasing in dendritic tree span with increasing eccentricity from the fovea. (Parts B and C, after Kolb et al., 1992, 1994.) (D) Electron micrograph of amacrine cell. (E) Ganglion cell body and adjacent nerve fibre bundles (NFB): ILM, inner limiting membrane; MC, Müller cell. Original magnifications: D,  $\times 7100$ ; E,  $\times 4200$ .

contain these pigments in the macular region. Impulses are received primarily from bipolar cells and amacrine cells via axodendritic and axosomatic synapses, the former occurring predominantly in the inner plexiform layer (Fig. 1-32B) where their dendrites repeatedly branch to form the ‘dendritic tree’, whose form and size varies considerably and may be correlated with location in the retina and therefore function (receptive field size) (Fig. 1-34B,C). The morphological diversity of ganglion cells (up to 25 types in mammalian and 18 types in human retinas) has prompted classification of these cells into categories,  $\alpha$ ,  $\beta$  and  $\gamma$ , or X, Y and W types, predominantly based on research in the cat.

Recently a non-rod, non-cone photoreceptive pathway, arising from a population of retinal ganglion cells, was discovered first in nocturnal rodents and then in primates. These ganglion cells express the putative photopigment melanopsin and by signalling gross changes in light intensity serve the subconscious, ‘non-image-forming’ functions of circadian photoentrainment and pupil constriction. The primate retina, in addition to being intrinsically photosensitive, is strongly activated by rods and cones to signal irradiance over the full dynamic range of human vision. Thus, in the diurnal trichromatic primate, ‘non-image-forming’ and conventional ‘image-forming’ retinal pathways are merged, and the melanopsin-based signal might contribute to conscious visual perception.

**Midget ganglion cells.** These cells synapse exclusively with amacrine cells and one midget bipolar cell (and thus usually one cone) (Fig. 1-32B). Dendritic spread is around 5–10  $\mu\text{m}$  in diameter in the central retina; however, this increases 10-fold in a zone of 2–6 mm eccentricity and attains a maximum of over 100  $\mu\text{m}$  (Fig. 1-34C). Neighbouring midget ganglion cell dendritic fields do not overlap but form mosaics. In humans they are also known as P-cells because they project to the parvocellular layer of the lateral geniculate nucleus (LGN).

**Diffuse (parasol) ganglion cells.** These comprise a large synaptic field with all types of bipolar cells except midget bipolar cells. They occur in the central retina and their cell bodies (soma) are 8–16  $\mu\text{m}$  in diameter with 30–70  $\mu\text{m}$  dendritic fields, these being

smaller nearer the fovea than the periphery. They are also known as M-cells because they project to the magnocellular layer of the LGN.

The finding that midget ganglion cells synapse exclusively with the midget bipolar cells, and that both are common near the fovea, provides the anatomical basis for the observation of small receptive fields and high visual acuity in this region. There are five types of diffuse ganglion cell, classified on the basis of morphology. The anatomical basis of antagonistic fields surrounding receptive fields is complex, although they do not appear to vary much in size from within an 8 mm radius of the fovea. The basis of the antagonist field may be the lateral extensions of the amacrine cell, with its extensive interconnections with ganglion cell dendrites and bipolar cells as well as fellow amacrine cells.

### Association neurones (amacrine and horizontal cells) (Figs 1-32B and 1-34A,B)

**Horizontal cells.** These cells derive their name from the extensive horizontal extensions of their cell processes. There are two distinct morphological varieties in the retina of most species, of which the cat is the most extensively studied: type A is a large sturdy axonless cell with stout dendrites that contact only cones; type B has a smaller bushier dendritic tree that contacts cones exclusively but, in addition, has an axon up to 300  $\mu\text{m}$  in length that ends in extensive arborization that is postsynaptic only to rods (Figs 1-32B and 1-34B). Type A cells have much larger receptive fields than type B. In primates it appears that the two types of horizontal cell, HI (approximates to type B) and HII (approximates to type A), both possess axons. A third type (HIII) has been described in the human

### BOX 1-19 CLINICAL CORRELATES

#### Proliferative vitreal retinopathy

When injured, the retina frequently responds by forming astroglial scars. Indeed, normal age-related degenerative processes in the peripheral retina (microcystoid degeneration) are accompanied by astrocyte proliferation. Disruption of the inner limiting membrane can lead to astrocyte proliferation in the subhyaloid space and in the vitreous itself.

retina. Each rod has connections with at least two horizontal cells and each cone with three or four horizontal cells of each type. In primates the stout dendrites of HII cell soma processes contact around seven cones near the fovea (dendritic tree covering 15 µm); this number increases to as many as 18 further from the fovea (dendritic tree covering 80–100 µm). The axon from HII cells passes laterally and terminates up to 1 mm away in a thickened axon terminal bearing a fan-shaped protrusion of lollipop-like endings in rod spherules (up to 100) (Fig. 1-34B). HII dendritic trees are more spidery and contact about twice as many cones. Their axons are generally shorter (100–200 µm) and contact cone pedicles by small wispy terminals. The manner of their insertion is depicted in Figure 1-32B. Their cell bodies are located primarily in the outer part of the inner nuclear layer. They have few distinctive cytoplasmic organelles except the crystallloids, a series of densely stacked tubules with associated ribosomes. Their processes ramify in the outer plexiform layer close to the cone pedicles. The overlap between horizontal cells is considerable and any one area of retina may be served by up to 20 horizontal cells. Horizontal cells have an integrative role in retinal processing and release inhibitory neurotransmitters, mainly  $\gamma$ -aminobutyric acid (GABA). Recent evidence suggests that there is some colour-specific wiring for the three types of horizontal cells in the human retina.

**Amacrine cells (Figs 1-32B and 1-34D).** These association neurones were thought to lack axons; however, recent studies have shown that some do indeed possess an axon. They are located in the vitread or inner aspect of the inner nuclear layer (bipolar cell layer) and are distinguishable as a result of their larger size (12 µm) and oval shape. They display a remarkable degree of diversity. There are at least 25 different types in the monkey and human retina. Their cell body is usually flask-shaped and the numerous dendritic processes of these cells ramify and terminate predominantly in the synaptic complexes formed by the bipolar and ganglion cell processes, namely the inner plexiform layer. The shape of their dendritic fields is highly variable and a few examples are shown in Figure 1-34A,B. They can be divided into subtypes on several criteria such as the stratification of their dendrites in the inner plexiform layer or their shape;

for example, diffuse, starburst and stratified. Diffuse types can cover narrow fields (approximately 25 µm wide), their fibres being cone-shaped. Other types may spread their axon-like processes several millimetres. They may also be classified on the basis of their neurotransmitters. Amacrine cells may be GABAergic and dopaminergic or can release acetylcholine indicating, together with their morphology, that these cells play a role in modulation (most probably inhibitory) of signals reaching ganglion cells. A subclass of amacrine cells are also thought to be the principal source of the peptide somatostatin, an important neuroactive peptide, in the retina. It may function as a neuromodulator or trophic factor.

### Retinal neuroglia

**Astrocytes.** Astrocytes are not the principal or predominant glial cell in the retina. This role is fulfilled by Müller cells, which are analogous to central nervous system oligodendrocytes. Astrocytes are predominantly located in the nerve fibre layer, ganglion cell layer, inner plexiform layer (site of cell bodies), and their outer limit is the vitread aspect of the inner nuclear layer in humans. They form an irregular honeycomb scaffold between vessels and neurones perpendicular to the Müller cells. They may occur as fibrous (elongated) or protoplasmic (rounded) astrocytes. They both contain abundant cytoplasmic structural fibrils (10 nm in diameter) consisting of glial fibrillary acid protein (GFAP) (Fig. 1-35B). Astrocytes are often oriented perpendicular to the direction of the neurone cell bodies or processes, such as in the nerve fibre layer (Fig. 1-35). It seems their role may be to isolate the receptive surfaces of neurones in the retina, thus preventing unwanted signals or effects in neighbouring neurones. They have abundant intracytoplasmic glycogen and form 'gap junctions' with neighbouring astrocytes. Their pedicles or foot processes were once believed to constitute an important functional component of the blood-retinal barrier (see below).

**Müller cells.** Müller cells (Fig. 1-36A,B) are the principal supporting glial cells of the retina and are considered analogous to central nervous system radial glial or ependymal cells. They have a radial orientation and extend through the depths of the retina from the inner surface, where their expanded 'foot process' lies

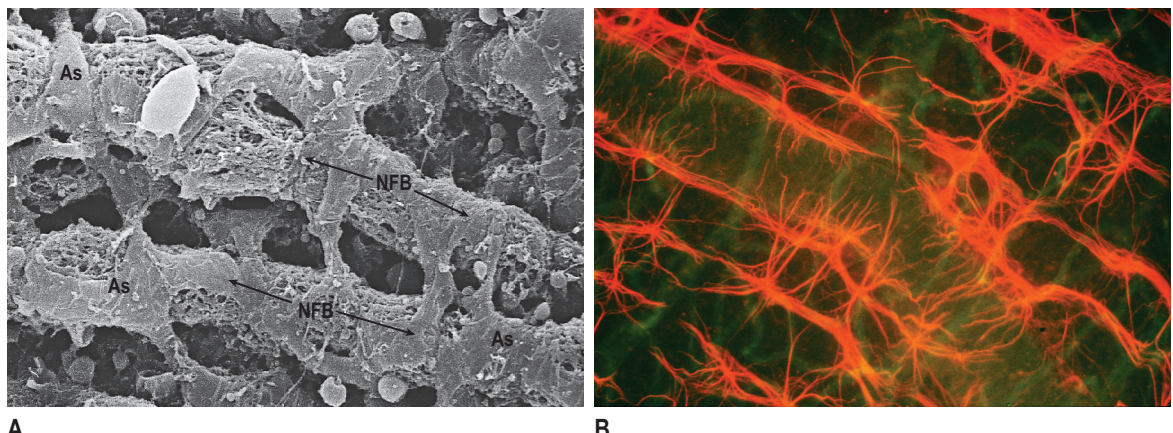


**FIGURE 1-35** (A) Scanning electron micrograph (viewed from the vitreous aspect) of astrocytes (As) surrounding nerve fibre bundles (NFB) in the inner retina (the inner limiting membrane has been removed to expose the underlying nerve fibre layer). (B) Double-colour immunofluorescence illustrating the relations of astrocytes shown with an antibody to glial acidic fibrillary protein (GFAP) (red) and lectin-stained vessels (pale green). Vn, retinal vein; C, capillaries. Original magnifications: **A**,  $\times 1500$ ; **B**,  $\times 150$ . (Part B courtesy of Dr T. Chan-Ling.)

adjacent to the inner limiting membrane, to their outer limit where they have adherens junctions with photoreceptor inner segments to form the external limiting membrane. They envelop blood vessels, neuronal cell bodies and processes, creating glial ‘tunnels’ via a series of cytoplasmic processes, as shown in Figure 1-36A,B. Müller cells in humans contain little glycogen, in contrast to species with avascular retinae. Their cytoplasm contains abundant endoplasmic reticulum and microtubules, reflecting their role in protein synthesis, intracellular transport and secretion (Fig. 1-36C). These cells may help to nourish and maintain the outer retina, which lacks a direct blood supply.

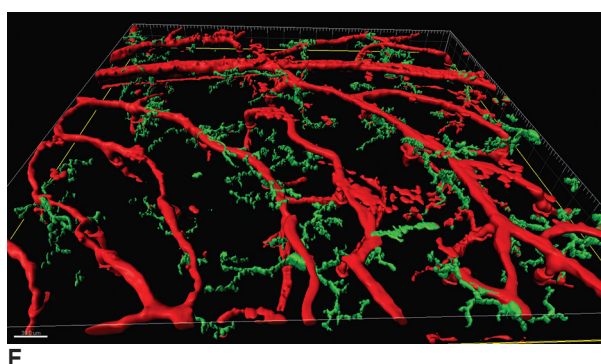
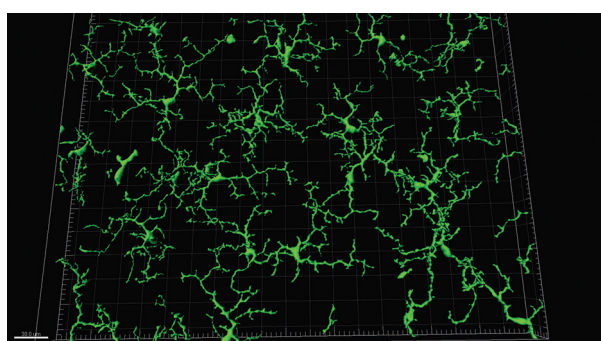
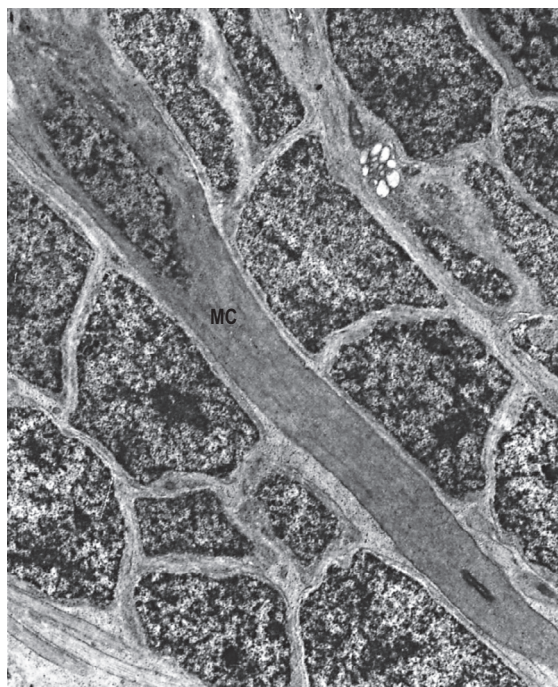
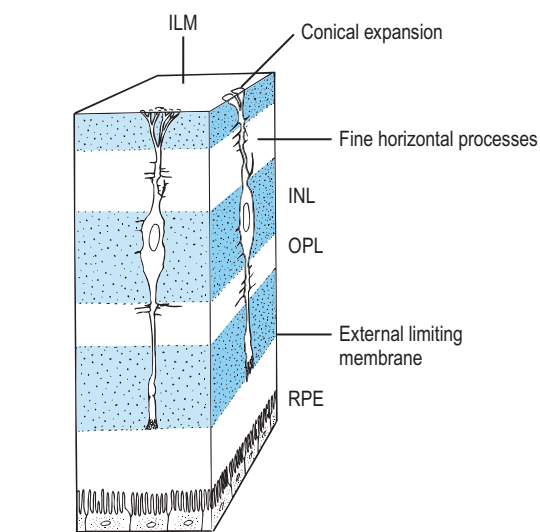
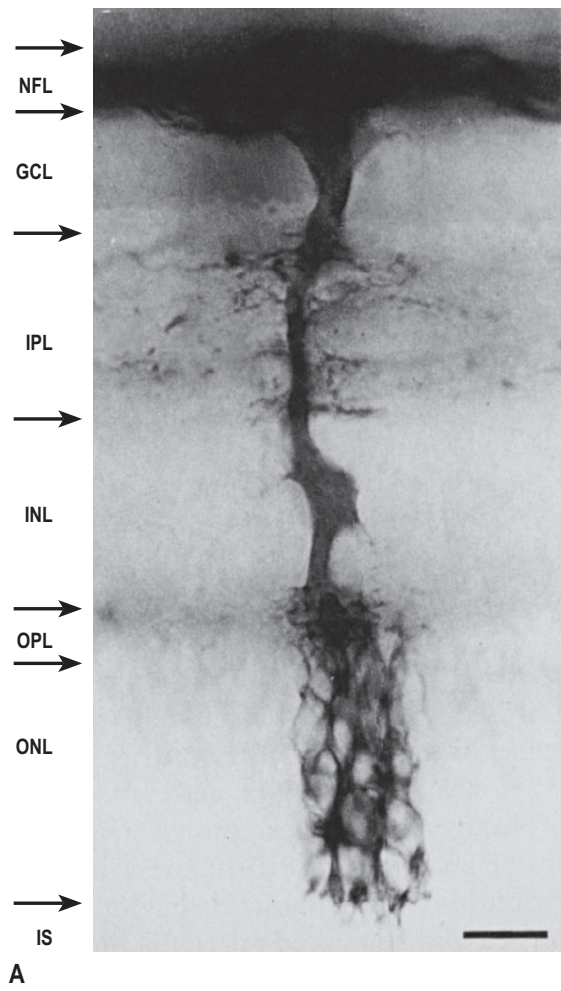
While there is extensive coupling between astrocytes and Müller cells, which allows the exchange of tracer molecules, recent studies have demonstrated an absence of significant spread of spatial buffer current between retinal glial cells. Both astrocytes and Müller

cells have high  $K^+$  membrane conductances, and most spatial buffer current will flow out through these conductances rather than spreading into neighbouring glial cells through gap junctions. In contrast to electrical coupling, chemical coupling between astrocytes is sufficiently strong to mediate propagation of intercellular signals such as the spread of metabolites and ions between glial cells. Coupling between glial cells, therefore, could serve to enhance the transport of key

#### BOX 1-20 AGEING CHANGES IN MACROPHAGE POPULATIONS IN THE RETINA

With age there is an increasing tendency in animals for microglia to assume a more amoeboid form and activated phenotype and migrate towards the subretinal space. In humans this is evident especially in the peripheral retina close to age-related cystoid retinal degeneration.

**FIGURE 1-36** (A) Micrograph of a horseradish peroxidase (HRP) filled Müller cell in the rabbit retina. The dark band at the top of the micrograph is composed of Müller cell endfeet and the labelled axons of ganglion cells in the nerve fibre layer. The Müller cells possess side-processes that form different strata in the inner plexiform and they send numerous processes to wrap around the somata of photoreceptors: NFL, nerve fibre layer; GCL, ganglion cell layer; IPL, inner plexiform layer; INL, inner nuclear layer; OPL, outer plexiform layer; ONL, outer nuclear layer; IS, inner segments. (B) Diagram of the shape and position of a Müller cell: RPE, retinal pigment epithelium. (C) Morphology of a Müller cell (MC) within the outer nuclear layer. Note the intracytoplasmic microfilaments. (D) Microglial cells (specialized macrophages) in a retinal whole mount from a transgenic mouse in which eGFP is expressed alongside the locus for the chemokine receptor CX<sub>3</sub>CR1. All microglia in these animals express CX<sub>3</sub>CR1 and thus appear fluorescent green in confocal microscopy. (E) 3D-rendered retinal microglial network in a retinal wholemount in which retinal vessels have been highlighted (red) by perfusion of a vascular dye. Original magnifications: **A**, bar 10 mm; **B**,  $\times 4400$ ; **C**,  $\times 200$ . (Part A courtesy of Dr. S. Robinson.)

**FIGURE 1-36**

For legend see opposite page.

metabolites, such as glutamate, glutamine and lactate, both into and out of glial cells, by allowing them to diffuse between neighbouring cells in the glial syncytium. Clearly the underlying arrangement of both astrocytes and Müller cells reflects this function.

**Microglia.** Microglia (Fig. 1-36D,E) are a highly specialized subpopulation of the mononuclear phagocyte system that reside in the parenchyma of the central nervous system. These cells most likely arise from yolk sac precursors during early development and may be replenished in adulthood by bone marrow-derived monocytes. They are characterized by an extremely arborized morphology and an immunophenotype of resting macrophages. In the retina, their cell bodies are located largely in three strata, one at the nerve fibre layer–ganglion cell layer interface, one in the inner nuclear layer and another in the outer plexiform layer, although the latter is more obvious in the rodent than human retina. Their processes form a lateral and vertical three-dimensional network within the retina extending only as far as the outer limiting membrane in the normal eye. Less arborized subtypes, sometimes referred to as perivascular macrophages, which closely resemble homologous cells in the parenchyma of the brain, are associated with the perivascular space of retinal capillaries (see Fig. 1-38C), although they are less numerous than brain perivascular macrophages. Retinal microglia share many properties with brain microglia including tissue homeostasis and host defence. Their highly arborized processes are constantly on the move sampling their immediate microenvironment. Upon injury to the retina these cells become activated and assume the role of wandering phagocytes. Activated microglia play a role as immune effectors, via the release of chemokines and cytokines; however, their role as potential antigen-presenting cells (they are predominantly MHC class II<sup>+</sup>), or indeed as immunomodulators limiting leucocyte infiltration of the retina, is controversial.

#### Blood supply of the retina (Figs 1-30A and 1-37)

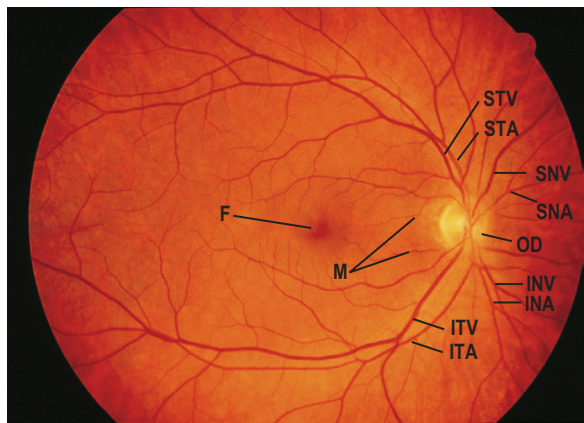
The retina is an extremely metabolically active sheet of neural tissue with the highest oxygen consumption (per weight) of any human tissue. Like the brain, the retina has a highly selective blood–tissue barrier, which serves primarily to regulate the optimal

extracellular environment to facilitate neural transmission. It also regulates the passage of pathogens and intravascular leucocytes, thus partly protecting the neural environment from ‘surveillance’ by immune cells. In humans, the retina has a dual blood supply (holangiotic), the inner two-thirds being nourished by branches from the central retinal vessels, while the outer one-third is nourished by the choroidal circulation. The choroidal circulation has a high flow rate (150 mm/s), low oxygen exchange and a fenestrated capillary bed; the retinal circulation has a low flow rate (25 mm/s) and high oxygen exchange. The blood–retinal barrier is defined by two sets of characteristics. The first is the structural character of the endothelial and RPE cells located at the endothelial and RPE tight junctions, and the second is the membrane-associated transport characteristics.

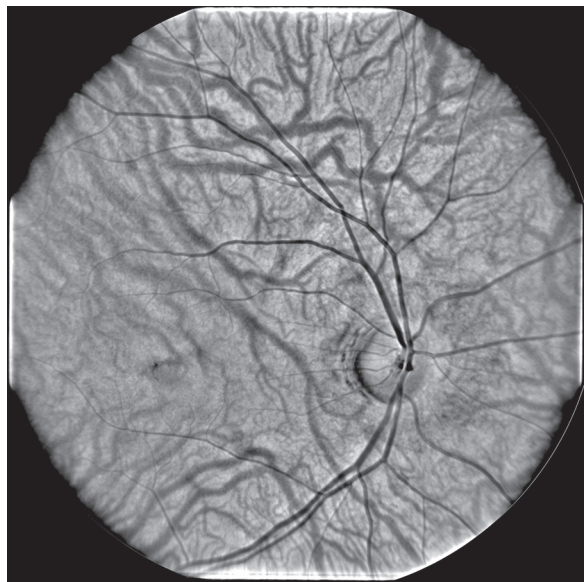
#### Central retinal artery and branches (Figs 1-30A,

1-37 and 1-38).

This vessel (0.3 mm in diameter) arises from the ophthalmic artery either in the optic canal or close to the optic foramen where the ophthalmic artery lies bound to the dural covering of the nerve (see p. 59). The central retinal artery then travels forward on the undersurface of the nerve within its dural covering. About 1–1.5 cm behind the eye it pierces the inferomedial aspect of the remainder of meningeal coverings to pass through the subarachnoid and then pierces the nerve. As it passes forward in the centre of the optic nerve, the artery is accompanied by the central retinal vein and a few sympathetic fibres. It resembles other muscular arteries and indeed is affected by conditions such as atheroma and giant cell arteritis. It pierces the papilla centrally, having passed through a constriction or gap in the lamina cribrosa (see Fig. 1-42E). This is a potential site for partial or complete occlusive disease. It branches into superior and inferior branches, which subdivide into nasal and temporal arteries, a pattern best appreciated and investigated clinically by fluorescein angiography. A small vessel, the cilioretinal artery, may be present near the optic nerve head and provide a small anastomotic connection between the choroidal and retinal circulations. The central retinal artery diameter decreases to 100 µm upon emerging from the disk. The large retinal arterial branches travel in the nerve fibre layer beneath the inner limiting membrane.



A



B

**FIGURE 1-37 (A)** Wide-field photograph of the normal human fundus: F, fovea; OD, optic disk; M, macular vessels; STV and STA, superior temporal vein and artery; ITV and ITA, inferior temporal vein and artery; INV and INA, inferior nasal vein and artery; SNV and SNA, superior nasal vein and artery. **(B)**, Multispectral digital ophthalmoscopic image of retinal and choroidal circulations. This new technique captures high-resolution image data through the retinal and subretinal layers and hence shows the larger vessels of the choroidal circulation. It both expands the examination wavelength range to include image data from invisible wavelengths of light and also generates the probe wavelengths to separate specific spectral regions for enhanced visibility and discrimination. No intravascular contrast is used in this method of visualizing the fundus. (Part A courtesy of C. Barry; Part B, courtesy of Annidis (Canada).)

These vessels have no internal elastic lamina (which is lost at the optic disk) and are thus not affected in temporal arteritis. They possess a well-developed muscularis, and numerous pericytes lie within the endothelial basal lamina. Each of its four major branches (Figs 1-30A and 1-37) supplies a sector of the retina between which there is no overlap, i.e. they are *functional end-arteries*. The superior and inferior temporal arteries curve above and below the macula and foveal region. Arteries pass over veins and may in some pathological situations cause ‘nipping’ or narrowing of the veins. There are two main levels of capillary networks, which spread like a vast cobweb throughout the retina (Fig. 1-38B). The inner plexus is situated at the level of the ganglion cell layer and the outer plexus at the level of the inner nuclear layer. The concept of these two laminae is not universally accepted, although patterns of vascular disease support the concept (see Ch. 9). There may be up to four layers of capillaries in the peripapillary zone, and single layers in the perifoveal region and at the ora serrata.

In the human, retinal capillaries pass only as far as the scleral margin of the inner nuclear layer, the outer retina being normally avascular. Capillaries are most dense in the macula but are absent from the fovea itself (capillary-free zone 500 µm in diameter), which is thus dependent on the choriocapillaris for nutritional support. Larger arterioles are surrounded by a capillary-free zone. Capillary network density decreases towards the peripheral retina.

Retinal capillaries are characterized by complete circumferentially oriented endothelial cells joined by non-leaky tight junctions (*zonulae occludentes*); however, the high number of endocytotic vesicles suggests that they are more permeable than brain capillaries (Fig. 1-38C,D). They are surrounded by a thick basal lamina, pericytes and astrocyte foot processes (Fig. 1-38C), which are four times more numerous around retinal vessels than brain capillaries and may act as a second front in the blood-retinal barrier and thus compensate for the more permeable nature of retinal vascular endothelium. The numbers of these supportive cells decrease in diabetes, macroglobulinaemia and other ischaemic diseases (see p. 503).

The luminal diameter of retinal capillaries (3.5–6 µm) is somewhat smaller than that of conventional capillaries. There is very little extravascular

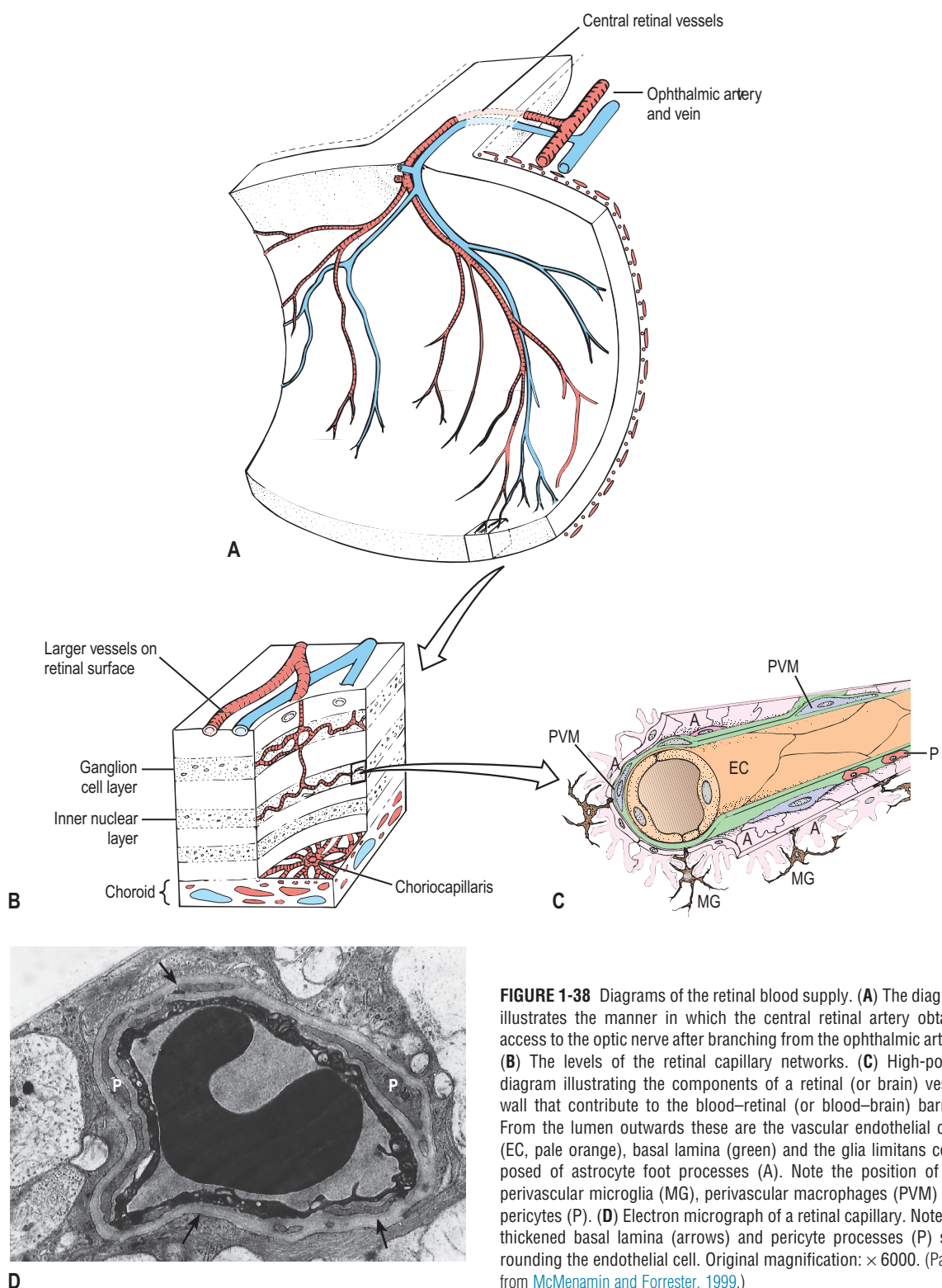


**FIGURE 1-38** Diagrams of the retinal blood supply. (A) The diagram illustrates the manner in which the central retinal artery obtains access to the optic nerve after branching from the ophthalmic artery. (B) The levels of the retinal capillary networks. (C) High-power diagram illustrating the components of a retinal (or brain) vessel wall that contribute to the blood-retinal (or blood-brain) barrier. From the lumen outwards these are the vascular endothelial cells (EC, pale orange), basal lamina (green) and the glia limitans composed of astrocyte foot processes (A). Note the position of the perivascular microglia (MG), perivascular macrophages (PVM) and pericytes (P). (D) Electron micrograph of a retinal capillary. Note the thickened basal lamina (arrows) and pericyte processes (P) surrounding the endothelial cell. Original magnification:  $\times 6000$ . (Part C from McMenamin and Forrester, 1999.)

**BOX 1-21 CLINICAL CORRELATES**

Besides the capillaries described above, a further lamina fans out over the nerve fibre layer in the peripapillary region. This unique radial capillary network may be more vulnerable to raised intraocular pressure in glaucoma because of the long course of these vessels (over 1000 µm), infrequent arterial input and lack of anastomoses. Flame-shaped haemorrhages (due to hypertension or papilloedema) or cotton-wool spots (in ischaemic disease) occur predominantly in this unusual capillary network.

connective tissue around retinal vessels. Mast cells, a common perivascular element in other tissues, including the choroid, are absent in the retina, which has a high threshold of tolerance to histamine. There are *no lymphatic vessels* in the retina.

**THE CHOROID**

The choroid (Fig. 1-39A–G) is the posterior portion of the middle vascular coat of the eye, the *uveal tract*. It is homologous to the pia–arachnoid of the brain. The choroid is a thin, highly pigmented, vascular, loose connective tissue situated between the sclera and the retina, whose principal function is to nourish the outer layers of the retina. It also acts as a conduit for vessels travelling to other parts of the eye and may also have a thermoregulatory role. Furthermore, absorption of light by choroidal pigment aids vision by preventing unwanted light from reflecting back through the retina as occurs in some nocturnal species that possess a tapetum. The regulation of blood flow in the choroid may also influence intraocular pressure by affecting perfusion rates of the ciliary processes.

The choroid extends from the optic nerve margins to the ciliary body and, although its thickness is probably dependent on blood flow dynamics and has a diurnal variation, it is quoted as being approximately 220 µm at the posterior pole and 100 µm anteriorly. Its inner surface is smooth and forms part of Bruch's membrane beneath the RPE. The outer surface, the suprachoroid, is irregular and firmly attached to the lamina fusca of the sclera. Histologically the human choroid consists of Bruch's membrane, the choriocapillaris, a vascular layer and the suprachoroid (Fig. 1-39C).

**BOX 1-22 CLINICAL CORRELATES****Central retinal artery occlusion**

This condition is a vivid reminder of the 'functional end-artery' status of the retinal blood supply. In complete central retinal artery occlusion, irreversible changes occur after 1–2 hours and the inner retina becomes white and oedematous except at the fovea, which survives owing to the underlying choroidal circulation, which shows through as a round red patch.

**Bruch's membrane (lamina vitrea)**

This modified connective tissue layer is 2–4 µm thick and histologically appears as an acellular glassy membrane beneath the RPE (Figs 1-31A,B and 1.39F,G). Bruch's membrane comprises five layers: the RPE basal lamina (0.3 µm thick) (not truly part of the choroid); an inner collagenous zone; a middle elastic layer (incomplete interwoven bands or perforated sheets of elastic 'fibres'); an outer collagenous zone (which blends with the stroma between the choriocapillaris); and the basement membrane of the endothelial cells in the choriocapillaris. Age-related changes in Bruch's membrane lead to areas of diffuse or discrete thickening known as drusen (see Ch. 9, pp. 514).

**Choriocapillaris**

This is an extraordinarily rich bed of wide-bore fenestrated capillaries that extends only as far anteriorly as the ora serrata and functions to provide nutritional support for the outer retina, especially the photoreceptors. The capillary 'network' is more akin to a perforated vascular 'net' than a network of capillaries (Fig. 1-39B,D,E).

The bore of the capillaries (20–40 µm) and the density of the 'net' (Fig. 1-39D) are greatest near the macula. The capillaries are fenestrated (75–85 nm diameter) on their retinal aspect (Fig. 1-39F,G) and these fenestrae occur at a density of approximately 46 per µm<sup>2</sup>. Smooth muscle cells are not usually present in this layer. This sheet or net of capillaries is fed from arterioles, from the layer composed of arterioles and venules (Sattler's) in the manner depicted in Figure 1-39B, i.e. hexagonal patches or 'lobules' of choriocapillaris are fed by a central precapillary arteriole that runs perpendicular to the flat choriocapillaris. This lobular pattern is clinically significant because

### BOX 1-23 COMPARATIVE ANATOMY

#### **Tapetum is the cause of 'eye shine'**

Many mammalian (carnivores, ruminants, cetaceans, seals) and non-mammalian (fish, crocodiles) species possess a reflective tapetum that may serve to increase photoreception in low light conditions. This may be located in the choroid or the retinal pigment epithelium (RPE). The choroidal tapetum may be cellular or fibrous and may occupy only part, usually the upper portion, of the globe. In carnivores it generally consists of several layers of flattened cells containing reflective material (e.g. guanine, zinc cysteine). In ruminants (e.g. cows, sheep) and cetaceans (dolphins) it is fibrous (tapetum fibrosum) and consists of fine regularly arranged collagen bundles which cause diffractive patterns depending on their orientation. A retinal tapetum generally consists of lipid (e.g. opossum) or guanine (fish, crocodiles) deposits within the RPE.



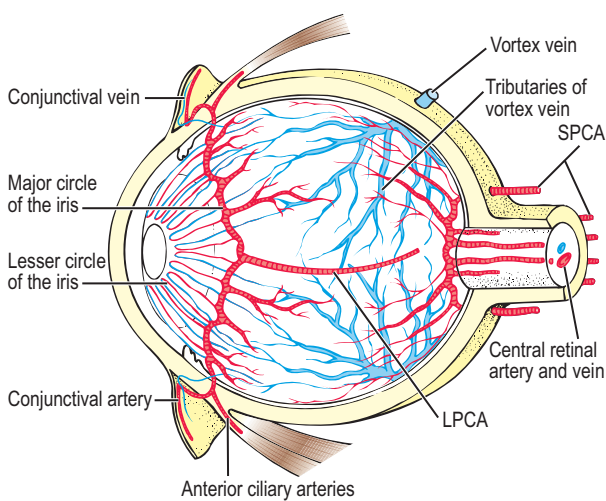
**FIGURE 1-39** (A) Diagram of the uveal tract blood supply. (B) Schematic representation of the hexagonal units in the choriocapillaris fed by small arterioles. (C) Semi-thin resin section of the outer retina and choroid in the primate eye. Note the heavy degree of pigmentation and the layers of the choroid. (D) Resin vascular cast of the choriocapillaris viewed from the retinal aspect. (E) Resin vascular cast of a quadrant of the choroid viewed from the external aspect showing a large vortex vein (VV). (F) Low-power electron micrograph of the retinal pigment epithelium, Bruch's membrane (BM) and the closely related choriocapillaris in a primate eye. (G) Higher-power electron micrograph of the basal aspect of the RPE with its basal lamina forming part of Bruch's membrane. Note the fenestrated capillaries (FC) in the endothelial lining of the choriocapillaris. Note the capillary endothelial cells are characterized by fenestrae (FC) on the retinal aspect adjacent to Bruch's membrane. RPE, retinal pigment epithelium; CC, choriocapillaris; HL, Haller's layer; SL, Sattler's layer; M, melanocyte; SPCA, short posterior ciliary arteries; LPCA, long posterior ciliary arteries. Original magnifications: C,  $\times 350$ ; D,  $\times 35$ ; E,  $\times 120$ ; F,  $\times 2400$ ; G,  $\times 14\,000$ .

choroidal ischaemia often occurs as pale hexagonal patches (mosaic pattern). The venous channels drain the periphery of these lobules (Fig. 1-39B).

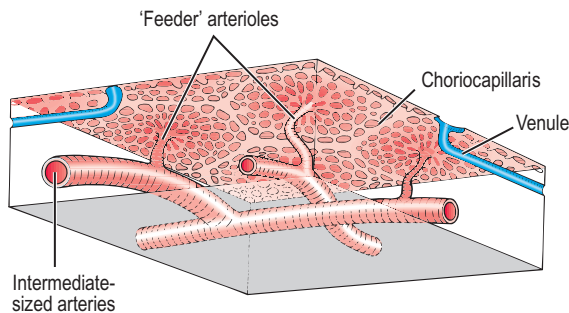
#### **Vascular layer**

This layer (Fig. 1-39C) lies beneath the choriocapillaris and can be subdivided into an inner layer of intermediate-sized vessels (arterioles and venules, Sattler's layer) and an outer component (major arteries and veins, Haller's layer). The blood supply of the choroid is chiefly from the long and short posterior ciliary arteries, although recurrent branches from the anterior ciliary arteries anastomose with anterior choroidal vessels (Fig. 1-39A). Venous drainage occurs via a series of large vortex veins (venae vorticosae), of which there are usually four (but may be up to six), each draining a sector of the choroid (Fig. 1-38B). These large veins pierce the sclera through emissary canals (Figs 1-17A, and 1-39A,E) and drain into the superior and inferior ophthalmic veins in the orbit.

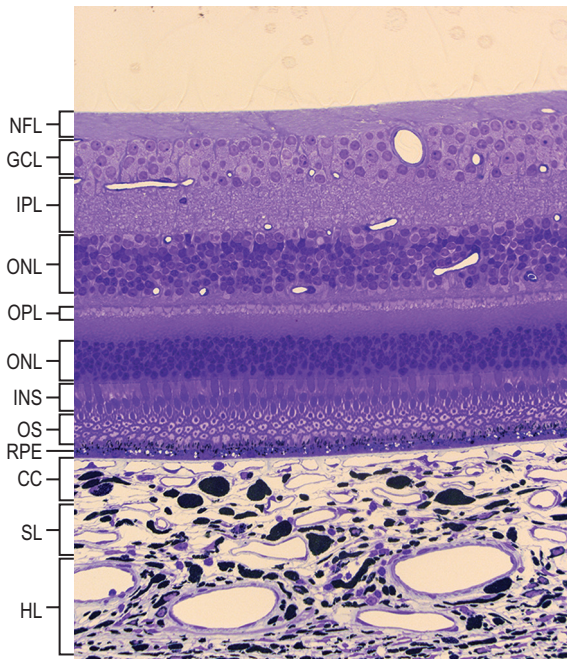
The choroidal stroma consists of randomly arranged collagen fibres (type I), flattened ribbon-like elastic fibres, fibrocytes and numerous melanocytes (Fig. 1-39C,F). The extent of choroidal pigmentation influences the appearance of the fundus, with the highly pigmented choroid of darker-skinned people showing through more than in the fundus of a person with less skin pigmentation, in which the red-orange reflex is primarily the result of the choroidal vasculature. The choroid, being a connective tissue, contains resident populations of immunocompetent cells including occasional plasma cells and lymphocytes, numerous perivascular mast cells (Fig. 1-40A, B) and networks of resident tissue macrophages and dendritic cells (Fig. 1-41).



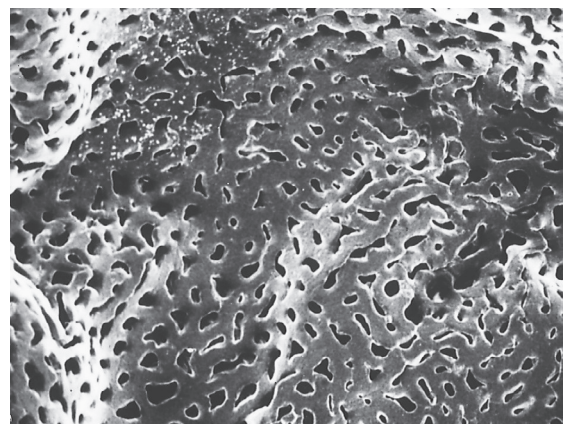
**A**



**B**



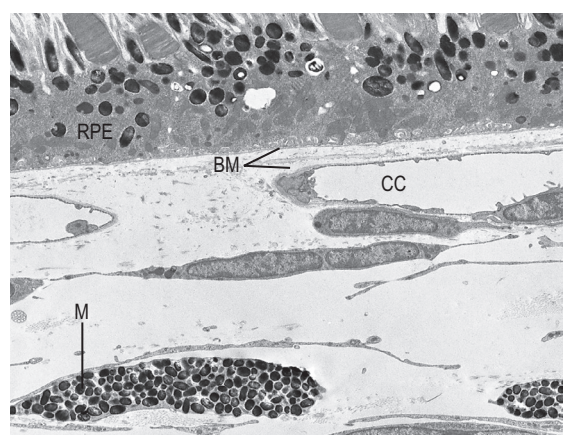
**C**



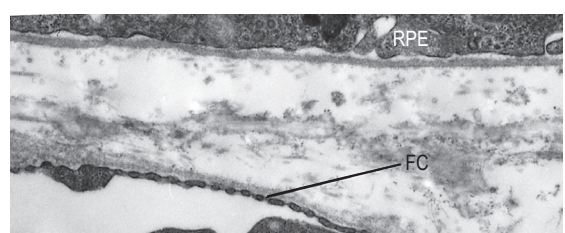
**D**



**E**



**F**



**G**

**FIGURE 1-39**

For legend see opposite page.

### Suprachoroid

This is a 30 µm thick transition zone between the choroid and the sclera. It consists of thin interconnected lamellae of melanocytes, fibroblasts and connective tissue fibres separated by a thin 'potential' (supra- or perichoroidal) space, which in pathological conditions may become separated by fluid and blood. It is frequently artefactually enlarged in histological preparations. It is an avascular layer, the only vessels being those that traverse the suprachoroid entering or leaving the choroid. The lamellae blend with the choroid and the lamina fusca of the sclera. The suprachoroidal space is continuous with the supraciliary space anteriorly. Recent research has unveiled a previously unrecognized, highly organized network of non-vascular smooth muscle cells in the suprachoroid. These networks were particularly evident behind the fovea, around the entry points of the posterior ciliary arteries and nerves and in bundles running parallel to vessels travelling anteriorly from the posterior pole as far as the exit points of the vortex veins. The function of this network of smooth muscle cells in the human choroid remains speculative.

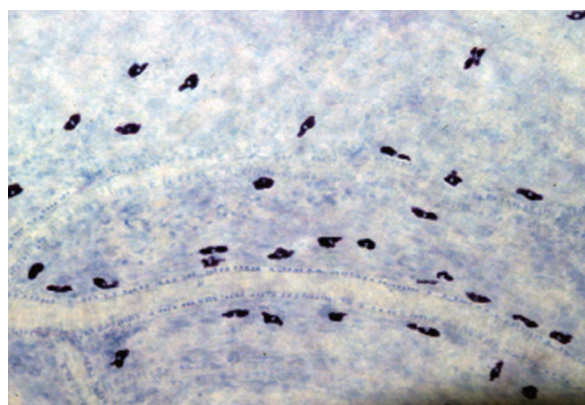
### Nerve supply of the choroid

The choroid is innervated by the *long and short ciliary nerves*. The long ciliary nerves (from the nasociliary branch of V<sub>1</sub>) pass through the choroid and transmit sensory fibres to the cornea, iris and ciliary body. Sympathetic fibres are also carried in these nerves to the dilator pupillae (see p. 28). The *short ciliary nerves* arise from the ciliary ganglion and carry sensory (from nasociliary), sympathetic and parasympathetic fibres (derived predominantly from nerve III, but also from

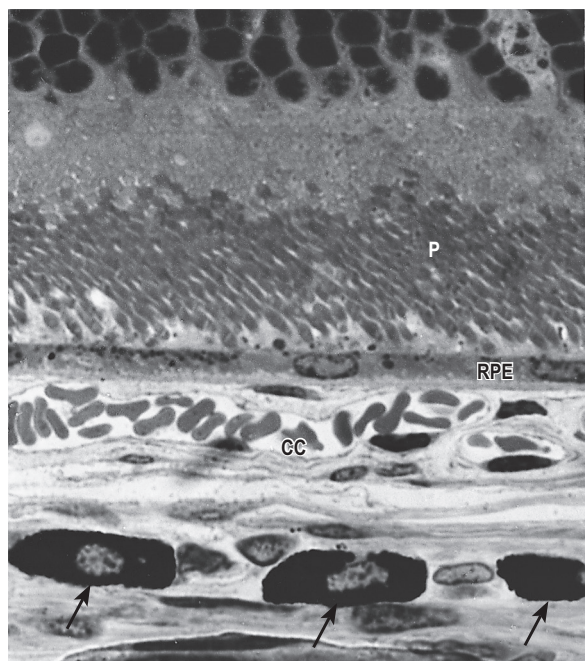
### BOX 1-24 AGEING CHANGES IN THE EYE

#### Choroidal immune cells and age-related macular degeneration (AMD)

The deposition of lipid, complement and immunoglobulin G that accompanies the senescent changes in Bruch's membrane may be augmented by impaired macrophage recruitment and/or decreased homeostatic scavenging by the resident macrophages and dendritic cells in the choroid and thus they may contribute to the accumulation of debris and the formation of drusen in 'dry AMD' and to the eventual choroidal neovascularization in 'wet AMD'.



A



B

**FIGURE 1-40** Mast cells in the choroid. (A) Low-power view of rat choroidal whole mount stained with toluidine blue which demonstrates the perivascular arrangement of mast cells: A, artery. (B) Semi-thin resin section of rat outer retina and choroid stained with toluidine blue showing three mast cells (arrows): P, photoreceptors; RPE, retinal pigment epithelium; CC, choriocapillaris. Original magnifications: A,  $\times 75$ ; B,  $\times 900$ .

VII). The latter have already synapsed in the pterygopalatine ganglion. Both long and short ciliary nerves pierce the sclera in the form of a ring 2–3 mm anterior to the optic nerve sheath, along with the long and short posterior ciliary arteries. The nerve terminals

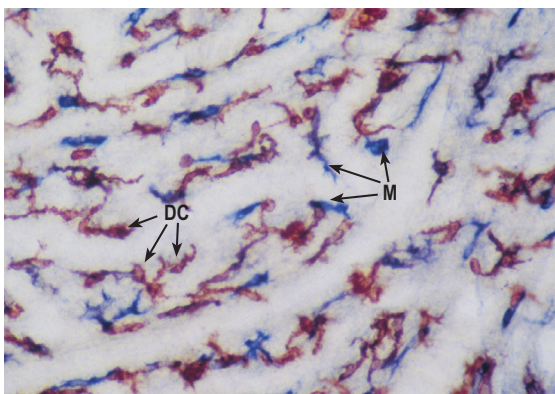


**FIGURE 1-41** Double-colour immunohistochemistry of rat choroidal whole mount stained with monoclonal antibodies specific for macrophages (M; blue) and major histocompatibility class II-positive dendritic cells (DC; red). This method of examining stained tissue provides a 'plan view' that clearly demonstrates the distinct networks of both these cell types in the choroid. Original magnification:  $\times 600$ .

branch extensively and form plexi of unmyelinated fibres in the choroid and suprachoroid adjacent to vascular smooth muscle cells; however, they do not extend into the choriocapillaris. Fibres containing vasoactive intestinal peptide (VIP) and neuropeptide Y have been identified in the choroid and probably act as vasodilator and vasoconstrictor agents, respectively. Multipolar and bipolar ganglion cell bodies immunoreactive for nitric oxide synthase (NOS) and VIP have been recently identified in the choroid and their axons may supply the choroidal vasculature (vasodilatory) or non-vascular smooth muscle cells. Their structure and immunohistochemical characteristics suggest that they may have a mechanosensory role.

## OPTIC NERVE

The optic nerve (Fig. 1-42) is unique anatomically as it is the only tract in the central nervous system to leave the cranial cavity. Furthermore, it is subdivided into fascicles by connective tissue and glial septae and is surrounded by cerebrospinal fluid. It is also unique in that it is the only central nervous system tract that can be visualized clinically.

The optic nerve is formed by convergence of ganglion cell axons at the optic disk, the commencement of the nerve. Foveal/macula fibres constitute around 90% of all axons leaving the eye and form the distinct *maculopapillary bundle*. From the disk, the axons

## BOX 1-25 CLINICAL CORRELATES

### Choroidal infarctions

These appear on angiograms to take the form of triangular areas near the equator, with the apex pointing towards the optic disk. There is probably less functional anastomosis between choriocapillaris lobules than was once suspected; however, some degree of anastomosis in the subcapillary arterioles exists. Peripheral retinal cobble or paving-stone degeneration represents chronic focal ischaemic changes in the anterior choroid.

extend along the nerve through the orbit to traverse the optic canal in the sphenoid bone.

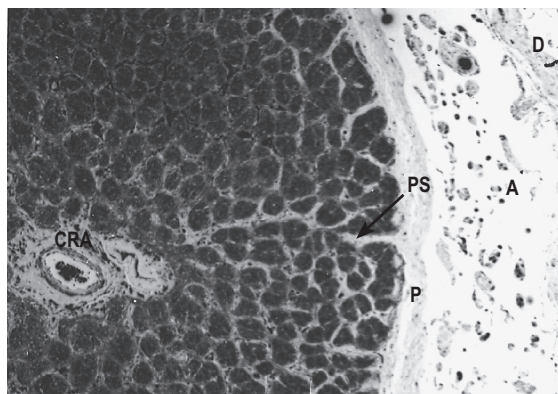
The optic nerve can be divided into four main portions: *intraocular* (1 mm in length), *orbital* (25–30 mm), *intracanalicular* (4–10 mm) and *intracranial* (10 mm). The latter portion is discussed on pp. 92 in the context of the visual pathways.

### Intraocular portion

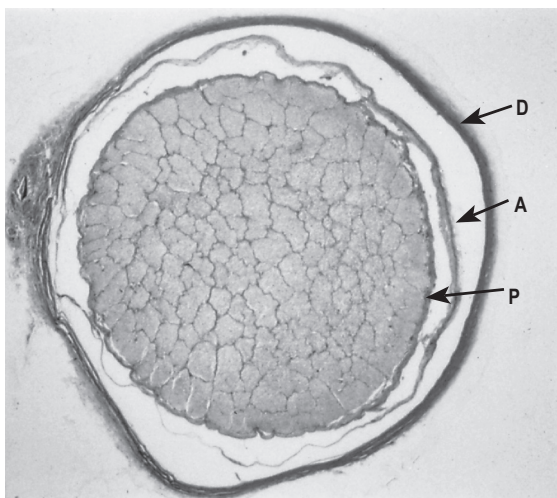
The *intraocular portion* (Fig. 1-42A) extends from the surface of the optic disk to the posterior margins of the sclera. The nerve fibres are not myelinated in this portion. It can be further subdivided into three regions: the retinal (pars retinalis), choroidal (pars choroidalis) and scleral (pars scleralis) portions. Myelination commences approximately level with the termination of the subarachnoid space at the posterior limits of the lamina cribrosa. As the fascicles of nerve fibres pass posteriorly from the optic disk into the intraocular portion, the glial cells become more common; columns of glial cell nuclei are especially prominent in the scleral portion, where they account for up to 40% of the tissue mass (Fig. 1-42A). The commencement of the optic nerve, the *optic disk*, varies depending on the method of measurement but is approximately between 1.7 and 2.8 mm in diameter, although variations both within a population and between races are observed and this variation has been linked to susceptibility to glaucoma. The layers of the retina and the choroid terminate at the edge of the disk as specialized regions of glial tissue, the intermediary tissue (of Kuhnt) and marginal border tissue (of Elschnig). The absence of retinal tissue in this region explains the '*blind spot*' phenomenon. As the 1.2 million ganglion cell axons in the nerve fibre layer become crowded towards the disk, they create a raised area or *papilla*, which is thickest on the lateral aspect owing to the large number of fibres in the



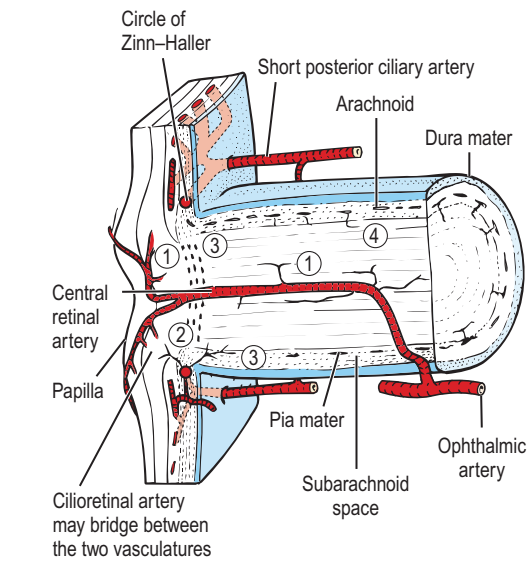
A



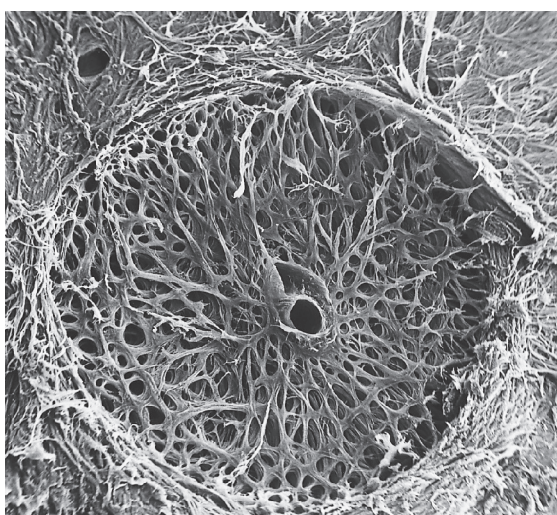
B



C



D



E

**FIGURE 1-42** (A) Histological section of the optic nerve head: LC, lamina cribrosa; A and V, central retinal artery and vein; SAS, subarachnoid space. (B) Transverse section (Loyez stain) of the orbital portion of the optic nerve revealing the arrangement of the myelinated nerve fascicles (darkly stained) separated by pial septae (PS) which penetrate as far as the central retinal artery (CRA) in the middle of the nerve. The three layers of meninges surrounding the nerve (D, dura; A, arachnoid; and P, pia mater) are clearly visible here and in C. (C) Cross-section (trichrome stain) of an entire optic nerve and surrounding meninges posterior to the entry of the central retinal artery. (D) Blood supply of the optic nerve. The four sources of vessels supplying the optic nerve include: 1, branches from the central retinal artery or its branches; 2, branches from the circle of Zinn-Haller; 3, choroidal branches; 4, pial branches. (E) Scanning electron microscopy of the lamina cribrosa (LC). A and V, apertures for the central artery and vein. Original magnifications: A,  $\times 60$ ; B,  $\times 290$ ; C,  $\times 40$ ; E,  $\times 75$  (Part E, courtesy of Dr A Thale).

*maculopapillary bundle*. The raised margin of the optic disk surrounds an indentation, the *physiological cup*. As the fibres pass posteriorly, they pierce the sieve-like connective tissue mesh, the *lamina cribrosa*, which fills the posterior scleral foramen. The lamina cribrosa is formed by irregular collagen fibre bundles continuous with the sclera. These bundles are arranged in the form of circles or a figure of eight (Fig. 1-42E). Elastic tissue from the choroid and Bruch's membrane is continuous with and 'anchored' to the adventitia surrounding the central retinal artery and vein. The collagenous bundles in the lamina cribrosa are separated from the axons by a covering of glial tissue, which may protect the nerve fibres as they pierce the irregular openings. The *scleral canal* is some 0.5 mm long and may vary in shape from cone-like (narrowest portion nearest the disk) to double cone or funnel-like. Posterior to the pars scleralis, the nerve fibres become myelinated by oligodendrocytes (Fig. 1-42B), causing a doubling of the thickness of the optic nerve.

### Orbital portion

The *orbital portion* of the optic nerve (Fig. 1-42C,D) extends backwards and medially from the back of the eye to the optic canal in the sphenoid at the apex of the orbit. It is covered by three layers of meninges: pia, arachnoid and dura. The dura and arachnoid blend with the sclera, and the subarachnoid space around the nerve terminates at the posterior surface of the sclera in the form of a fluid-filled ring (Fig. 1-42A). The central retinal vessels must cross the subarachnoid space and are therefore vulnerable, particularly the vein, in cases of raised intracranial pressure.

The majority of the axons in the nerve are 1 µm in diameter and approximately 10% are between 2 and 10 µm. The glial septae between fascicles present in the intraocular portions extend into the orbital portion but become less distinct as the orbital apex is approached. The orbital portion of the optic nerve has a slight S-shaped bend, which allows a full range of ocular movement without stretching the nerve. As the optic nerve approaches the orbital apex it is surrounded by the tendinous annulus, which gives origin to the rectus muscles.

### Intracanalicular portion

The *intracanalicular portion* of the optic nerve passes through the optic canal (foramen), accompanied by

## BOX 1-26 CLINICAL CORRELATES

### Glaucoma

The intraocular portion is that part of the optic nerve damaged in glaucoma. Axonal damage may be a consequence of either interference with blood flow or interruption of axonal transport and raised intraocular pressure is a significant risk factor. No single hypothesis has been proposed that adequately explains why specific regions of the nerve are more likely to be damaged than others, resulting in the characteristic visual field defects or *scotomas*. Recent research has highlighted the differential pressure gradient across the lamina cribrosa between the cerebrospinal fluid pressure and the intraocular pressure (IOP) (the translaminar pressure gradient (TLPG)) and how it may influence central retinal venous pressure as it traverses the lamina cribrosa, including the 'arteriolization' of the vessel wall and endothelial lining. It appears that other factors such as the buffering effects of orbital tissue, pia mater and the conformation of the lamina itself may further influence the TLPG and this previously unsuspected pressure gradient may in part be responsible for the outward bowing of the lamina in the optic cup. Increased TLPG and its relationship to IOP may have a role in the progression of optic nerve damage and glaucoma.

the ophthalmic artery and sympathetic nerves. The dura surrounding the nerve splits at the orbital opening, the majority continuing as the dural sheath of the nerve inside the canal and a thinner portion blending with the periorbita (Fig. 1-43).

### Blood supply

The optic nerve has a complex blood supply, which has been extensively investigated because of its importance in the pathogenesis of glaucoma (see Ch. 9). The intraocular portion is supplied by branches from four sources: central retinal vessels and their branches, scleral vessels (the circle of Zinn–Haller), choroidal vessels and pial vessels (see Fig. 1-42D). The first three are derived from the ophthalmic or central retinal artery, and pial vessels from the adjacent branches of the internal carotid artery. The majority of capillaries pierce the nerve and course longitudinally within the nerve via the glial septae.

### Orbital contents

#### GENERAL ARRANGEMENT

The orbits are a pair of bony sockets, with each orbital cavity having a volume of about 30 cm<sup>3</sup>.

## PERIORBITA AND ORBITAL FIBROADIPOSE TISSUE (Figs 1-43 and 1-44)

The orbital contents are bound together and supported by fibroadipose tissue. This connective tissue has classically been divided into separate components.

- *Periorbita* or periosteum of the orbit. This layer of connective tissue is frequently described as having a dense outer layer and a looser inner layer, which invests orbital nerves and the lacrimal gland. It is tightly bound to the bones only at the sutures, fissures and foraminae in the orbital walls, and also to the posterior lacrimal crest where it covers the lacrimal sac and is continuous with the fibrous lining of the nasolacrimal duct. It forms a dense membrane over the inferior and superior orbital fissures, with sufficient gaps for transmission of nerves and vessels. It is continuous with the periosteum lining the optic foramen and with the sheath of the optic nerve, itself an extension of dura mater of the brain. The periorbita is firmly attached at the orbital margins anteriorly where it becomes continuous with the orbital septum (palpebral fascia) in the eyelids (see pp. 84).

## BOX 1-27 CLINICAL CORRELATES

### PAPILLOEDEMA

Papilloedema is the swelling of the papillary fibres, which appears as a raised white disk margin, and is partly the result of the lack of Müller cells in this region. These cells serve to bind the nerve fibres together in the remainder of the retina. Papilloedema may be a cardinal sign of raised intracranial pressure which is transmitted to the subarachnoid space which envelopes the optic nerve as far anteriorly as the sclera surrounding the optic nerve.

### MENINGITIS

The continuation of the subarachnoid space from the cranial cavity along the nerve may facilitate the spread of infection or tumours from the orbit to the cranium and vice versa.

- *Bulbar fascia (Tenon's capsule)*, a thick fibrous sheath enclosing the globe but separated from it by a layer of loose connective tissue.
- *Muscular fascial sheaths* that surround the extraocular muscles and blend with the bulbar fascia.
- *Medial and lateral check ligaments*.
- *Suspensory ligament (of Lockwood)*.

The fibrous intermuscular membrane connecting the four rectus muscles helps create the intraconal space (best developed in the anterior part of the orbit;

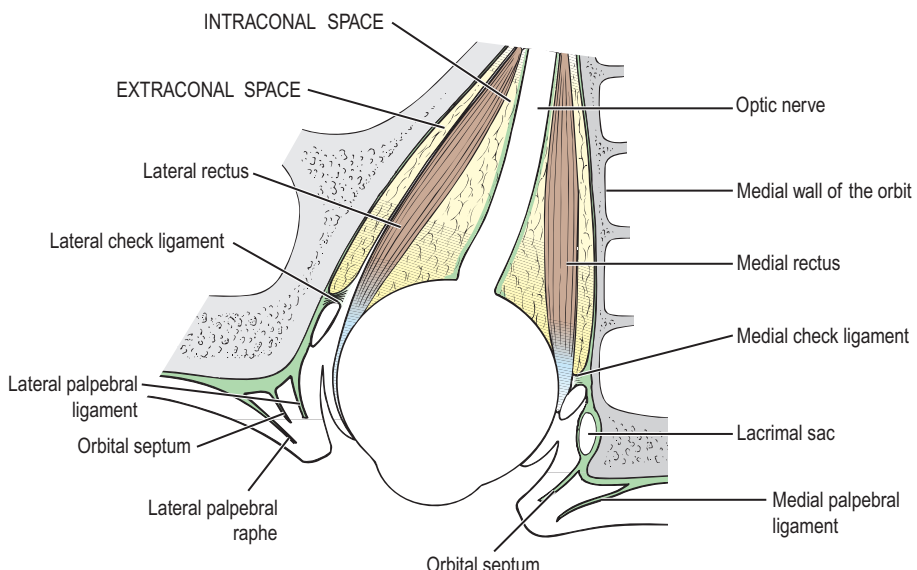


**FIGURE 1-43** Diagram of a horizontal section through the orbit illustrating the formation of an intra- and extraconal space by the four rectus muscles (only medial and lateral rectus shown in this section).

incomplete behind the globe) (Fig. 1-44B,C). Besides the ‘check’ ligaments there are other specific attachments via fibrous bands to the orbital walls throughout their course (Fig. 1-44A–C). A theoretical framework, known as the ‘active pulley hypothesis’ postulates a crucial role for these connective tissue bands, known as ‘pulley suspensions’, in understanding the kinematics of extraocular muscle action. These suspensions pass between the orbital wall and the ‘pulley sleeve’ of each muscle, which is described as a ring-like extension of the connective tissue from Tenon’s capsule posteriorly around the muscle. The tone of the pulleys is possibly under neuronal control because of the presence of smooth muscle fibres. The ‘active pulley hypothesis’ proposes that the rectus muscles have a so-called ‘orbital layer’ of fibres that are continuous with (or ‘blend with’ or ‘insert into’) these sleeves (and thus also into the pulley suspensions), in essence one part of a bifid insertion. The inner half or ‘global layer’ of the rectus muscle continues through the sleeve and bulbar fascia to insert

directly into the sclera. The newly postulated function for orbital connective tissue in the ‘active pulley hypothesis’, which states in effect that this dual insertion allows the pulleys to act as a second ‘origin’ and thus influence the direction of pull of the extraocular muscles, has gained wide acceptance but some investigators have questioned the anatomical evidence of orbital muscle fibres terminating in connective tissue other than the sclera.

There are well-recognized but variable amounts of smooth muscle within the orbital connective tissue, including the sleeves of some of the recti muscles, whose functions (besides the superior and inferior palpebral muscles) are presently unclear. It has been suggested that like the smooth muscle covering the inferior orbital fissure (orbitalis or Müller’s muscle) they may represent a redundant evolutionary remnant.

Veins passing through the orbit are supported by connective tissue septae (Fig. 1-44B); arteries, instead, travel among the fat locules and frequently pierce the septae. A thickened band of orbital fibrous tissue

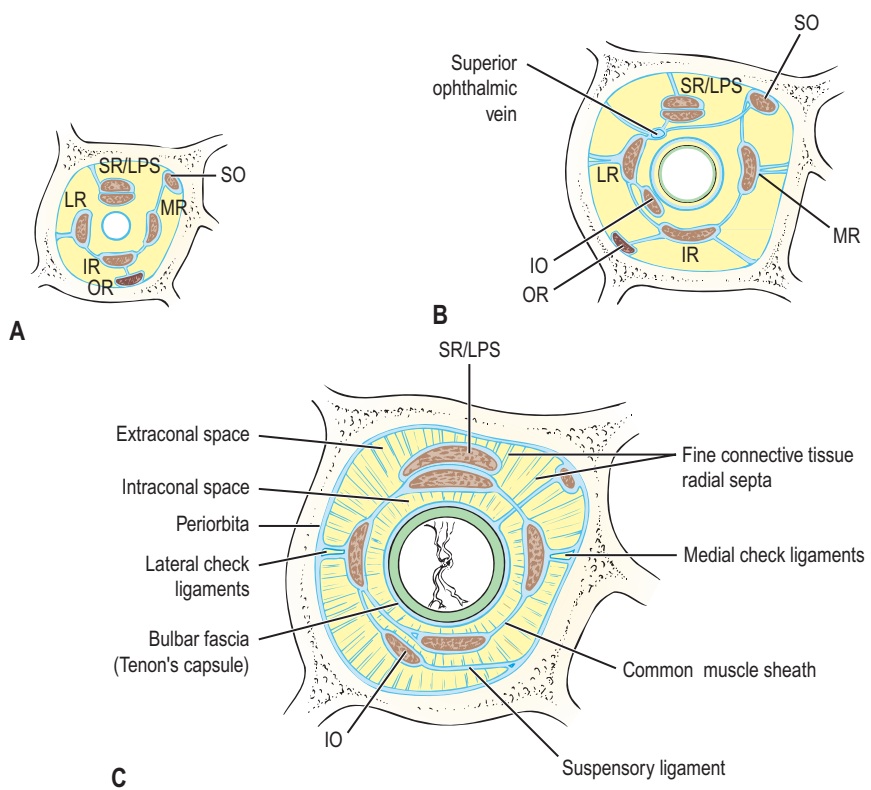


**FIGURE 1-44** Schematic diagrams of the connective tissue septae associated with each extraocular muscle at three levels in the orbit: (A) near orbital apex; (B) posterior part of the globe; (C) close to the equator of the globe. SO, superior oblique; MR, medial rectus; LR, lateral rectus; IR, inferior rectus; SR, superior rectus; LPS, levator palpebrae superioris; IO, inferior oblique; OR, orbitalis. (Modified from Koornneef, 1982.)

connects the superior rectus and the levator palpebrae superioris. This aids in coordinating lifting of the eyelid when the eye is directed upwards by the superior rectus.

The complex and interlinked nature of the fibroadipose system of connective tissue septae may explain why patients with orbital floor ‘blow-out’ fractures display vertical ocular mobility problems. It is not necessary to invoke the incarceration of the inferior rectus and inferior oblique muscles in the fracture to explain the symptoms.

### EXTRAOCULAR MUSCLES

There are six true extraocular muscles responsible for movements of the globe. In addition there is one further ‘orbital’ muscle, the levator palpebrae superioris, which originates at the orbital apex and inserts into the tarsal plate and upper eyelid (see pp. 81).

The true extraocular muscles comprise *four rectus muscles*, which arise from the tendinous ring at the apex of the orbit and insert into the sclera about 4–8 mm behind the limbus, and *two oblique muscles* (superior and inferior), whose tendons approach the globe from in front and insert into the posterior aspect of the sclera (Figs 1-45 and 1-48). Details of the six true extraocular muscles, including their innervation, origin, insertion, tendon length (important in the surgical management of strabismus), length of muscle belly, the angle subtended by the muscle axis to the vertical, and the size of the motor units, are provided in Table 1-2. The origins of the muscles are shown in Figure 1-47 and the pattern of insertion into the sclera is shown in Figure 1-48. The collagen bundles of the tendons blend with the scleral collagen as shown in Figure 1-17C. The relations of the orbital muscles to each other and to the orbital nerves are summarized diagrammatically in Figures 1-45 and 1-46. Movements are discussed in Chapter 5 (pp. 326).

### Microscopic anatomy of extraocular muscle

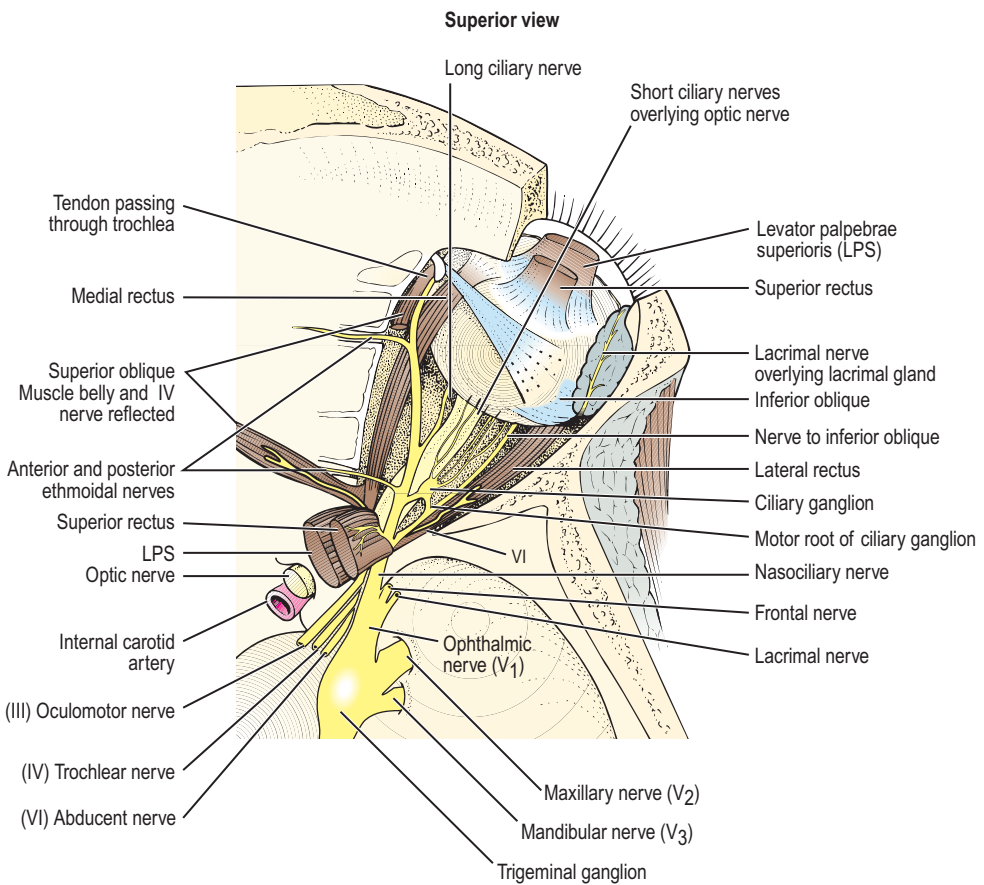
Histologically, extraocular muscle differs from skeletal muscle in the following respects (compare Fig. 1-49A with Fig. 1-49B).

- The epimysium or muscle sheath of extraocular muscle is generally very thin by comparison with other muscles.
- The fibres are not tightly packed but are separated by unusually large amounts of connective

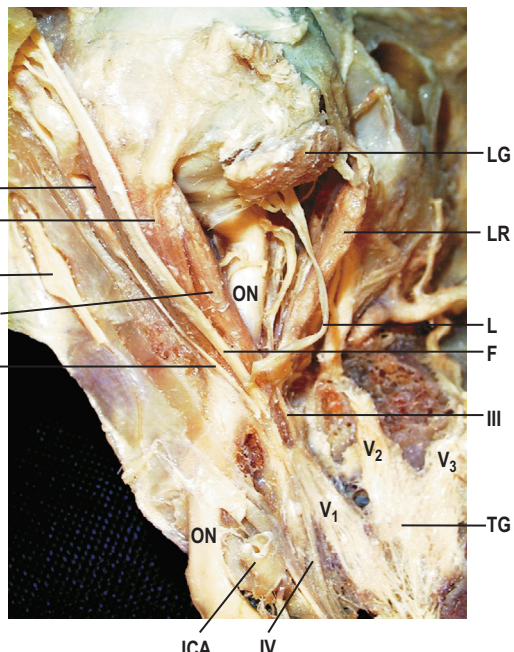
tissue (perimysium) rich in reticulin and elastic fibres.

- The muscle fibres are rounded or oval in shape with small fibres (5–15 µm) around the periphery of the muscle and larger fibres (10–40 µm) in the centre.
- Extraocular muscle is the most vascular in the body, next to myocardium. The most vascularized region is the orbital aspect.
- In normal extraocular muscle there often appear to be histopathological or ultrastructural changes normally associated with myopathy, i.e. mild mononuclear cellular infiltrate, centrally placed nuclei, disorganization of the sarcolemma, disruption of the Z lines, and mitochondrial clumping.
- Extraocular muscle contains large numbers of specialized sensory or proprioceptive endings, including large muscle spindles up to 1 mm long (nuclear bag fibres, nuclear chain fibres and annular nerve terminals). Golgi tendon organs are also numerous and are generally found within the tendons of extraocular muscles in greater numbers than in skeletal muscle (Fig. 1-49). The afferent fibres from extraocular muscles are transmitted initially for part of their course in the respective cranial nerve innervating the muscle (either III, IV or VI); however, they leave these nerves and join the ophthalmic division of the trigeminal, either in the cavernous sinus or in the brainstem. Their cell bodies are situated in the mesencephalic nucleus, although some muscle afferents have been traced to Purkinje cells in the cerebellum, and play an important role in positional sense and control of ocular movements (both saccadic and tracking).

The structural differences between extraocular and skeletal muscle outlined above are not surprising in light of the fundamental differences in function, namely the constancy of activity (even during sleeping) and the rapidity and fine gradation of contraction of extraocular muscle required to fixate subjects of interest on the fovea. Since both eyes must move together, both sets of six muscles must be highly coordinated and move simultaneously (see Ch. 5). Up to six types of muscle fibre have been identified morphologically, but functionally there appear to be three main types (Table 1-3).



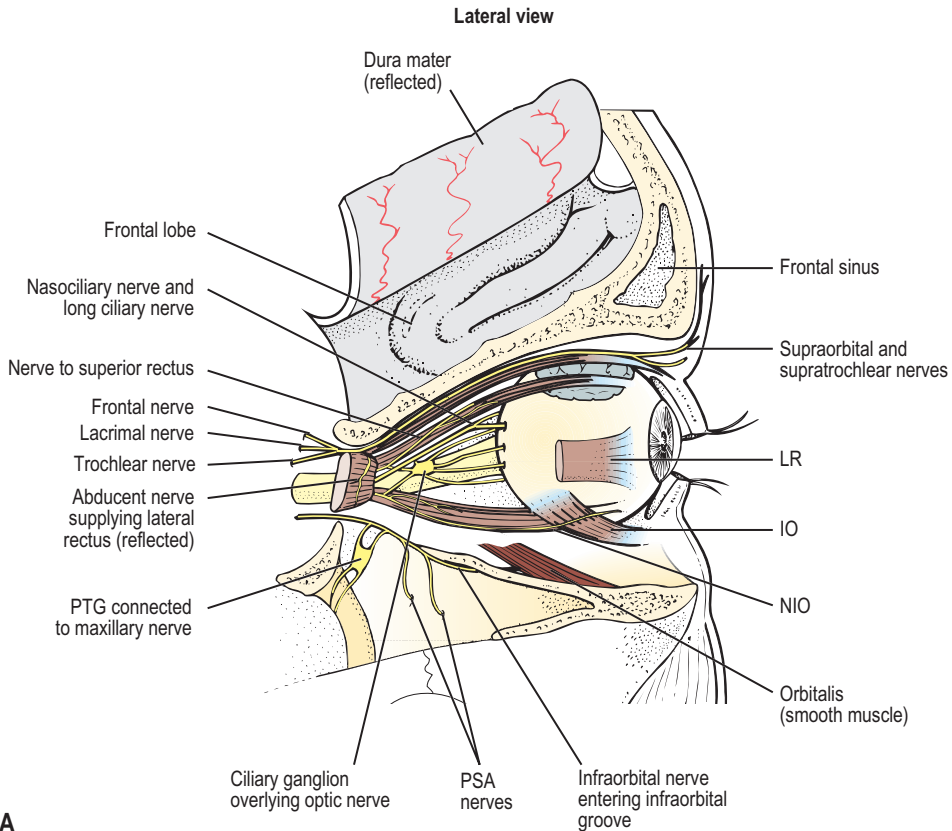
A



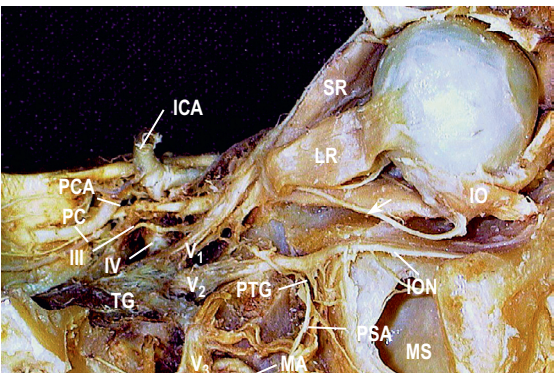
B

**FIGURE 1-45** Diagram (A) and prosected specimen (B) of the orbit viewed from above, revealing the relations of the orbital nerves and extraocular muscles. Orbital fat and vessels have been excluded for the purposes of clarity.

- The roof of the orbit and superior orbital fissure have been removed and the periorbita divided.
- In (A) the lacrimal (L), frontal (F) and trochlear (IV) nerves have been cut. In (B) these nerves are intact as they pass external to the tendinous ring or annulus.
- In (A) only one long ciliary nerve is shown arising from the nasociliary nerve.
- The sensory root of the ciliary ganglion emerges from the nasociliary. The motor root (parasympathetic fibres) arises from the branch of the oculomotor supplying inferior oblique.
- In (A) and (B) the lateral dural covering of the cavernous sinus has been removed to expose the cranial nerves before they pass through the superior orbital fissure: TG, trigeminal ganglion;  $V_1$ ,  $V_2$ ,  $V_3$ , divisions of the trigeminal nerve; OB, olfactory bulb; ICA, internal carotid artery; III, oculomotor nerve; VI, abducens nerve; SO, superior oblique; LR, lateral rectus; LG, lacrimal gland; LPS, levator palpebrae superioris; SR, superior rectus; ON, optic nerve.
- The optic canal has not been opened.



**A**



**B**

- The lateral wall has been removed and the infratemporal fossa has been dissected to expose the pterygomaxillary fissure and pterygopalatine fossa.
- The cranial cavity has been opened to reveal the dura (reflected) covering the frontal lobe.
- The lateral rectus has been divided and reflected to expose the optic nerve and other cranial nerves entering the orbit through the tendinous ring. Note the abducent nerve entering its bulbar surface.
- The ciliary ganglion lies between the lateral rectus and the optic nerve. Note the motor root and sensory root as seen in the superior view. The nerve to inferior oblique (NIO) is a useful landmark for finding the ciliary ganglion. The short ciliary nerves emerge from the ganglion and enter the globe around the optic nerve.
- Note the three nerves which enter the orbit outside the tendinous ring: lacrimal, frontal and trochlear.
- The nerve to superior rectus (branch of superior division of III nerve) pierces the muscle and enters the levator palpebrae superioris, which it supplies, from below.
- Branches of the pterygopalatine ganglion (PTG) enter the orbit through the inferior orbital fissure and contribute to the formation of the retrobulbar plexus (not shown).
- Inferior oblique passes backwards, laterally and superiorly beneath the inferior rectus.
- Orbitalis (Müller's muscle), a band of smooth muscle, covers the inferior orbital fissure.

**FIGURE 1-46 (A)** Diagram illustrating a lateral view of a dissected orbit revealing the relations of the orbital nerves and extraocular muscles (vessels have been excluded for the purposes of clarity). **(B)** Dissection of the orbit similar to the diagram above except that lateral rectus has not been cut and the course of the orbital nerves within the cavernous sinus is also shown (by removal of the lateral dural wall). ICA, internal carotid artery; PCA, posterior communicating artery; PC, posterior cerebral artery; MA, maxillary artery; TG, trigeminal ganglion; V<sub>1</sub>, V<sub>2</sub>, V<sub>3</sub>, divisions of the trigeminal nerve; PTG, pterygopalatine ganglion; PSA, posterior superior alveolar nerves; ION, infraorbital nerve; IO, inferior oblique; LR, lateral rectus; SR, superior rectus; arrow, nerve to superior oblique branch of oculomotor nerve (III); IV, trochlear nerve; MS, maxillary sinus.

TABLE 1-2 Summary of anatomical features of human extraocular muscles

Muscle	Innervation	Origin	Insertion (mm from cornea)	Tendon length (mm)	Length of muscle belly (mm)	Size of motor unit	Comment
Medial rectus	III (inf)	Tendinous ring	5.6	3.6	40	1 : 1.7-1 : 4	Largest of the ocular muscles
Inferior rectus	III (inf)	Tendinous ring	6.6	5	40	1 : 2-1 : 6	
Lateral rectus	VI	Tendinous ring via two heads	7.0	8.4	40	1 : 3-1 : 6	Opening between the two heads bridging the medial end of superior orbital fissure
Superior rectus	III (sup)	Tendinous ring	7.8	5.4	41	1 : 4	Lies beneath levator palpebrae superioris
Superior oblique	IV	Superomedial to optic canal	Lateral aspect of posterosuperior quadrant	Tendon forms 10 mm before winding around trochlea	32	1 : 5-1 : 6	The only extraocular muscle with a fusiform shape. IV nerve enters the muscle on its upper border
Inferior oblique	III (inf)	Behind orbital margin lateral to nasolacrimal canal	Posteriorlateral quadrant, mostly below horizontal	Very short tendon; muscle fibres almost reach the sclera	34	1 : 7	The only extraocular muscle not to originate at apex of orbit. Passes between the eye and lateral rectus

Values are approximate means based on several studies; for full details and ranges see Eggers (1982). III (inf), inferior division of oculomotor nerve; III (sup), superior division of oculomotor nerve.

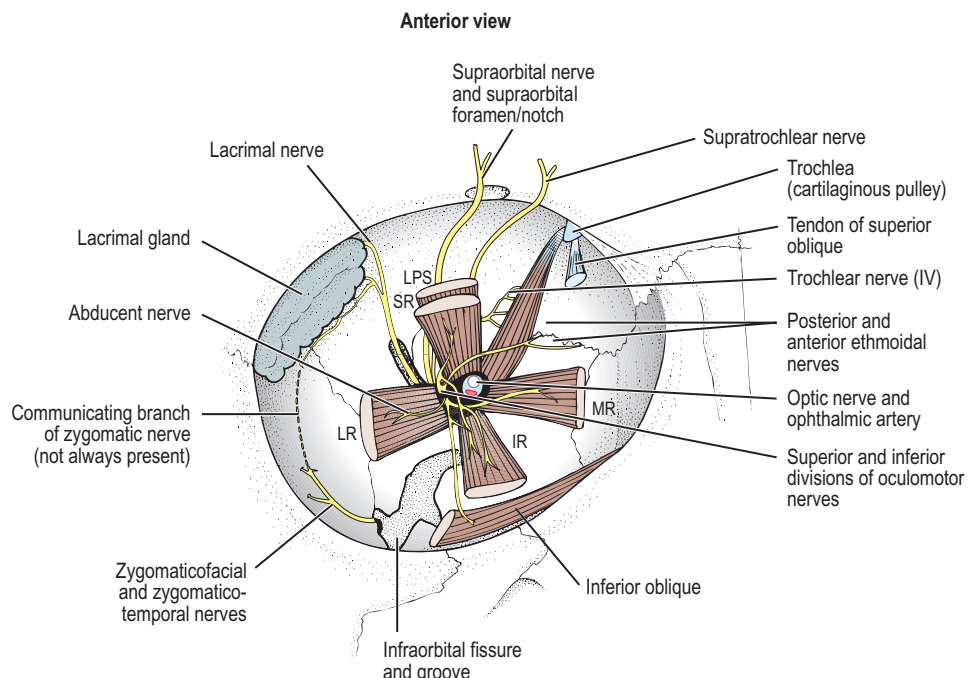


**FIGURE 1-47** The orbit from in front with the globe removed to show the origins of the extraocular muscles and the orbital nerves (vessels and fat are not included in this diagram).

### BLOOD VESSELS OF THE ORBIT (Fig. 1-50)

The orbital contents are supplied chiefly by the ophthalmic artery, which usually arises from the internal carotid artery shortly after it emerges from the roof of the cavernous sinus. It commences its course beneath the optic nerve, closely bound to the dura while in the optic canal, then winds around its lateral aspect, and finally passes above the nerve. It then proceeds forward above the medial rectus and under the superior oblique. It ends its tortuous course by dividing into dorsal nasal and supratrochlear branches. The branches are summarized in Figure 1-50. There are several important points of anastomosis between arteries derived from the internal carotid and the external carotid arteries (Table 1-4).

These anastomoses may be important during occlusive vascular disease of the ophthalmic artery by serving as alternative routes of blood supply to the eye and orbit. The veins that accompany the above arteries, in common with most veins of the head and neck, lack valves and thus there are several sites of communication between veins on the upper face and lids with intraorbital veins (superior and inferior

ophthalmic veins) which drain posteriorly into the cavernous sinuses. The inferior ophthalmic vein may drain via the inferior orbital fissure into the pterygoid venous plexus. These communications are important clinically as they act as potential routes for the spread of infection from the face around the nose and eye to the cavernous sinuses and the cranial cavity.

### Cranial nerves associated with the eye and orbit

#### GENERAL FUNCTIONAL ARRANGEMENT

Cranial nerves contain a diversity of functional components. Besides those found in spinal nerves (somatic efferents, somatic afferents, general visceral efferents, general visceral afferents), cranial nerves also contain additional functional categories including special visceral efferents (branchiomotor), special somatic afferents (special senses, hearing and balance), and special visceral afferents (taste and smell). The functional classification of cranial nerve components and their target organs and tissues are summarized in eTable 1-1.



**eTABLE 1-1 Functional analysis of cranial nerve components**

Functional classification	Modality/target (ontogeny/phytogeny)	Present in cranial nerves
Somatic efferent (general motor)	Supplies skeletal muscle of somatic origin (preotic somites – extraocular muscles; occipital somites – tongue musculature)	III, IV and VI XII
Somatic afferent (general sensory)	Pain, temperature and touch. Supplies skin and mucous membranes of the head and neck	Predominantly in V but several minor elements in VII, IX and X
General visceral efferents* (parasympathetic)	Supplies smooth muscle (viscera), cardiac muscle, glands, blood vessels and intrinsic eye muscles (ciliary muscle and sphincter pupillae)	III, VII, IX, X and XI. X (vagus) is largest parasympathetic nerve in the body
General visceral afferents	Pain and sensibility of viscera	VII, IX and X
Special visceral efferents (branchiomotor)	Skeletal muscles of mastication and facial expression (i.e. pharyngeal arch or visceral evolutionary origin)	V, VII, IX, X and XI
Special somatic afferent (special senses concerned with body position, excluding vision)	Maintenance of balance and reception of sound (vestibulocochlear organ)	VII
Special visceral afferent (special visceral senses, taste and smell)	Olfactory epithelium in nasal cavity and taste receptors in tongue and palate	Olfaction (smell) in I; taste in VII, IX and X

\*Sympathetic nerve fibres, originating from upper thoracic segments of the spinal cord and synapsing in cervical ganglia may 'hitch-hike' with various cranial nerves and/or blood vessels to reach ocular and orbital structures, e.g. dilator pupillae muscle and tarsal muscle (see Fig. 1-65).

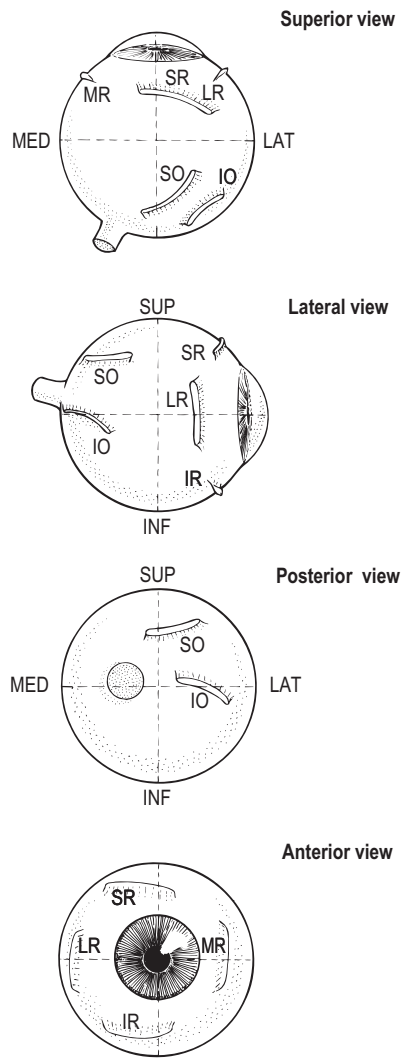


**FIGURE 1-48** Four views of the right globe to demonstrate the insertions of the extraocular muscles.

The sites of origin of the cranial nerves from the brainstem are illustrated in [Figures 1-51](#) and [1-52](#).

### OCULOMOTOR NERVE (CRANIAL NERVE III) ([Fig. 1-52](#))

This is the largest of the extraocular nerves and supplies all the extraocular muscles except the lateral rectus and superior oblique.

#### Origin

The oculomotor nerve nuclei comprise two main types:

- a complex of five individual motor (*somatic efferent*) nuclei containing the cell bodies of the

multipolar motor neurones whose axons directly innervate their respective extraocular muscles

- a general visceral efferent nucleus, the Edinger-Westphal nucleus, containing small spindle-shaped preganglionic (first-order) *parasympathetic* neurones.

The oculomotor nuclei lie at the level of the superior colliculus in the ventral region of the periaqueductal grey matter and extend cranially for a short distance into the floor of the third ventricle. The *medial longitudinal fasciculus* lies lateral to the nucleus and contains the axons of internuclear neurones that pass vertically between the brainstem nuclei of the III, IV and VI nerves. The fibres emerge from the oculomotor nuclei, pass anteriorly through the tegmentum of the midbrain and red nucleus, and emerge medial to the cerebral peduncle at the upper border of the pons ([Figs 1-51](#) and [1-52](#)).

#### Intracranial and intracavernous course

The nerve passes forward, laterally and slightly downward in the interpeduncular fossa (one of the enlargements of the subarachnoid space or cisterns) lateral to the posterior communicating artery ([Fig. 1-52](#)). It passes between the posterior cerebral artery (above) and the superior cerebellar artery (below). It grooves the posterior clinoid process and courses forward before it passes through the dural roof of the cavernous sinus ([Fig. 1-46B](#)). The nerve runs forward in the upper part of the lateral wall of the cavernous sinus ([Fig. 1-9C](#) and [eFig. 1-2B](#)) and enters the intraconal space of the orbit through the superior orbital fissure within the tendinous ring ([Figs 1-5](#) and [1-6](#)), where it divides into superior and inferior divisions.

#### Intraorbital course

In the orbit the nasociliary nerve is interposed between the two divisions of the oculomotor nerve. The superior supplies the superior rectus, which it pierces to reach levator palpebrae superioris. The inferior division splits into several branches which supply the medial rectus and inferior rectus, and a long branch passes forward on the lateral aspect of inferior rectus to reach inferior oblique ([Fig. 1-46B](#)). It is from this latter branch that the stout motor root (preganglionic parasympathetic fibres) passes to the ciliary ganglion, the site of postganglionic parasympathetic (second-order) neurones ([Fig. 1-45A](#)). Axons from the

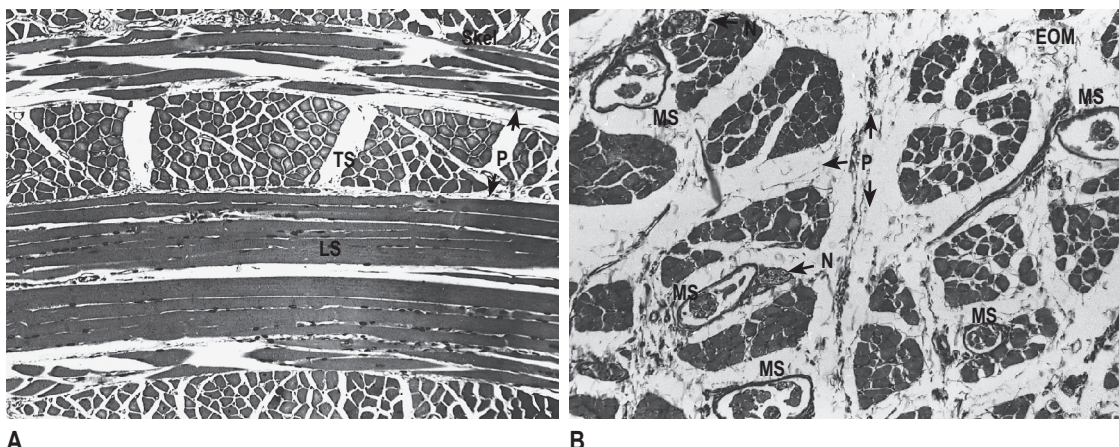


**FIGURE 1-49** Histological section of (A) normal human skeletal muscle fibres (SKel) and (B) extraocular muscle fibres (EOM): LS, longitudinal section of fibres; TS, fibres in transverse section; P, perimysium; MS, muscle spindles; N, nerve. Original magnifications: A and B,  $\times 100$ .

**TABLE 1-3 Classification of mammalian extraocular muscle fibres**

Type A	Type B	Type C
Large diameter	Intermediate diameter	Small diameter
Single end-plate	Multiple end-plates	Small <i>en grappe</i> plates
Fast twitch	Slow twitch	Tonic contractions
Required for saccadic movements	Needed for smooth pursuit movements	Function to align both visual axes, i.e. fine local contractions

**TABLE 1-4 Sites of anastomosis between branches of the internal and external carotid arteries**

External carotid branch	Internal carotid branch	Region of anastomosis
Angular artery (facial)	Dorsalis nasi (ophthalmic)	Medial palpebral margin
Transverse facial artery (superficial temporal)	Lacrimal artery (ophthalmic)	Lateral palpebral margin
Middle meningeal artery and deep temporal artery	Lacrimal artery (ophthalmic)	Orbit

**Blood supply of the orbit**

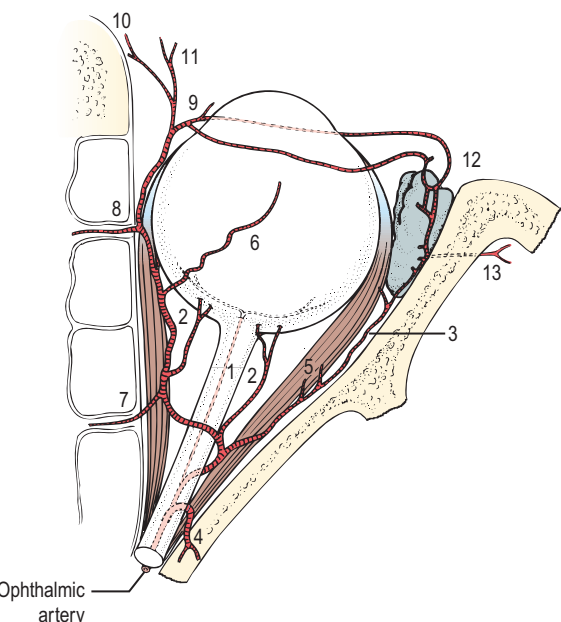


**FIGURE 1-50** Diagram summarizing the blood supply of the orbit as seen in a superior view: 1, central retinal artery; 2, posterior ciliary arteries (usually emerge as two trunks that divide into the short posterior ciliary arteries (seven or more) and the long posterior ciliary arteries (usually two, medial and lateral)); 3, lacrimal artery; 4, recurrent branches (to meninges); 5, muscular branches (give rise to anterior ciliary arteries); 6, supraorbital artery; 7, posterior ethmoidal artery; 8, anterior ethmoidal artery; 9, superior and inferior medial palpebral arteries; 10, dorsalis nasi; 11, supratrochlear; 12, superior and inferior lateral palpebral arteries; 13, zygomatic branches of the lacrimal artery.

**BOX 1-28 CLINICAL CORRELATES****Intracavernous lesions of cranial III nerve**

The oculomotor, like other cranial nerves coursing through the cavernous sinus, can become involved in pathological processes such as venous thrombosis or aneurysms of the internal artery. Pituitary enlargements more commonly affect the oculomotor and trochlear nerves than the abducent, which is protected by the internal carotid artery. Meningioma or expanding lesions in the region of the superior orbital fissure can also compress the nerve.

**BOX 1-29 CLINICAL CORRELATES****Lesions of the oculomotor nerve**

*Complete lesions* of the oculomotor nerve (e.g. trauma) result in:

- inability to look upwards, downwards or medially
- lateral or *external strabismus* because of unopposed action of lateral rectus
- diplopia
- complete ptosis (paralysis of levator palpebrae superioris and unopposed orbicularis oculi)
- dilated non-reactive pupils (unopposed dilator pupillae)
- lack of accommodation.

*Incomplete lesions* – some of the symptoms above may be present.

*Internal ophthalmoplegia* – loss of parasympathetic components only. This may be the first sign of nerve palsy as the parasympathetic fibres are located superficially in the nerve and they may be damaged first in intracranial lesions; thus, pupil dilation is a crucial sign of compression within the cranial cavity following head injury.

*External ophthalmoplegia* – the loss of extraocular muscle supply.

*Intracranial lesions affecting the oculomotor nerve*

- aneurysms of adjacent arteries around the brainstem may cause compression of the nearby nerve. Meningitis can involve the nerve along its course in the subarachnoid space.

postganglionic neurones travel in the short ciliary nerves to supply the choroid, sphincter pupillae of the iris and the ciliary muscle (Fig. 1-52).

The nerves that supply extraocular muscles generally pierce the muscle one-third of the way along the muscle belly on the bulbar aspect.

**TROCHLEAR NERVE (CRANIAL NERVE IV) (Fig. 1-53)**

This is the only somatic efferent nerve to emerge from the posterior aspect of the central nervous system. It

**BOX 1-30 CLINICAL CORRELATES****Intracranial lesions affecting the trochlear nerve**

The trochlear nerve is rarely paralysed alone, although it is particularly vulnerable at its posterior exit from the brainstem and as it winds round the midbrain. Lesions causing compression on the undersurface of the tentorium may affect the trochlear nerve. It may also be involved in pathological processes in the cavernous sinus. Patients suffering paralysis of the superior oblique because of trochlear nerve lesions suffer diplopia when looking down and have difficulty in looking down when the eye is adducted because the superior oblique is the only depressor in the adducted state. Patients characteristically carry the head tilted to the non-affected side with the chin lowered to compensate for the overaction of the inferior oblique producing unopposed torsion on the eye.

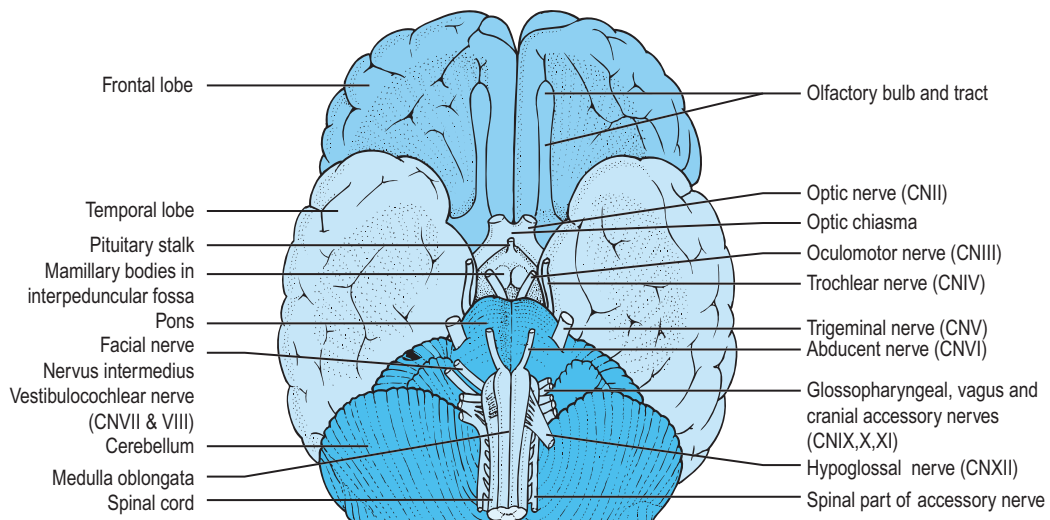
is also unusual in that it decussates before leaving the brainstem. It supplies only one extraocular muscle, the *superior oblique*.

**Origin**

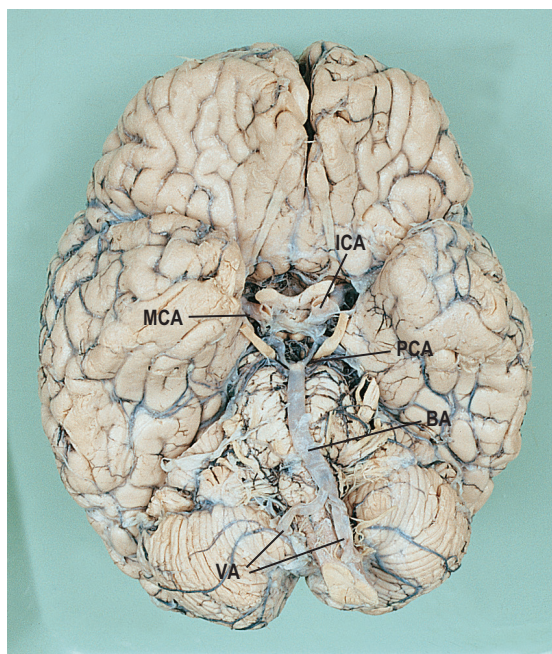
The nucleus lies in the anterior part of the periaqueductal grey matter at the level of the inferior colliculus (caudal to III nerve nucleus) in line with the other oculomotor nuclei. The fibres first pass anteriorly and laterally towards the tegmentum before turning and passing posteriorly around the periaqueductal grey matter and into the superior medullary velum (part of the roof of the fourth ventricle) where they decussate before emerging from the posterior surface of the brainstem in the posterior cranial fossa (Fig. 1-53).

**Intracranial and intracavernous course**

The trochlear nerve winds around the crus of the midbrain (cerebral peduncles) above the superior cerebellar artery and the pons and below the posterior cerebral artery. It continues anteriorly immediately beneath the free edge of the tentorium cerebelli (Fig. 1-53). It pierces this dura and enters the lateral wall of the cavernous sinus beneath the oculomotor nerve (Figs 1-9C and eFig. 1-2B; 1-45B and 1-46B). The trochlear nerve then passes upwards, thus coming to lie above the oculomotor nerve before entering the orbit outside the tendinous ring in the lateral part of the superior orbital fissure.



A



B

**FIGURE 1-51** Ventral views of the brain to demonstrate the origin of the cranial nerves: (A) diagram without vessels; (B) photograph of a whole brain with vessels. ICA, internal carotid artery; MCA, middle cerebral artery; PCA, posterior cerebral artery; BA, basilar artery; VA, vertebral artery.

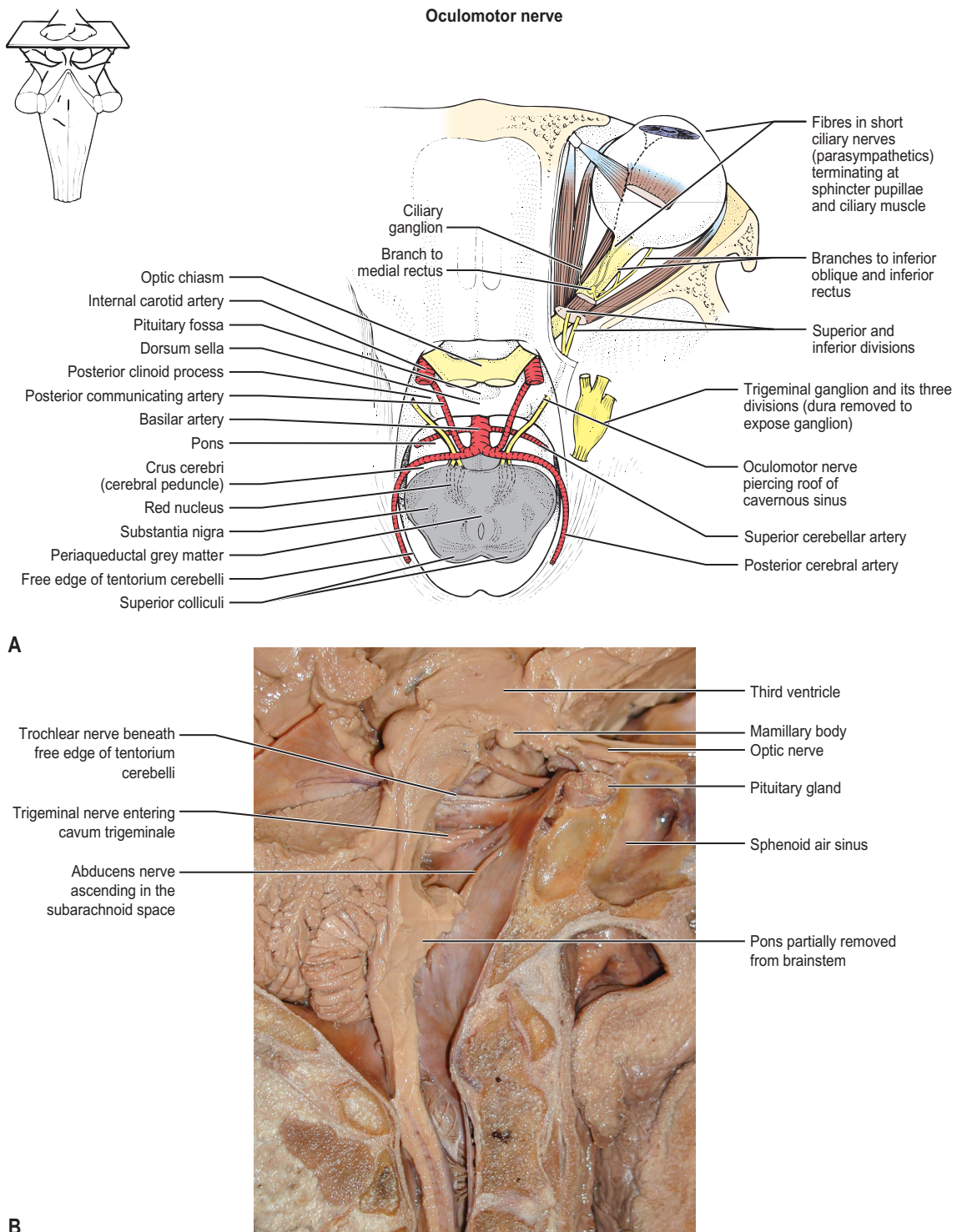


**FIGURE 1-52 (A)** Diagram summarizing the brainstem origin (inset shows level of section), intracranial, intracavernous and intraorbital course of the oculomotor nerve. **(B)** Brainstem cranial nerves.

### Intraorbital course

It passes forward above the origin of levator palpebrae superioris close to the bone, to enter the upper free edge of the superior oblique (Figs 1-45A,B; 1-47 and 1-53).

### ABDUCENT NERVE (CRANIAL NERVE VI) (Fig. 1-54)

The abducens nucleus lies in the mid-pons beneath the floor of the upper part of the fourth ventricle, close to the midline beneath the facial colliculus. The fibres pass anteriorly to emerge on the lower border of the pons above the medulla near the midline (Figs 1-51 and 1-54).

### Intracranial and intracavernous course

The abducent nerve has the longest intracranial course of any cranial nerve. It courses upwards in the pontine cistern between the brainstem and the clivus, either side of the basilar artery. It is crossed or 'bound down' to the brainstem close to its origin by the anterior inferior cerebellar artery. It may pierce the dura early in its upward course upon the clivus close to the inferior petrosal sinus (2 cm below the posterior clinoid process). On reaching the upper border of the apex of the petrous temporal bone, it crosses the inferior petrosal sinus from medial to lateral and changes direction sharply from a vertical to a horizontal course and runs forward beneath the *petrosphenoidal ligament (of Gruber)* and *superior petrosal sinus* (Fig. 1-54). The abducent nerve passes forward within the *cavernous sinus*, surrounded by venous spaces and suspended by fine connective tissue trabeculae. It lies *lateral* to the ascending portion of the internal carotid artery and then inferolateral to its horizontal portion (Fig. 1-9C and eFig. 1-2B). The abducent nerve enters the intraconal space of the orbit by passing within the tendinous ring (Figs 1-5 and 1-6).

### Intraorbital course

The abducent nerve has a short intraorbital course. It enters the bulbar surface of the lateral rectus one-third of the way from its origin. This is the only muscle supplied by the abducent nerve.

### Sensory endings in oculomotor nerves

The cell bodies of proprioceptive fibres in the extraocular muscles are located in the mesencephalic nucleus of the trigeminal nerve. The mesencephalic nucleus also receives proprioceptive terminals from neck and face musculature. The coordination of simultaneous movements of the head and eyes is dependent on conjugation of sensory (proprioceptive) information from the musculature of the neck and eyes, and input from cerebellar oculomotor centres (see Ch. 5).

### TRIGEMINAL NERVE (CRANIAL NERVE V) (Fig. 1-55)

The trigeminal is the largest of the cranial nerves. It is the main sensory nerve of the head, supplying the mucous membranes of the oronasal cavities, middle ear, paranasal sinuses, skin of the face, the teeth, the cornea, the temporomandibular joint, and the dura of the anterior and middle cranial fossae (Fig. 1-55A,B). The dermatomes corresponding to its three major subdivisions and the cutaneous branches of the ophthalmic and maxillary nerves are shown in Figure 1-55A.

The mandibular division, besides its sensory component, supplies motor fibres to the muscles of mastication and also receives proprioceptive fibres from these muscles, together with the muscles of facial expression.

The trigeminal nerve arises from the brainstem in the posterior cranial fossa as a large *sensory root* and a small *motor root*. The sensory root consists of the central processes of pseudo-unipolar sensory neurones whose cell bodies lie in the large *trigeminal ganglion* located in the *cavum trigeminale*, a bony depression near the apex of the petrous temporal bone lined by evaginating dura mater from the edge of the *tentorium cerebelli* and roofed over by dura of the middle cranial fossa. The ganglion is partly surrounded by cerebrospinal fluid, which is continuous with the subarachnoid space of the posterior cranial fossa. The ganglion is homologous to a dorsal root or sensory ganglion of a spinal nerve. It is from the anterolateral convex surface of this flattened ganglion that the three named branches emerge: the *ophthalmic (V<sub>1</sub>)*, *maxillary (V<sub>2</sub>)* and *mandibular (V<sub>3</sub>)* (Fig. 1-55B).

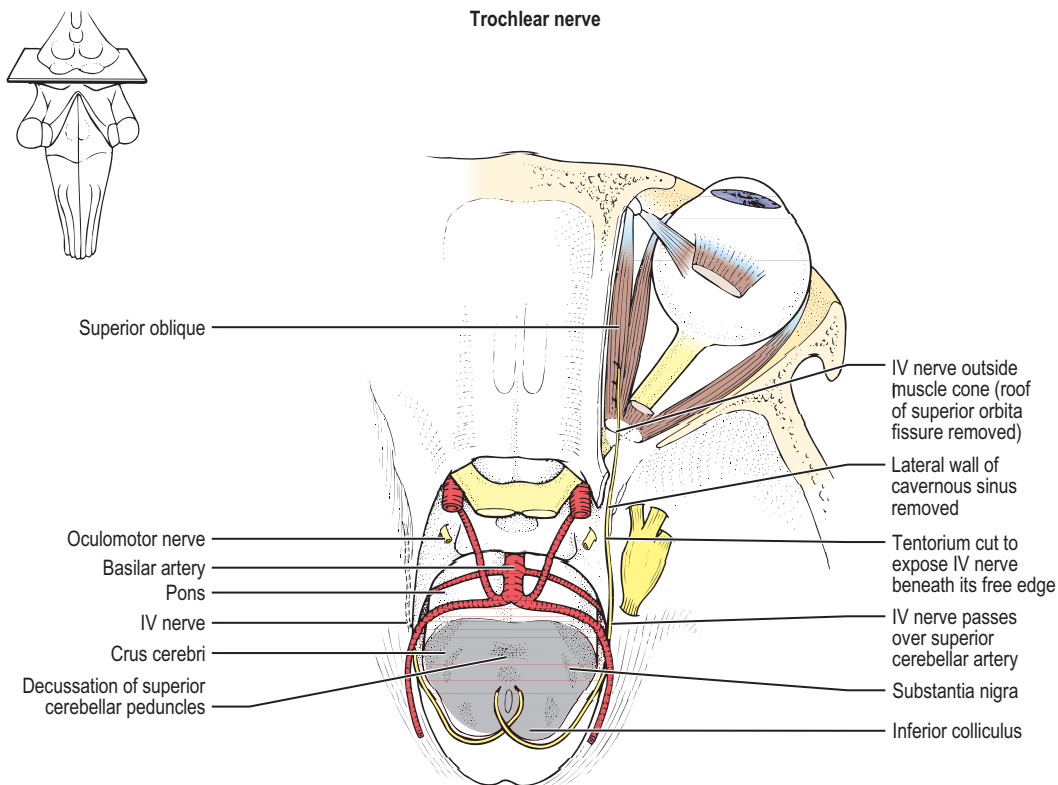


**FIGURE 1-53** Diagram summarizing the brainstem origin (inset shows level of section), intracranial, intracavernous and intraorbital course of the trochlear nerve.

The ophthalmic division or nerve (Fig. 1-56A) splits in the anterolateral portion of the cavernous sinus into three main branches: the lacrimal, frontal and nasociliary. The pathway and termination of these nerves are summarized in Figures 1-45–1-47, 1-55B and 1-56A.

The maxillary nerve (Figs 1-55B and 1-56B) passes through the foramen rotundum and spans the pterygopalatine fossa before entering the orbit through the inferior orbital fissure as the *infraorbital nerve*. It lies beneath the periorbita and is thus not truly an orbital content. The nerve passes forward from the inferior orbital fissure to the *infraorbital groove*, which becomes the *infraorbital canal*, the nerve eventually emerging through the *infraorbital foramen* (Fig. 1-57). Here it radiates out as a number of cutaneous branches supplying the lower eyelid, the nose, upper lip and cheek (Fig. 1-55A). The *zygomatic nerve*, a branch of the

infraorbital, runs along in the inferior orbital fissure, beneath the periorbita, to the lateral wall of the orbit where it pierces the zygomatic bone as two branches, the *zygomaticotemporal* and *zygomaticofacial* nerves (both cutaneous). Traditionally, a communicating branch is described as passing up the lateral wall of the orbit to join the lacrimal nerve; however, the presence and importance of this nerve has been disputed. Other branches of the maxillary nerve, which pass through the *pterygopalatine ganglion* (without synapsing), supply the nasal cavity, upper alveolar arch and hard and soft palate (Fig. 1-55B). More details of these branches and those of the mandibular division are provided in standard anatomical texts.

The four parasympathetic ganglia of the head and neck (ciliary, pterygopalatine, otic and submandibular) are associated with the branches of the trigeminal (Fig. 1-55B). They are generally connected by short

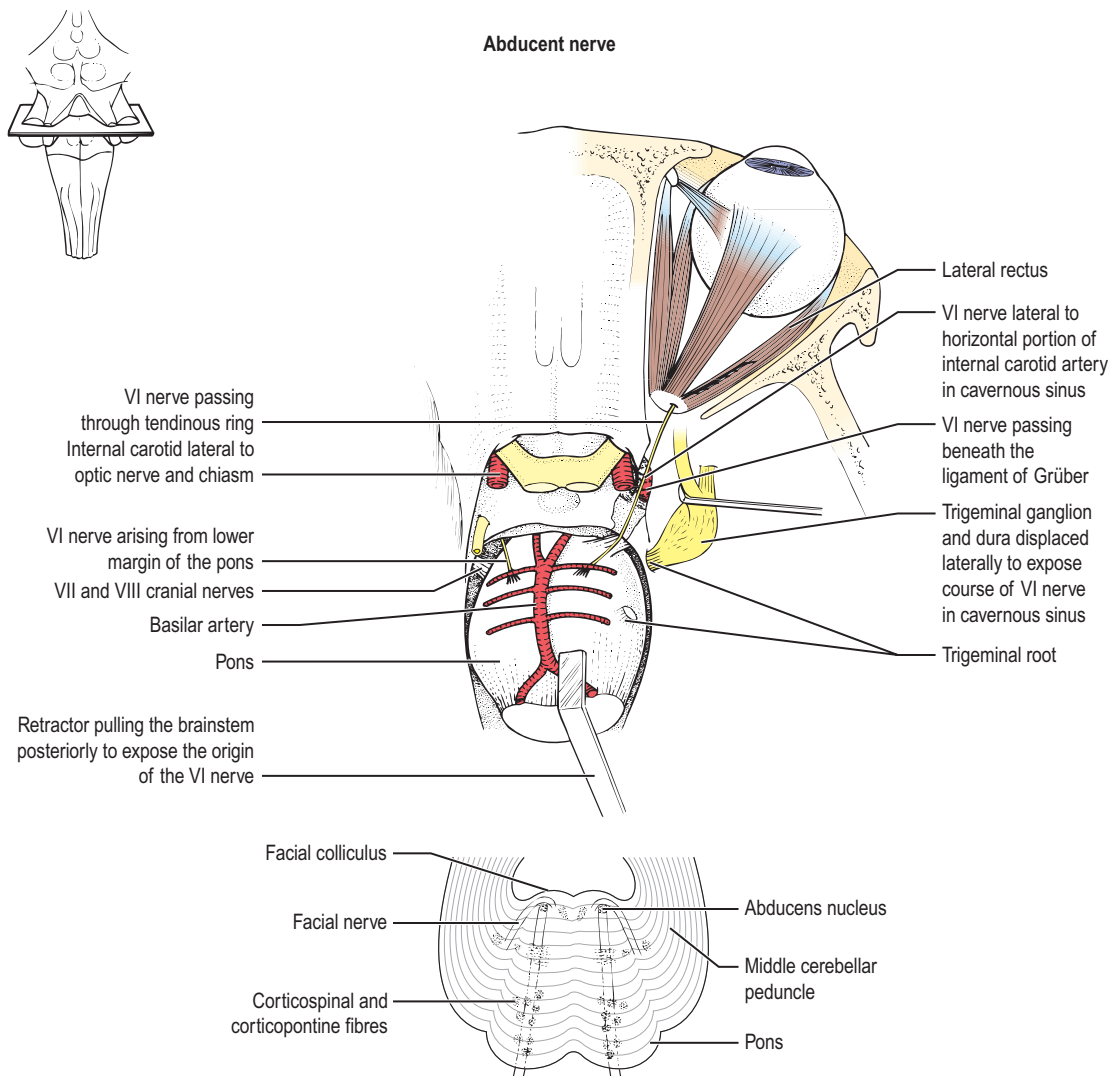


**FIGURE 1-54** Main diagram summarizes the intracranial, intracavernous and intraorbital course of the abducent nerve. The smaller lower diagram shows the neurohistological features at the level of the abducens nuclei (level of mid-pons on brainstem).

### BOX 1-31 CLINICAL CORRELATES

#### Intracranial lesions affecting the abducent nerve

The abducent nerve is considered the ‘weakening’ of the cranial contents. It is very susceptible to damage in head injuries, such as fractures to the base of the skull or any type of expanding cerebral lesion, owing to its long intracranial course. If the brainstem is displaced downwards (due to raised intracranial pressure) the nerve may be compressed against the inferior cerebellar artery or severed where it bends sharply over the apex or crest of the petrous

temporal bone. Within the *cavernous sinus* the nerve, not being protected by the dura of the lateral wall, is more susceptible than the other intracavernous nerves. For example, atheromatous changes in the internal carotid artery may compress the abducent nerve. Lesions of the abducent nerve result in paralysis of lateral rectus; thus, the patient is unable to abduct the eye and suffers esotropia (*internal strabismus*) as a result of the unopposed action of the medial rectus.

stalks containing pre- and postganglionic fibres, and the terminal fibres are distributed with the branches of the trigeminal – they may share the same perineurial sheath for part of their course ('hitch-hikers'). Sympathetics may also hitch-hike with branches of the trigeminal for part of their course and be distributed to the territories of this large nerve.

### Sensory nuclei of the trigeminal nerve

There are three sensory nuclei in the brainstem associated with the trigeminal nerve:

- **Mesencephalic nucleus.** This receives sensory (proprioceptive) information from muscles of mastication, muscles of facial expression and extraocular muscles. The peripheral processes are distributed with all three divisions of the trigeminal.
- **Pontine nucleus.** This is concerned with discriminative tactile information from the face. Fibres from all three divisions enter this nucleus.
- **Spinal nucleus.** This is continuous with the substantia gelatinosa of the posterior grey horn of the spinal cord. It is concerned with tactile, nociceptive and thermal information from the territories of the three divisions.

The afferent fibres terminating in the last two nuclei are the central processes of sensory neurones whose cell bodies are located in the trigeminal (Gasserian) ganglion. The peripheral processes terminate in appropriate sensory receptors in the territories of the three divisions.

### FACIAL NERVE (CRANIAL NERVE VII)

The facial nerve contains a number of functional components (eTable 1-1). The *facial nerve proper* (containing *branchiomotor* or *special visceral efferents*) supplies the muscles of facial expression, stapedius (small muscle in middle ear), stylohyoid, and the posterior belly of the digastric. The second component, the *nervus intermedius*, contains *secretomotor* or *parasympathetic* fibres (*general visceral efferent*), which synapse in the pterygopalatine ganglion and supply the lacrimal gland and choroid in addition to other glands in and around the nose and mouth. The nerve also transmits taste fibres (*special visceral afferents*) from the anterior two-thirds of the tongue. The extracranial branch of cranial nerve VII exits the skull through the

*stylomastoid foramen* and pierces the parotid gland to emerge at the anterior border of that gland (Fig. 1-58). The facial nerve is important to the eye and orbit primarily because of its parasympathetic supply to the lacrimal gland (and some intraocular branches) and its motor supply to the periorbital facial muscles (especially *orbicularis oculi*). It is the most frequently paralysed of all peripheral nerves.

There are three reflex arcs in the brainstem involving the facial nerve, of which the corneal reflex is an important clinical test (Table 1-5).

## Ocular appendages (adnexa)

### MUSCLES OF THE EYELIDS AND ADJACENT FACE

The muscles that are primarily responsible for movement of each eyelid include the *orbicularis oculi* (a muscle of facial expression), which is responsible for lid closure, and the *levator palpebrae superioris* (an extraocular muscle), which raises the lid.

Other muscles of facial expression of primary interest around the eye and eyelids are the *corrugator supercilii* and *occipitofrontalis*.

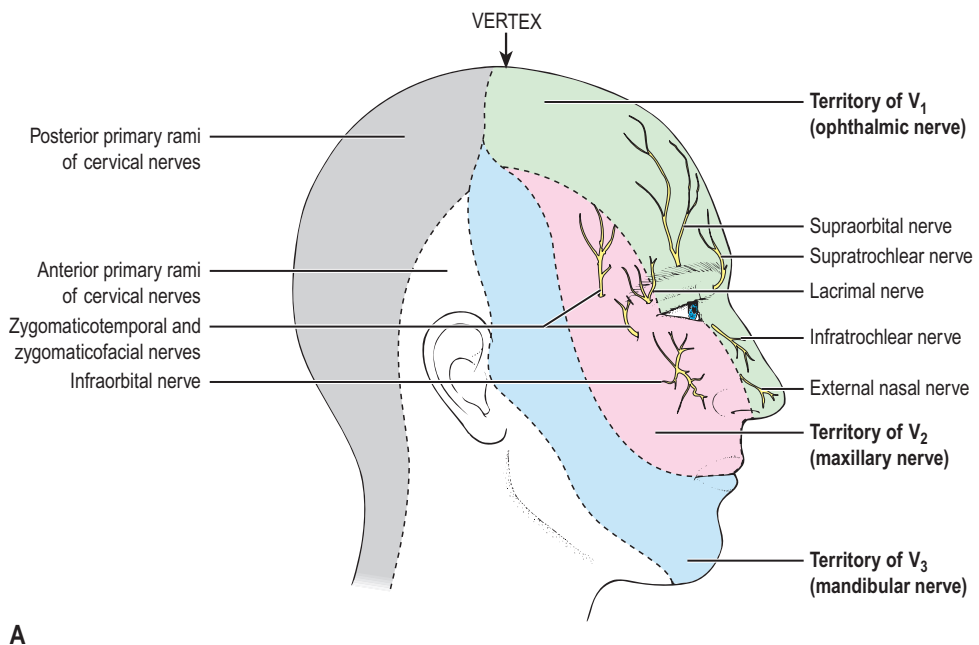
### Orbicularis oculi (Fig. 1-58)

**Shape.** The orbicularis oculi muscle is a broad, flat, sheet of skeletal muscle with orbital, palpebral and lacrimal portions. The circular orientation of the fibres is a reflection of the sphincter-like function of this muscle. The *orbital portion* arises from the medial palpebral ligament and the adjacent orbital margin

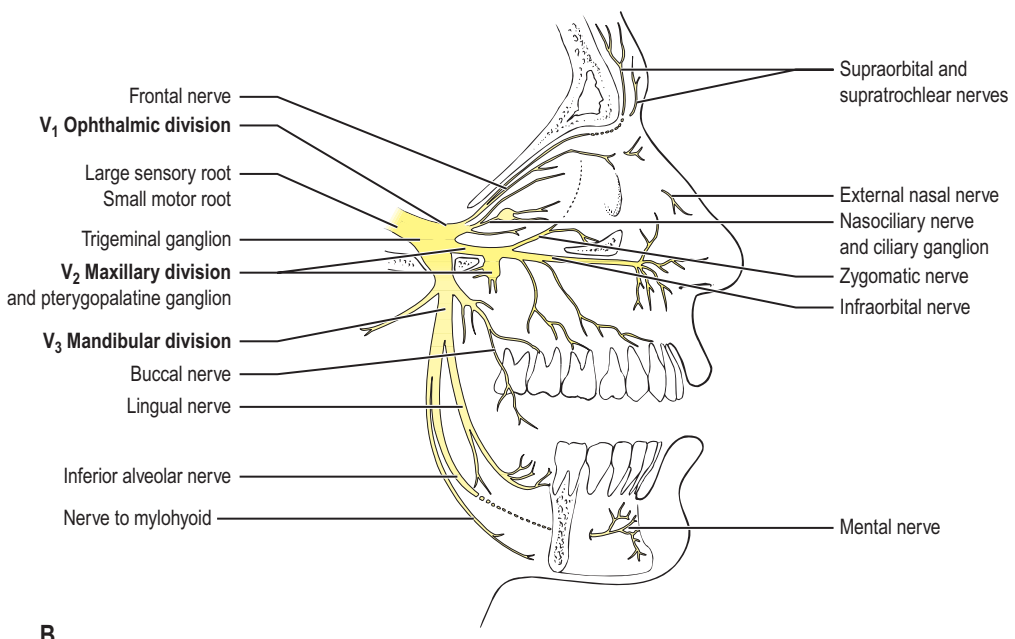
### BOX 1-32 CLINICAL CORRELATES

#### Trigeminal neuralgia ('tic douloureux')

This is a condition characterized by excruciating pain in the territory of one or more of the divisions of the trigeminal nerve. Thus, the clinician should be familiar with structures supplied by each division. Many causes have been suggested, including osteitis of the petrous temporal bone or compression of the root or ganglion in the cavum trigeminale by enlarged or engorged vessels; however, in many cases the aetiology is unknown. The territory of the maxillary nerve is most frequently involved, then the mandibular, and less commonly the ophthalmic nerve. Three commonly performed surgeries are glycerol rhizotomy, stereotactic radio-surgery (Gamma Knife) and endoscopic vascular decompression.



A



B

**FIGURE 1-55 (A)** Sensory ‘map’ of the head and neck. Note the limits of the territories of the skin of the face and scalp supplied by the three divisions of the trigeminal nerve (ophthalmic, maxillary and mandibular). **(B)** Stylized diagram showing the origin of the motor and sensory roots of the trigeminal, the position of the pterygopalatine and ciliary ganglia, and the territories of some of the major branches of the three divisions.

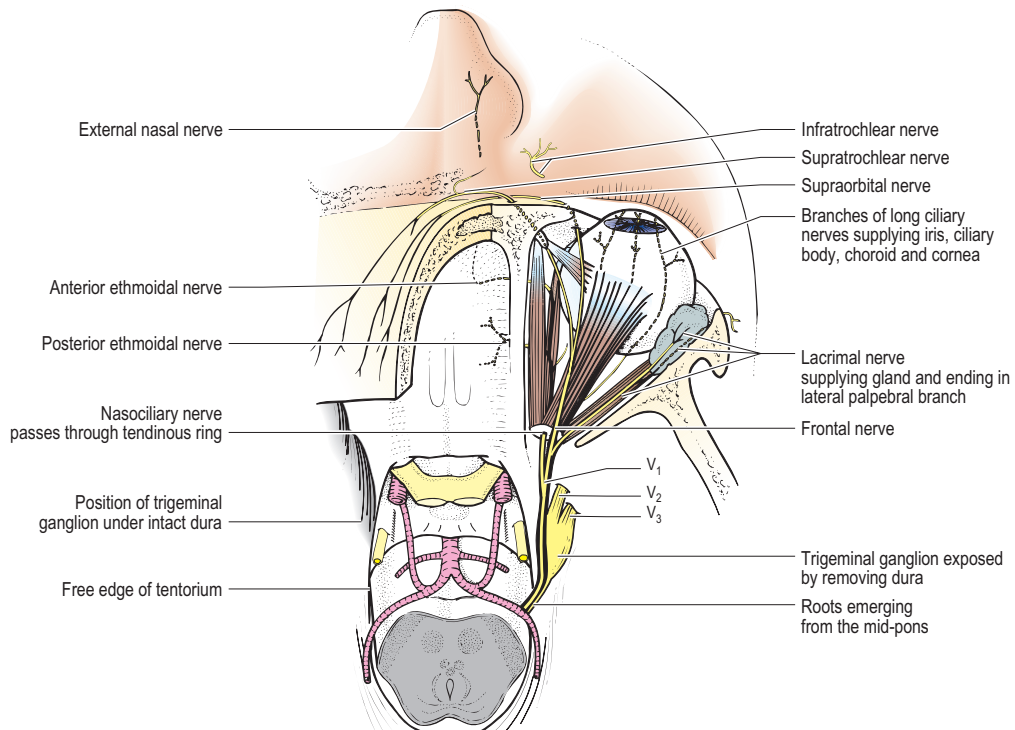


**FIGURE 1-56** Diagram summarizing the origin, intracranial, intracavernous and intraorbital course of the ophthalmic nerve and its three main branches.

- The **frontal nerve** passes obliquely above the levator palpebrae superioris and divides into the supraorbital nerve and the supratrochlear nerve.
- The supraorbital nerve passes through the supraorbital notch or foramen and ascends in the subcutaneous tissue of the forehead to supply the skin.
- The supratrochlear nerve passes along the medial wall of the orbit to pass above the trochlea and supply the skin at the root of the nose, upper eyelid and the medial part of the forehead.
- The **lacrimal nerve** travels forward along the upper border of the lateral rectus and sends fibres to the gland before ending as *lateral palpebral branches* to the conjunctiva and skin of this region.
- Branches of the **nasociliary nerve** include the *sensory root* to the ciliary ganglion (from which the short ciliary nerves emerge), *long ciliary nerves*, *posterior ethmoidal nerve* (supplies ethmoidal and sphenoidal sinuses), the *anterior ethmoidal nerve* and *infratrochlear nerves*.
- The anterior ethmoidal briefly re-enters the cranial cavity at the cribriform plate (beneath the dura) before piercing the bone to exit the cavity to terminate as the *medial and lateral internal nasal branches* (supply the nasal cavity), the latter of which ends as the *external nasal branch* which supplies the skin on the lower half of the nose.
- The infratrochlear nerve runs along close to the medial orbital wall, passes beneath the trochlea and supplies the skin at the angle of the eye and upper part of the skin of the nose.

(Fig. 1-58, inset). Its fibres run circumferentially in an elliptical fashion around and beyond the orbital margin. Most pass round the lateral orbital margin without interruption, although some fibres (known as *depressor supercilii*) are inserted into the skin and connective tissue of the eyebrow. The *palpebral part* is an extremely thin muscle that originates from the *medial*

*palpebral ligament*. Its fibres pass laterally within the eyelid anterior to the orbital septum and tarsal plate (see below), and interlace to form the *lateral palpebral raphe*. The small *lacrimal component* of the muscle passes deep to the medial palpebral ligament and is attached to the posterior lacrimal crest (behind the lacrimal sac) as two muscle slips (upper and lower).

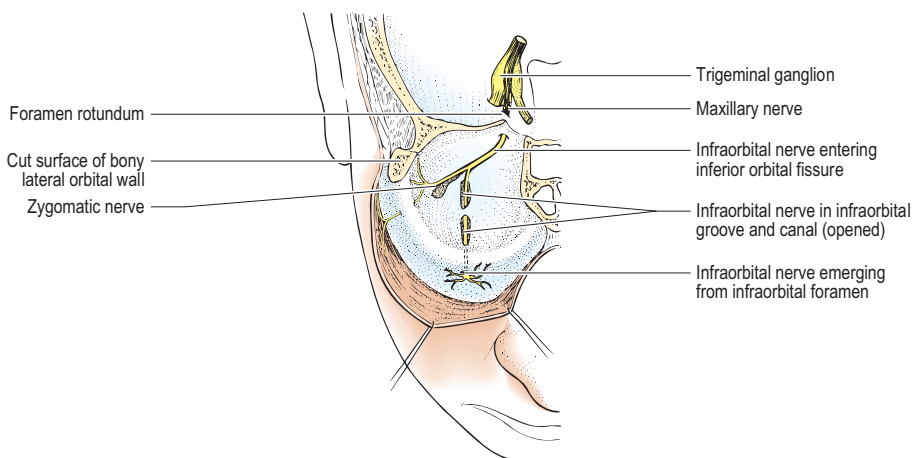


**FIGURE 1-57** Diagram of the orbital floor and the course of the maxillary and infraorbital nerves.

### BOX 1-33 CLINICAL CORRELATES

#### Lesions of the facial nerve

**Supranuclear lesions** – caused by vascular stroke in which descending corticonuclear and corticospinal fibres are damaged in the internal capsule. The upper facial motor nucleus (supplying upper half of facial muscles) receives input from ‘face’ areas of both the ipsilateral and contralateral motor cortices. The lower part of the facial nucleus has only contralateral input. The effect of a stroke, therefore, is to cause contralateral paralysis or weakness of the limbs and lower face. The upper face survives because of the bilateral supranuclear supply to the upper part of the facial nucleus.

**Nuclear lesions** – direct damage to the facial nucleus, such as thrombosis of the pontine branches of the basilar artery, results in complete paralysis of

structures supplied by the facial nerve (and abducent nerve; see Fig. 1-54) together with motor weakness of the limbs on the opposite side (owing to pyramidal decussation occurring below this level).

**Intranuclear lesions** – *Bell's palsy* involves direct neuritis of the facial nerve in the bony canal within the temporal bone and results usually in complete facial paralysis. The patient is unable to move the lips (saliva and food drools from the corner of the mouth), eyebrows or close the eyelids (lids may be lax, causing epiphora), and suffers hyperacusis (due to paralysis of the stapedius). Some patients may also have reduced lacrimal and salivary secretions and loss of taste to the anterior two-thirds of the tongue. Other causes of intranuclear lesions include multiple sclerosis, tumours of the cerebellopontine angle (acoustic neuromas), middle ear disease and tumours of the parotid gland.

These fibres are inserted laterally into the tarsi close to the lacrimal canaliculi; they help draw the eyelids and lacrimal papillae medially and in addition dilate the lacrimal sac during blinking. This helps to suck tears into the lacrimal punctum from the lacus lacrimalis.

**Nerve supply.** Temporal and zygomatic branches of the facial nerve.

**Action.** The *orbital* portion, owing to its elliptical form and medial attachments, acts like a purse string, drawing the skin of the forehead, temple, cheek and orbital margin towards the medial angle of the orbit, firmly closing the lids (for example, when in very

bright light). The *palpebral* portion of orbicularis oculi can act under both voluntary and involuntary control to close the eyelids during normal blinking (and sleeping). This blinking reflex (Table 1-5) is essential to the integrity of the ocular tear film and function of the cornea.

#### Corrugator supercilii

This is a small pyramidal muscle at the medial aspect of the eyebrow (Fig. 1-58), beneath the occipitofrontalis and orbicularis oculi. It draws the eyebrow downwards and medially (frowning), producing vertical skin furrows on the forehead. It assists in

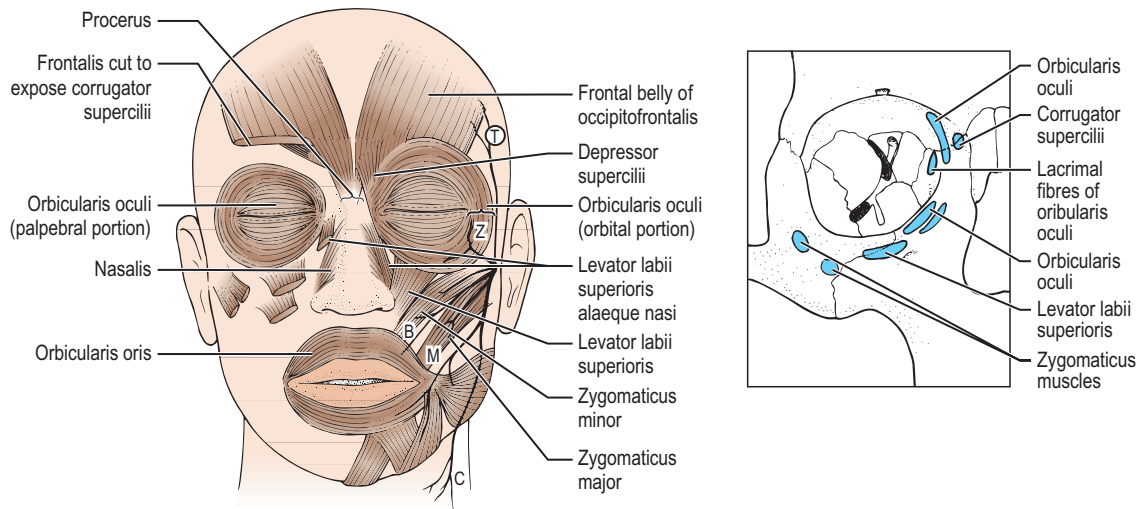


**FIGURE 1-58** The muscles of facial expression, particularly those of relevance to the eye and orbit. Inset shows the bony origins of some of these muscles around the orbit. Some of orbicularis oculi and frontalis muscle fibres have been removed on the right side of the face to display underlying musculature. The extracranial motor branches of the facial nerve that supply the muscles are shown on the right: T, temporal or frontal branches; Z, zygomatic branches; B, buccal branches; M, marginal mandibular branch; C, cervical branches.

protecting the eyes in bright light. It is supplied by small subdivisions of the temporal branch of the facial nerve.

### Occipitofrontalis

This fibromuscular layer covers the dome of the skull from the eyebrows to the nuchal lines. It consists of two occipital bellies posteriorly attached via a thick fibrous layer, the *galea aponeurotica*, to the two frontal bellies. Only the frontal part is of relevance to the eye and orbit. Its fibres form a thin quadrangular sheet that is attached to the superficial fascia above the eyebrows. The medial fibres are continuous with procerus (Fig. 1-58), the intermediate fibres with corrugator supercilii and orbicularis oculi, and the lateral fibres with orbicularis oculi. The frontal belly is supplied by the temporal branches of the facial nerve. Upon contraction it draws the scalp backwards and elevates the eyebrows, causing transverse wrinkles on the scalp as in expressions of surprise, horror, fright, or when glancing upwards.

### Levator palpebrae superioris

This muscle lies within the orbit and is responsible for opening the eyelids and, upon relaxation, allows

lid closure due to gravity. The muscle has its origin from the lesser wing of sphenoid, above and in front of the optic foramen, blending with the origin of superior rectus. The muscle belly passes horizontally forward above superior rectus, close to the orbital roof (Fig. 1-45). Behind the orbital margin it curves downwards into the lid where it becomes aponeurotic. The aponeurosis fans out, on either side, to form medial and lateral horns, which extend the whole width of the eyelid. The levator palpebrae superioris inserts into the skin of the upper lid (causing the horizontal palpebral sulcus or furrow) and the anterior surface of the tarsal plate (see Fig. 1-60C). The lateral horn of the aponeurosis forms the *lateral palpebral ligament*, which inserts into the lateral orbital tubercle, and the medial horn forms the *medial palpebral ligament*, which inserts into the frontolacrimal suture. The levator palpebrae superioris is supplied by the superior division of the oculomotor nerve (see p. 69 and Fig. 1-52). Upon contraction it elevates the upper lid, thereby opening the palpebral fissure. On the inferior aspect of the levator palpebrae superioris is a small band of smooth muscle, the *superior tarsal* or *Müller's muscle*. It is attached anteriorly to the upper surface of the tarsal plate and conjunctival fornix (see

**TABLE 1-5 Reflexes involving the facial nerve**

	<b>Corneal reflex</b>	<b>Blinking to light or fast-approaching object</b>	<b>Blinking to noise</b>
<i>Receptor</i>	Sensory ending in corneal epithelium	Retina	Cochlea
<i>Afferent pathway</i>	Long ciliary nerves, nasociliary nerve, ophthalmic nerve	Optic nerve	Vestibulocochlear nerve
<i>First synapse</i>	Spinal nucleus of trigeminal	Superior colliculus	Inferior colliculus
<i>Second synapse</i>	Facial nucleus	Facial nucleus	Facial nucleus
<i>Efferent pathway</i>	Temporal and zygomatic branches of facial nerve	Temporal and zygomatic branches of facial nerve	Temporal and zygomatic branches of facial nerve
<i>Effector muscle</i>	Orbicularis oculi	Orbicularis oculi	Orbicularis oculi

Fig. 1-60C). It has a sympathetic innervation and upon contraction assists the levator in elevating the eyelid. While there is no equivalent muscle to the levator in the lower lid, there is a small group of smooth muscle fibres (inferior tarsal muscle) that originate from the fascial sheath of the inferior rectus and insert into the lower tarsus.

## THE EYELIDS

The eyelids are thin curtains of skin, muscle, fibrous tissue and mucous membrane that serve to protect the eyes from injury and excessive light and also to distribute tears over the ocular surface during blinking. The upper lid, when open, normally just overlaps the corneoscleral junction, and it is this lid that undergoes most displacement during eyelid closure, the lower lid moving only minimally during normal blinking.

On external examination (Fig. 1-59) each lid is seen to be divided into *orbital* and *tarsal portions* by a horizontal *palpebral sulcus*, which is most evident on the upper lid. The upper lid is limited superiorly by the eyebrow, whereas the lower lid blends with the skin of the cheek. The upper and lower lids meet at the *medial* and *lateral canthi* or angles, and are separated from one another by an elliptical opening – the *palpebral fissure*. The lateral canthus is an acute angle (60°) and lies close to the eyeball; the medial canthus is rounded, elongated medially, and lies 6 mm from the eyeball. It is separated from the eye by a triangular zone, the *lacus lacrimalis* (lake of tears), in which a small raised red swelling, the *curuncula lacrimalis*, is situated. There are obvious racial differences in the shape and form of the eyelids and canthi, the most

conspicuous being the vertical *epicanthal fold* in Oriental and Asian races.

The eyelid margins (Figs 1-59 and 1-60) are approximately 30 mm in length, 2 mm in thickness, and relatively square in profile along most of their length, except the medial one-sixth, which is rounded and lacks eyelashes. Eyelashes are modified, thick, stiff hairs that occur as double or triple rows close to the anterior lid margin. They curl away from the lashes of the opposite lid. Notable features on the lid margins include:

- *Lacrimal puncta* located at the medial ends of the upper and lower lids. These drain tears from the *lacus lacrimalis*. The puncta are more easily identified if tension is placed on the lids, causing the papillae to blanch.
- Openings of *tarsal (meibomian) glands* are visible to the naked eye as a row of minute openings on the lid margin posterior to the eyelash follicles. There are around 30 in the upper lid and slightly fewer in the lower lid.
- The *skin/conjunctival transition zone* mucocutaneous junction occurs at the level of the opening of the tarsal glands.
- The *grey line* marks the anterior boundary of the tarsal plate and is a useful landmark for surgical incisions.

The histological structure of the eyelid is summarized in Figures 1-60 and 1-62. Note that the fibrous framework of the lids is formed by the *orbital septum* arising from the orbital margin (Fig. 1-43) and the *tarsal plates*. The *tarsal plates* are modified regional thickenings of the orbital septum that provide rigidity to the upper and lower lids and separate the orbit and its contents from the lids.

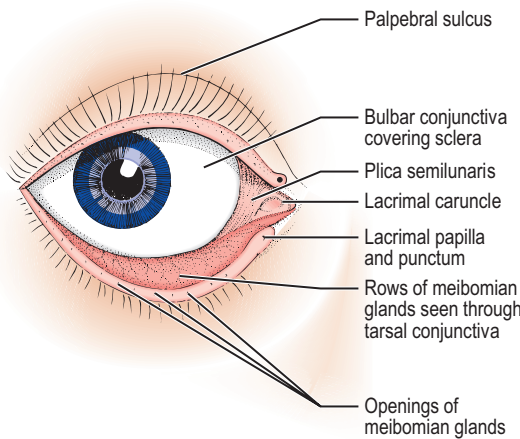


**FIGURE 1-59** Surface anatomy of the eye and eyelids. The bottom lid has been slightly everted to reveal the inner surface of the lid, lacrimal papillae and puncta and the openings of the meibomian glands along the lid margin.

#### BOX 1-34 AGEING CHANGES

Herniation of orbital fat through weakened regions of the septum occurs in the elderly, producing bulging, sagging lids (blepharochalasis).

The tarsal plates consist of dense fibrous connective tissue and are approximately 25–30 mm from the medial to lateral borders. They are 1 mm thick and the upper plate is greater in height (10–12 mm) than the lower plate (5 mm). They are attached at either end via their continuations, the *medial* and *lateral palpebral ligaments*. Skin moves freely over their anterior surface, although the conjunctiva is tightly bound to the posterior surface. External examination of an everted eyelid reveals vertical rows of yellowish tarsal glands (see inset, Box 1-35). They are embedded in the matrix of the tarsal plate and consist of modified sebaceous glands. Histologically the acinar cells are replete with lipid droplets that are secreted in a holocrine manner on to the eyelid margin, which functions to retain tears in the conjunctival sac and contributes to the lipid layer of the precorneal tear film.

The blood supply and nerve supply of the lids and surrounding areas are summarized in Figure 1-61. Lymphatics drain to the superficial parotid or submandibular lymph nodes. The pretarsal portion derives its arterial supply from the superficial temporal

#### BOX 1-35 CLINICAL CORRELATE

##### Chalazion, hordeolum and ectropion

A *chalazion* is a localized, painless swelling in the lid due to obstruction and chronic inflammation of a tarsal gland (see Fig. 1-60B).

A *hordeolum* (sty) may be an acute infection of an eyelash follicle or its sebaceous gland, infection of a ciliary sweat gland (external hordeolum) or acute infection of a tarsal gland (internal hordeolum).

*Ectropion* is drooping of the lower lid owing to paralysis of orbicularis oculi. Because of paralysis of the fibres of orbicularis that enclose the lacrimal sac, the puncta no longer suck up tears, which may thus pass over the lid margin (*epiphora*).

and facial arteries (branches of the external carotid), while the post-tarsal portion is supplied by branches of the ophthalmic artery (branch of internal carotid artery) (see Fig. 1-50). Venous drainage follows a similar pattern to the arterial supply (see p. 70 for consideration of anastomoses between the internal and external carotid arteries). The post-tarsal venous drainage is via the ophthalmic veins to the cavernous sinus.

#### Movements of the eyelids

The eyelids close as a result of the action of the palpebral fibres of the orbicularis oculi and relaxation of the levator palpebrae superioris. Opening of the lids occurs via the pull of levator palpebrae superioris on the skin, tarsal plate and fornecal conjunctiva. The nerve supply to these muscles is from three sources: orbicularis oculi – the facial nerve (VII); levator palpebrae superioris – the oculomotor nerve (III); while its smooth muscle component, superior tarsal (Müller's) muscle, is supplied by sympathetic nerves. The latter is important in times of fear or excitement when the width of the palpebral fissure is further increased.

#### THE CONJUNCTIVA

The conjunctiva (Figs 1-60A,C and 1-62) is a thin translucent mucous membrane that derives its name from the fact that it attaches the eyeball to the lids. It consists of a superficial conjunctival epithelium overlying a loose connective tissue stroma. The epithelium is continuous with the corneal epithelium at the limbus and with the skin at the mucocutaneous

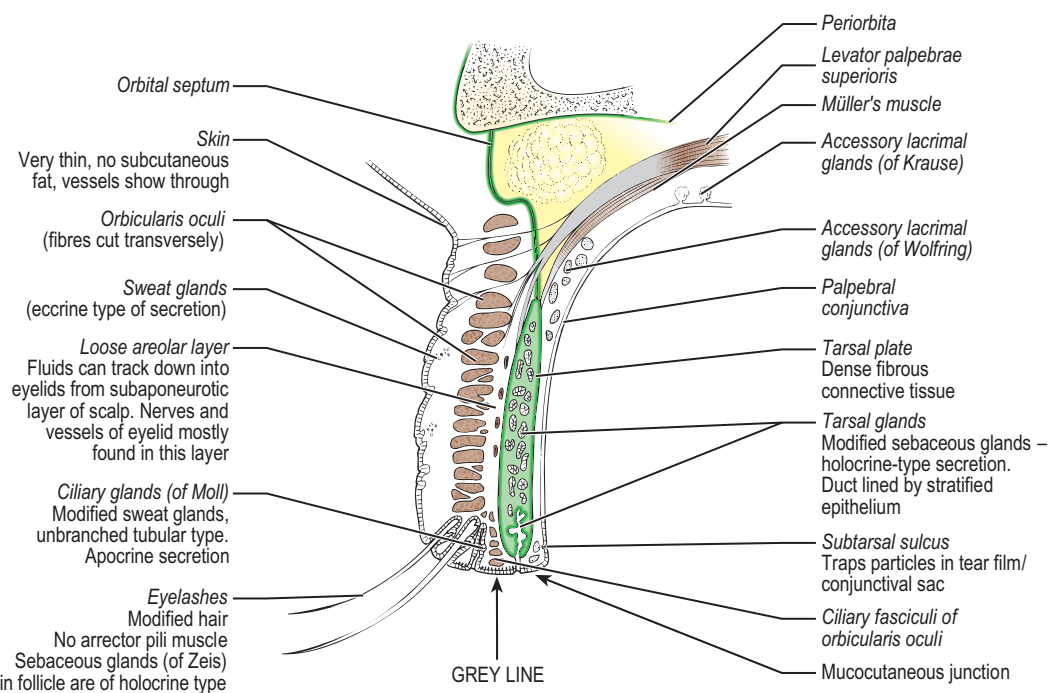


FIGURE 1-60

For legend see opposite page.

## BOX 1-36 CLINICAL CORRELATES

### Horner syndrome

Because of the complex neuroanatomy of the sympathetic nervous system, Horner syndrome, which is characterized by classical symptoms of unilateral ptosis, miosis and dry facial skin (anhidrosis) and blushing on the affected side, may result from a wide variety of lesions in the central and peripheral nervous system. These include iatrogenic interruption of the sympathetic chain in the neck, dissection of the internal carotid artery, cervical disk dislocation and the lysis of the first rib affecting the stellate ganglion associated with Pancoast tumour. Other symptoms may include heterochromia and enophthalmos, although the latter is debatable in humans.

junction on the lid margin. The conjunctiva is reflected from the anterior portion of the sclera at the superior and inferior fornices on to the tarsal surface of the eyelids. Thus, when the lids are closed a potential sac, the *conjunctival sac*, is formed. The volume of this sac is approximately 7 µL, which explains the tendency for eye drops from commercial dispensers (volume 50–70 mL) to overflow unless the lower lid is held away from the globe. The conjunctiva is responsible for the production of the mucous component of the tear film and, in common with other mucous membranes, has a variety of immunological defence mechanisms that protect the ocular surface from infection (see Ch. 7). For descriptive purposes the conjunctiva can be divided into three main regions.

### Palpebral conjunctiva (Fig. 1-60A,C)

This part lines the inner surfaces of the eyelids. It is tightly bound to the tarsal plate, the subepithelial connective tissue stroma being thin in this region. The lacrimal puncta open on to the palpebral conjunctiva; thus the conjunctival epithelium is continuous with the lining of the inferior meatus of the nasal cavity, which explains the manner in which infection spreads between these two sites. A small *subtarsal sulcus*, close to the lid margin, is important in trapping and removing foreign particles and debris on the ocular surface.

## BOX 1-37 CLINICAL CORRELATES

### Allergic responses in the conjunctiva

Clinical examination of the everted lid for signs of ocular allergy and infection is a common procedure. Two major types of abnormal accumulations of immune cells may occur: *follicles*, which are similar to mucosal-associated lymphoid follicles elsewhere and consist primarily of lymphocytes; and *papillae*, which are focal aggregates of chronic inflammatory cellular infiltrates and accompanying vascular changes. These are usually associated with allergic conditions and irritation of the ocular surface, such as in contact lens wear.

### Forniceal conjunctiva (Fig. 1-60A)

The superior and inferior fornices are continuous at the medial and lateral canthi, thus forming a circular *cul de sac*. It is into the superolateral fornix that the ducts of the main lacrimal gland and the bulk of accessory lacrimal glands empty. The forniceal conjunctiva is loosely attached to the fascial sheaths of levator palpebrae superioris and the rectus muscles, and thus moves slightly with the eye during contraction of these muscles.

### Bulbar conjunctiva

The white sclera is visible through the normal translucent bulbar conjunctiva (see Figs 1-20A and 1-59). It clothes the anterior part of the eyeball including the extraocular muscle insertions and Tenon's capsule. Near the limbus the conjunctiva is tightly bound to the globe, but further from the limbus there is a loose episcleral tissue layer (Fig. 1-62A) within which lies the pericorneal vascular plexus (Fig. 1-62D). These vessels can become dilated and conspicuous as a result of physical and inflammatory stimuli.

There are two specializations of the conjunctiva in the medial fornix. First, the semilunar fold (*plica semilunaris*), which is probably homologous to the nictitating membrane of lower mammals and many non-mammalian vertebrates. It is highly vascular and

**FIGURE 1-60** (A) Histological preparation of the upper eyelid, conjunctiva and anterior segment: PC, palpebral conjunctiva; FC, forniceal conjunctiva; BC, bulbar conjunctiva; C, cornea. (B) Primate upper eyelid as viewed from the inner aspect to reveal the rows of tarsal glands (arrowheads) and their openings (arrows) on the lid margin. (C) Schematic diagram of the upper eyelid in longitudinal section (sagittal plane). Original magnification: A,  $\times 15$ . (Part A courtesy of W.R. Lee and Springer-Verlag.)

rich in goblet cells and interstitial immunocompetent cells. The function of this loose fold may be to facilitate lateral movement of the eye. Second, the *caruncle* (*caruncula lacrimalis*) is a highly vascular nodule of modified skin in the medial corner of the eye containing large nests of accessory lacrimal and sebaceous glandular tissue.

### Structure of the conjunctiva

Histologically the conjunctival epithelium varies in structure, depending on location, from a stratified squamous non-keratinizing epithelium (close to the lid margin) to a stratified columnar epithelium (bulbar). In general it consists of between two and seven layers of epithelial cells that are organized into three main types: basal, intermediate and superficial. There is no

margin) to a stratified columnar epithelium (bulbar). In general it consists of between two and seven layers of epithelial cells that are organized into three main types: basal, intermediate and superficial. There is no

### BOX 1-38 CLINICAL CORRELATES

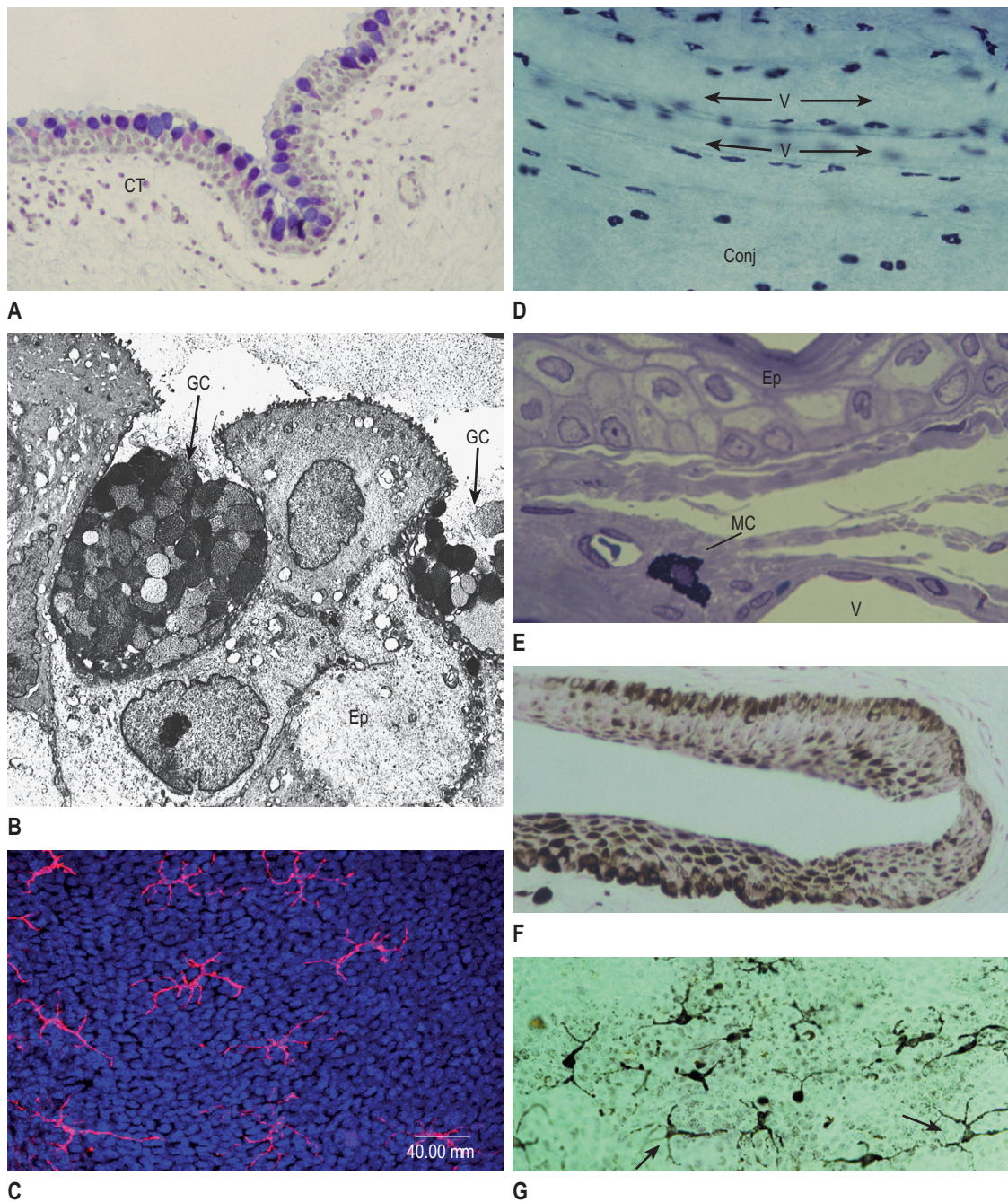
#### Systemic disease evident in the conjunctiva

The conjunctiva may manifest signs of several important systemic diseases: pathognomonic signs are present in sickle cell anaemia (comma sign), jaundice (scleral icterus (yellowing)) and vitamin A deficiency (Bitot's spots).



**FIGURE 1-61** Summary of the blood supply and sensory nerve supply of the eyelids and adjacent areas from cutaneous branches of the ophthalmic ( $V_1$ ) and maxillary ( $V_2$ ) divisions of the trigeminal nerve.

**FIGURE 1-62** Histology of the conjunctiva. (A) Low-power light micrograph of human conjunctiva (periodic acid–Schiff (PAS) stain) showing the irregular nature and goblet cell content (purple and red PAS<sup>+</sup> profiles) of the epithelium (compare to corneal epithelium; Figs 1-12, 1-14 and 1-16). Note the accumulations of lymphoid cells in the highly vascular connective tissue stroma, a common feature in eyes of elderly patients. CT, subepithelial connective tissue or connective tissue stroma. (B) Electron micrograph of goblet cells (GC) in the conjunctival epithelium: Ep, epithelium. (C) 'Plan view' of + intraepithelial dendritic cells (sometimes called Langerhans cells (LC)) in the limbal/conjunctival epithelium in wholemount preparation from Cx3cr1-GFP transgenic mouse (green – Cx<sub>3</sub>cr1<sup>+</sup> myeloid-derived cells; red – MHC class II; blue – DAPI-stained nuclei). Note the Langerhans cells are Cx<sub>3</sub>cr1<sup>+</sup> MHC class II<sup>+</sup>. The Z-profile shows how some of the cell processes act as 'periscopes' and project towards the superficial aspect of the conjunctival/limbal epithelium. (D) Toluidine blue-stained conjunctival whole mount illustrating the orientation and distribution of mast cells around limbal vessels (V) and in the bulbar conjunctiva (Conj) where they are more rounded. (E) Toluidine blue-stained semi-thin resin section of the limbal region showing a mast cell (MC) adjacent to a large venule (V). (F) Primate conjunctiva (histological preparation, H&E) showing melanocytes in the basal layer of the conjunctival/limbal epithelium. Note the intraepithelial melanin granules throughout the conjunctival epithelial layers. (G) Melanocytes as seen in a limbal whole mount preparation. Note their highly dendriform shape (arrows) and how they form a halo (dotted lines) of melanin granules within the adjacent epithelial cells ('epithelial-melanin unit'). Original magnifications: A,  $\times 150$ ; B,  $\times 3000$ ; C,  $\times 200$ ; D,  $\times 100$ ; E,  $\times 650$ ; F,  $\times 150$ ; G,  $\times 160$ . (Part B courtesy of W.R. Lee.)

**FIGURE 1-62**

For legend see opposite page.

'prickle' layer as found in corneal epithelium, indicating that there are fewer desmosomes between the conjunctival epithelial cells. There are numerous other cell types resident within the epithelium, reflecting its protective function, including the following:

- *Goblet cells* (Fig. 1-62A,B) – unicellular mucus-secreting cells that vary in density in different regions of the conjunctiva, being most numerous in the fornices and plica semilunaris. They are responsible for the secretion of the majority of conjunctival mucins.
- *Melanocytes* (Fig. 1-62E,G) – degree of melanization varies dependent on race, although melanocytes are present in all eyes. Melanosomes are synthesized within the melanocyte before exocytosis and subsequent uptake by surrounding epithelial cells as occurs in the epidermis.
- *Intraepithelial MHC class II-positive dendritic cells* (sometimes referred to as Langerhans cells because of their similar morphology to analogous dendritic cell populations in the epidermis of the skin) (Fig. 1-62C) – function as 'sentinels' on the ocular surface and are responsible for trapping and internalizing antigens and transporting these signals to either local lymph nodes (such as the preauricular nodes) or conjunctival associated lymphoid tissue (CALT) or follicles, where they are capable of presenting antigens to naïve T cells and inducing primary immune responses or driving antigen-specific B-cell maturation and immunoglobulin production (see Ch. 7).
- *Intraepithelial lymphocytes* – a feature of normal conjunctiva, but increased numbers occur in inflammatory conditions and close to subepithelial lymphoid accumulations. These are predominantly CD3<sup>+</sup> T cells, although occasional B cells are present.

The epithelium has an irregular basal aspect adjacent to the underlying connective tissue which is sometimes described as having a looser lymphoid layer and a deeper fibrous layer. Distinct papillae, finger-like protrusions of connective tissue stroma that project into the epithelium, are found only near the limbus. The subepithelial connective tissue contains numerous immunocompetent cells such as mast cells (Fig. 1-62D, E), eosinophils, plasma cells and lymphocytes

scattered among the matrix. In some eyes, particularly of older individuals, these may form diffuse or discrete aggregates. Some of these follicles contain pale germinal centres and represent the local mucosal lymphoid tissue (MALT) or CALT. There is no clear evidence of the specialized antigen-transporting intraepithelial M cells that are typically found in other similar MALT such as Peyer's patches or tonsils. The diffuse subepithelial aggregates along with intraepithelial lymphocytes form the efferent arm of the immune system and aid in immunological protection of the ocular surface. The topographical distribution of the small (~0.3 mm) lenticular lymphoid follicles and epithelial crypts in the tarso-orbital conjunctiva suggests that they may approximate to the cornea during eye closure and thus function as an 'immunological cushion'.

The loose connective tissue stroma contains a rich vascular network, similar to the eyelids. In addition, it also receives blood from the anterior ciliary arteries (see Fig. 1-50).

The sensory nerve supply of the palpebral conjunctiva is almost entirely from branches of the ophthalmic division of the trigeminal (supraorbital, supratrochlear and lacrimal nerves). These contain the neurotransmitters substance P, calcitonin gene-related peptide (CGRP) and gallanin. Only the medial portion of the inferior fornical and palpebral conjunctiva derives its nerve supply from the maxillary division (infraorbital nerve) (see Fig. 1-61). The long ciliary nerves supply the bulbar conjunctiva. Parasympathetic nerves from the pterygopalatine ganglion (containing the neurotransmitters acetylcholine and VIP) and sympathetics (containing norepinephrine and neuropeptide Y) travelling with branches of the ophthalmic artery are also present in the conjunctiva. Both parasympathetics and sympathetics have been identified around goblet cells, whereas the sensory nerve endings occur only among the stratified squamous epithelial cells.

### Glands in the conjunctiva

Besides the unicellular mucous glands (goblet cells) distributed throughout the conjunctiva, there are several small collections of named glands, some of which are accessory lacrimal glands (glands of Krause in the upper fornices, glands of Wolfring in the upper border of the tarsus); others secrete mucus (glands of Henle). The

accessory lacrimal glands are under sympathetic stimulation and are responsible for baseline tear production.

### LACRIMAL APPARATUS (Fig. 1-63)

The lacrimal apparatus consists of the *lacrimal gland*, *lacrimal puncta*, *lacrimal canaliculi*, *lacrimal sac* and *nasolacrimal duct*. The lacrimal apparatus functions to produce tears that moisten the ocular surface, thus preventing desiccation of delicate ocular cells and tissues, and facilitating non-friction-bearing movements of the lids on the globe. Tears are thus essential in maintaining the functional integrity of the eye.

**Tear film.** The tear film (7–9 µm) is composed of three layers: an outer oily or lipid layer (from meibomian and Zeis glands), a middle aqueous layer containing protein, electrolytes and water (mainly from lacrimal glands but also small contributions from conjunctival epithelia and cornea) and a deep hydrophilic mucin layer (from goblet cells and conjunctival epithelial cells and some from the corneal epithelium) associated with the microvilli-rich surface of the conjunctival epithelium (Fig. 1-62B).

### Lacrimal gland

The lacrimal gland measures approximately  $20 \times 12 \times 5$  mm and weighs approximately 78 mg. It is divided by the lateral horn of the aponeurosis of the levator palpebrae superioris into a large *orbital* and small *palpebral portion*, which are continuous via a small isthmus around the lateral border of the aponeurosis. The orbital portion is shaped like an almond

with a convex outer surface that is lodged in the *lacrimal fossa* (see Fig. 1-47). The concave inferior surface is moulded around the tendons of levator palpebrae superioris and lateral rectus (Fig. 1-63). The palpebral portion of the gland is approximately one-quarter of the total gland and its inferior surface lies close to the eye; indeed the gland can usually be seen when the upper lid is everted. In the orbital portion, fine interlobular ducts unite to form three to five main excretory ducts which then traverse the palpebral portion, joining a further five to seven from this part of the gland before entering the superotemporal conjunctival fornix. As a result of this arrangement, removal of the palpebral portion renders the entire gland non-functional.

**Histological structure (Fig. 1-64A–C).** The lacrimal gland is a branched tubuloacinar gland of the serous type. It is composed of many lobules separated by interstitial fibrovascular septae that are continuous with the poorly developed capsule. On section, each lobule contains numerous acini separated by abundant loose intralobular connective and adipose tissue. Histologically the acini resemble those of the parotid gland and appear as a series of rounded profiles in cross-section (Fig. 1-64A,B). Each acinus or tubuloacinar unit consists of a single layer of cuboidal or columnar cells whose apices are directed towards a central lumen (Fig. 1-64B–D). A layer of stellate-shaped myoepithelial cells surrounds each acinus. The central lumen of several acini unite to form intralobular ducts (Fig. 1-64A), which eventually form

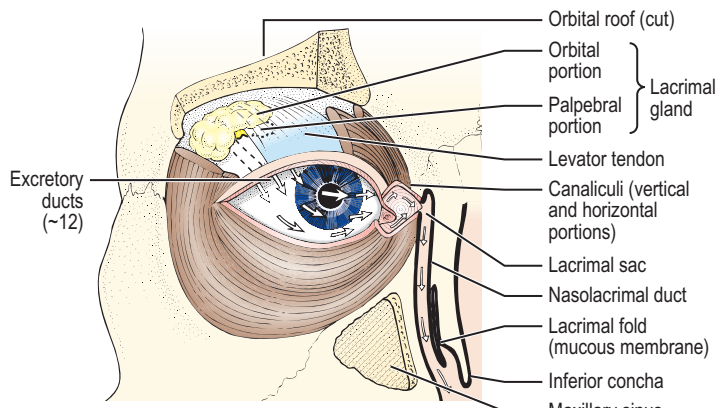


**FIGURE 1-63** Schematic diagram summarizing the entire lacrimal apparatus. Arrows indicate the direction of tears from the site of production to the site of drainage.

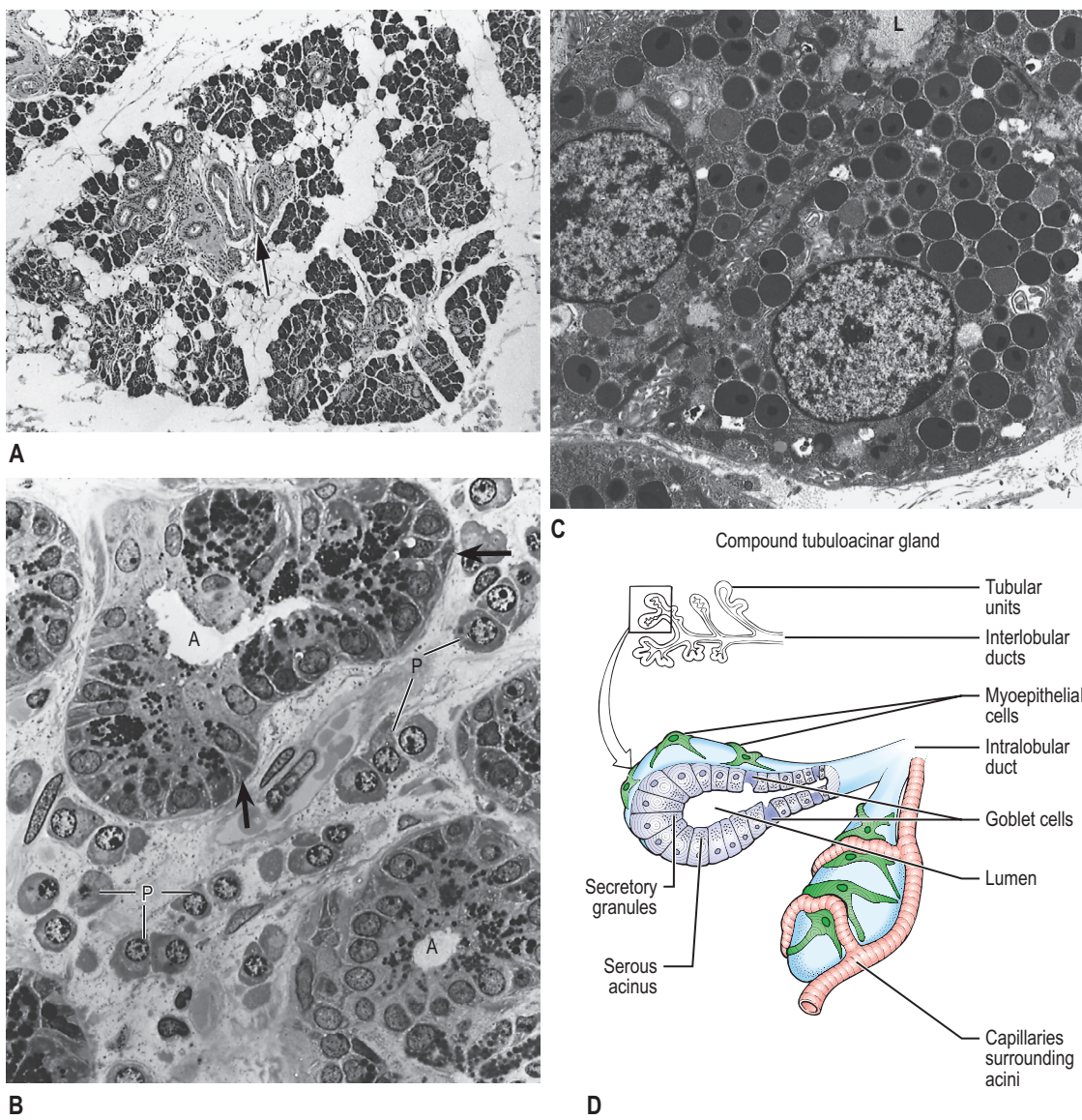


**FIGURE 1-64** Histology of the lacrimal gland. **(A)** Low-power micrograph of an entire lobule containing a series of large intralobular ducts (arrow). **(B)** Semi-thin section illustrating the arrangement of the glandular epithelial cells, containing numerous secretory granules, in acinar units (A). The vascular intralobular connective tissue is extremely rich in mature plasma cells (P). Arrows, myoepithelial cells. **(C)** Electron micrograph revealing the ultrastructure of a few pyramidal-shaped acinar cells whose apices are directed toward the central lumen (L). Note the numerous electron-dense zymogenic granules in the apical portion of the cells. An intracellular canalculus is indicated (arrow); N, nucleus. **(D)** Three-dimensional diagram summarizing the arrangement of the epithelial cells, myoepithelial cells and capillaries in the lacrimal gland. Original magnifications: **A**,  $\times 40$ ; **B**,  $\times 630$ ; **C**,  $\times 4400$ . (Part B courtesy of W.R. Lee.)

larger interlobular ducts that unite to form the main excretory duct system. The glandular epithelial cells have the characteristic histological and ultrastructural appearance of serous cells, namely basophilic cytoplasm, owing to large numbers of round or oval

secretory ('zymogen') granules. The epithelial cells have been subdivided into various subtypes depending on the size and electron density of these granules; however, there is still debate as to whether these are functional subtypes or different stages in the life

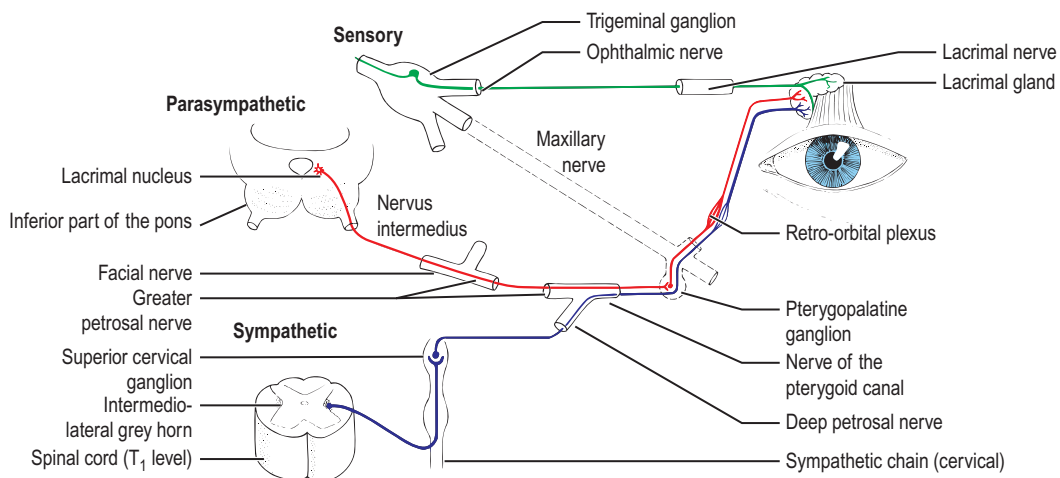


**FIGURE 1-65** Diagram summarizing the sensory (trigeminal nerve – green), secretomotor (facial nerve – red) and sympathetic (blue) innervation of the lacrimal gland.

cycle of one cell type. The presence of true intracellular canaliculi (Fig. 1-64C), as observed in salivary glands, is also still controversial. The secretion of the gland is primarily proteinaceous, although some granules contain glycosaminoglycans and the lumen on histological examination contains strongly eosinophilic and mucoid-like secretory material. The secretion also contains lysozymes, lactoferrin, B-lysin and immunoglobulin A (IgA), which are important in defence of the ocular surface against microbial infection. The IgA is derived from numerous plasma cells, present along with other immunocompetent cells such as lymphocytes and mast cells, in the intralobular connective tissue (Fig. 1-64B). The number of these cells increases with age concomitant with increased fibrosis and fatty infiltration and a decrease in the acinar elements especially in the orbital lobe.

**Nerve supply.** The nerve supply of the lacrimal gland and the complex course of the secretomotor fibres is summarized in Figure 1-65. The lacrimary nucleus of the facial nerve lies at the rostral end of the general visceral efferent column of cell bodies in the brainstem, which include the superior and inferior salivatory nuclei. The cells are under the influence of the hypothalamus via descending autonomic pathways, thus explaining the neuronal pathways involved in excess lacrimation, which accompanies various

emotional states. Reflex excess lacrimation occurs following irritation of the cornea, conjunctiva and nasal epithelia (afferent pathways in ophthalmic and maxillary divisions of the trigeminal). Interneurones connect the trigeminal sensory nuclei with the lacrimary nucleus.

**Blood supply.** The lacrimal gland derives its blood supply principally from the lacrimal artery, an early branch of the ophthalmic artery, although a variable branch from the infraorbital artery (originating indirectly from the external carotid) may also aid in its supply. Venous blood drains posteriorly, usually to the superior ophthalmic vein in the orbit, and lymph drains to the preauricular node.

#### Collecting portion of the lacrimal apparatus (Fig. 1-64)

The collecting system serves to drain normal tears that have not evaporated (normally only a very small quantity) and those produced in times of increased lacrimation. Excess tears are drained from the medial aspect of the conjunctival sac via the canaliculi into the lacrimal sac and nasolacrimal duct, to empty into the inferior meatus of the nasal cavity (Fig. 1-63).

The *puncta* are small openings (visible to the naked eye on the medial margin of each lid) at the summit of small swellings, the *papillae lacrimalis* (see Fig. 1-59). Tears that enter the puncta from the *lacus lacrimalis* during blinking pass into the *lacrimal canaliculi*

situated in the upper and lower lid behind the medial palpebral ligament. Each canaliculus is about 10 mm long (0.5 mm in diameter) and has vertical and horizontal components (Fig. 1-63) that may unite to form a common canaliculus before entering the lacrimal sac. The canaliculi are lined by stratified squamous non-keratinizing cells. They enter the lacrimal sac by piercing the fascial covering. This sac is 12 mm long and in its upper portion the walls are usually in apposition. It lies in the lacrimal fossa (see p. 2; Fig. 1-5B), protected by the medial palpebral ligament anteriorly and the lacrimal fibres of orbicularis oculi posteriorly. It is related medially to the ethmoidal air cells and the middle meatus of the nasal cavity. The walls of the lacrimal sac consist of fibroelastic tissue and are lined by a mucous membrane consisting of stratified cuboidal/columnar epithelium containing goblet cells. This epithelium is continuous with that lining the canaliculi and the nasolacrimal duct inferiorly.

The nasolacrimal duct empties into the anterior part of the inferior meatus of the nasal cavity, the opening being protected by a flap of mucous membrane, which prevents air and debris passing up the duct during nose 'blowing'. The duct lies in a bony nasolacrimal canal formed by the maxilla, the lacrimal bone and the inferior nasal concha. The duct is lined by a stratified columnar ciliated epithelium, which rests upon a vascular substantia propria. Knowledge of the position of a variety of constrictions and mucous membrane folds or 'valves' along the course of the canal is important during reconstruction of congenitally malformed lacrimal drainage systems.

## Anatomy of the visual pathway

The visual pathway is made up of the retina, optic nerves, optic chiasma, optic tracts, lateral geniculate bodies, optic radiations and visual cortex (summarized in Fig. 1-66). There are other areas of the cortex also associated with vision such as the frontal eye fields (see Ch. 5 for full description of visual physiology). The visual pathway is effectively a tract within the central nervous system because the retinae develop as evaginations of the diencephalon (see Ch. 5) and, as discussed above, the optic nerves are covered by layers of meninges; even the corneoscleral envelope and uveal tract of the eye itself can be considered as

homologous to the dura mater and pia–arachnoid, respectively.

The retina has been described on p. 38. The intraocular, orbital and intracanalicular portions of the optic nerve were described on p. 59. Description of the visual pathway will commence at the intracranial portion of the optic nerve.

## INTRACRANIAL PORTION OF THE OPTIC NERVE (Figs 1-51 and 1-66)

The optic nerves leave the cranial end of the optic canal and pass medially, backwards and slightly upwards within the subarachnoid space of the middle cranial fossa. They end by forming the optic chiasma in the floor of the third ventricle. Important relations include the olfactory tracts, frontal lobe (gyrus rectus) and the anterior cerebral arteries above. Each internal carotid artery as it emerges from the roof of the cavernous sinus lies lateral to the junction of the optic nerve and chiasma (Fig. 1-45). Below the optic nerves lies the jugum of the sphenoid and the sulcus chiasmaticus or optic groove.

## OPTIC CHIASMA

The optic chiasma (Figs 1-66 and 1-67) is situated at the junction of the anterior wall and the floor of the third ventricle, approximately 5–10 mm above the diaphragma sella and the hypophysis cerebri. It is a flattened quadrangular bundle of nerves measuring 12 × 8 mm whose anterolateral angles are continuous with the optic nerves, and its posterolateral angles form the optic tracts. It usually lies just behind the optic groove or sulcus chiasmaticus, but may rarely lie partly within the sulcus. The tuber cinereum (a sheet of grey matter that forms a median eminence around the base of the pituitary stalk or infundibulum) lies behind and below the chiasma between the mamillary bodies. The anterior perforated substance is an important lateral relation. The anterior communicating artery passes between the two anterior cerebral arteries, and lies above the chiasma. The partial crossing of optic nerve fibres in the optic chiasma is an essential requirement for binocular vision. The fibres from the nasal hemiretina of each eye cross the midline to enter the contralateral optic tract after taking a short loop in the ipsilateral tract or into the contralateral optic nerve. Nerve fibres from the

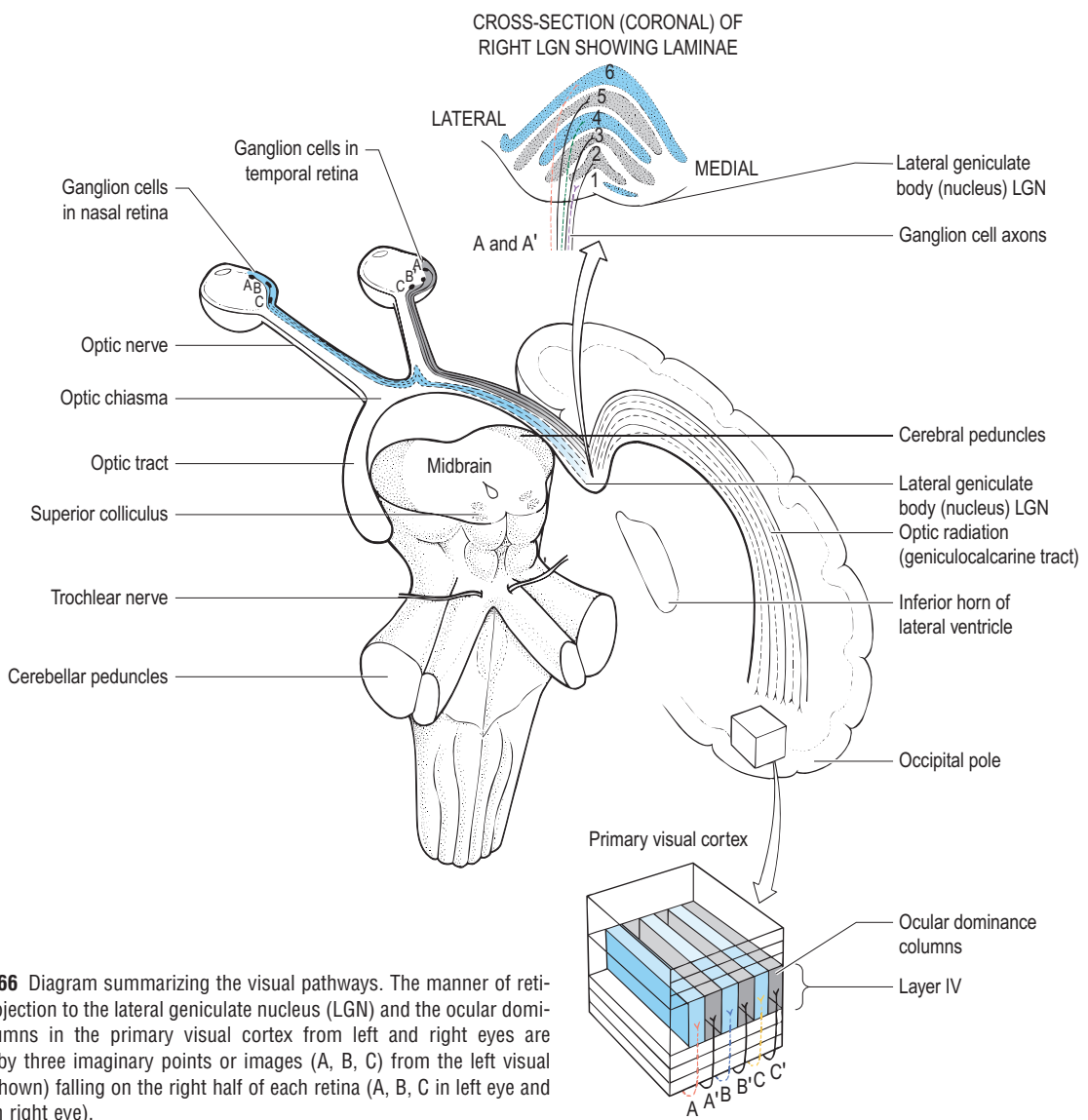


**FIGURE 1-66** Diagram summarizing the visual pathways. The manner of retinotopic projection to the lateral geniculate nucleus (LGN) and the ocular dominance columns in the primary visual cortex from left and right eyes are illustrated by three imaginary points or images (A, B, C) from the left visual field (not shown) falling on the right half of each retina (A, B, C in left eye and A', B', C' in right eye).

temporal hemiretina do not cross at the chiasma (Fig. 1-66).

## OPTIC TRACTS

The optic tracts (Figs 1-66 and 1-67) wind round the cerebral peduncles of the rostral midbrain and each divides into a large *lateral root*, which terminates posteriorly in the lateral geniculate body and is concerned with conscious visual sensation, and a smaller

*medial root*. The medial root is connected both to the *pretectal area* and *superior colliculus* by the *superior brachium* and carries around 10% of tract fibres, which functionally are not concerned with conscious vision. They contain six groups of fibres, three of which target the *superior colliculus* (involved in the visual grasp reflex, automatic scanning of images and visual association pathways); the remaining three enter either the *pretectal nucleus* (serve the pupillary light reflex), the *parvocellular reticular formation*

(arousal function), or the retinohypothalamic tract, which terminates in the suprachiasmatic nucleus of the hypothalamus (possibly involved in photoperiod regulation and has been invoked to account for the beneficial effect of bright artificial light or sunshine on mood).

The *superior colliculi* are two small rounded elevations located on the dorsal surface of the midbrain above the inferior colliculi, visible on external examination of the brainstem. The pineal body lies between and above the superior colliculi. The two pairs of colliculi are referred to collectively as the *tectum*. The mesencephalic or tectal termination of optic tract fibres is phylogenetically older than the forebrain termination (visual cortex).

The *lateral root of the optic tract* passes backwards, a little upwards, and terminates in the lateral geniculate nucleus (LGN), part of the thalamus (a relay station for ascending sensory information). The lateral root does not lie completely free because its medial aspect is attached to the outer wall of the third ventricle by a narrow band of tissue. It rotates slightly on its own axis (90° inward twist) as it passes round the cerebral peduncles. It runs above the dorsum sella and crosses the third nerve from medial to lateral. Below and parallel to the optic tract runs the posterior cerebral artery (Figs 1-52 and 1-71). The middle portion

of the tract is overlapped by the uncus and parahippocampal gyrus.

### LATERAL GENICULATE BODIES

Each lateral geniculate body (Figs 1-66 and 1-67) is distinguishable on the surface of the brain as an ovoid projection on the posteroinferior aspect of the thalamus, partly obscured by the overhanging temporal lobe (Fig. 1-67). It consists of a body, head, spur and hilum. The hilum is continuous with the groove between the medial and lateral root of the optic tract, which enters its anterior aspect. It lies at the anterior aspect of the pulvinar, which also partly surrounds it, particularly from above. The LGN in which the great majority of the optic tract fibres terminate consists of six laminae or cell layers (numbered 1 to 6 beginning at the hilum), oriented in a dome-shaped mound similar to a stack of hats (Fig. 1-66). On coronal section, the layers of cell nuclei (approximately 1 million) are separated by white matter (optic tract fibres). Nerve fibres derived from the contralateral eye (crossed fibres from the nasal half of the retina) terminate on cell bodies in layers 1, 4 and 6. Those of the ipsilateral eye (uncrossed) terminate in layers 2, 3 and 5. Thus each LGN receives information from both retinas. Each retinal ganglion cell axon may terminate on up to six geniculate cells; however, these are located

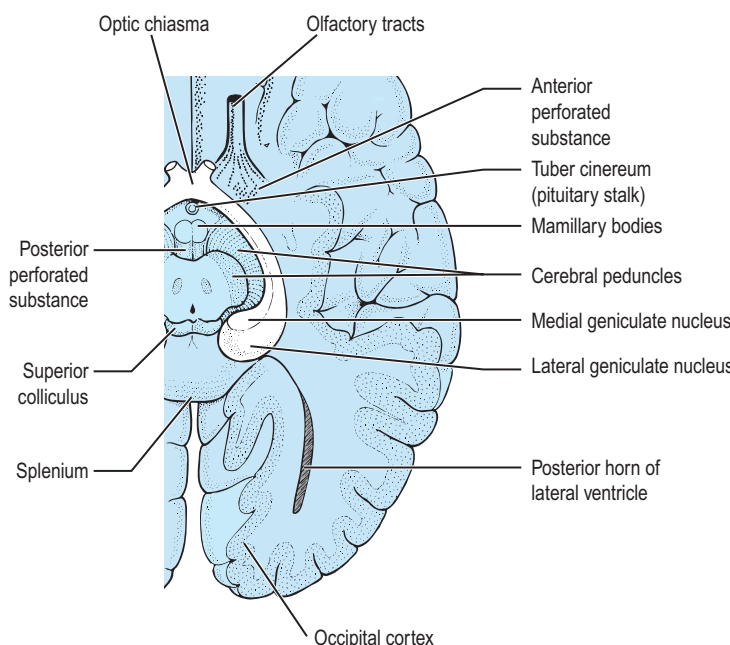


**FIGURE 1-67** The base of the brain with the brainstem and cerebellum removed to expose the optic nerves, optic chiasma, optic tracts and lateral geniculate nucleus and their relations.

in one lamina. Fibres from the upper quadrants of peripheral retinae synapse on the medial aspect of the LGN and those of the lower quadrant on the lateral aspect. The *macula* projects to a disproportionately large central wedge of the LGN. The posterior aspect of the LGN is dome-shaped, and it is from here that the geniculate cell axons that form the optic radiation emerge. The bulk of the LGN sends its fibres via the optic radiation to the visual cortex (area 17). The LGN has input from areas 17, 18, 19, oculomotor centres and the reticular formation.

### OPTIC RADIATIONS (GENICULOCALCARINE TRACTS)

These tracts (Fig. 1-66) consist of nerve fibre bundles whose cell bodies lie in the LGN. Their axons terminate in the visual (striate) cortex. The fibres form a wide forward and inferiorly directed fan-shaped loop (of Meyer), firstly into the retroレンicular portion of the internal capsule (posterior to sensory fibres and medial to auditory fibres). The fibres then pass into the temporal lobe around the inferior horn of the lateral ventricle (Fig. 1-68). Each tract then passes posteriorly along the lateral aspect of the posterior horn of the lateral ventricle before turning medially to enter the visual cortex. The optic radiations are of major clinical importance as they are frequently involved in cerebrovascular disturbance or tumours (Fig. 1-76). Not all fibres loop to the same degree (Fig. 1-68A,B). Those destined for the lower half of the visual cortex take a wider sweep into the loop around the tip of the inferior horn of the lateral ventricle than those designed for the upper half of the visual cortex (Fig. 1-68B). The fibres that swing furthest into the loop are associated with peripheral retina; those that pass more directly posteriorly originate closer to or within the macula region of the retina.

### PRIMARY VISUAL CORTEX (AREA 17)

The myelinated fibres of the geniculocalcarine tract (containing fibres from both eyes) enter the primary visual cortex, which lies within the depths of the calcarine sulcus and extends both above and below its margins on the medial surface of the occipital cortex, extending as far posteriorly as the occipital pole (Fig. 1-69B) and as far anteriorly as the parieto-occipital sulcus. The area above the fissure is known as the *cuneus gyrus* and below is the *lingual gyrus*.

Fibres from the superior retinal quadrants (representing the inferior visual field) pass to the upper lip of the calcarine sulcus. The fibres representing the macula account for one-third of the visual cortex (posterior portion of area 17). The myelinated fibres of the geniculocalcarine tract entering this area of cortex create the conspicuous white line or stria (of Gennari). This represents layer IV in the cortex (Fig. 1-70). The six basic layers of the primary visual cortex are shown in Figure 1-70. This region of cortex, although thinner (1.5 mm), is more cellular than other areas of cortex, the predominant cell type not being pyramidal but small stellate cells. Alternating *ocular dominance columns* of these cells receive input from right and left eyes (Fig. 1-66). The geniculocalcarine projection is ordered in a manner whereby matching points from the retinae of both eyes are registered side by side in contiguous columns (see Ch. 5 for a discussion of binocular vision, colour vision, etc.). The cells in laminae II and III project to the secondary visual cortex (areas 18 and 19; Fig. 1-69B,C). Those in lamina V project to the superior colliculus, and those of VI are a major source of 'feed-forward' to the LGN.

### SECONDARY VISUAL ASSOCIATION AREAS (AREAS 18 AND 19)

These association areas (Fig. 1-69B,C), which lack the characteristic 'extra' stria found in the primary visual cortex, lie above and below area 17 and extend on to the lateral surfaces of the cerebral hemispheres. They possess the usual six layers, although layer IV is less extensive. Areas 18 and 19 receive afferent input fibres from area 17, the thalamus and pulvinar, together with other regions of the cerebral cortex. The connections of areas 18 and 19 mainly follow dorsal and ventral pathways (Fig. 1-69C). Outputs to area 7 in the parietal cortex are mainly involved in stereopsis and movement. Ventral outputs to the inferotemporal cortex are concerned with analysis of colour and form, and connections to area 37 are associated with recognition of faces. Area 18 is also likely to be involved in sensory-motor eye coordination, as this is known to be linked to the frontal eye fields and oculomotor nuclei via descending pathways. This area also integrates information from two halves of the visual field via commissural fibres crossing the midline in the splenium of the corpus callosum (Fig. 1-67).

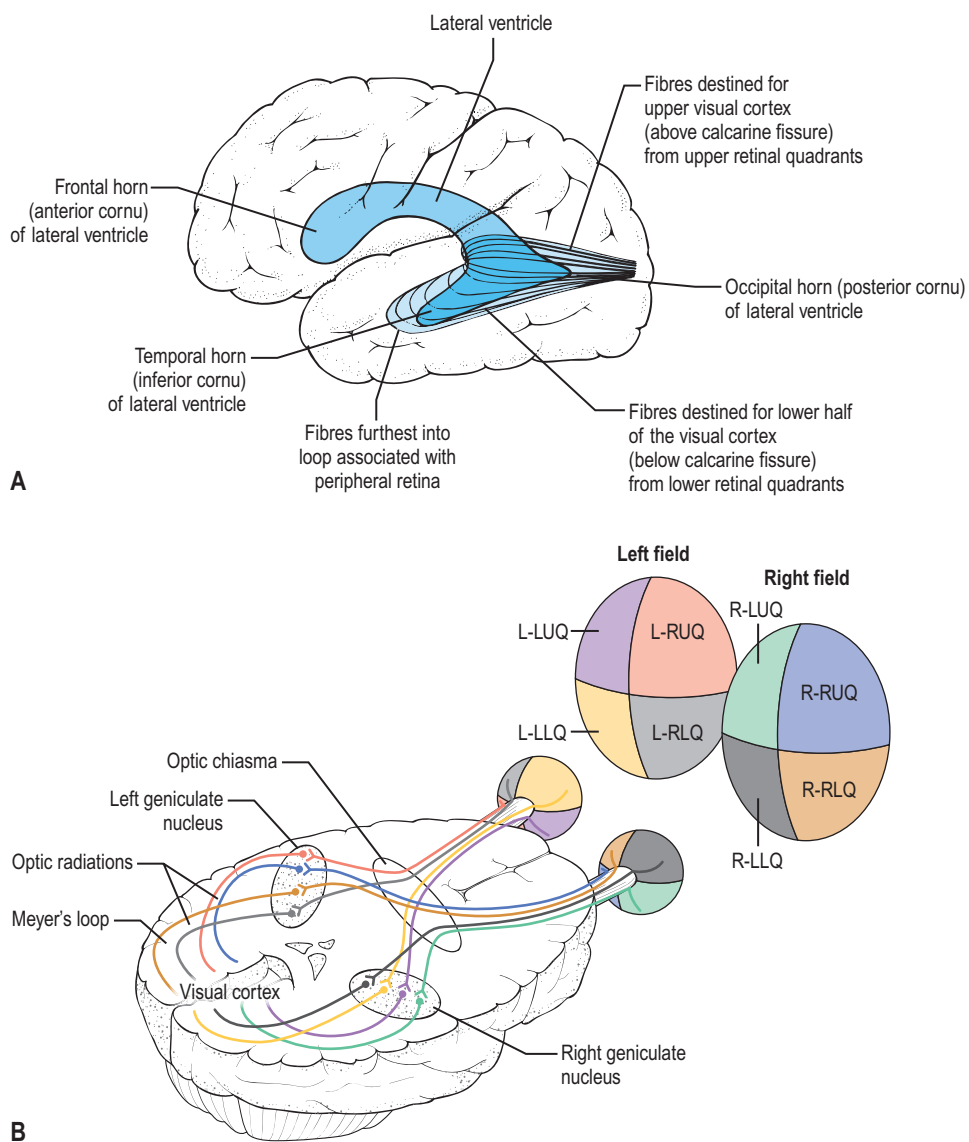


**FIGURE 1-68** (A) The optic radiation and its relation to the lateral ventricle, viewed from the left side. (B) Diagram showing the retinotopic organization of fibres within the optic radiations. (Part B courtesy of Wikimedia Commons.)

## FRONTAL EYE FIELD

This frontal area (Fig. 1-69C) corresponds to Brodmann's areas 6, 8 and 9, and is concerned with voluntary control of eye movements (saccades). Fibres pass from here to the superior colliculus, and in turn

are connected to the 'extraocular' cranial nerve nuclei (III, IV and VI) and anterior horn cells (motor neurones) in cervical spinal cord segments, thus allowing coordination of head and neck movements with eye movements.

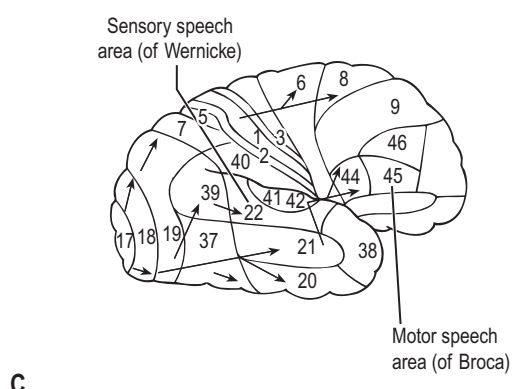
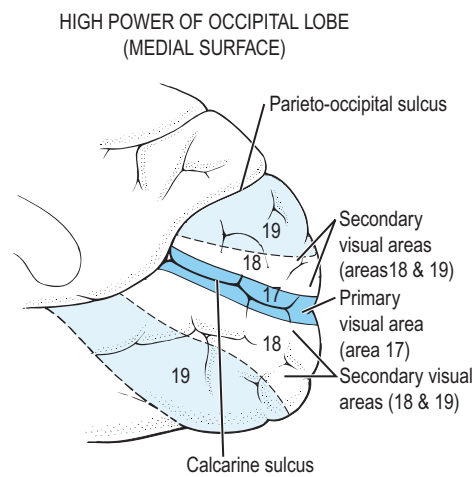
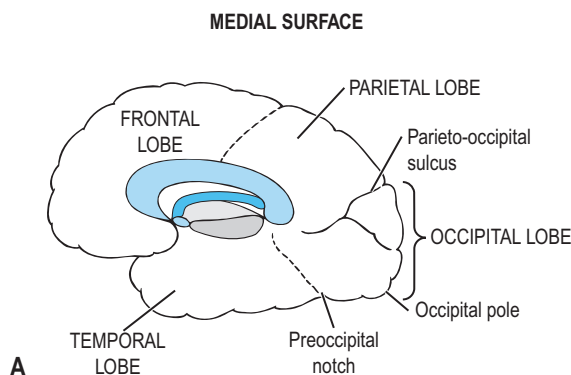


**FIGURE 1-69** (A) Simplified diagram showing the boundaries of the lobes of the brain as viewed from the medial aspect. (B) The medial surface of the right occipital lobe indicating the sites of the primary and secondary visual areas. (C) The cytoarchitectural areas of the cortex as described by Brodmann. Higher visual projections are from area 17 of the left hemisphere. Those to and from area 20/21 are concerned with detail and colour. Projections to and from area 7 are associated with stereopsis and movement, while those to and from area 39 are concerned with recognition of letters and numbers.

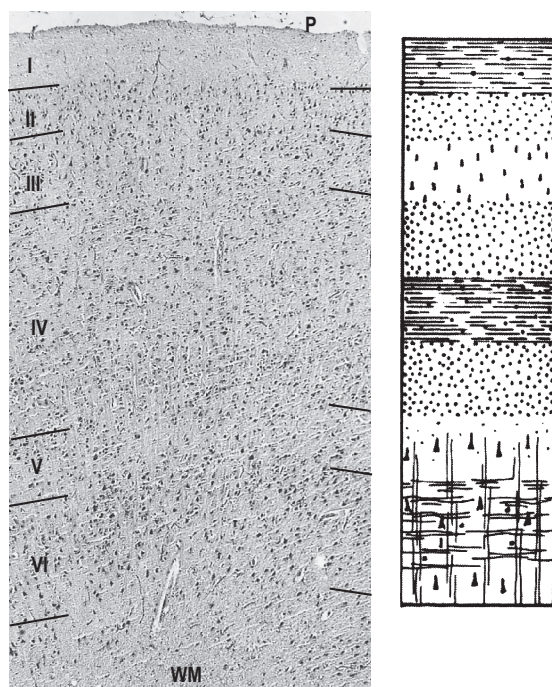


**FIGURE 1-70** Histology and cytoarchitecture of the primary visual cortex. Layers I–VI are indicated on the micrograph and adjacent diagram: P, pia; WM, white matter. Original magnification:  $\times 35$ .

## RETINOTOPIC ORGANIZATION OF THE VISUAL PATHWAY AND VISUAL PATHWAY DISTURBANCES (Figs 1-71–1-77)

A large amount of neurobiological research in primates and non-primates, together with observations of visual dysfunction or abnormalities in human subjects by neuro-ophthalmologists, has led to a considerable body of knowledge regarding the position along the visual pathway of fibres originating from various points on the retina. This information has been crucial to our understanding of the physiology of vision (see Ch. 5), but in addition helps to explain the specific patterns of visual field disturbances following localized lesions in the pathway. Examples of these lesions and the resultant visual field loss are provided in Figures 1-72–1-77.

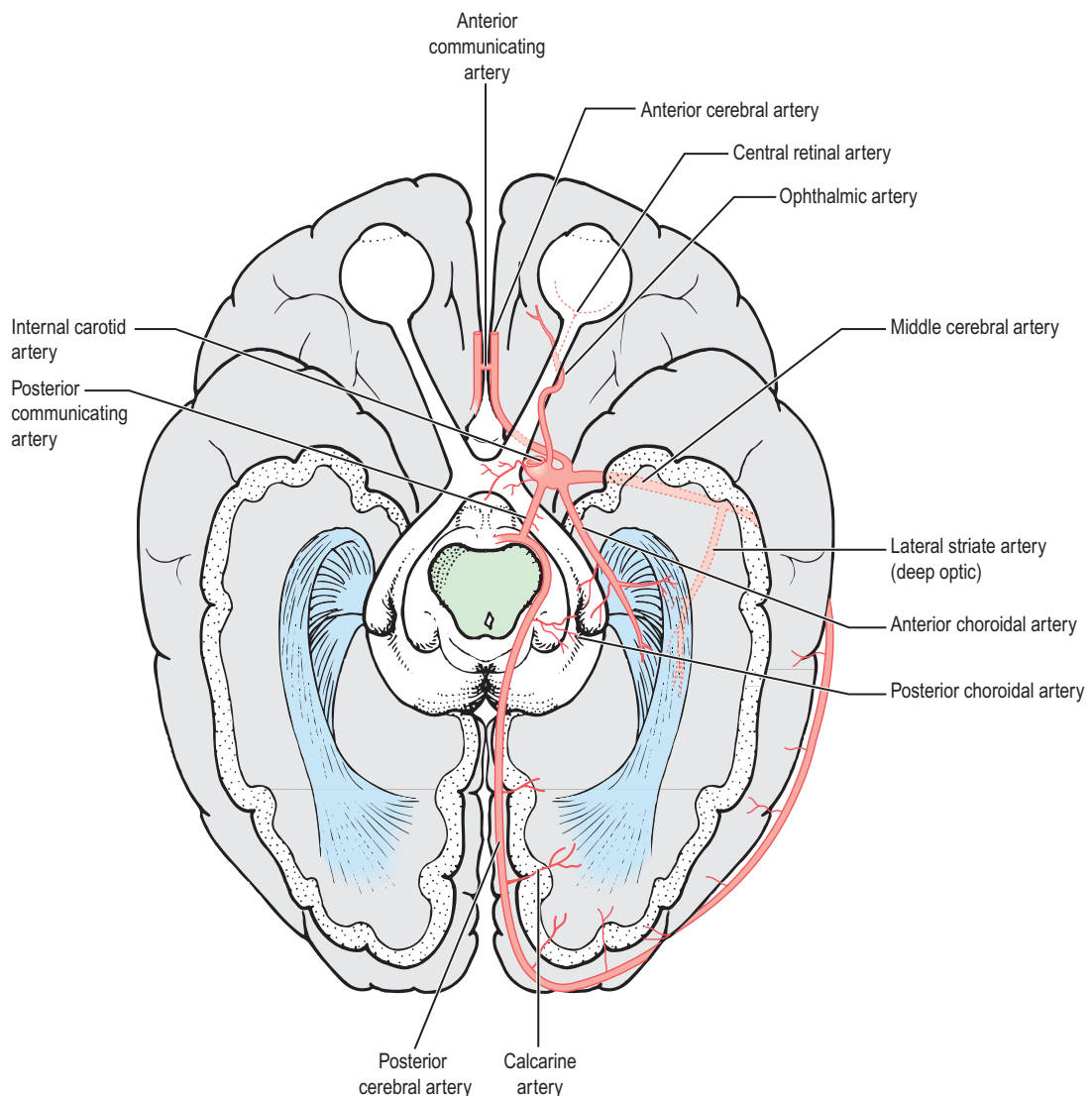


**FIGURE 1-71** Diagram of a brain dissected to display the visual pathways as seen from the ventral aspect. The blood supply to the various parts of the visual pathways is shown in red on the right-hand side of the diagram (corresponding to the *left side of the brain*). Note the blood supply to the following areas:

- Intracranial optic nerve: ophthalmic artery (an important inferior relation) and pial branches of the hypophyseal artery.
- Optic chiasma: adjacent related vessels including the superior hypophysial, internal carotid, posterior communicating, anterior cerebral and anterior communicating artery.
- Lateral root of the optic tract: anterior choroidal artery.
- Lateral geniculate body: anterior choroidal artery and branches of posterior cerebral artery.
- Commencement of the optic radiation (geniculocalcarine tract): anterior choroidal artery.
- Posteriorly directed fibres: lateral striate (deep optic) branch of the middle cerebral artery.
- Termination of geniculocalcarine tract and visual cortex: perforating branches of cortical arteries, principally the calcarine branch of the posterior cerebral although the middle cerebral may anastomose and aid in the supply of the cortex at the anterior end of the calcarine sulcus and at the posterior pole.

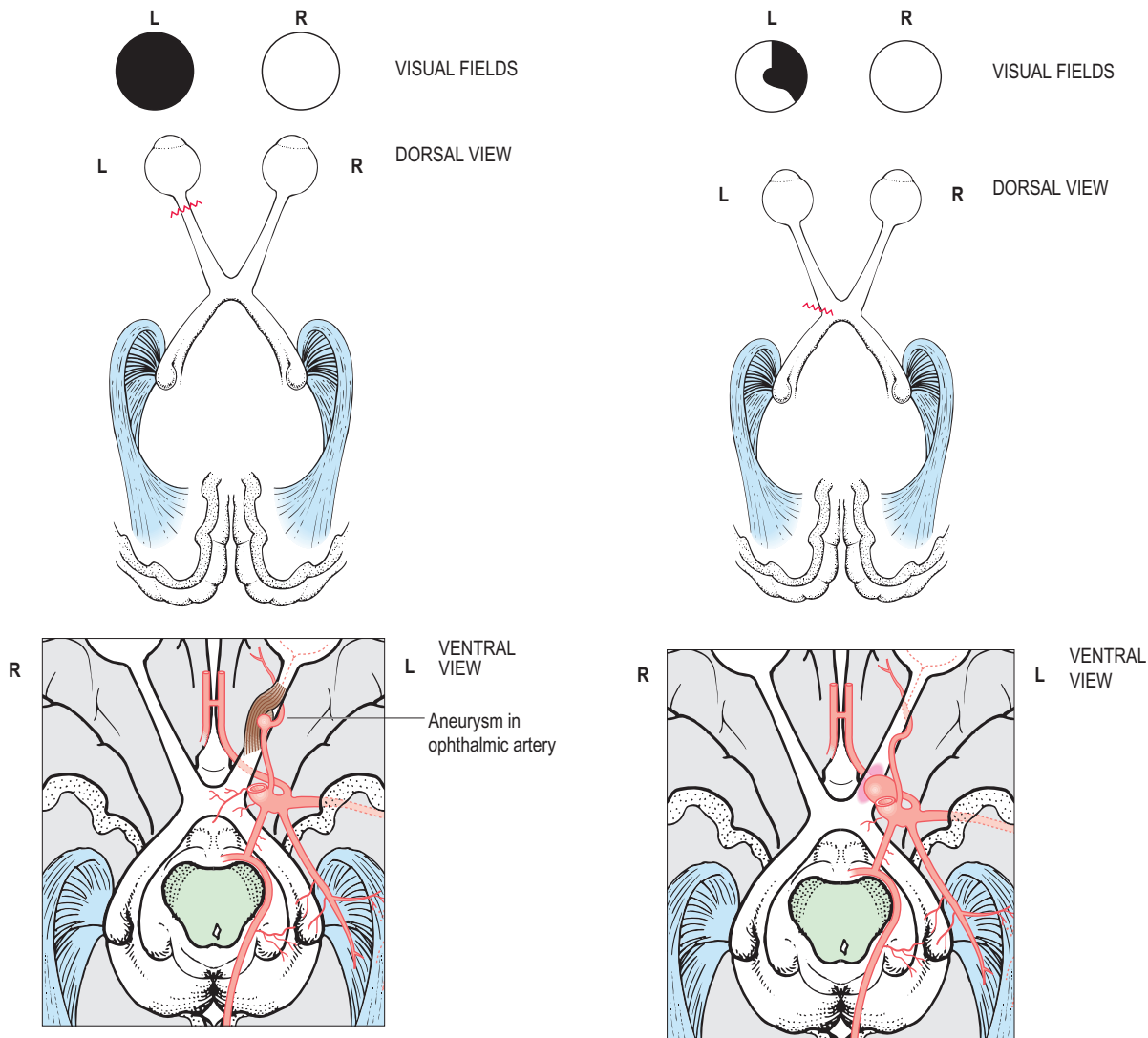


**FIGURE 1-72** Blindness in the left eye (top panel shows visual field deficit) caused by a lesion in the left optic nerve (middle panel). An example of such a lesion, an aneurysm in the ophthalmic artery, is illustrated (bottom panel: ventral view of the brain).

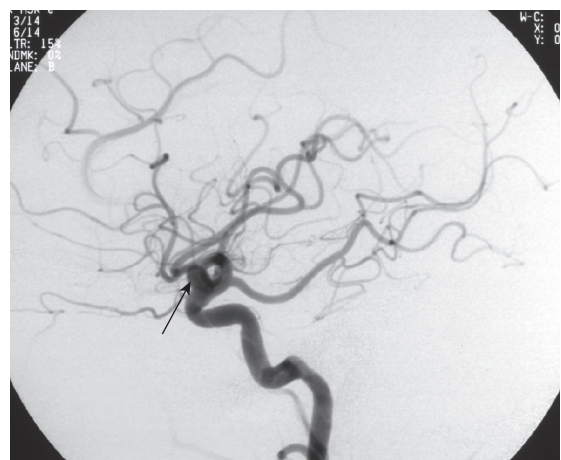


**FIGURE 1-73** (see right) Incongruous ipsilateral nasal hemianopia (top panel) caused by a lesion on the left side of the optic chiasma (middle panel). An example of such a lesion is an aneurysm of the terminal portion of the internal carotid artery (bottom panel). The radiographic image shows the digitally subtracted arterial phase of a carotid arteriogram of a 48-year-old patient suffering incongruous ipsilateral nasal hemianopia due to such an aneurysm (arrow). (Radiographic image courtesy of Prof. T. Chakera, Royal Perth Hospital.)

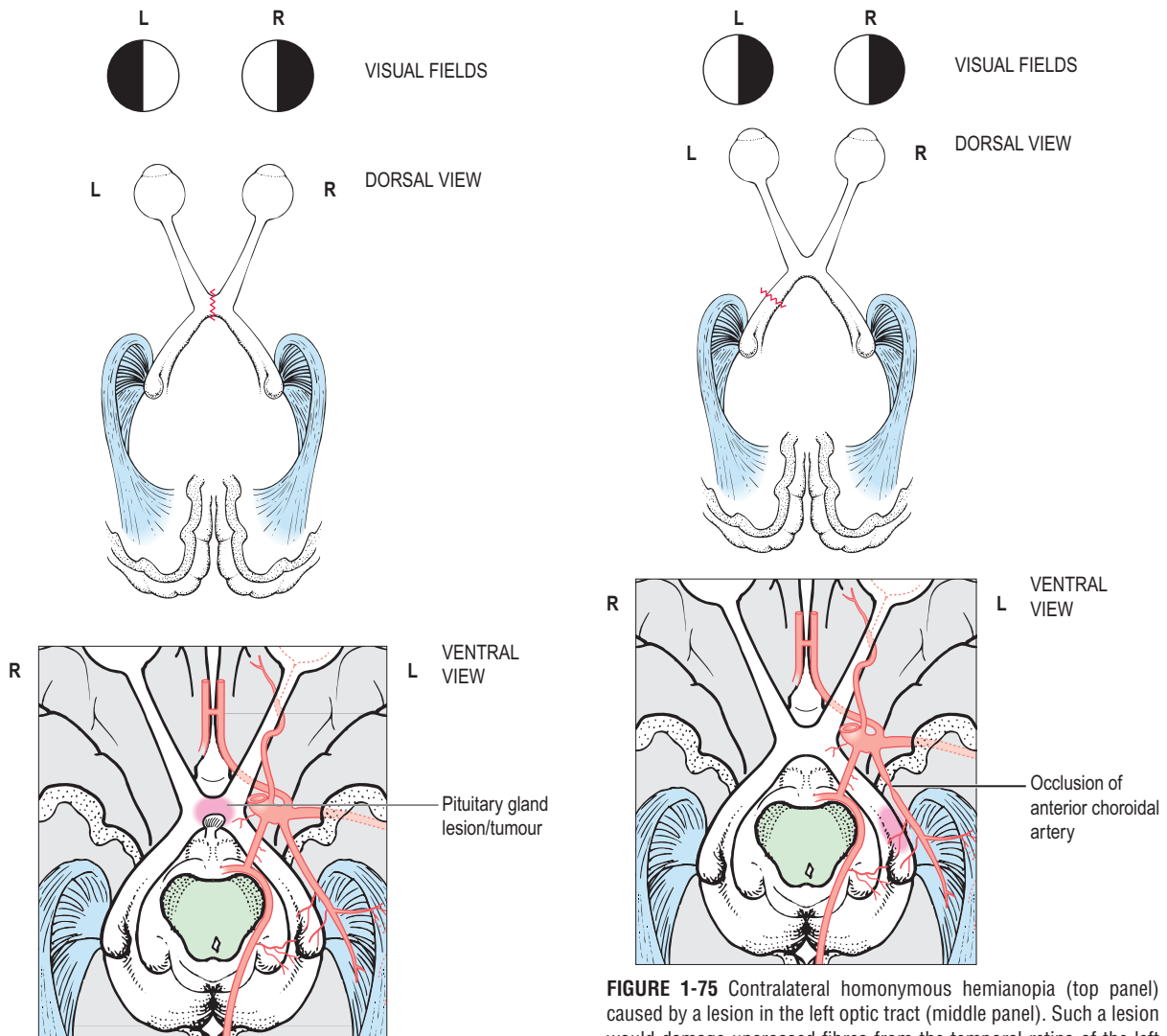


**FIGURE 1-75** Contralateral homonymous hemianopia (top panel) caused by a lesion in the left optic tract (middle panel). Such a lesion would damage uncrossed fibres from the temporal retina of the left eye and crossed fibres from the nasal retina of the right eye and therefore cause disturbances in the right visual field. Causes of this type of deficit may include vascular disturbances such as occlusion of the anterior choroidal artery (bottom panel).

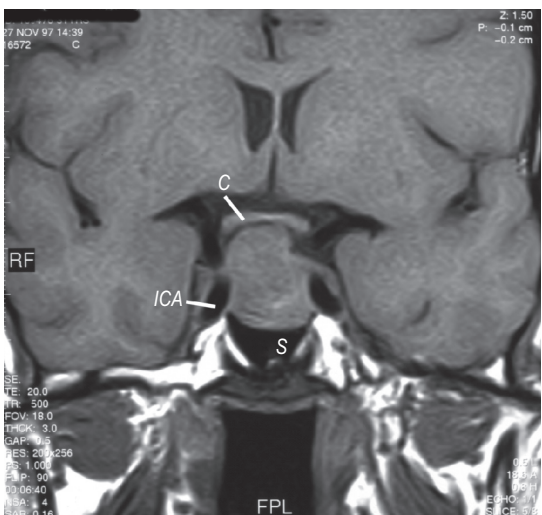


**FIGURE 1-74** (see left) Contralateral bitemporal homonymous hemianopia (top panel) caused by interruption or damage to the nasal retinal fibres decussating in the optic chiasma (middle panel). A common cause of such deficits is pituitary tumours (bottom panel). Radiograph: coronal MR image of the sellar region in a 31-year-old patient who presented with bitemporal hemianopia. A large pituitary tumour can be seen compressing the optic chiasm (C). S, sphenoid sinus; ICA, internal carotid artery. (Radiographic image courtesy of Prof. T. Chakera, Royal Perth Hospital.)

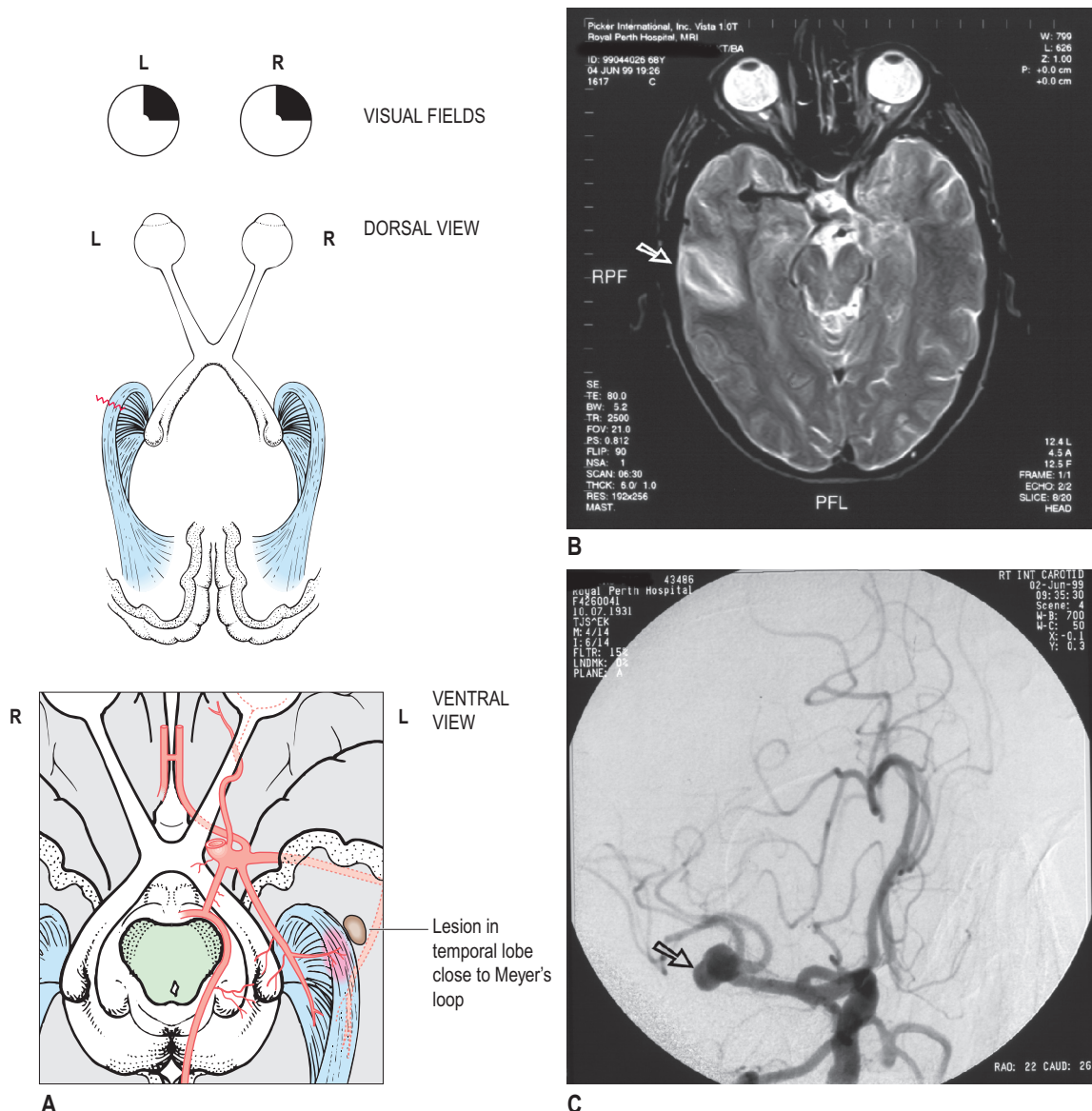


**FIGURE 1-76** (A) Contralateral homonymous superior quadrantanopia (top panel) – so called ‘pie in the sky’ defects – may result from lesions in the temporal lobe affecting the fibres furthest into the optic radiation (middle panel) (see Fig. 1-68B), which are derived from the inferior retinal quadrants and therefore cause deficits in the superior visual field. (B) Radiographic image of the brain of a 68-year-old patient with a stroke in the right middle cerebral artery (MCA) territory. Axial MR scan (diffusion weighted) shows the size and limits of the right temporo-parietal infarct (arrow). (C) The digital subtraction carotid arteriogram (anteroposterior projection) shows the aneurysm (arrowhead) at the bifurcation of the right MCA. The extent of the ischaemic changes in the temporal lobe (involving the optic radiation) are consistent with the patient’s loss of the left visual field causing him to bump into objects. (Radiographic images courtesy of Prof. T. Chakera, Royal Perth Hospital.)

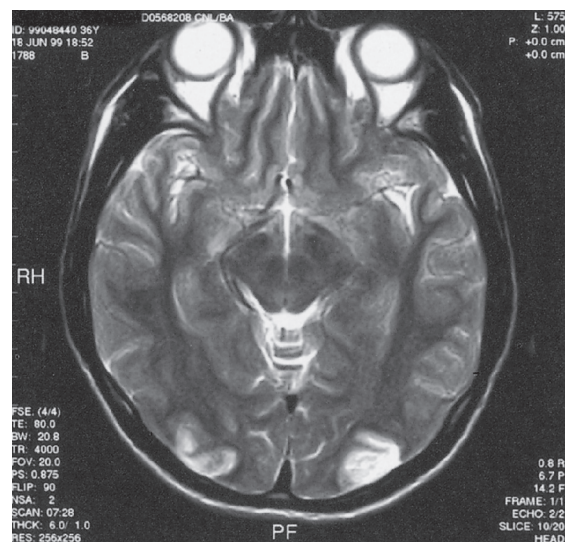
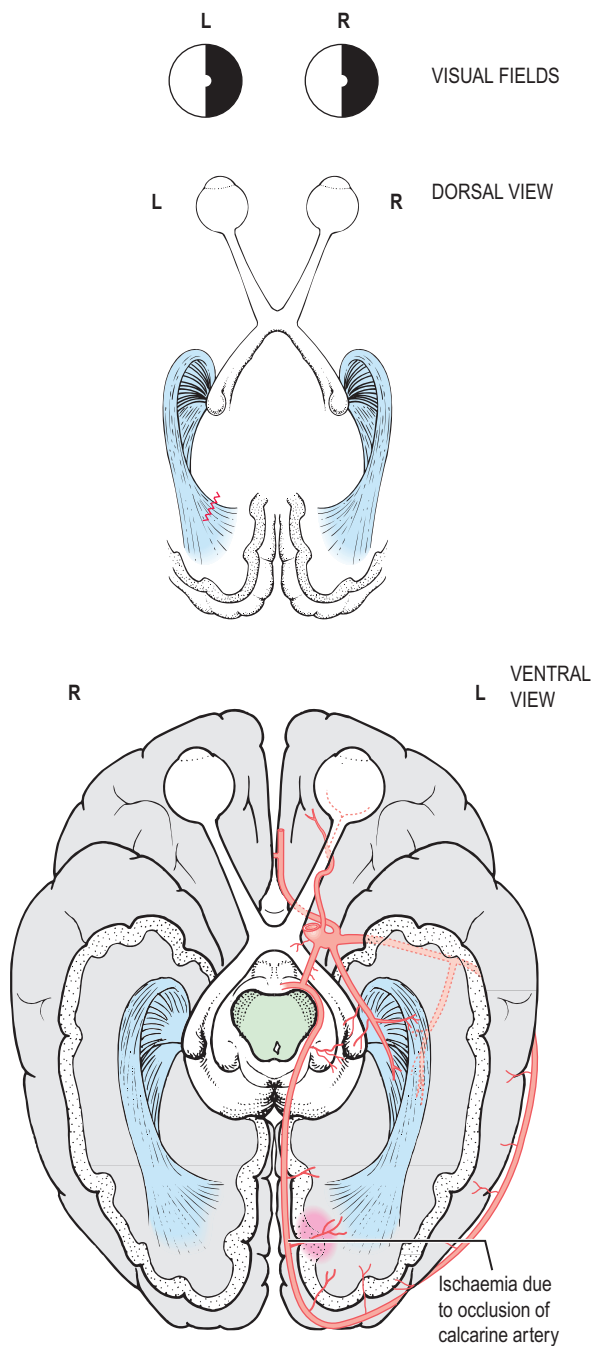


**FIGURE 1-77** Contralateral homonymous hemianopia with macular sparing (top left panel). This may be the result of lesions affecting portions of the occipital cortex, such as tumours or infarcts (bottom panel). Lesions affecting the entire occipital cortex can cause complete blindness. One such case is shown: MR scan of the brain in a 36-year-old intravenous drug user who presented with occipital headaches after injecting speed (amphetamine sulphate) with a dirty needle and waking 2 days later with total blindness and occipital headaches. Early CT scan (not shown) showed no sign of infarction but MR scan and diffusion-weighted imaging (not shown) clearly show bilateral occipital lobe infarcts which would explain the bilateral cortical blindness in this subject. (Radiographic image courtesy of Prof. T. Chakera, Royal Perth Hospital.)

## BLOOD SUPPLY OF THE VISUAL PATHWAY

The blood supply of the visual pathways is summarized in [Figure 1-71](#).

## FURTHER READING

A full reading list is available online at <https://expertconsult.inkling.com/>.



## FURTHER READING

- Ahnelt, P., Kolb, H., 1994. Horizontal cells and cone photoreceptors in human retina: a Golgi-electron microscopic study of spectral connectivity. *J. Comp. Neurol.* 343, 406–427.
- Ambati, J., Anand, A., Fernandez, S., Sakurai, E., Lynn, B.C., Kuziel, W.A., et al., 2003. An animal model of age-related macular degeneration in senescent Ccl-2- or Ccr-2-deficient mice. *Nat. Med.* 9 (11), 1390–1397.
- Balazs, E.A., 1982. Functional anatomy of the vitreous. In: Jakobiec, F.A. (Ed.), *Ocular anatomy, embryology and teratology*. Harper and Row, Philadelphia, pp. 425–440.
- Bishop, P.N., 2000. Structural macromolecules and supramolecular organisation of the vitreous gel. *Prog. Retin. Eye Res.* 19, 323–344.
- Bishop, P.N., Takanosu, M., Le Goff, M., Mayne, R., 2002. The role of the posterior ciliary body in the biosynthesis of vitreous humour. *Eye* 16 (4), 454–460.
- Butler, T.L., McMenamin, P.G., 1996. Resident and infiltrating immune cells in the uveal tract in the early and late stages of experimental autoimmune uveoretinitis. *Invest. Ophthalmol. Vis. Sci.* 37, 2195–2210.
- Ceelen, P.W., Lockridge, A., Newman, E.A., 2001. Electrical coupling between glial cells in the rat retina. *Glia* 35, 1–13.
- Chan-Ling, T., 1994. Glial, neuronal and vascular interactions in the mammalian retina. *Prog. Ret. Eye Res.* 13, 357–389.
- Chinnery, H.R., Ruitenberg, M.J., Plant, G.W., Pearlman, E., Jung, S., McMenamin, P.G., 2007. The chemokine receptor CX3CR1 mediates homing of MHC class II-positive cells to the normal mouse corneal epithelium. *Invest. Ophthalmol. Vis. Sci.* 48, 1568–1574.
- Christensen, A.M., 2004. Assessing the variation in individual frontal sinus outlines. *Am. J. Phys. Anthropol.* 127, 291–295.
- Cruzat, A., Witkin, D., Baniasadi, N., Zheng, L., Ciolino, J.B., Jurkunas, U.V., et al., 2011. Inflammation and the nervous system: the connection in the cornea in patients with infectious keratitis. *Invest. Ophthalmol. Vis. Sci.* 52 (8), 5136–5143.
- Dacey, D.M., Liao, H.W., Peterson, B.B., Robinson, F.R., Smith, V.C., Pokorny, J., et al., 2005. Melanopsin-expressing ganglion cells in primate retina signal colour and irradiance and project to the LGN. *Nature* 433, 749–754.
- Dartt, D.A., 2002. Regulation of mucin and fluid secretion by conjunctival epithelial cells. *Prog. Ret. Eye Res.* 21, 555–576.
- Demer, J.L., 2004. Pivotal role of orbital connective tissue in binocular alignment and strabismus. *Invest. Ophthalmol. Vis. Sci.* 45, 729–738.
- Demer, J.L., Poukens, V., Miller, J.M., Micevych, P., 1997. Innervation of extraocular pulley smooth muscle in monkeys and humans. *Invest. Ophthalmol. Vis. Sci.* 38, 1774–1785.
- Diaz-Araya, C.M., Provis, J.M., Penfold, P.L., Billson, F.A., 1995. Development of microglial topography in human retina. *J. Comp. Neurol.* 363, 53–68.
- Dick, A.D., Carter, D., Robertson, M., Broderick, C., Hughes, E., Forrester, J.V., et al., 2003. Control of myeloid activity during retinal inflammation. *J. Leuk. Biol.* 74 (2), 161–166.
- Eggers, H.M., 1982. Functional anatomy of the extraocular muscles. In: Jakobiec, F.A. (Ed.), *Ocular anatomy, embryology and teratology*. Harper and Row, Philadelphia, pp. 783–834.
- Eisner, G., 1982. Clinical anatomy of the vitreous. In: Jakobiec, F.A. (Ed.), *Ocular anatomy, embryology and teratology*. Harper and Row, Philadelphia, pp. 391–424.
- Ertrurk, M., Kayalioglu, G., Govsa, F., Varol, T., Ozgur, T., 2005. The crano-orbital foramen, the groove on the lateral wall of the human orbit, and the orbital branch of the middle meningeal artery. *Clin. Anat.* 18, 10–14.
- Fitzgerald, M.J.F., 1992. *Neuroanatomy. Basic and clinical*, second ed. Baillière Tindall, London.
- Forrester, J.V., 2003. Macrophages eyed in macular degeneration. *Nat. Med.* 9, 1350–1351.
- Gausas, R.E., 2004. Advances in applied anatomy of the eyelid and orbit. *Curr. Opin. Ophthalmol.* 15, 422–425.
- Gebert, A., Pabst, R., 1999. M cells at locations outside the gut. *Semin. Immunol.* 11, 165–170.
- Guymer, R.H., Bird, A., Hageman, G., 2005. Cytoarchitecture of choroid capillary endothelial cells. *Invest. Ophthalmol. Vis. Sci.* 45, 1660–1666.
- Halfter, W., Dong, S., Schurer, B., Ring, C., Cole, G.J., Eller, A., 2005. Embryonic synthesis of the inner limiting membrane and vitreous body. *Invest. Ophthalmol. Vis. Sci.* 46 (6), 2202–2209.
- Hamrah, P., Zhang, Q., Liu, Y., Dana, M.R., 2002. Novel characterization of MHC class II-negative population of resident corneal Langerhans cell-type dendritic cells. *Invest. Ophthalmol. Vis. Sci.* 43, 639–646.
- Hingorani, M., Metz, D., Lightman, S.L., 1997. Characterisation of the normal conjunctival leukocyte population. *Exp. Eye Res.* 64, 905–912.
- Ihanamaki, T., Pelliniemi, L.J., Vuorio, E., 2004. Collagens and collagen-related matrix components in the human and mouse eye. *Prog. Ret. Eye Res.* 23, 403–434.
- Jakobiec, F.A., 1982. *Ocular anatomy, embryology and teratology*. Harper and Row, Philadelphia.
- Kabil, M.S., Eby, J.B., Shahinian, H.K., 2005. Endoscopic vascular decompression versus microvascular decompression of the trigeminal nerve. *Minim. Invasive Neurosurg.* 48 (4), 207–212.
- Knop, E., Knop, N., 2005. The role of eye-associated lymphoid tissue in corneal immune protection. *J. Anat.* 206, 271–285.
- Kolb, H., Linberg, K.A., Fisher, S.K., 1992. Neurons of the human retina: a Golgi study. *J. Comp. Neurol.* 318, 147–187.
- Kolb, H., Fernandez, E., Schouten, J., Ahnelt, P., Linberg, K.A., Fisher, S.K., 1994. Are there three types of horizontal cell in the human retina? *J. Comp. Neurol.* 343, 370–386.
- Koornneef, L., 1982. Orbital connective tissue. In: Jakobiec, F.A. (Ed.), *Ocular anatomy, embryology and teratology*. Harper and Row, Philadelphia, pp. 835–857.
- Last, R.J., 1968. *Wolff's anatomy of the eye and orbit*. Lewis, London.
- Lockwood, C., 1886. The anatomy of the muscles, ligaments, fascia of the orbit etc. *J. Anat. Physiol.* 20, 1.
- Lütjen-Drecoll, E., 1998. Functional morphology of the trabecular meshwork in primate eyes. *Prog. Retin. Eye Res.* 18, 91–119.
- Mariani, A.P., 1990. Amacrine cells of the rhesus monkey retina. *J. Comp. Neurol.* 301, 382–400.
- May, C.A., 2005. Non-vascular smooth muscle cells in the human choroid: distribution, development and further characterization. *J. Anat.* 207, 381–390.
- May, C.A., Neuhuber, W., Lutjen-Drecoll, E., 2004. Immunohistochemical classification and functional morphology of human choroidal ganglion cells. *Invest. Ophthalmol. Vis. Sci.* 45, 361–367.
- McClung, J.R., Allman, B.L., Dimitrova, D.M., Goldberg, S.J., 2006. Extraocular connective tissues: a role in human eye movements? *Invest. Ophthalmol. Vis. Sci.* 47, 202–205.
- McMenamin, P.G., Lee, W.R., Aitken, D.A.N., 1986. Age-related changes in the human outflow apparatus. *Ophthalmol.* 93, 194–208.

## 102.e2 1 Anatomy of the eye and orbit

- McMenamin, P.G., Forrester, J.V., 1999. Dendritic cells in the central nervous system and eye and their associated supporting tissues. In: Lotze, M.T., Thomson, A.W. (Eds.), *Dendritic cells: biology and applications*. Academic Press, San Diego, pp. 205–248.
- Muller, L.J., Pels, L., Vrensen, F.J.M., 1995. Novel aspects of the organisation of human corneal keratocytes. *Invest. Ophthalmol. Vis. Sci.* 36, 2557–2567.
- Muller, L.J., Marfurt, C.F., Kruse, F., Tervo, T.M.T., 2003. Corneal nerves: structure, contents and function. *Exp. Eye Res.* 76, 521–542.
- Nimmerjahn, A., Kirchhoff, F., Helmchen, F., 2005. Resting microglial cells are highly dynamic surveillants of brain parenchyma in vivo. *Science* 308 (5726), 1314–1318.
- Obata, H., Yamamoto, S., Horiuchi, H., Machinami, R., 1995. Histopathologic study of human lacrimal gland. *Ophthalmol.* 102, 678–686.
- Penfold, P.L., Madigan, M.C., Provis, J.M., 1991. Antibodies to human leucocyte antigens indicate subpopulations of microglia in human retina. *Vis. Neurosci.* 7, 383–388.
- Qiao, H., Hisatomi, T., Sonoda, K.H., Kura, S., Sassa, Y., Kinoshita, S., et al., 2005. The characterisation of hyalocytes: the origin, phenotype, and turnover. *Br. J. Ophthalmol.* 89 (4), 513–517.
- Rada, J.A., Shelton, S., Norton, T.T., 2006. The sclera and myopia. *Exp. Eye Res.* 82, 185–200.
- Raviola, G., 1977. The structural basis of the blood–ocular barriers. *Exp. Eye Res. (suppl.)* 25, 27–63.
- Robinson, S., Dreher, Z., 1990. Müller cells in the adult rabbit retinae: morphology, distribution and implications for function and development. *J. Comp. Neurol.* 292, 178–192.
- Rohen, J., 1964. Ciliarkörper. In: von Möllendorff, W. (Ed.), *Das Auge und seine Hilfsorgane. Ergänzung zu Band 11 1/2. Haut und Sinnesorgane. 4 Teil. Handbuch der mikroskopischen Anatomie des Menschen*. Springer, Berlin, pp. 189–238.
- Rowe, M.H., 1991. Functional organisation of the retina. In: Dreker, B., Robinson, S.R. (Eds.), *Neuroanatomy of the visual pathways and their development. Vision and visual dysfunction* (Cronly-Dillon J, general ed.), Vol. 3. Macmillan UK, Basingstoke, pp. 1–68.
- Rowland, L.P., 1985. Blood–brain barrier, cerebrospinal fluid, brain edema, and hydrocephalus. In: Kandel, E.R., Schwartz, J.H. (Eds.), *Principles of neuroscience*. Elsevier, New York, pp. 837–844.
- Ruskell, G.L., 1971a. Facial parasympathetic innervation of the choroidal blood vessels in the monkey. *Exp. Eye Res.* 12, 166–172.
- Ruskell, G.L., 1971b. The distribution of autonomic postganglionic nerve fibres to the lacrimal gland in monkeys. *J. Anat.* 109, 229–242.
- Ruskell, G.L., 2004. Distribution of pteryopalatine ganglion efferents to the lacrimal gland in man. *Exp. Eye Res.* 78, 329–335.
- Ruskell, G.L., Kjellevold Haugen, I.B., Bruenech, J.R., van der Werf, F., 2005. Double insertions of extraocular rectus muscles in humans and the pulley theory. *J. Anat.* 206, 295–306.
- Sebag, J., 2004. Seeing the invisible: the challenge of imaging vitreous. *J. Biomed. Opt.* 9 (1), 38–46.
- Snell, R.S., Lemp, M.A., 1989. *Clinical anatomy of the eye*. Blackwell Scientific, Boston.
- Stewart, P.A., Tuor, U.I., 1994. Blood–eye barriers in the rat: correlation of ultrastructure with function. *J. Comp. Neurol.* 340, 566–576.
- Stiemke, M.M., Watsky, M.A., Kangas, T.A., Edelhauser, H.F., 1995. The establishment and maintenance of corneal transparency. *Prog. Ret. Eye. Res.* 14 (1), 109–140.
- Thale, A., Tillman, B., 1993. The collagen architecture of the sclera: SEM and immunohistochemical studies. *Ann. Anat.* 175, 215–220.
- Thermos, K., 2003. Functional mapping of somatostatin receptors in the retina: a review. *Vision Res.* 43 (17), 1805–1815.
- Van Buskirk, E.M., 1989. The anatomy of the limbus. *Eye* 3, 101–108.
- Waring, G.O., Bourne, W.M., Edelhauser, H.F., Kenyon, K.R., 1982. The corneal endothelium. Normal and pathologic structure and function. *Ophthalmol.* 89, 531–590.
- Watson, P.G., Young, R.D., 2004. Scleral structure, organisation and disease. A review. *Exp. Eye Res.* 78, 609–623.
- Williams, P.L., Warwick, R., 1980. *Gray's anatomy*, thirty-sixth ed. Churchill Livingstone, Edinburgh.
- Wotherspoon, A.C., Hardman-Lea, S., Isacsson, P.G., 1994. Mucosa-associated lymphoid tissue (MALT) in the human conjunctiva. *J. Pathol.* 174, 33–37.
- Yemelyanov, A.Y., Katz, N.B., Bernstein, P.S., 2001. Ligand-binding characterization of xanthophyll carotenoids to solubilized membrane proteins derived from human retina. *Exp. Eye Res.* 72 (4), 381–392.
- Young, R.W., 1967. The renewal of photoreceptor cell outer segments. *J. Cell Biol.* 33, 61–72.
- Zhang, H.R., 1994. Scanning electron-microscopic study of corrosion casts on retinal and choroidal angioarchitecture in man and animals. *Prog. Ret. Eye Res.* 13, 243–270.
- Zhivotov, A., Stave, J., Vollmar, B., Guthoff, R., 2005. In vivo confocal microscopic evaluation of Langerhans cell density and distribution in the normal human corneal epithelium. *Graefes Arch. Clin. Exp. Ophthalmol.* 243 (10), 1056–1061.